1151

File Cy

AD A057404

CONTRACT REPORT ARBRL-CR-00372

SPECTRAL RADIOMETRIC MEASUREMENTS OF SUB-ARCTIC STRATOSPHERIC CONSTITUENTS

Prepared by

University of Denver
Department of Physics
Denver, Colorado 80208

April 1978

US ARMY ARMAMENT RESEARCH AND DEVELOPMENT COMMAND
BALLISTIC RESEARCH LABORATORY
ABERDEEN PROVING GROUND, MARYLAND

Approved for public release; distribution unlimited.

UNCLASSIFIED

SECURITY CLASSIFICATION OF THIS PAGE (When Data Entered)

REPORT DOCUMENTATION PAGE		READ INSTRUCTIONS BEFORE COMPLETING FORM
1. REPORT NUMBER: CONTRACT REPORT ARBRL-CR-00372	2. GOVT ACCESSION NO.	3. RECIPIENT'S CATALOG NUMBER
4. TITLE (and Subtitle): SPECTRAL RADIOMETRIC MEASUREMENTS OF SUB-ARCTIC STRATOSPHERIC CONSTITUENTS		5. TYPE OF REPORT & PERIOD COVERED: Scientific Report
		6. PERFORMING ORG. REPORT NUMBER
7. AUTHOR(s): David G. Murcray, Frank H. Murcray, Aaron Goldman, Walter J. Williams, John J. Kosters		8. CONTRACT OR GRANT NUMBER(s): DAAD05-76-C-0740
9. PERFORMING ORGANIZATION NAME AND ADDRESS: University of Denver (Colorado Seminary), Department of Physics, Denver, Colorado 80208		10. PROGRAM ELEMENT, PROJECT, TASK AREA & WORK UNIT NUMBERS
11. CONTROLLING OFFICE NAME AND ADDRESS: US Army Armament Research & Development Command, US Army Ballistic Research Laboratory (ATTN: DRDAR-BL), Aberdeen Proving Ground, MD 21005		12. REPORT DATE: APRIL 1978
		13. NUMBER OF PAGES: 174
14. MONITORING AGENCY NAME & ADDRESS (if different from Controlling Office)		15. SECURITY CLASS. (of this report): UNCLASSIFIED
		15a. DECLASSIFICATION/DOWNGRADING SCHEDULE

16. DISTRIBUTION STATEMENT (of this Report)

Approved for public release; distribution unlimited.

17. DISTRIBUTION STATEMENT (of the abstract entered in Block 20, if different from Report)

18. SUPPLEMENTARY NOTES

19. KEY WORDS (Continue on reverse side if necessary and identify by block number)

Spectral Radiometry
Water Vapor
Nitric Acid
Ozone
Fluorocarbons
Atmospheric Constituent Profiles
Atmospheric Emission Spectroscopy

20. ABSTRACT (Continue on reverse side if necessary and identify by block number)

Constituent height profiles are derived for HNO_3, O_3, H_2O, CF_2Cl_2, $CFCl_3$ and two unidentified constituents from spectral radiance data observed on a balloon flight to 37.56 km on 29 April 1976 from Fairbanks, Alaska. Improvements in the band model techniques used are discussed and comparative results are shown. Spectral radiance data observed at selected altitudes and zenith angles are shown covering the spectral ranges of 8 to 13.6 μm and 18.8 to 27.6 μm. Tables of spectral radiance for selected spectral regions as a function of altitude are included.

DD FORM 1 JAN 73 1473 EDITION OF 1 NOV 65 IS OBSOLETE

S/N 0102-014-6601

UNCLASSIFIED

SECURITY CLASSIFICATION OF THIS PAGE (When Data Entered)

TABLE OF CONTENTS

LIST OF TABLES

LIST OF FIGURES

FIGURE PAGE

I. INTRODUCTION

This report contains the scientific results of a balloon flight on 29 April 1976. The emphasis in this report is on changes in the experimental approach from those reported to BRL in the flight report of 27 June 1974 and 19 February 1975[1] and on several additional data analysis techniques. The flight reported here was the first in a series of four made from Eielson AFB, Alaska, in the spring of 1976. Three of the flights measured atmospheric thermal emission and one measured atmospheric transmission. This will be the only data report on the emission flights except for a report by Snider et al.[2]. The second emission flight obtained data similar to that on this flight except that much of it contained interference from one of the piggyback instruments. The third emission flight had no usable data due to a bad launch. These flights are summarized in the Final Reports on two Contracts.[3]

---

[1] D. G. Murcray, J. N. Brooks, A. Goldman, J. J. Kosters and W. J. Williams, "Water Vapor, Nitric Acid and Ozone Mixing Ratio Height Profiles Derived from Spectral Radiometric Measurements" Report No. BRL CR332 on Contract DAAD05-74-C-0795 by Department of Physics, University of Denver, Feb. 1977. (AD #A037375)

[2] D. E. Snider, D. G. Murcray, W. J. Williams and F. H. Murcray, "Investigation of High Altitude Enhanced Infrared Background Emissions -Results from COSMEP III and IV" Electronics Command Report No. 5824, OSD-1366, June 1977.

[3] D. G. Murcray, R. C. Amme and J. R. Olson, Final Reports on Contracts DAAD05-74-C-0795 and DAAD05-76-C-0740 by Department of Physics, University of Denver, in preparation, 1978.

The purpose of this flight was to obtain data on the height distributions of a number of neutral minor atmospheric constituents and to measure any time-varying emissions present in the spectral bandpass of the instruments. These measurements were to be made near the auroral zone in the spring. This report contains the constituent data and a separate report by Snider et al.[2] contains the time-varying results.

A large volume of spectral radiometric data was obtained on this flight. An extensive analysis of some aspects of the data has not only provided numerous constituent height profiles (some of unknown constituents), but has generated better reduction and analysis techniques, has raised interesting questions on how to deal with gray emitting matter and has led to a better understanding of the significant radiometric instrument parameters. The data are presented here in various comparative forms to provide the viewer with a diversity of perspective. Constituent height profiles are derived from the data and are compared with similar data from other flights.

II. INSTRUMENTATION AND CALIBRATION

A. Instrumentation

The payload for the flight included a number of complementary instruments. The liquid helium cooled spectral radiometer described in detail in a previous report[1] was intended to measure constituent height profiles during ascent and to measure time variations in the window radiance at float. Toward this end a scan-stop mode was incorporated which allowed one window wavelength to be monitored for several minutes at a time before returning to the normal scan mode. This was accomplished by stopping the scan reference ramp at a pre-selected point. Table I includes a list of the instruments and their parameters for this flight.

A liquid nitrogen cooled filter radiometer was also flown with four detectors mounted in a vertically linear array. Each detector has a 1° F.O.V. and is offset from the next by 3° center to center. This radiometer had a spectral bandpass that covered the HNO_3 band at $11.3\mu m$. The elevation angles associated with each detector correspond to some of the programmed angles for the spectral radiometer. This instrument has been described in detail elsewhere.[4] For this flight the principal function of the filter radiometer was to measure the temporal and spatial character of the 11 to $12\mu m$ window radiance at float.

---

[4] D. G. Murcray, "Optical Properties of the Atmosphere" Six Month Technical Report on Contract F19628-68-C-0233 for AFCRL by Department of Physics, University of Denver, Sept. 1969.

In addition, a four-channel x-ray counter was flown to provide a monitor of possible temporal variations in other portions of the energy spectrum. This experiment has been described in more detail by Snider et al.[2] A number of independent experiments were also performed during the course of this flight. Rawinsonde and ozonesonde balloon flights were flown from Poker Flats in addition to a rocket sonde for a temperature profile. Special runs were performed with the Chatanika radar and data was collected from a number of monitors operated by the Geophysical Institute of the University of Alaska.

Table I. Flight and Instrument Parameters

29 April 1976 Flight

Flight Date: 29 April 1976

Location: Eielson A. F. B., Alaska

Primary Instruments:
1. Liquid helium cooled spectrometer with cold window.
2. 4-Detector LN_2 radiometers.

Auxiliary Instruments:
1. X-ray (Barcus)

Purpose of Flight: To measure constituent height profiles and to measure temporal and spatial radiance fluctuations at float altitude in atmospheric windows.

Time Log:		
	Launch	0430 ADT
	Float	0740 ADT (37.6 km)
	Cut Down	0905 ADT

LHe Spectrometer Parameters:

Window material	KRS 5
Scan Time	43 sec
λ Equation	See Figure 3

Grating Order	2	1
λ Range	8.0-13.6μm	18.8-27.7μm
Resolution	.03μm	.06μm
Sample Interval	.005μm	.01μm
Detector Bias	+15 v	+15 v
Amplifier Gain	4.0/160	4.0/160
Band Pass	12.5Hz	12.5Hz
NER (Realized during flight)	4×10^{-8} $wcm^{-2} sr^{-1} \mu m^{-1}$	2×10^{-8} $wcm^{-2} sr^{-1} \mu m^{-1}$

B. Calibration Procedure

The calibration procedure used prior to this flight is the same as described previously.[1] Briefly, a double-walled cavity is placed in the field of view directly in front of the vacuum window. The window is maintained at LN_2 temperature while the black body is allowed to slowly vary in temperature over the range from LN_2 to $170^{\circ}K$, above which the preamp is saturated. The differential calibration technique, which eliminates the window emission and scatter effects, was used to derive the spectral calibration coefficient from pairs of black body scans at different temperatures. The spectral calibration coefficients are shown in Figures 1 and 2 and reflect the product of the blocking filters and the grating efficiency functions.

The wavelength function is derived from the grating equation and the constants are determined by fitting the equation to water vapor emission or absorption line positions. Figure 3 shows this function for the calibration data as well as for the flight data.

The spectrometer was calibrated in Denver prior to the Alaskan series and then in Alaska prior to each flight. Also, the flight data are checked for specific radiance values under selected conditions which serves as an in-flight check of the calibration. This procedure is discussed later (section IV.C., Data Testing).

The experience gained during this calibration established four points worth noting. 1) The black body must be thermally stabilized at each temperature used to obtain a good radiometric calibration. Both the temperature sensor of the black body and the radiometric measurement of the spectrometer should be monitored to confirm stability. This should eliminate temperature errors, the effect of which was discussed in the previous report.[1] 2) At high detector

bias levels a random short-term breakdown occurs at the detector causing high frequency spikes. The number of these spikes per unit time depends both on the bias level and the total photon level. The time duration of these spikes is short compared to a resolution element and can be differentiated against if the electrical bandpass is wide compared to a resolution element. Bias values of 15v were picked as a compromise between this effect and optimum signal to noise. It should also be noted that the signal is linearly proportional to the bias voltage within the normal range of photon levels. 3) As noted in the previous report the cross talk between the short and long wavelength channels is $< 0.1\%$. If it is present at all, it may be slightly noticeable at the high altitudes and in the long wavelength data where the strong signal from the $9.6 \mu m$ O_3 band may be reducing the signal level slightly around $19 \mu m$. 4) The effects of scattered radiation from the vacuum window have been greatly reduced for this flight series but have not been eliminated (see IV. B., Window Correction, Eq. (1)). A further improvement has since been made on the balloon spectrometer window baffle assembly. In addition, a modified optical design has been successfully tried on the U-2 aircraft spectrometer in which the window was placed as near as possible to the internal cold baffles.

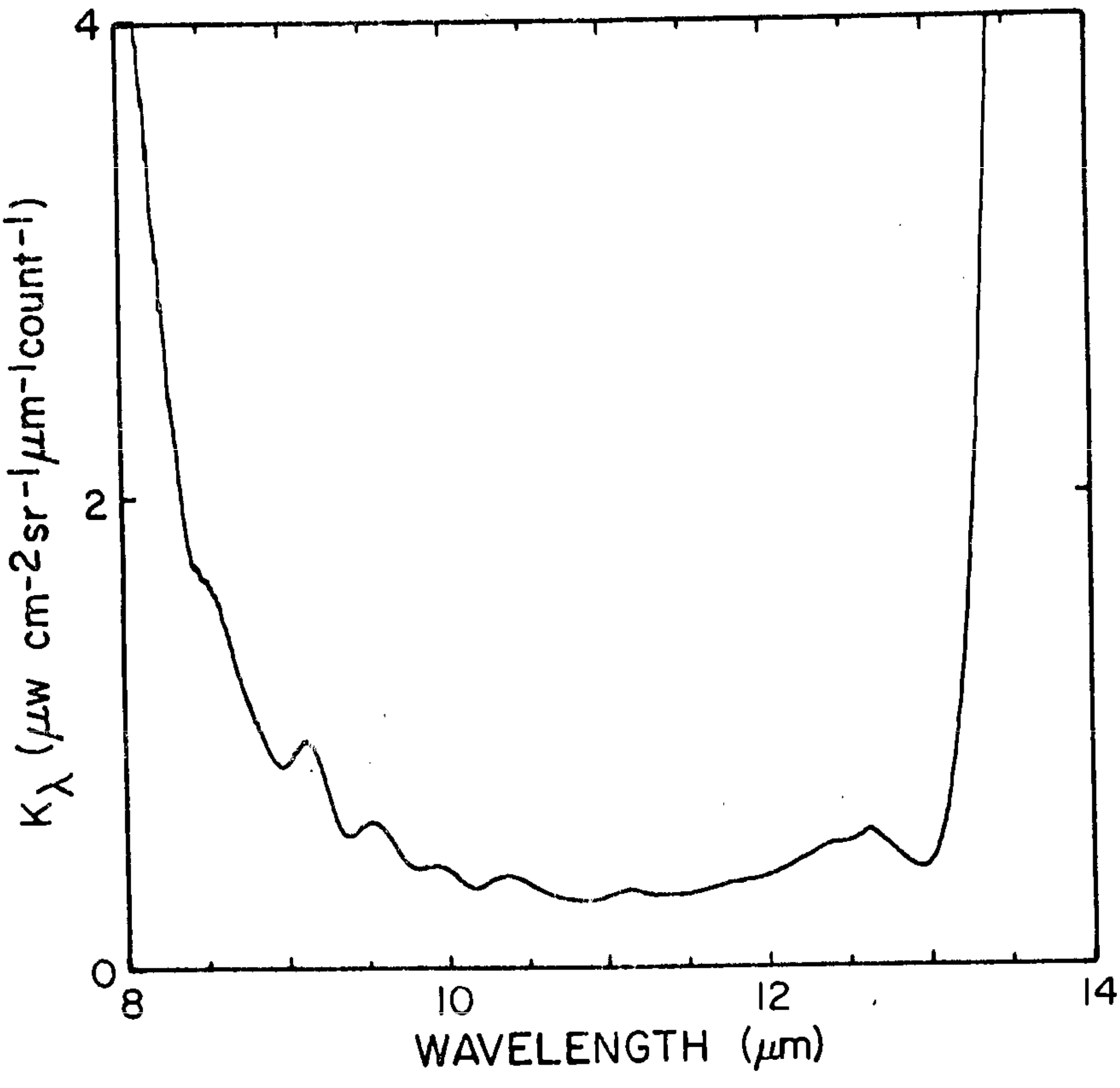

Figure 1. Spectral calibration coefficient for the second order spectral region.

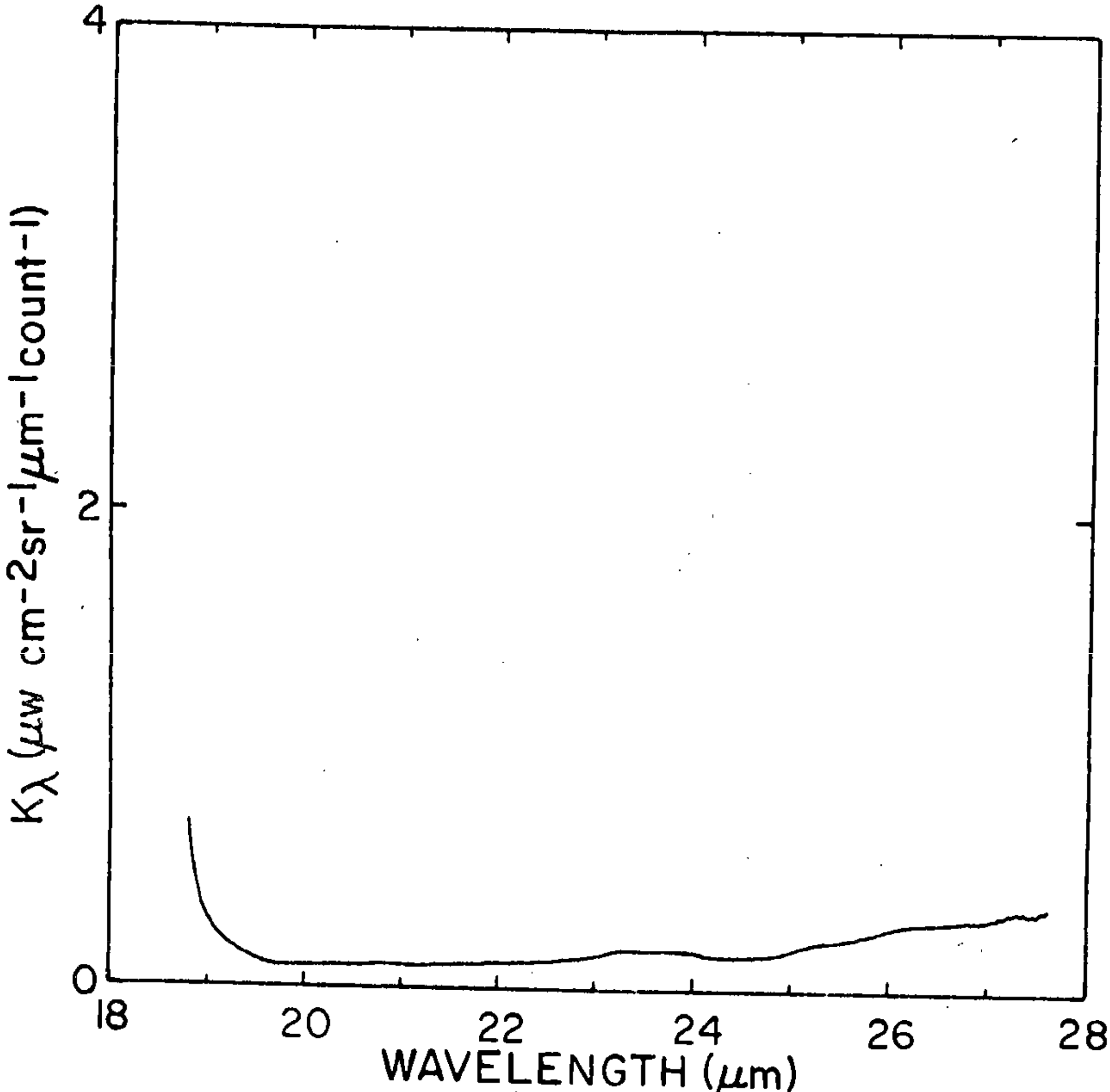

Figure 2. Spectral calibration coefficient for the first order spectral region.

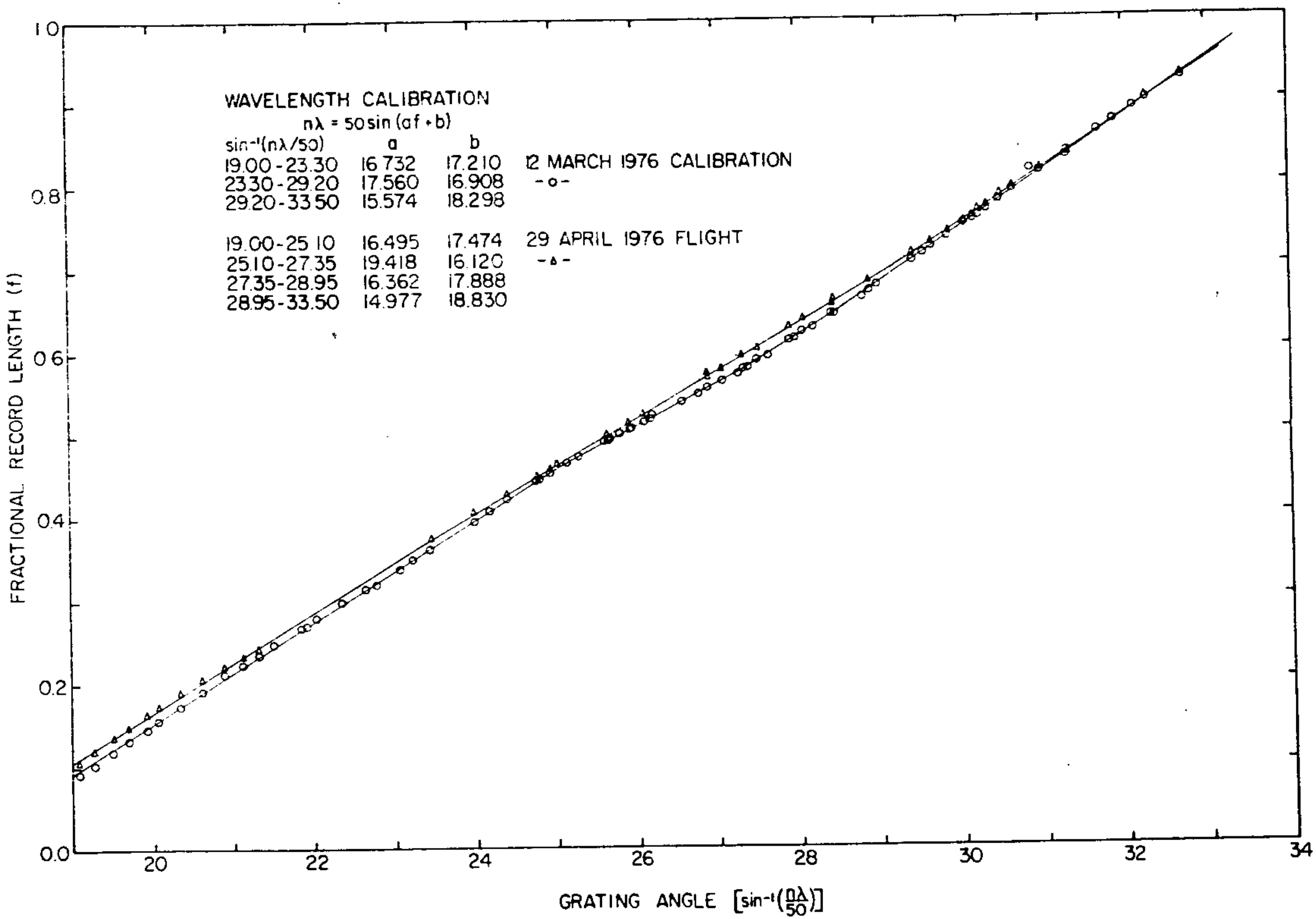

Figure 3. Wavelength equations for 12 March 1976 calibration and 29 April 1976 balloon flight.

III. FLIGHT DETAILS (29 April 1976)

Project personnel arrived at Eielson AFB on 19 April 1976 to prepare for a series of four balloon flights. Assembly and testing was begun on 20 April of the LHe grating spectrometer, the LN_2 interferometer, the LN_2 filter radiometer with a four-detector vertically linear array, and the auxilliary instrumentation such as the x-ray sensors, gyrocompass servo control, tape recorders, etc. Delays in shipment of liquid helium prevented early testing of any of the infrared experiments. Tests of the laser and white light outputs of the interferometer indicated that that instrument had sustained considerable shock during shipment and required total re-alignment. The radiometer and the grating spectrometer fared better and with the arrival of the LHe were calibrated against cold black bodies on 24 April and 25 April, respectively. By 26 April these instruments were assembled in a gondola and ready for flight. Marginal weather prevented flights on the mornings of the 27th and 28th, but forecasts for the 29th were favorable.

On 29 April 1976 at 0115 ADT, the balloon instrumentation, including the liquid helium cooled spectrometer, the liquid nitrogen cooled four-field radiometer, the four-level x-ray counter, and support instruments, was moved out to the launch area on the taxi strip at Eielson AFB after weighing the payload at 863 kg plus parachute. A complete pre-flight check was made prior to moving the gondola to the launch area, and it was repeated at the site. Preparations continued and the balloon was launched at 0430 ADT.

Since the LHe grating spectrometer was aboard, one of the flight objectives was to measure constituent height distribution. For this purpose the 3.28×10^5 m^3 Winzen balloon weighing 549 kg was used to obtain a higher float altitude. The balloon ascended at a uniform rate of about 4.0 meters/second and reached a float altitude of 37.6 km at 0740 ADT. The ascent to 18 km was to the NNE, from there to near float it was to the SW and float winds were to the west. The balloon height profile and atmospheric temperature profile are shown in Fig. 4. The trajectory (see Fig. 5) carried the balloon over Nenanna and the flight was terminated at 0905 ADT, 85 nautical miles west of Eielson AFB. The payload impacted 3 miles south of Bear Lake in a tall stand of trees. The equipment was returned at 2100 ADT the same day using the H-3 rescue helicopter from Eielson AFB. The gondola and instruments were in excellent condition.

During the flight the trajectory tracking was excellent from both x-band and s-band at Poker Flats, and the GMD tracks from the Air Force proved reliable after an azimuth correction was determined by comparison with theodolite observations. The O-2 chase aircraft also provided a fix some time prior to cut-down.

Real time readouts of the gyrocompass and the magnetometers provided direction of look data during the flight by using the Nova 1220 computer to decommutate and digitize the multiplexed data containing this information and then calculate the angles with appropriate, precalibrated equations.

The LHe spectrometer and the x-ray monitor worked well during the flight. The radiometer was working at launch but soon lost sensitivity. It was determined after the flight that this was

due to a bad bias battery and possibly due to difficulties with the tuning fork chopper which were more pronounced on later flights.

A series of command controls were executed during the flight which varied both the azimuth and zenith angle of observation of the spectral radiometer. The zenith angles were pre-programmed for 47, 50, 53, 56, 70, 85, 90.5, and 93.5°, sequentially. There is some evidence from the float altitude data that the effective angles were about 0.2° less than those stated. The instrument was set at 50° at launch and, as the constituent radiances fell off with altitude, the angle was increased to provide a greater optical path (see Table II). Once at float the remaining angles were stepped through and the instrument was set at 47° to look for temporal data. At the end of the flight the instrument was parked at 70°. Thus, there are two points in the flight where several angles are sampled over a short time-span, allowing secant air mass extrapolations to be made.

The azimuth control system was turned on during ascent at about 0540 ADT. The recorder containing the azimuth direction data cannot be well correlated to real-time due to failure of the end-of-record switch. However, a number of things can be said about the pointing, even if it cannot be correlated with the radiance data on a fine time base. The azimuth control was pre-set at 25° true. The gondola did not stabilize immediately following turn-on due to the driving torques associated with the ascending balloon. The platform had stabilized by 0650 ADT (30 km altitude) and was pointing at 25.5° ± 5° true. The period of the 10° oscillation was 15.5 sec which was relatively constant until the angle was changed. At 0715 ADT the gondola was rotated slightly to 118° true and the

oscillation continued. At about 1730 ADT the gondola was again rotated to 152° true, and at 0755 ADT a full rotation was instituted (200 seconds of command) which ended at an azimuth of 159° true with an oscillation of ± 15° over a period of 36.2 seconds. A final change in the azimuth was made at about 0830 ADT with a resulting angle of 182° ± 15°.

A list of the parameters associated with each of the spectral scans can be found in Table II. The skin and window temperatures are used in radiometric corrections discussed later. The air and dew point temperatures are from rawinsonde data (Figure 4). The air mass along the optical path was calculated for each scan ($m = p/p_o \sec \theta$) for angles less than 80° and derived from air mass tables[5] for greater angles. Temperatures are listed to 60 km for each kilometer above the balloon float altitude at the end of the table. These were derived from a rocketsonde launched near the time of the balloon flight from Poker Flats. The pressure data were measured on-board the balloon payload. This data was converted to altitude with a model atmosphere derived from the local meteorological data for the preceding several days.

---

[5] D. E. Snider and A. Goldman, "Refractive Effects in Remote Sensing of the Atmosphere with Infrared Transmission Spectroscopy" BRL Report No. 1790, Ballistic Research Laboratories, Aberdeen Proving Ground, Maryland, June 1975. (AD #A011253)

Table II. Atmospheric and Instrument Parameters for 29 April 1976.

Rec. No.	Time (ADT)	Altitude (km)	Pressure (mb)	Zenith Angle (°)	Air Temp. (K)	Skin Temp. (K)	Window Temp. (K)	Air Mass (atm)	Dew Point (K)
Launch	0438.0	0.00	1002.0	50	280.3	242.7	106.2	1.539	
32	0438.2	0.06	994.9	50	280.3	242.7	106.2	1.528	
33	0438.9	0.30	969.8	50	280.2	242.7	106.2	1.489	271.8
34	0439.6	0.50	944.8	50	280.1	242.7	106.2	1.451	270.6
35	0440.3	0.72	919.8	50	279.9	242.4	106.2	1.413	269.2
36	0441.0	0.95	894.8	50	279.3	242.0	106.2	1.374	267.9
37	0441.7	1.06	873.3	50	279.0	242.2	106.2	1.341	267.4
38	0442.4	1.33	852.0	50	277.3	242.5	106.2	1.308	266.7
39	0443.1	1.41	843.6	50	276.8	242.5	106.2	1.296	266.5
40	0443.8	1.50	833.8	50	276.2	243.0	106.2	1.281	266.2
41	0444.5	1.60	824.0	50	275.7	242.0	106.2	1.265	265.8
42	0445.3	1.71	812.8	50	275.1	242.0	106.2	1.248	265.2
43	0446.0	1.80	803.0	50	274.5	243.0	106.2	1.233	264.8
44	0446.7	2.10	784.5	50	274.1	243.5	106.2	1.205	259.5
45	0447.4	2.30	765.9	50	273.4	243.5	106.1	1.176	256.3
46	0448.1	2.40	747.4	50	272.8	243.0	106.1	1.148	254.7
47	0448.8	2.60	728.8	50	271.3	242.0	106.0	1.119	254.8
48	0449.5	2.80	710.3	50	269.6	242.0	106.0	1.091	256.3
49	0450.2	3.00	692.2	50	268.1	242.3	105.9	1.063	258.8
50	0450.9	3.15	677.8	50	266.9	242.8	105.7	1.041	261.6
51	0451.7	3.42	656.2	50	265.0	242.9	105.5	1.008	256.9
52	0452.4	3.75	638.2	50	262.8	242.1	105.3	0.980	251.4
53	0453.0	3.85	622.0	50	262.2	241.8	105.2	0.955	249.8
54	0453.8	4.00	600.4	50	261.2	241.6	105.0	0.922	247.3
55	0454.5	4.23	584.5	50	259.6	241.5	104.8	0.898	243.6
56	0455.2	4.50	569.8	50	258.2	241.4	104.5	0.875	241.2
57	0455.9	4.70	555.1	50	257.1	240.8	104.2	0.852	239.7
58	0456.6	4.90	541.9	50	256.1	240.8	103.8	0.832	238.1
59	0457.3	5.07	529.0	50	255.1	241.0	103.5	0.812	236.9
60	0458.0	5.25	516.0	50	254.0	241.0	103.0	0.792	235.8
61	0458.7	5.35	508.3	50	253.2	240.7	102.4	0.781	235.5
62	0459.5	5.50	499.5	50	252.1	240.2	101.8	0.767	235.0
63	0500.2	5.82	477.5	50	249.4	240.2	101.1	0.733	233.4
64	0500.9	6.02	465.3	50	247.8	240.2	100.3	0.715	232.0
65	0501.6	6.20	453.0	50	246.2	239.9	99.2	0.696	230.9
66	0502.3	6.45	438.8	50	244.2	239.1	98.4	0.674	229.2
67	0503.0	6.60	429.8	50	243.0	238.8	97.8	0.660	228.3
68	0503.7	6.82	415.4	50	241.2	238.5	97.3	0.638	226.9
69	0504.4	7.10	403.2	50	239.1	238.3	96.7	0.619	225.1
70	0505.1	7.30	391.3	50	237.6	238.1	96.0	0.601	224.0
71	0505.8	7.50	379.4	50	235.7	237.8	95.1	0.583	
72	0506.5	7.70	368.4	50	234.2	237.6	94.3	0.566	
73	0507.2	7.95	356.2	50	232.0	237.4	93.5	0.547	
74	0507.9	8.10	347.0	50	230.7	237.1	92.9	0.533	
75	0508.7	8.35	334.8	50	228.7	236.9	92.4	0.514	

Table II. Atmospheric and Instrument Parameters for 29 April 1976. (Continued)

Rec. No.	Time (ADT)	Altitude (km)	Pressure (mb)	Zenith Angle (°)	Air Temp. (K)	Skin Temp. (K)	Window Temp. (K)	Air Mass (atm)	Dew Point (K)
76	0509.4	8.60	324.2	50	226.8	236.6	91.8	0.498	
77	0510.1	8.80	313.6	50	225.4	236.3	91.4	0.482	
78	0510.8	9.05	303.5	50	223.4	236.0	91.0	0.466	
79	0511.6	9.32	290.6	50	221.5	235.8	90.7	0.446	
80	0512.3	9.55	280.6	50	220.1	235.6	90.4	0.431	
81	0513.0	9.78	270.8	50	218.5	235.3	90.2	0.416	
82	0513.7	9.92	264.8	50	217.6	234.8	89.9	0.407	
83	0514.4	10.13	256.4	50	216.2	234.4	89.6	0.3938	
84	0515.1	10.30	248.0	50	215.3	234.1	89.4	0.3809	Trop
85	0515.8	10.53	241.3	50	214.6	233.6	89.1	0.3706	
86	0516.5	10.65	235.5	50	214.4	233.4	88.7	0.3617	
87	0517.2	10.80	229.7	50	214.2	233.0	88.4	0.3528	
88	0517.9	11.00	223.8	50	213.9	232.5	88.1	0.3437	
89	0518.6	11.10	219.8	50	213.8	232.1	87.9	0.3376	
90	0519.3	11.15	216.0	50	213.7	231.8	87.6	0.3317	
91	0520.0	11.30	212.2	50	213.5	231.4	87.3	0.3259	
92	0520.7	11.42	208.4	50	213.4	231.2	87.0	0.3201	
93	0521.5	11.55	204.1	50	213.3	230.9	86.7	0.3134	
94	0522.2	11.70	200.3	50	213.2	230.6	86.5	0.3076	Min. Temp.
95	0522.9	11.80	196.5	50	213.3	230.3	86.2	0.3018	
96	0523.6	11.90	192.8	50	213.4	230.1	85.9	0.2961	
97	0524.3	12.00	189.0	50	213.5	229.8	85.6	0.2903	
98	0525.0	12.15	185.2	50	213.9	229.5	85.4	0.2844	
99	0525.7	12.30	181.4	50	214.5	229.4	85.2	0.2786	
100	0526.4	12.45	177.6	50	215.6	229.1	84.9	0.2728	
101	0527.1	12.60	173.3	50	216.1	228.8	84.7	0.2661	
102	0527.8	12.70	170.2	50	216.2	228.5	84.4	0.2614	
103	0528.5	12.90	166.6	50	216.2	228.3	84.2	0.2559	
104	0529.3	13.00	162.8	50	216.1	228.1	83.9	0.2500	
105	0530.0	13.15	159.4	50	216.0	227.8	83.7	0.2448	
106	0530.7	13.25	156.2	50	215.9	227.6	83.5	0.2399	
107	0531.4	13.42	152.7	50	215.8	227.4	83.4	0.2345	
108	0532.1	13.55	149.3	50	215.7	227.2	83.2	0.2293	
109	0532.8	13.70	146.0	50	215.6	227.0	83.0	0.2242	
110	0533.5	13.85	142.8	50	215.6	226.8	82.9	0.2193	
111	0534.2	14.00	139.7	50	215.7	226.6	82.7	0.2145	
112	0534.9	14.10	136.6	50	215.8	226.5	82.6	0.2098	
113	0535.7	14.27	133.1	50	215.9	226.2	82.4	0.2044	
114	0536.4	14.40	130.0	50	216.1	226.1	82.3	0.1996	
115	0537.1	14.60	127.0	50	216.5	225.9	82.2	0.1950	
116	0537.8	14.80	123.9	50	217.1	225.7	82.3	0.1903	
117	0538.5	14.90	121.4	50	217.5	225.5	82.4	0.1864	
118	0539.2	15.00	119.2	50	217.8	225.3	82.7	0.1831	
119	0539.9	15.10	117.0	50	218.1	225.1	83.1	0.1797	
120	0540.6	15.20	114.8	50	218.5	224.9	83.5	0.1763	

Table II. Atmospheric and Instrument Parameters for 29 April 1976. (Continued)

Rec. No.	Time (ADT)	Altitude (km)	Pressure (mb)	Zenith Angle (°)	Air Temp. (K)	Skin Temp. (K)	Window Temp. (K)	Air Mass (atm)	Dew Point (K)
121	0541.3	15.35	112.6	50	218.8	224.8	83.9	0.1729	
122	0542.0	15.45	110.4	50	219.1	224.5	84.2	0.1695	
123	0542.8	15.60	107.9	50	219.5	224.4	84.6	0.1657	
124	0543.5	15.70	105.7	50	219.8	224.2	85.1	0.1623	
125	0544.2	15.87	103.5	50	220.1	224.0	85.4	0.1590	
126	0544.9	16.00	101.3	50	220.3	223.9	85.7	0.1556	
127	0545.6	16.10	99.4	50	220.5	223.7	86.2	0.1527	
128	0546.3	16.25	97.5	50	220.6	223.5	86.6	0.1497	
129	0547.0	16.40	95.7	50	220.7	223.4	87.0	0.1470	
130	0547.7	16.50	93.8	50	220.7	223.3	87.4	0.1441	
131	0548.4	16.70	91.8	50	220.7	223.1	87.7	0.1410	
132	0549.1	16.80	89.7	50	220.8	222.9	88.1	0.1378	
133	0549.9	17.00	87.3	50	220.8	222.7	88.5	0.1341	
134	0550.6	17.15	85.2	50	220.8	222.6	88.9	0.1308	
135	0551.3	17.30	83.1	50	220.9	222.5	89.2	0.1276	
136	0552.0	17.45	81.0	50	221.0	222.2	89.6	0.1244	
137	0552.7	17.62	78.9	50	221.0	222.1	90.0	0.1212	
138	0553.4	17.80	77.1	50	221.1	221.9	90.4	0.1184	
139	0554.1	17.92	75.6	50	221.1	221.8	90.7	0.1161	
140	0554.8	18.05	74.0	50	221.2	221.7	91.0	0.1136	
141	0555.5	18.20	72.5	50	221.2	221.4	91.4	0.1113	
142	0556.2	18.30	71.0	50	221.2	221.3	91.8	0.1090	
143	0557.0	18.45	69.2	50	221.3	221.2	92.2	0.1063	
144	0557.7	18.68	67.7	50	221.2	221.0	92.6	0.1040	
145	0558.4	18.80	66.3	50	221.2	220.9	93.0	0.1018	
146	0559.1	18.90	65.0	50	221.1	220.7	93.4	0.0998	
147	0559.8	19.00	63.8	50	221.0	220.5	93.8	0.0980	
148	0600.5	19.18	62.5	50	220.9	220.4	94.2	0.0960	
151	0602.7	19.60	58.5	50	220.4	220.0	95.1	0.0898	
152	0603.4	19.75	57.1	50	220.2	219.8	95.4	0.0877	
153	0604.1	19.95	55.6	50	220.0	219.7	95.7	0.0854	
154	0604.8	20.10	54.1	50	219.8	219.7	95.9	0.0831	
155	0605.5	20.30	52.6	50	219.6	219.4	96.1	0.0808	
156	0606.2	20.50	51.1	50	219.5	219.3	96.3	0.0785	
157	0606.9	20.68	49.6	50	219.4	219.2	96.5	0.0762	
158	0607.6	20.85	48.1	50	219.3	219.1	96.8	0.0739	
159	0608.3	21.05	46.6	50	219.2	219.0	97.0	0.0716	
160	0609.1	21.28	44.9	50	219.1	218.8	97.2	0.0690	
161	0609.8	21.48	43.4	50	219.0	218.7	97.5	0.0666	
162	0610.5	21.65	42.4	50	219.0	218.6	97.8	0.0651	
163	0611.2	21.76	41.8	53	218.9	218.4	98.1	0.0686	
164	0611.9	21.91	40.8	53	218.9	218.3	98.3	0.0669	
168	0614.8	22.58	36.8	53	218.9	217.9	99.4	0.0604	
169	0615.5	22.74	35.9	53	218.9	217.7	99.7	0.0589	
170	0616.2	22.91	34.9	56	218.9	217.6	99.9	0.0616	

Table II. Atmospheric and Instrument Parameters for 29 April 1976. (Continued)

Rec. No.	Time (ADT)	Altitude (km)	Pressure (mb)	Zenith Angle (°)	Air Temp. (K)	Skin Temp. (K)	Window Temp. (K)	Air Mass (atm)	Dew Point (K)
171	0616.9	23.07	34.1	56	218.9	217.6	100.2	0.0602	
172	0617.6	23.23	33.2	56/70	219.0	217.5	100.5		
173	0618.3	23.39	32.4	70	219.0	217.4	100.8	0.0935	
174	0619.0	23.56	31.6	70	219.0	217.3	101.0	0.0912	
175	0619.8	23.74	30.7	70	219.0	217.2	101.2	0.0886	
176	0620.5	23.90	29.94	70	219.0	217.1	101.4	0.0864	
177	0621.2	24.07	29.16	70	219.1	217.0	101.6	0.0842	
178	0621.9	24.23	28.44	70	219.1	216.9	101.9	0.0821	
179	0622.6	24.39	27.75	70	219.2	216.8	102.1	0.0801	
180	0623.3	24.55	27.06	70	219.2	216.7	102.3	0.0781	
181	0624.0	24.72	26.36	70	219.3	216.6	102.5	0.0761	
182	0624.7	24.88	25.71	70	219.4	216.5	102.7	0.0742	
183	0625.4	25.04	25.08	70	219.5	216.5	102.9	0.0724	
184	0626.1	25.20	24.46	70	219.7	216.4	103.1	0.0706	
185	0626.9	25.39	23.75	70	219.8	216.3	103.3	0.0686	
186	0627.6	25.55	23.17	70	220.0	216.2	103.4	0.0669	
187	0628.3	25.71	22.60	70	220.1	216.1	103.6	0.0652	
188	0629.0	25.85	22.11	70	220.2	216.0	103.8	0.0638	
189	0629.7	26.04	21.47	70	220.4	215.9	104.0	0.0620	
190	0630.4	26.20	20.94	70	220.5	215.9	104.2	0.0604	
191	0631.1	26.36	20.43	70	220.7	215.8	104.4	0.0590	
192	0631.8	26.53	19.90	70	220.9	215.8	104.6	0.0574	
193	0632.5	26.69	19.41	70	221.1	215.7	104.8	0.0560	
194	0633.2	26.85	18.93	70	221.3	215.6	104.9	0.0546	
195	0634.0	27.04	18.38	70	221.5	215.5	105.1	0.0530	
196	0634.7	27.20	17.93	70	221.8	215.5	105.3	0.0518	
197	0635.4	27.36	17.49	70	222.1	215.4	105.4	0.0505	
198	0636.1	27.52	17.06	70	222.5	215.3	105.5	0.0492	
199	0636.8	27.69	16.61	70	222.9	215.2	105.7	0.0479	
200	0637.5	27.85	16.21	70	223.3	215.2	105.9	0.0468	
201	0638.2	28.01	15.82	70	223.6	215.1	106.1	0.0457	
202	0638.9	28.17	15.44	70	224.0	215.1	106.3	0.0446	
203	0639.6	28.34	15.05	70	224.5	215.0	106.5	0.0434	
204	0640.3	28.50	14.69	70	225.0	215.0	106.6	0.0424	
205	0641.1	28.68	14.29	70	225.5	214.9	106.8	0.0412	
206	0641.8	28.85	13.93	70	226.0	214.8	106.9	0.0402	
207	0642.5	29.01	13.60	70	226.4	214.8	107.1	0.0392	
208	0643.2	29.17	13.28	70	226.8	214.7	107.3	0.0383	
209	0643.9	29.33	12.96	70	227.3	214.7	107.4	0.0374	
210	0644.6	29.50	12.64	70	227.8	214.6	107.5	0.0365	
211	0645.3	29.67	12.32	70	228.3	214.6	107.6	0.0356	
212	0646.0	29.85	11.99	70	228.8	214.5	107.8	0.0346	
213	0646.7	30.04	11.66	70	229.3	214.4	107.9	0.0336	
214	0647.4	30.22	11.35	70	229.8	214.4	108.0	0.0328	
215	0648.2	30.40	11.05	70	230.3	214.4	108.1	0.0319	

Table II. Atmospheric and Instrument Parameters for 29 April 1976. (Continued)

Rec. No.	Time (ADT)	Altitude (km)	Pressure (mb)	Zenith Angle (°)	Air Temp. (K)	Skin Temp. (K)	Window Temp. (K)	Air Mass (atm)	Dew Point (K)
216	0648.9	30.50	10.88	70	230.6	214.4	108.2	0.0314	
217	0649.6	30.60	10.72	70	230.9	214.3	108.3	0.0309	
218	0650.3	30.72	10.53	70	231.2	214.3	108.3	0.0304	
219	0651.0	30.88	10.29	70	231.7	214.3	108.4	0.0297	
220	0651.7	31.03	10.06	70	232.1	214.2	108.4	0.0290	
221	0652.4	31.16	9.87	70	232.4	214.2	108.4	0.0285	
222	0653.1	31.29	9.68	70	232.8	214.2	108.3	0.0279	
223	0653.8	31.38	9.55	70	233.1	214.1	108.2	0.0276	
224	0654.6	31.51	9.37	70	233.4	214.0	108.0	0.0270	
225	0655.3	31.65	9.18	70	233.8	214.1	107.8	0.0265	
226	0656.0	31.83	8.94	70	234.3	214.0	107.6	0.0258	
227	0656.7	31.99	8.73	70	234.8	214.0	107.4	0.0252	
228	0657.4	32.13	8.55	70	235.2	213.9	107.1	0.0247	
229	0658.1	32.22	8.44	70	235.4	213.9	106.9	0.0244	
230	0658.8	32.30	8.34	70	235.6	213.8	106.6	0.0241	
231	0659.5	32.37	8.26	70	235.8	213.8	106.3	0.0238	
232	0700.2	32.45	8.16	70	236.1	213.7	105.9	0.0236	
233	0700.9	32.53	8.07	70	236.3	213.7	105.5	0.0233	
234	0701.7	32.68	7.89	70	236.7	213.7	105.2	0.0228	
235	0702.4	32.88	7.66	70	237.3	213.7	104.8	0.0221	
236	0703.1	33.03	7.50	70	237.7	213.6	104.4	0.0216	
237	0703.8	33.17	7.35	70	238.1	213.6	103.9	0.0212	
238	0704.5	33.26	7.25	70	238.3	213.6	103.3	0.0209	
239	0705.2	33.36	7.15	70	238.6	213.6	102.7	0.0206	
240	0705.9	33.50	7.00	70	239.0	213.6	102.1	0.0202	
241	0706.6	33.70	6.80	70	239.6	213.5	101.5	0.0196	
242	0707.3	33.86	6.65	70	240.0	213.5	101.1	0.0192	
243	0708.0	33.99	6.52	70	240.4	213.5	100.7	0.0188	
244	0708.8	34.09	6.43	70	240.7	213.5	100.3	0.0186	
245	0709.5	34.16	6.36	70	240.8	213.4	99.7	0.0184	
246	0710.2	34.26	6.27	70/85	241.1	213.4	99.2		
247	0710.9	34.39	6.15	85	241.5	213.3	98.5	0.070	
248	0711.6	34.52	6.04	85	241.9	213.3	97.9	0.069	
249	0712.3	34.63	5.95	85	242.2	213.3	97.3	0.068	
250	0713.0	34.70	5.89	85	242.4	213.2	96.7	0.067	
251	0713.7	34.78	5.82	85	242.6	213.2	95.9	0.066	
252	0714.4	34.86	5.75	85	242.8	213.2	95.2	0.065	
253	0715.1	34.95	5.68	85	243.1	213.2	94.5	0.064	
254	0715.9	35.07	5.58	85	243.4	213.2	94.0	0.063	
255	0716.6	35.16	5.51	85	243.6	213.1	93.2	0.063	
256	0717.3	35.24	5.45	85	243.9	213.1	92.4	0.062	
257	0718.0	35.29	5.41	85	244.0	213.1	91.7	0.062	
258	0718.7	35.32	5.38	85	244.1	213.1	91.0	0.061	
259	0719.4	35.36	5.35	85	244.2	213.2	90.1	0.061	
260	0720.1	35.45	5.28	85/90.5	244.5	213.3	89.6		

Table II. Atmospheric and Instrument Parameters for 29 April 1976. (Continued)

Rec. No.	Time (ADT)	Altitude (km)	Pressure (mb)	Zenith Angle (°)	Air Temp. (K)	Skin Temp. (K)	Window Temp. (K)	Air Mass (atm)	Dew Point (K)
261	0720.8	35.59	5.18	90.5	244.9	213.4	89.2	0.272	
262	0721.5	35.74	5.07	90.5	245.3	213.6	88.9	0.266	
263	0722.2	35.88	4.97	90.5	245.7	213.7	88.6	0.260	
264	0723.0	35.98	4.90	90.5	245.9	213.9	88.4	0.256	
265	0723.7	36.02	4.87	90.5	246.1	214.1	88.2	0.254	
266	0724.4	36.05	4.85	90.5	246.1	214.3	88.1	0.253	
267	0725.1	36.11	4.81	90.5/93.5	246.3	214.5	88.0		
268	0725.8	36.21	4.74	93.5	246.6	214.8	87.9	2.394	
269	0726.5	36.31	4.67	93.5	246.9	215.0	87.9	2.358	
270	0727.2	36.38	4.63	93.5	247.1	215.2	87.9	2.333	
271	0727.9	36.43	4.59	93.5	247.2	215.4	88.0	2.315	
272	0728.6	36.48	4.56	93.5	247.3	215.8	88.0	2.298	
273	0729.3	36.54	4.52	93.5	247.5	216.0	88.0	2.276	
274	0730.1	36.62	4.47	93.5/47	247.7	216.2	88.1		Long Scan
275	0733.1	36.82	4.35	47	248.3	216.9	88.2	0.0063	Long Scan
276	0735.9	37.07	4.20	47	249.0	217.4	88.2	0.0061	Long Scan
277	0738.7	37.32	4.05	47	249.7	218.0	88.3	0.0059	Long Scan
278	0741.5	37.56	3.92	47	250.4	218.6	88.4	0.0057	
279	0742.2	37.56	3.92	47	250.4	218.9	88.5	0.0057	
280	0742.9	37.56	3.92	47	250.4	219.0	88.6	0.0057	
281	0743.7	37.56	3.92	47	250.4	219.2	88.6	0.0057	
282	0744.4	37.56	3.92	47	250.4	219.4	88.7	0.0057	
283	0745.1	37.56	3.92	47	250.4	219.6	88.8	0.0057	
284	0745.8	37.56	3.92	47	250.4	219.8	88.9	0.0057	
285	0746.5	37.56	3.92	47	250.4	220.0	89.0	0.0057	
286	0747.2	37.56	3.92	47	250.4	220.2	89.0	0.0057	
287	0747.9	37.56	3.92	47	250.4	220.4	89.1	0.0057	
288	0748.6	37.56	3.92	47	250.4	220.6	89.2	0.0057	
289	0749.3	37.56	3.92	47	250.4	220.8	89.2	0.0057	
290	0750.0	37.56	3.92	47	250.4	221.1	89.3	0.0057	
291	0750.7	37.56	3.92	47	250.4	221.2	89.4	0.0057	
292	0751.5	37.56	3.92	47	250.4	221.5	89.5	0.0057	
293	0752.2	37.56	3.92	47	250.4	221.7	89.6	0.0057	
294	0752.9	37.56	3.92	47	250.4	221.9	89.7	0.0057	
295	0753.6	37.56	3.92	47	250.4	221.1	89.8	0.0057	
296	0754.3	37.56	3.92	47	250.4	222.4	89.8	0.0057	
297	0755.0	37.56	3.92	47	250.4	222.6	89.9	0.0057	
298	0755.7	37.56	3.92	47	250.4	222.8	90.0	0.0057	
299	0756.4	37.56	3.92	47	250.4	223.1	90.1	0.0057	
300	0757.1	37.56	3.92	47	250.4	223.3	90.2	0.0057	
301	0757.8	37.56	3.92	47	250.4	223.6	90.3	0.0057	
302	0758.6	37.56	3.92	47	250.4	223.9	90.4	0.0057	
303	0759.3	37.56	3.92	47	250.4	224.1	90.5	0.0057	
304	0800.0	37.56	3.92	47	250.4	224.3	90.6	0.0057	
305	0800.7	37.56	3.92	47	250.4	224.5	90.7	0.0057	

Table II. Atmospheric and Instrument Parameters for 29 April 1976. (Continued)

Rec. No.	Time (ADT)	Altitude (km)	Pressure (mb)	Zenith Angle (°)	Air Temp. (K)	Skin Temp. (K)	Window Temp. (K)	Air Mass (atm)	Dew Point (K)
306	0801.4	37.56	3.92	47	250.4	224.7	90.8	0.0057	
307	0802.1	37.56	3.92	47	250.4	224.9	90.9	0.0057	
308	0802.8	37.56	3.92	47	250.4	225.1	90.9	0.0057	
309	0803.5	37.56	3.92	47	250.4	225.3	91.0	0.0057	
310	0804.2	37.56	3.92	47	250.4	225.5	91.1	0.0057	
311	0804.9	37.56	3.92	47	250.4	225.7	91.1	0.0057	
312	0805.7	37.56	3.92	47	250.4	226.0	91.2	0.0057	
313	0806.4	37.56	3.92	47	250.4	226.2	91.2	0.0057	
314	0807.1	37.56	3.92	47	250.4	226.5	91.3	0.0057	
315	0807.8	37.56	3.92	47	250.4	226.7	91.4	0.0057	
316	0808.5	37.56	3.92	47	250.4	227.0	91.5	0.0057	
317	0809.2	37.56	3.92	47	250.4	227.3	91.5	0.0057	
318	0809.9	37.56	3.92	47	250.4	227.5	91.6	0.0057	
319	0810.6	37.56	3.92	47	250.4	227.8	91.6	0.0057	
320	0811.3	37.56	3.92	47	250.4	228.0	91.7	0.0057	
321	0812.0	37.56	3.92	47	250.4	228.3	91.8	0.0057	
322	0812.8	37.56	3.92	47	250.4	228.5	91.8	0.0057	
323	0813.5	37.56	3.92	47	250.4	228.8	91.9	0.0057	
324	0814.2	37.56	3.92	47	250.4	229.0	92.0	0.0057	
325	0814.9	37.56	3.92	47	250.4	229.3	92.1	0.0057	
326	0815.6	37.56	3.92	47	250.4	229.6	92.2	0.0057	
327	0816.3	37.56	3.92	47	250.4	229.8	92.2	0.0057	
328	0817.0	37.56	3.92	47	250.4	230.1	92.3	0.0057	
329	0817.7	37.56	3.92	47	250.4	230.3	92.4	0.0057	
330	0818.4	37.56	3.92	47	250.4	230.6	92.5	0.0057	
331	0819.1	37.56	3.92	47	250.4	230.8	92.5	0.0057	
332	0819.9	37.56	3.92	47	250.4	231.1	92.6	0.0057	
333	0820.6	37.56	3.92	47	250.4	231.4	92.6	0.0057	
334	0821.3	37.56	3.92	47	250.4	231.6	92.7	0.0057	
335	0822.0	37.56	3.92	47	250.4	231.8	92.7	0.0057	
336	0822.7	37.56	3.92	47	250.4	232.1	92.8	0.0057	
337	0823.4	37.56	3.92	47	250.4	232.3	92.9	0.0057	
338	0824.1	37.56	3.92	47	250.4	232.6	92.9	0.0057	
339	0824.8	37.56	3.92	47	250.4	232.8	93.0	0.0057	
340	0825.5	37.56	3.92	47	250.4	233.1	93.0	0.0057	
341	0826.2	37.56	3.92	47	250.4	233.4	93.1	0.0057	
342	0827.0	37.56	3.92	47	250.4	233.6	93.2	0.0057	
343	0827.7	37.56	3.92	47	250.4	233.9	93.2	0.0057	
344	0828.5	37.56	3.92	47	250.4	234.1	93.3	0.0057	
345	0829.1	37.56	3.92	47	250.4	234.4	93.3	0.0057	
346	0829.8	37.56	3.92	47	250.4	234.6	93.4	0.0057	
347	0830.5	37.56	3.92	47	250.4	234.8	93.4	0.0057	
348	0831.2	37.56	3.92	47	250.4	235.1	93.5	0.0057	
349	0831.9	37.56	3.92	47	250.4	235.3	93.5	0.0057	
350	0832.6	37.56	3.92	47	250.4	235.6	93.6	0.0057	

Table II. Atmospheric and Instrument Parameters for 29 April 1976. (Continued)

Rec. No.	Time (ADT)	Altitude (km)	Pressure (mb)	Zenith Angle (°)	Air Temp. (K)	Skin Temp. (K)	Window Temp. (K)	Air Mass (atm)	Dew Point (K)
351	0833.3	37.56	3.92	47	250.4	235.8	93.6	0.0057	
352	0834.0	37.56	3.92	47	250.4	236.1	93.6	0.0057	
353	0834.8	37.56	3.92	47	250.4	236.4	93.7	0.0057	
354	0835.5	37.56	3.92	47	250.4	236.7	93.7	0.0057	
355	0836.2	37.56	3.92	47	250.4	237.1	93.7	0.0057	
356	0836.9	37.56	3.92	47	250.4	237.4	93.7	0.0057	
357	0837.6	37.56	3.92	47	250.4	237.8	93.8	0.0057	
358	0838.3	37.56	3.92	47	250.4	238.1	93.8	0.0057	
359	0839.0	37.56	3.92	47	250.4	238.4	93.8	0.0057	
360	0839.7	37.56	3.92	47	250.4	238.8	93.8	0.0057	
361	0840.4	37.56	3.92	47	250.4	239.1	93.8	0.0057	
362	0841.2	37.56	3.92	47	250.4	239.4	93.9	0.0057	
364	0842.6	37.56	3.92	47	250.4	240.0	93.9	0.0057	
365	0843.3	37.56	3.92	47	250.4	240.3	93.9	0.0057	
366	0844.0	37.56	3.92	47	250.4	240.7	93.9	0.0057	
367	0844.7	37.56	3.92	47	250.4	240.8	93.9	0.0057	
368	0845.4	37.56	3.92	47/50	250.4	241.2	94.0		
369	0846.1	37.56	3.92	50	250.4	241.6	94.0	0.0060	
370	0846.8	37.56	3.92	50	250.4	241.8	94.0	0.0060	
371	0847.5	37.56	3.92	50	250.4	242.1	94.0	0.0060	
372	0848.3	37.56	3.92	50/53	250.4	242.4	94.0		
373	0849.0	37.56	3.92	53	250.4	242.7	94.0	0.0064	
374	0849.7	37.56	3.92	53/56	250.4	243.0	94.0		
375	0850.4	37.56	3.92	56	250.4	243.2	94.0	0.0069	
376	0851.1	37.56	3.92	56/70	250.4	243.6	94.0		
377	0851.8	37.56	3.92	70	250.4	243.8	94.0	0.0113	
378	0852.5	37.56	3.92	70	250.4	244.1	94.0	0.0113	
		38.00			251.6				
		39.00			254.4				
		40.00			257.2				
		41.00			260.0				
		42.00			262.8				
		43.00			265.5				
		44.00			268.2				
		45.00			270.9				
		46.00			273.4				
		47.00			276.0				
		48.00			275.2				
		49.00			274.4				
		50.00			273.6				
		51.00			273.2				
		52.00			274.7				
		53.00			273.4				
		54.00			272.0				
		55.00			270.6				
		56.00			269.2				
		57.00			267.8				
		58.00			266.4				
		59.00			265.0				
		60.00			263.6				

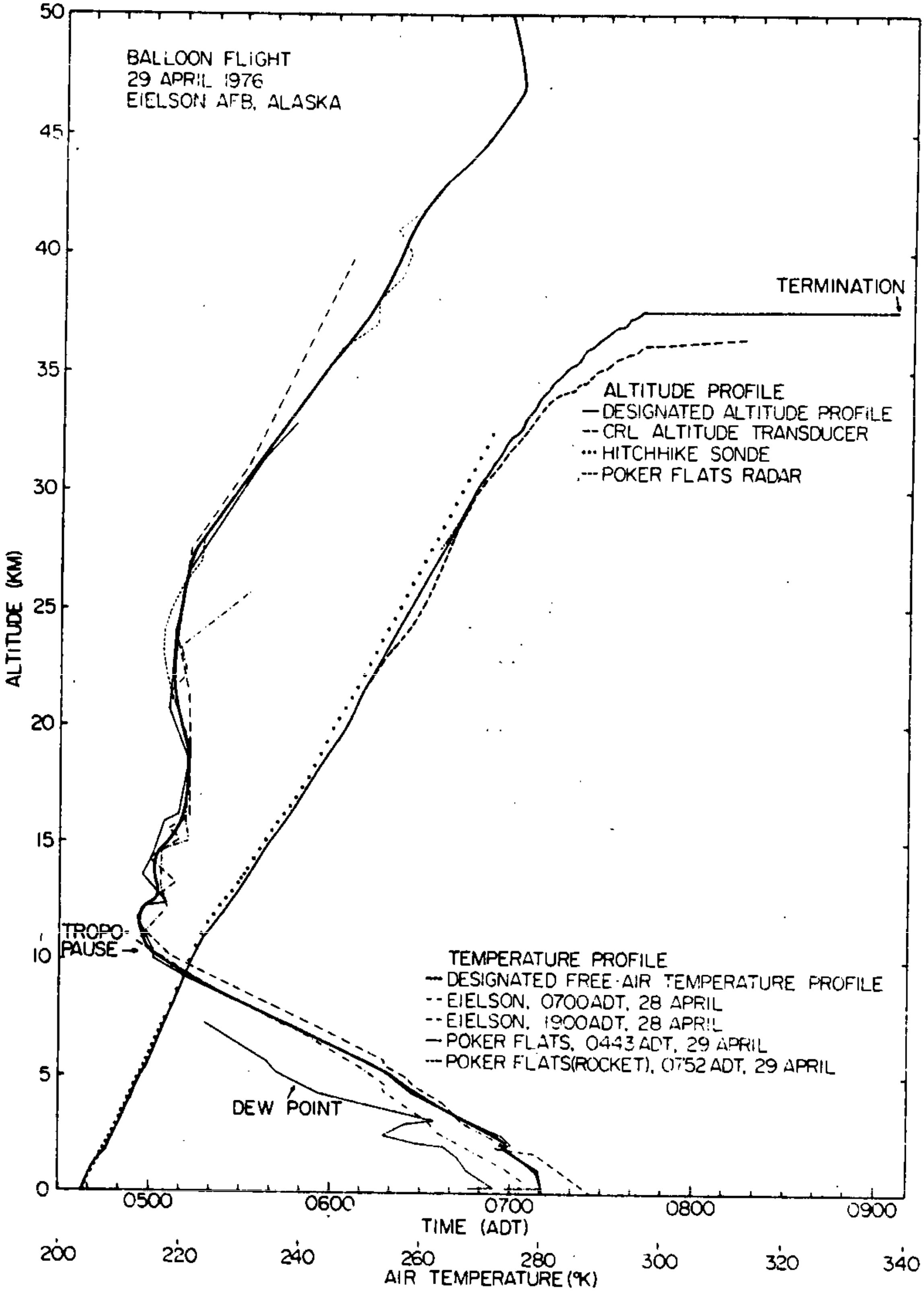

Figure 4. Balloon height profile and atmospheric temperature profile for 29 April 1976.

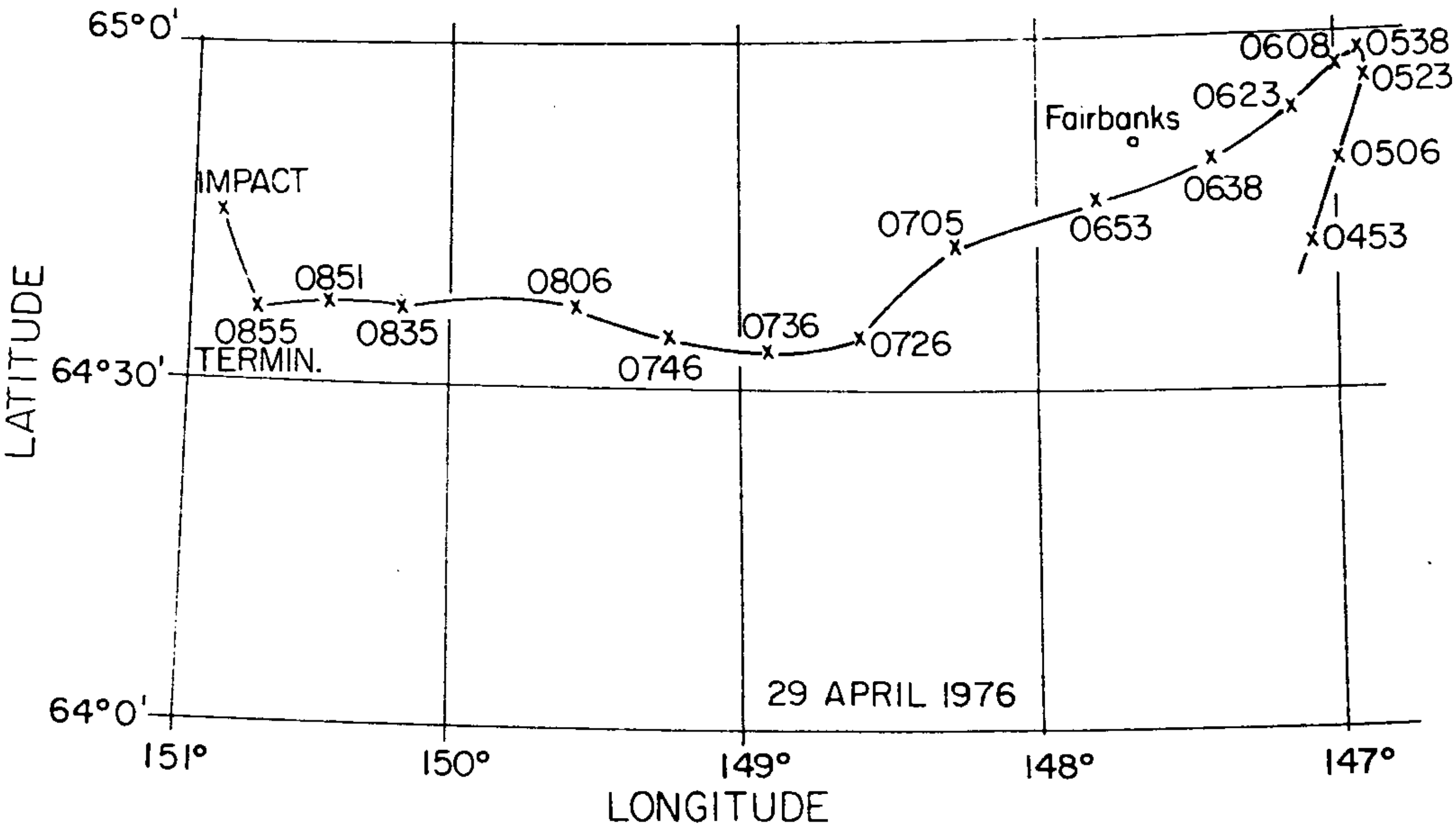

Figure 5. Trajectory for balloon flight of 29 April 1976.

IV. DATA REDUCTION

A. Conversion to Radiance

The purpose of the data reduction process is to numerically reproduce, as faithfully as possible, the incident radiance at the spectrometer window at the time of observation. This requires an accurate instrument calibration and suitable corrections for various instrumentally-induced signals. It also requires some testing of the reduced data to confirm the radiometric accuracy.

The data reduction procedure is similar to that described in the previous report. A wavelength equation is determined from the low altitude flight data based on selected H_2O lines (see Figure 3). Minor linear corrections ($< \pm 1.5\%$) to this equation are determined for each spectral scan based on reference features such as the CO_2 Q-branch at 12.6μm in the 2nd order and numerous H_2O rotational lines in the 1st order. The wavelength equation is, of course, the same for both orders except for a factor of 2. Electrical and optical zeroes are obtained for each spectrum from a region at the beginning of each scan where an optical filter blocks all radiation from the detectors. This point is both an electrical and optical zero since the measured signal is derived only from optically chopped radiation which is referenced to a radiometric zero (4K).

A few voltage spikes induced by the high bias voltage are present in the recorded data. These spikes are removed by a computer program that distinguishes the rapid rise time of the spike from the slower rise time of a spectral resolution element. These spikes normally consist of one or two data points. Substitute

values based on linear smoothing of the edge points are provided. The spectral radiance is then calculated using the calibration factors shown in Figures 1 and 2. This is the total spectral radiance incident at the detector and includes emission and scattering from the KRS5 vacuum window, the only optical element not at LHe temperature.

B. Window Corrections

The corrections for radiant sources associated with the KRS5 window based on the following four assumptions are derived from the flight data. 1) Both the scattering and emissions are gray in nature (i.e., they do not have a spectral dependence for their functional emission or scattering). Thus, if this gray constant is determined at one wavelength, it can be used at all wavelengths and for the entire flight. 2) The temperature associated with the window emission is the measured window temperature. 3) The temperature associated with the scattering varies in a manner similar to the measured skin temperature (which is measured at a point not far from where the scattering probably occurs). The scattered radiation probably comes from surfaces which are at a finite range of temperatures; however, one temperature will be associated with the window scattering for each spectral scan. 4) The atmospheric "window" radiance does not vary at float altitude with either time or azimuth angle. Thus, both time (instrument temperature) and secant caused variations of the window radiance can be used to derive the three necessary constants of emissivity, scattering coefficient, and temperature offset from the measured skin temperature. By using two wavelengths relatively far apart (12 and 24μm), a fairly accurate

determination can be made for the three constants. The 12μm corrections are very sensitive to the scattering term while the 24μm corrections are more sensitive to window temperature.

The data reduction equation takes the following form after the above considerations are empirically met:

$$N = K V - [.0042 \, B(T_s - 55) + .0476 \, B(T_w)] \quad (1)$$

where

N is spectral radiance in w cm^{-2} sr^{-1} μm^{-1},

K is the spectral calibration coefficient,

V is the recorded detector signal,

$B(T_s - 55)$ is the Planck radiance for a temperature 55°K below the measured skin temperature, and

$B(T_w)$ is the Plank radiance for the window temperature.

An earlier correction for this flight of

$$-[.0035 \, B(T_s - 50) + .056 \, B(T_w)]$$

was close to satisfactory, but over-corrected slightly on some scans. The difference in value of these two corrections may represent the absolute uncertainty in the radiance data.

As will be pointed out later, some parts of the ascent data are not quite adequately corrected. The temperature used for the scattering correction implies gradients with possible time lags and these are different during ascent than at float since the skin is primarily cooling during ascent and warming at float. Most of the residual radiance errors are not important for determining constituent

profiles and are only of interest in evaluating atmospheric window radiance for dust layers, etc. The reduced data, radiance vs. wavelength, are stored on magnetic tape and selected portions of this data are presented in the next section.

C. Data Testing

The only possible in-flight test of the data is to compare some of the measured data with known radiance sources. This can be in the form of an in-flight black body, but none were present on this flight. There are some molecular bands in the wavelength range covered on this flight that are optically black under certain viewing conditions. At the lower altitudes where the concentrations are high, the water vapor bands are usually black, and at high altitudes at large zenith angles ($\geq 90^{\circ}$) a number of bands become opaque, such as O_3 and CO_2.

On this flight the 9.6μm O_3 band observed from float altitude at a zenith angle of 93.5° is about 95% black. The optical path is tangent to the limb at 24 km but the peak radiance in the center of the band exceeds the Planck function for the temperature at 24 km. It is equivalent to the Planck radiation from about 30 km. The O_3 band is not as good a test from this altitude as from a lower altitude where the temperature is more nearly constant with altitude and the optical path penetrates more O_3. Nevertheless, this data provides a roughly $\pm$ 10% test of the short wavelength calibration.

A similar test of the long wavelength data was made using a low altitude scan where the center of the H_2O lines were still black. This data was observed at a small zenith angle and because of the low altitude there is a significant temperature gradient above the

height of observation. However, by looking at several black lines and fitting the peak values with a Planck curve, it is apparent that the best fit is for a temperature a few km above the point of observation, indicating an absolute calibration error of $< \pm 10\%$.

V. RADIANCE DATA

The radiance data contained in this report are presented in several formats. In all cases the intention is to provide convenient intercomparison of the observed data at different parametric values. For this report, since the principle result of this flight is constituent height profiles, as much data as possible relating to constituents is included in both tabular and graphical form.

Thirty-four regions were selected within the spectral bandpass of the instrument, each of which has a dominant emitting species or is an atmospheric reference window. These regions are listed in Table III along with the constituent identification. Most of the spectral regions included here are the same as used in the previous report.[1] A few new regions have been added around 11μm and 12μm to better define some of the minor constituents measurable near the tropopause. The spectral radiance from each scan is integrated over these regions and normalized by the spectral band width. These values for all spectral scans are presented in tabular form in Tables IVA, IVB, and V. All of the constituent height profiles in this report were derived using data from these tables.

Selected spectral radiance data are plotted in Figures 6 through 61. The selection is based on showing significant change in the spectral features as a function of either height or zenith angle. The 8 to 13.6μm data are presented in several ways. First, Figures 6 through 20 contain linear radiance plots of representative scans at approximately 0.5 km intervals in observation height. Each figure contains five scans offset from one another for clarity. Because of

the dynamic range of the radiance values in this spectral region, the higher altitude plots do not show much detail in the window areas. A second set of plots with a logarithmic radiance scale are shown in Figures 21 and 22. Again, several scans are shown in each figure with a 1/2 decade offset between successive spectra. Scans were selected at about 2 km intervals and each scan shown is a composite of three co-added spectra. Since the radiance scale is difficult to read in these figures, the individual spectral scans are replotted in Figures 23 through 35. As the balloon neared float altitude the spectrometer was rotated through several zenith angles. Figure 36 shows a composite of representative spectra for five zenith angles at altitudes between 34 and 37.5 km. These spectra have not been offset from one another; the difference in radiance levels is the result of the change in optical path. Each spectrum is a composite average of from 5 to 10 scans.

A number of interesting spectral features were observable in the 10 to 13μm region in the upper troposphere and lower stratosphere. Some of these are analyzed in a later section. To help the reader understand the detail of information available in this region, every spectral scan from 3 to 15 km is shown in Figures 37 through 47. Only the spectral range from 10.3 to 13μm is included to permit an expanded linear radiance scale. Again there are five scans per figure and they are offset for clarity.

The long wavelength region from 18.8 to 27.6μm is shown in Figures 48 through 60, representing approximately 0.5 km height steps. These figures also contain five scans each, which are offset for clarity. A slight residual instrument window emission can be observed in the higher altitude data. This can easily be subtracted

from the constituent data when calculating profiles. A plot similar to Figure 36, showing the zenith angle dependence of the long wavelength radiance, is shown in Figure 61. Here the radiance scale is linear and each scan is offset from the next.

There are a few points relative to the above data that should be noted since they affect the analysis of constituent profiles. The radiance values for each spectral region of Tables IV and V are usually plotted as a function of record number (time) to check the data for consistency, noise and observable errors which would affect the analysis process. Such plots are best made with a specific purpose of analysis in mind and are therefore not included here. There are three features found in these plots which will be discussed here.

At about record 77 (9 km) there is a sharp radiance fall-off in all the data (short and long wavelength) of ~0.5μw cm^{-2} sr^{-1} μm^{-1}. This occurs just below the tropopause (10.3 km) and is probably associated with Cirrus clouds. This feature has made the analysis of the F-11 ($CFCl_3$) and F-12 (CF_2Cl_2) data more difficult, as will be discussed later. The second sudden radiance decline of a similar magnitude occurs only in the long wavelength data near record 118 (15 km). There is no apparent atmospheric reason for this change; although this is very near the point where the minimum instrument window temperature occurs. The measured radiance change represents a 25% change in the window radiance contribution, which is not indicated by the calculated radiance change due to the window (or skin) temperature change over the few records involved. When this effect is removed from the constituent radiance data (i.e. H_2O) at those wavelengths, by subtracting the atmospheric window radiance,

the constituent radiance curves are smooth and no longer show a rapid change near 15 km. It would appear that the change near 9 km is atmospheric and the change near 15 km is instrumental; however, it is possible to postulate other mechanisms for these changes which leaves the question open.

The third feature of interest is the change in radiance of several species as a function of time at float. This should not be the case for uniformly mixed species without diurnal variation. In the time (0736 to 0845 ADT) that the instrument was set at a constant elevation angle at float altitude the following changes were observed: O_3 region 2, slight decrease $<3\%$; O_3 region 3, slight increase $\sim 1.6\%$; CO_2 region 21, slight decrease $< 2\%$; CO_2 region 23, slight increase $\sim 5\%$; H_2O region 28, slight increase $\sim 5\%$. The interpretation of the changes could be many and varied; it can be stated, however, that any change in radiance related to these constituents is small over this period of time. Additional analyses of the radiance data are found in the following section.

Table III. Spectral Regions of Interest

	Wavelength Range	Constituent of Interest
	Short Wavelength Region (see Table IVA)	
1.	8.245- 8.310μm	Window
2.	8.810- 9.020	Ozone
3.	9.740- 9.780	Ozone
4.	10.420-10.425	Minimum
5.	10.480-10.540	CO_2 P-Branch
6.	10.660-10.680	Window
7.	10.740-10.770	F-12 R-Branch
8.	10.820-10.865	F-12 Q-Branch
9.	10.870-11.765	HNO_3 Band
10.	11.035-11.065	HNO_3
11.	11.215-11.315	HNO_3
12.	11.315-11.415	HNO_3 Q-Branch
	Short Wavelength Region (see Table IVB)	
13.	11.415-11.465	HNO_3
14.	11.630-11.655	Minimum
15.	11.725-11.815	F-11
16.	11.960-11.985	Window
17.	12.005-12.070	Unknown
18.	12.175-12.215	Unknown
19.	12.415-12.480	CO_2
20.	12.485-12.585	CCl_4
21.	12.585-12.680	CO_2 Q-Branch
22.	12.680-12.690	CO_2 Edge
23.	13.205-13.265	CO_2

Table III. Spectral Regions of Interest (Continued)

Long Wavelength Region (see Table V)

24.	20.05-20.11	Window
25.	20.75-21.02	HNO_3
26.	24.42-24.46	Window
27.	24.67-24.78	Window
28.	24.78-25.56	H_2O
29.	25.56	Window
30.	25.72-25.76	Window
31.	25.76-26.20	H_2O
32.	26.20	Window
33.	26.37	Window
34.	27.33-27.56	Window

Table IVA. Average Spectral Radiances in Spectral Regions 1-12 (μw cm^{-2} sr^{-1} μm^{-1}). Spectral Regions are in Table III and Pressures, Temperatures and Zenith Angles are in Table II.

Rec. No.	Spectral Region											
	1	2	3	4	5	6	7	8	9	10	11	12
35	71.29	55.19	178.28	39.10	58.32	43.05	44.48	69.54	66.53	50.49	69.05	60.43
36	63.17	51.12	172.97	36.16	54.81	38.93	40.92	65.05	62.34	46.53	62.83	56.23
37	58.47	46.13	164.94	32.84	49.23	35.18	37.99	57.33	59.68	43.09	60.86	53.37
38	55.54	42.14	162.62	28.70	44.69	29.23	32.94	46.82	51.49	34.64	52.85	45.36
39	51.96	39.15	157.68	31.59	44.77	34.90	34.37	50.38	51.31	33.13	51.75	45.47
40	46.88	34.89	150.66	21.40	36.30	27.94	28.71	45.56	46.32	37.78	46.86	40.81
41	42.33	30.50	150.15	18.81	30.76	18.05	19.41	28.96	30.78	17.72	31.63	25.61
42	40.85	29.16	149.06	19.96	30.90	20.65	21.88	28.90	33.27	20.98	34.91	28.67
43	38.05	27.31	143.19	16.25	26.79	16.40	17.45	25.84	27.68	17.60	27.85	24.25
44	37.18	26.01	139.79	17.89	27.25	18.00	18.01	26.42	26.61	19.20	28.15	25.00
45	34.570	22.879	136.95	13.665	22.121	14.283	16.034	21.763	23.669	15.863	23.131	19.937
46	32.379	21.882	133.01	12.554	20.376	14.326	14.676	19.615	21.125	13.592	21.526	17.936
47	28.772	19.817	129.37	10.981	17.692	12.453	12.726	17.128	16.556	11.631	17.697	16.001
48	26.745	18.606	126.78	10.337	15.975	12.257	12.286	14.934	16.418	10.245	15.760	14.013
49	24.107	16.557	123.42	8.509	13.609	9.376	9.776	12.686	12.925	8.628	12.125	11.176
50	21.004	16.251	118.43	8.377	12.103	9.996	9.447	11.969	12.264	8.707	12.458	10.799
51	19.220	14.448	116.43	7.998	11.244	8.231	9.253	11.046	11.024	9.060	11.163	9.110
52	17.274	13.781	114.36	6.807	9.336	6.671	7.122	8.464	8.940	6.992	9.273	7.919
53	14.724	12.980	115.24	6.302	8.396	6.530	6.465	7.806	7.564	6.630	7.425	7.056
54	12.535	11.995	114.51	5.335	7.277	6.024	5.931	6.197	6.802	6.008	6.652	6.407
55	11.624	11.414	111.70	4.965	6.862	5.747	5.723	6.093	6.250	5.786	6.431	6.141
56	9.520	10.972	110.39	4.693	6.335	5.133	5.148	5.561	5.495	4.376	5.729	5.355
57	7.951	10.410	108.44	4.847	6.455	4.998	5.340	5.738	5.716	5.248	5.536	5.298
58	7.199	10.353	104.52	5.531	6.931	5.688	6.065	6.297	6.330	5.952	6.166	6.116
59	5.385	9.620	101.94	4.874	6.102	5.085	5.484	5.922	5.662	5.311	5.757	5.442
60	4.452	8.929	98.80	4.454	5.428	4.708	5.123	5.561	5.599	5.151	5.693	5.346
61	3.386	8.139	99.74	2.973	3.975	3.262	3.624	4.091	4.322	3.870	4.656	4.314
62	2.620	7.586	98.33	2.927	3.781	3.055	3.601	4.096	4.568	4.130	4.086	4.571
63	2.985	7.629	96.04	3.250	3.873	3.319	3.668	4.219	4.566	4.343	4.639	4.656
64	3.053	7.027	94.90	2.586	3.133	2.606	2.903	3.268	3.660	3.496	4.261	4.057
65	2.382	6.954	93.15	2.514	2.976	2.463	2.776	3.223	3.751	3.417	4.226	3.930
66	2.029	7.019	91.69	2.831	3.419	2.986	3.468	3.792	4.456	4.141	4.679	4.654
67	2.304	7.027	90.03	2.998	3.439	2.930	3.292	3.627	4.171	3.976	4.582	4.411
68	1.756	6.599	88.53	2.413	2.704	2.317	2.614	3.016	3.740	3.524	4.274	4.025
69	1.812	6.104	87.62	2.150	2.444	2.031	2.345	2.655	3.504	3.231	4.066	3.955
70	1.685	5.830	86.96	2.062	2.374	1.964	2.284	2.577	3.478	3.235	4.090	3.669
71	1.601	5.628	86.02	1.876	2.137	1.728	1.991	2.305	3.249	2.968	3.885	3.694
72	1.402	5.224	85.36	1.691	1.925	1.590	1.796	2.062	3.046	2.770	3.718	3.536
73	1.183	5.034	84.72	1.685	1.863	1.510	1.721	1.969	2.997	2.736	3.659	3.460
74	1.236	4.998	84.19	1.581	1.771	1.387	1.617	1.860	2.868	2.603	3.545	3.335
75	1.260	4.882	83.58	1.399	1.585	1.215	1.465	1.663	2.731	2.459	3.410	3.227
76	1.053	4.627	82.87	1.320	1.472	1.133	1.317	1.509	2.622	2.318	3.321	3.160
77	.916	4.535	82.73	1.238	1.403	1.070	1.245	1.404	2.489	2.191	3.196	3.012
78	.623	3.999	81.74	.624	.768	.422	.559	.690	1.729	1.363	2.411	2.277
79	.393	3.742	81.93	.364	.555	.267	.381	.491	1.512	1.126	2.196	2.076
80	.348	3.600	81.19	.358	.486	.175	.301	.396	1.434	1.056	2.160	2.010
81	.349	3.597	80.42	.353	.465	.189	.236	.368	1.433	1.049	2.157	2.026
82	.499	3.673	81.04	.335	.456	.196	.277	.397	1.427	1.107	2.131	2.015
83	.396	3.544	80.33	.369	.446	.185	.286	.365	1.413	1.066	2.122	2.001
84	.210	3.532	80.85	.337	.449	.203	.232	.354	1.373	1.051	2.086	1.983

Table IVB. Average Spectral Radiances in Spectral Regions 13-23 ($\mu w\ cm^{-2}\ sr^{-1} \mu m^{-1}$). Spectral Regions are in Table III and Pressures, Temperatures and Zenith Angles are in Table II.

Rec. No.	Spectral Region 13	14	15	16	17	18	19	20	21	22	23
35	63.83	63.12	108.41	92.03	113.63	96.66	152.65	238.78	179.17	84.80	374.48
36	53.63	54.72	99.93	79.41	100.28	81.14	138.10	218.66	166.07	77.29	349.24
37	53.85	54.57	89.56	70.99	97.58	78.11	123.72	205.24	146.92	69.47	319.84
38	50.75	50.76	75.36	66.31	94.66	80.83	112.49	185.16	128.43	67.05	290.23
39	46.77	47.92	76.23	57.11	80.41	66.27	103.43	170.83	120.84	54.69	279.20
40	42.75	40.35	66.16	51.16	71.66	56.22	88.01	153.12	108.87	49.73	256.93
41	30.65	29.44	49.95	38.37	63.82	51.17	79.47	139.9[illegible]	94.29	43.82	235.85
42	33.25	32.47	49.38	42.19	67.76	52.17	75.58	129.57	87.18	43.47	219.01
43	27.83	25.87	43.56	34.64	55.45	43.68	66.44	119.46	82.33	36.59	211.35
44	27.85	28.10	44.67	35.83	54.54	41.81	59.68	110.14	77.13	34.23	193.20
45	24.957	24.629	38.595	29.306	47.652	37.820	53.282	95.993	66.253	30.246	176.05
46	21.167	20.697	33.139	26.954	42.848	33.636	48.696	86.74[illegible]	[illegible]	27.742	162.49
47	18.884	18.385	30.516	25.299	36.889	29.804	41.417	76.165	53.635	24.676	146.39
48	16.761	17.736	25.893	20.125	32.693	25.666	36.223	65.406	46.470	21.430	129.16
49	12.873	12.438	21.870	19.653	28.083	21.947	31.573	57.462	44.377	20.243	120.36
50	11.530	11.321	20.523	16.628	23.007	18.160	24.393	47.037	37.874	15.506	138.91
51	10.539	10.134	16.765	13.473	20.744	16.935	21.398	40.337	33.392	15.292	96.36
52	8.345	8.152	14.087	11.627	17.532	13.046	17.213	33.076	30.235	14.543	88.45
53	7.066	6.847	11.800	10.096	14.385	11.758	14.168	25.499	25.884	11.221	79.75
54	6.457	6.395	10.155	8.488	12.460	10.035	11.713	20.642	21.923	10.632	66.73
55	6.117	5.788	8.565	7.713	11.147	9.550	11.093	17.438	20.257	9.896	62.89
56	5.142	4.910	7.125	7.328	9.225	9.094	10.454	15.306	19.044	9.438	55.22
57	5.339	5.626	7.644	7.961	9.823	9.455	10.792	16.812	19.678	10.567	55.08
58	6.017	5.958	8.364	7.927	10.304	9.212	10.437	15.400	16.105	9.241	54.32
59	5.287	5.070	7.368	7.314	9.086	8.686	9.648	14.554	17.553	9.047	48.30
60	5.466	5.410	7.113	7.489	8.328	8.492	9.746	14.047	15.900	8.924	41.40
61	4.168	3.762	5.732	4.989	6.670	6.069	6.817	11.272	14.397	6.882	39.79
62	4.506	4.062	6.014	5.328	6.896	6.444	7.260	11.249	14.211	7.230	38.85
63	4.383	3.974	5.732	5.066	6.326	5.677	6.420	10.015	13.151	6.660	36.16
64	3.757	3.183	4.757	3.943	5.246	4.744	5.595	8.935	11.946	6.200	33.72
65	3.723	3.150	4.526	3.805	4.907	4.551	5.219	8.266	10.953	5.802	31.74
66	4.368	3.881	5.192	4.660	5.635	5.366	6.029	8.622	11.357	6.605	30.91
67	4.091	3.481	4.753	4.221	4.969	4.849	5.720	8.113	10.641	6.106	29.78
68	3.689	3.133	4.200	3.627	4.554	4.316	4.876	6.945	9.453	5.431	27.68
69	3.514	2.856	3.830	3.247	3.980	3.852	4.401	6.359	8.868	5.070	25.78
70	3.500	2.844	3.722	3.161	3.860	3.741	4.314	5.987	8.484	4.872	25.13
71	3.339	2.624	3.383	2.802	3.455	3.322	3.709	5.215	7.747	4.402	23.54
72	3.154	2.389	3.066	2.543	3.089	3.008	3.473	4.761	7.120	4.095	22.27
73	3.109	2.398	2.966	2.537	2.993	2.873	3.357	4.520	6.833	4.006	21.40
74	3.005	2.242	2.783	2.361	2.788	2.672	3.130	4.215	6.476	3.790	20.57
75	2.878	2.123	2.622	2.160	2.555	2.475	2.805	3.739	5.939	3.470	19.61
76	2.797	1.998	2.441	2.044	2.382	2.277	2.487	3.336	5.458	3.153	19.36
77	2.669	1.863	2.227	1.796	2.094	1.960	2.174	2.626	4.841	2.734	17.71
78	1.951	1.146	1.462	1.069	1.263	1.052	1.186	1.714	3.559	1.742	16.53
79	1.731	.964	1.253	.841	1.070	.900	1.016	1.509	3.289	1.587	15.49
80	1.646	.924	1.117	.747	.942	.812	.884	1.324	2.979	1.377	15.15
81	1.658	.866	1.073	.685	.909	.720	.875	1.259	2.924	1.460	14.91
82	1.651	.848	1.047	.677	.878	.744	.869	1.228	2.851	1.452	14.45
83	1.639	.894	1.011	.664	.861	.690	.817	1.196	2.777	1.326	13.84
84	1.603	.823	.942	.685	.804	.667	.818	1.147	2.688	1.346	14.03

Table IVA. Average Spectral Radiances in Spectral Regions 1-12 ($\mu w\ cm^{-2}\ sr^{-1}\ \mu m^{-1}$). Spectral Regions are in Table III and Pressures, Temperatures and Zenith Angles are in Table II. (Continued)

Rec. No.	Spectral Region 1	2	3	4	5	6	7	8	9	10	11	12
85	.340	3.448	80.48	.344	.440	.154	.207	.318	1.330	1.007	2.005	1.905
86	.332	3.485	80.22	.351	.405	.150	.224	.279	1.276	.901	1.953	1.937
87	.314	3.542	79.39	.309	.406	.185	.223	.274	1.297	.973	1.982	1.964
88	.116	3.441	79.12	.378	.408	.160	.211	.265	1.289	.948	1.970	1.901
89	.380	3.430	79.07	.314	.403	.150	.211	.207	1.268	.955	1.952	1.899
90	.283	3.458	78.61	.256	.386	.159	.174	.250	1.244	.925	1.875	1.854
91	.248	3.432	78.39	.269	.385	.105	.182	.243	1.229	.888	1.905	1.833
92	.169	3.376	78.05	.281	.364	.149	.151	.227	1.205	.901	1.874	1.773
93	.340	3.312	77.61	.267	.365	.127	.175	.204	1.200	.879	1.852	1.806
94	.349	3.402	78.28	.280	.364	.094	.113	.231	1.227	.946	1.908	1.865
95	.288	3.328	76.77	.260	.345	.167	.131	.200	1.161	.903	1.793	1.771
96	.285	3.320	77.10	.242	.329	.114	.115	.194	1.153	.873	1.780	1.749
97	.247	3.293	76.78	.302	.357	.163	.101	.181	1.141	.882	1.772	1.730
98	.340	3.255	76.62	.257	.353	.087	.153	.207	1.126	.856	1.745	1.732
99	.259	3.297	76.74	.248	.352	.113	.138	.189	1.139	.829	1.772	1.719
100	.279	3.215	76.11	.286	.341	.130	.128	.162	1.132	.881	1.743	1.731
101	.227	3.190	75.67	.221	.331	.140	.134	.182	1.112	.860	1.732	1.712
102	.226	3.196	75.60	.298	.307	.141	.115	.164	1.116	.872	1.741	1.729
103	.176	3.181	75.24	.357	.324	.145	.095	.158	1.109	.879	1.725	1.716
104	.325	3.240	74.83	.316	.308	.073	.100	.114	1.074	.794	1.685	1.690
105	.393	3.210	74.91	.226	.316	.053	.103	.153	1.074	.801	1.676	1.681
106	.242	3.231	74.66	.219	.301	.098	.096	.131	1.074	.785	1.676	1.686
107	.230	3.184	74.88	.261	.290	.152	.104	.139	1.059	.819	1.651	1.635
108	.224	3.141	74.66	.305	.312	.127	.107	.152	1.058	.825	1.651	1.646
109	.158	3.099	74.07	.290	.283	.092	.091	.092	1.041	.804	1.638	1.621
110	.290	3.151	74.45	.239	.300	.104	.085	.136	1.054	.813	1.674	1.632
111	.221	3.150	74.26	.240	.298	.113	.062	.102	1.020	.790	1.583	1.606
112	.274	3.171	74.61	.209	.290	.062	.066	.107	1.036	.784	1.631	1.648
113	.191	3.160	74.08	.240	.286	.085	.049	.122	1.005	.778	1.590	1.576
114	.208	3.141	74.13	.265	.279	.106	.097	.106	1.015	.744	1.585	1.590
115	.214	3.089	73.88	.231	.286	.071	.064	.116	.969	.724	1.553	1.508
116	.153	3.074	74.55	.282	.288	.079	.063	.110	.960	.740	1.523	1.465
117	.295	3.041	73.67	.167	.287	.043	.066	.086	.939	.712	1.459	1.447
118	.246	2.996	73.06	.199	.278	.085	.064	.096	.915	.656	1.439	1.412
119	.279	2.976	72.50	.315	.272	.084	.031	.084	.901	.716	1.446	1.401
120	.224	2.865	71.88	.269	.266	.083	.066	.077	.877	.679	1.387	1.358
121	.132	2.936	71.75	.214	.263	.067	.076	.080	.864	.640	1.372	1.366
122	.258	2.827	71.61	.267	.259	.061	.044	.064	.832	.603	1.309	1.296
123	.239	2.863	71.57	.215	.262	.089	.020	.102	.819	.614	1.322	1.283
124	.217	2.902	70.98	.227	.254	.077	.035	.089	.814	.622	1.291	1.274
125	.138	2.849	71.28	.169	.266	.130	.420	.077	.811	.614	1.271	1.265
126	.130	2.825	70.87	.125	.359	.090	.053	.066	.783	.597	1.227	1.222
127	.188	2.819	69.57	.279	.245	.084	.034	.091	.752	.569	1.178	1.180
128	.288	2.759	68.46	.221	.242	.023	.058	.065	.738	.591	1.164	1.145
129	.203	2.691	67.93	.206	.226	.043	.059	.079	.718	.508	1.115	1.150
130	.339	2.618	67.02	.175	.246	.096	.032	.065	.712	.570	1.086	1.111
131	.188	2.646	66.00	.171	.258	.033	.023	.095	.707	.544	1.110	1.108
132	.248	2.647	65.38	.232	.235	.057	.065	.080	.684	.478	1.065	1.095
133	.219	2.581	63.98	.262	.227	.048	.038	.067	.651	.509	1.033	1.007
134	.201	2.511	62.82	.185	.239	.060	.020	.094	.633	.511	.992	.984

Table IVB. Average Spectral Radiances in Spectral Regions 13-23 (μw cm^{-2} sr^{-1} μm^{-1}). Spectral Regions are in Table III and Pressures, Temperatures and Zenith Angles are in Table II. (Continued)

Rec. No.	Spectral Region 13	14	15	16	17	18	19	20	21	22	23
85	1.521	.741	.895	.642	.783	.653	.738	1.071	2.662	1.366	13.75
86	1.492	.823	.901	.619	.785	.675	.796	1.097	2.599	1.265	13.58
87	1.531	.786	.864	.539	.759	.584	.705	1.012	2.409	1.096	12.72
88	1.494	.772	.868	.607	.768	.623	.850	1.070	2.468	1.218	12.73
89	1.464	.804	.828	.549	.756	.619	.698	1.024	2.410	1.160	13.25
90	1.477	.796	.841	.555	.721	.639	.758	1.043	2.537	1.168	13.13
91	1.457	.769	.807	.551	.709	.626	.726	1.021	2.394	1.225	12.85
92	1.429	.778	.793	.568	.691	.604	.660	.947	2.309	1.096	12.91
93	1.386	.733	.758	.484	.696	.582	.694	.937	2.276	1.015	12.91
94	1.423	.782	.748	.552	.645	.627	.667	.905	2.272	1.081	12.66
95	1.362	.735	.731	.503	.690	.561	.668	.969	2.235	1.02[illegible]	12.87
96	1.345	.727	.701	.512	.653	.556	.627	.686	2.189	1.102	12.49
97	1.341	.716	.716	.450	.654	.522	.641	.961	2.136	1.020	11.93
98	1.320	.711	.692	.489	.660	.528	.640	.892	2.133	1.118	11.72
99	1.353	.711	.679	.484	.599	.522	.631	.851	2.039	1.071	11.46
100	1.380	.703	.670	.493	.606	.533	.645	.847	2.073	.994	11.57
101	1.296	.708	.654	.455	.614	.508	.630	.825	2.060	.985	11.82
102	1.304	.676	.634	.416	.605	.505	.613	.794	2.036	.938	11.86
103	1.318	.692	.615	.403	.610	.494	.601	.794	1.979	.980	12.08
104	1.249	.711	.595	.411	.550	.477	.552	.799	1.933	.977	11.72
105	1.268	.702	.565	.406	.543	.455	.600	.816	1.975	.984	11.38
106	1.247	.685	.579	.437	.556	.460	.581	.814	1.974	1.065	11.11
107	1.263	.691	.579	.388	.557	.419	.582	.819	1.926	.939	10.91
108	1.254	.696	.553	.400	.548	.458	.597	.776	1.903	.910	11.06
109	1.246	.636	.506	.377	.532	.442	.601	.771	1.857	.946	10.69
110	1.258	.641	.522	.374	.515	.453	.556	.772	1.833	.962	10.48
111	1.215	.673	.510	.380	.518	.443	.578	.767	1.847	.912	10.73
112	1.231	.651	.473	.363	.495	.429	.553	.740	1.733	.909	10.52
113	1.225	.615	.477	.364	.467	.403	.550	.721	1.750	.937	9.99
114	1.221	.649	.473	.354	.472	.412	.544	.746	1.770	.916	10.40
115	1.167	.615	.429	.311	.428	.368	.535	.680	1.691	.842	9.83
116	1.199	.568	.446	.308	.438	.374	.563	.744	1.741	.979	10.07
117	1.149	.585	.443	.354	.435	.346	.554	.721	1.697	.792	9.49
118	1.137	.611	.435	.336	.412	.356	.527	.717	1.654	.901	9.53
119	1.072	.546	.407	.310	.427	.351	.497	.695	1.630	.917	9.16
120	1.059	.494	.405	.313	.409	.342	.499	.663	1.598	.920	9.42
121	1.044	.549	.399	.312	.412	.335	.533	.685	1.594	.774	9.19
122	1.067	.476	.369	.299	.368	.315	.510	.710	1.559	.966	8.82
123	1.016	.479	.373	.282	.428	.324	.465	.630	1.556	.867	8.93
124	1.006	.472	.384	.280	.372	.318	.501	.643	1.546	.905	9.02
125	1.002	.490	.375	.215	.392	.364	.473	.665	1.547	.779	9.34
126	.969	.442	.391	.293	.356	.324	.491	.640	1.512	.746	9.05
127	.949	.545	.369	.276	.367	.323	.517	.631	1.537	.816	8.81
128	.888	.527	.356	.360	.354	.317	.499	.626	1.537	.775	8.54
129	.873	.449	.355	.268	.345	.290	.437	.617	1.511	.767	8.39
130	.898	.439	.320	.226	.335	.303	.455	.636	1.470	.764	8.21
131	.854	.463	.365	.275	.335	.287	.466	.605	1.433	.683	8.23
132	.847	.423	.321	.239	.344	.265	.447	.591	1.433	.723	8.01
133	.765	.435	.312	.274	.302	.266	.407	.592	1.391	.653	7.53
134	.816	.374	.242	.303	.304	.323	.495	.620	1.414	.707	7.65

Table IVA. Average Spectral Radiances in Spectral Regions 1-12 ($\mu w\ cm^{-2}\ sr^{-1}\ \mu m^{-1}$). Spectral Regions are in Table III and Pressures, Temperatures and Zenith Angles are in Table II. (Continued)

Rec. No.	Spectral Region											
	1	2	3	4	5	6	7	8	9	10	11	12
135	.194	2.494	62.24	.228	.224	.101	.039	.061	.627	.500	.966	.969
136	.183	2.479	60.94	.233	.234	.087	.020	.070	.633	.479	.946	.937
137	.180	2.456	60.56	.227	.213	.054	.044	.054	.595	.431	.891	.925
138	.057	2.443	59.59	.184	.213	.103	.054	.068	.561	.447	.871	.876
139	.140	2.376	58.32	.135	.193	.045	.020	.069	.545	.411	.845	.854
140	.221	2.375	58.73	.207	.219	.059	.039	.037	.531	.392	.853	.827
141	.262	2.366	57.50	.236	.218	.053	.024	.066	.534	.415	.851	.834
142	.194	2.304	56.60	.184	.181	.038	.113	.032	.513	.394	.790	.797
143	.176	2.283	56.71	.220	.166	.033	.055	.070	.503	.353	.779	.786
144	.148	2.305	56.57	.202	.180	.089	.023	.041	.494	.387	.749	.745
145	.265	2.325	55.54	.246	.212	.043	.031	.047	.483	.383	.757	.765
146	.460	2.207	54.91	.281	.216	.023	.052	.041	.475	.493	.726	.735
147	.128	2.176	54.10	.181	.219	.124	.048	.037	.449	.356	.695	.704
148	.198	2.207	53.46	.311	.234	.066	.020	.061	.439	.311	.674	.678
151	.255	2.090	51.22	.266	.187	.049	.045	.062	.415	.285	.637	.633
152	.157	2.059	50.89	.220	.189	.055	.039	.041	.403	.304	.613	.631
153	.222	2.041	49.98	.165	.176	.094	.030	.075	.383	.274	.593	.598
154	.212	2.039	48.85	.230	.217	.083	.020	.060	.368	.324	.565	.531
155	.305	1.995	47.99	.173	.162	.096	.039	.050	.357	.302	.555	.526
156	.195	1.899	47.30	.147	.181	.054	.041	.031	.325	.257	.500	.514
157	.209	1.900	45.67	.149	.159	.086	.033	.053	.311	.261	.464	.492
158	.122	1.791	44.82	.115	.169	.074	.042	.039	.300	.269	.456	.457
159	.221	1.805	44.39	.129	.176	.087	.020	.115	.234	.220	.462	.465
160	.119	1.788	43.56	.171	.174	.086	.032	.042	.265	.226	.411	.403
161	.090	1.680	42.80	.133	.147	.072	.026	.039	.249	.217	.385	.390
162	.127	1.686	42.43	.098	.171	.027	.021	.033	.251	.197	.404	.382
163	.126	1.703	43.07	.228	.200	.048	.047	.030	.272	.234	.401	.427
164	.066	1.736	43.22	.226	.182	.123	.083	.026	.245	.160	.371	.388
168	.043	1.650	40.58	.235	.156	.047	.040	.061	.200	.146	.297	.296
169	.100	1.641	39.93	.180	.155	.046	.049	.023	.187	.180	.275	.298
170	.071	1.749	40.93	.342	.144	.068	.029	.030	.221	.170	.330	.362
171	.292	1.817	40.45	.273	.226	.077	.034	.036	.213	.161	.302	.331
172	.303	1.768	39.69	.184	.216	.074	.042	.048	.206	.159	.296	.317
173	.127	2.445	52.02	.320	.315	.111	.026	.061	.326	.283	.468	.482
174	.171	2.474	50.43	.296	.298	.149	.058	.058	.307	.263	.457	.456
175	.269	2.429	50.14	.315	.319	.133	.070	.044	.290	.239	.429	.434
176	.140	2.392	50.37	.367	.313	.094	.040	.042	.264	.193	.387	.402
177	.132	2.365	49.25	.301	.313	.130	.026	.050	.254	.195	.366	.389
178	.159	2.361	48.45	.274	.282	.119	.065	.044	.262	.226	.385	.384
179	.175	2.317	49.32	.342	.297	.105	.062	.038	.234	.185	.338	.364
180	.113	2.329	49.07	.390	.303	.089	.036	.031	.236	.164	.345	.344
181	.113	2.266	47.61	.314	.294	.144	.036	.033	.228	.199	.327	.336
182	.096	2.192	47.14	.322	.273	.121	.066	.041	.222	.170	.314	.327
183	.383	2.296	47.60	.303	.267	.132	.064	.046	.223	.145	.314	.326
184	.159	2.241	47.01	.343	.311	.171	.060	.049	.216	.167	.319	.315
185	.194	2.256	46.52	.286	.316	.139	.062	.052	.209	.173	.298	.302
186	.284	2.149	46.17	.390	.313	.105	.061	.069	.197	.147	.271	.296
187	.142	2.260	46.36	.324	.300	.169	.041	.061	.198	.185	.265	.327
188	.235	2.199	45.93	.342	.320	.131	.088	.056	.195	.127	.266	.277
189	.098	2.110	46.03	.333	.316	.127	.068	.047	.195	.170	.265	.297

Table IVB. Average Spectral Radiances in Spectral Regions 13-23 ($\mu w\ cm^{-2}\ sr^{-1}\ \mu m^{-1}$). Spectral Regions are in Table III and Pressures, Temperatures and Zenith Angles are in Table II. (Continued)

Rec. No.	Spectral Region										
	13	14	15	16	17	18	19	20	21	22	23
135	.783	.402	.291	.271	.286	.325	.439	.600	1.410	.660	7.45
136	.752	.445	.296	.271	.305	.251	.472	.564	1.364	.577	7.35
137	.721	.418	.299	.194	.256	.267	.410	.573	1.377	.686	7.33
138	.698	.317	.262	.175	.296	.180	.424	.551	1.357	.620	6.69
139	.690	.305	.246	.145	.271	.286	.416	.543	1.310	.697	6.85
140	.684	.331	.233	.177	.262	.230	.412	.523	1.328	.556	6.89
141	.659	.364	.248	.178	.251	.202	.407	.546	1.239	.555	6.60
142	.645	.271	.233	.179	.226	.220	.430	.529	1.137	.569	6.43
143	.624	.312	.236	.159	.249	.207	.373	.544	1.232	.659	6.37
144	.612	.327	.224	.215	.256	.237	.384	.545	1.226	.684	6.57
145	.586	.327	.219	.122	.239	.249	.399	.484	1.259	.550	6.45
146	.561	.288	.186	.150	.195	.220	.396	.503	1.175	.548	6.49
147	.572	.301	.206	.209	.249	.185	.356	.497	1.195	.540	6.28
148	.529	.322	.204	.180	.217	.227	.385	.511	1.205	.598	6.02
151	.517	.233	.177	.163	.199	.226	.400	.506	1.061	.542	5.49
152	.533	.262	.175	.147	.184	.217	.392	.496	1.096	.497	5.61
153	.476	.292	.174	.133	.237	.209	.409	.460	1.074	.475	5.57
154	.438	.292	.162	.092	.210	.233	.377	.451	1.064	.493	5.61
155	.423	.249	.186	.144	.212	.170	.358	.419	1.034	.494	5.69
156	.397	.255	.127	.125	.203	.191	.328	.388	1.054	.609	5.42
157	.401	.256	.131	.101	.181	.199	.302	.417	.993	.434	5.11
158	.392	.233	.172	.109	.197	.098	.301	.388	1.003	.521	4.82
159	.363	.226	.127	.128	.164	.153	.308	.426	.993	.500	4.96
160	.318	.197	.137	.065	.181	.126	.229	.393	.970	.411	4.85
161	.310	.202	.102	.147	.161	.136	.261	.413	.901	.441	4.67
162	.317	.210	.101	.073	.137	.154	.310	.39[illegible]	.906	.493	4.75
163	.317	.203	.127	.118	.189	.161	.307	.417	1.004	.507	5.30
164	.318	.161	.166	.142	.143	.138	.315	.419	1.014	.466	5.94
168	.245	.123	.080	.068	.114	.116	.283	.363	.908	.472	4.39
169	.215	.139	.086	.091	.132	.143	.239	.354	.878	.489	4.43
170	.248	.185	.118	.139	.179	.201	.350	.420	.990	.405	4.94
171	.283	.132	.121	.100	.205	.182	.335	.420	.939	.406	4.81
172	.231	.168	.155	.031	.131	.232	.495	.618	1.518	.667	7.51
173	.389	.330	.209	.144	.299	.291	.483	.683	1.576	.784	7.22
174	.384	.240	.178	.239	.265	.269	.503	.688	1.522	.777	6.63
175	.320	.255	.172	.242	.231	.253	.513	.668	1.497	.797	6.67
176	.327	.179	.155	.189	.248	.297	.528	.631	1.482	.751	6.25
177	.311	.224	.155	.156	.257	.253	.484	.646	1.472	.689	6.15
178	.302	.229	.160	.202	.262	.173	.478	.624	1.444	.776	6.24
179	.282	.175	.139	.183	.238	.283	.496	.642	1.466	.726	6.35
180	.297	.227	.160	.170	.214	.259	.526	.598	1.442	.602	6.25
181	.292	.183	.154	.141	.255	.245	.466	.636	1.350	.534	6.14
182	.262	.189	.162	.214	.242	.262	.485	.607	1.342	.750	6.65
183	.276	.182	.158	.196	.245	.244	.457	.616	1.445	.647	6.36
184	.245	.206	.145	.099	.258	.301	.470	.621	1.426	.733	6.11
185	.240	.170	.165	.200	.262	.277	.457	.602	1.423	.944	5.85
186	.240	.157	.152	.171	.234	.318	.478	.593	1.376	.951	6.12
187	.221	.181	.144	.189	.262	.252	.467	.606	1.372	.712	5.91
188	.230	.145	.139	.188	.243	.248	.466	.572	1.352	.640	6.13
189	.232	.178	.148	.173	.242	.262	.578	.570	1.376	.705	5.97

Table IVA. Average Spectral Radiances in Spectral Regions 1-12 ($\mu w\ cm^{-2}\ sr^{-1}\ \mu m^{-1}$). Spectral Regions are in Table III and Pressures, Temperatures and Zenith Angles are in Table II. (Continued)

Rec. No.	Spectral Region 1	2	3	4	5	6	7	8	9	10	11	12
190	.143	2.151	45.38	.370	.269	.107	.049	.054	.167	.133	.212	.225
191	.197	2.093	45.34	.254	.281	.106	.072	.050	.134	.169	.249	.265
192	.060	2.067	45.49	.303	.317	.145	.093	.060	.166	.152	.218	.234
193	.082	2.027	45.03	.311	.273	.111	.032	.040	.175	.154	.247	.258
194	.383	2.007	45.35	.329	.281	.098	.064	.041	.153	.088	.234	.258
195	.127	2.052	45.19	.253	.288	.160	.108	.036	.167	.147	.212	.263
196	.126	1.991	44.78	.300	.305	.150	.059	.071	.174	.119	.233	.245
197	.212	2.049	45.10	.285	.289	.121	.075	.048	.162	.133	.207	.224
198	.176	1.995	44.61	.308	.310	.170	.071	.073	.165	.134	.213	.242
199	.099	2.012	44.55	.276	.292	.150	.076	.063	.149	.133	.214	.175
200	.150	2.027	44.51	.325	.301	.117	.068	.068	.166	.145	.199	.267
201	.077	1.984	44.92	.315	.312	.117	.086	.049	.147	.122	.202	.215
202	.087	1.927	43.33	.421	.308	.143	.053	.063	.154	.139	.193	.217
203	.314	2.067	43.19	.328	.324	.128	.083	.043	.132	.122	.149	.195
204	.075	1.970	43.02	.365	.318	.126	.074	.067	.151	.145	.195	.216
205	.289	1.925	42.07	.341	.281	.148	.068	.066	.153	.186	.190	.198
206	.230	1.902	41.60	.304	.295	.161	.056	.059	.136	.130	.183	.176
207	.181	1.848	40.84	.275	.299	.151	.076	.074	.128	.129	.167	.175
208	.039	1.863	40.34	.340	.324	.141	.125	.089	.134	.115	.182	.139
209	.245	1.853	40.76	.340	.307	.154	.088	.051	.135	.156	.161	.150
210	.163	1.800	39.93	.316	.317	.135	.093	.097	.121	.132	.157	.169
211	.236	1.771	38.67	.296	.336	.138	.094	.048	.120	.112	.158	.142
212	.163	1.782	39.73	.311	.319	.177	.067	.079	.123	.123	.146	.165
213	.232	1.753	39.56	.399	.329	.155	.062	.060	.118	.121	.148	.171
214	.251	1.702	38.08	.350	.304	.096	.072	.070	.113	.106	.138	.163
215	.105	1.694	37.93	.341	.306	.166	.087	.064	.164	.146	.192	.177
216	.099	1.685	37.91	.321	.323	.281	.102	.075	.115	.135	.147	.155
217	.281	1.657	37.79	.325	.306	.033	.105	.068	.102	.086	.130	.137
218	.107	1.629	37.40	.378	.288	.105	.090	.060	.102	.070	.121	.131
219	.363	1.632	37.77	.312	.305	.191	.105	.047	.101	.090	.133	.129
220	.231	1.635	37.24	.391	.299	.106	.085	.070	.100	.114	.124	.145
221	.148	1.642	37.29	.312	.268	.110	.086	.064	.100	.099	.120	.136
222	.175	1.552	36.26	.333	.306	.120	.083	.049	.115	.104	.133	.173
223	.096	1.562	35.93	.301	.297	.161	.072	.046	.099	.116	.135	.136
224	.115	1.549	35.65	.439	.283	.135	.089	.054	.094	.104	.118	.129
225	.088	1.565	35.59	.305	.307	.153	.065	.072	.091	.093	.110	.125
226	.156	1.534	35.67	.288	.291	.131	.105	.066	.030	.119	.102	.128
227	.061	1.585	34.93	.295	.307	.125	.075	.063	.090	.074	.101	.130
228	.108	1.474	34.34	.317	.295	.154	.074	.044	.092	.091	.113	.101
229	.066	1.453	33.97	.321	.286	.170	.057	.057	.095	.110	.118	.108
230	.026	1.415	33.76	.359	.290	.126	.076	.047	.094	.145	.106	.120
231	.110	1.476	33.75	.282	.284	.116	.060	.064	.080	.085	.109	.109
232	.518	1.433	33.74	.328	.288	.149	.047	.057	.093	.110	.120	.106
233	.094	1.450	33.35	.289	.293	.155	.084	.065	.083	.091	.103	.102
234	.130	1.381	32.75	.266	.300	.162	.067	.061	.083	.066	.097	.109
235	.159	1.374	31.94	.305	.289	.139	.068	.053	.078	.092	.094	.109
236	.122	1.331	31.47	.255	.265	.156	.111	.051	.076	.074	.095	.096
237	.080	1.332	31.41	.303	.261	.165	.068	.105	.084	.093	.082	.132
238	.109	1.340	30.95	.273	.294	.160	.080	.048	.074	.100	.072	.086
239	.016	1.251	30.48	.367	.290	.143	.066	.050	.071	.079	.071	.106

Table IVB. Average Spectral Radiances in Spectral Regions 13-23 ($\mu w\ cm^{-2}\ sr^{-1}\ \mu m^{-1}$). Spectral Regions are in Table III and Pressures, Temperatures and Zenith Angles are in Table II. (Continued)

Rec. No.	Spectral Region 13	14	15	16	17	18	19	20	21	22	23
190	.212	.168	.135	.143	.212	.252	.419	.569	1.272	.687	5.78
191	.219	.152	.156	.351	.273	.267	.430	.570	1.334	.631	5.86
192	.201	.156	.149	.165	.259	.283	.410	.512	1.306	.624	5.66
193	.209	.176	.183	.168	.258	.235	.392	.552	1.308	.636	5.18
194	.208	.134	.125	.184	.197	.280	.419	.587	1.336	.591	5.33
195	.188	.129	.135	.156	.246	.242	.418	.547	1.273	.607	5.12
196	.189	.165	.152	.153	.247	.228	.393	.537	1.281	.627	5.33
197	.189	.175	.143	.159	.277	.232	.460	.545	1.276	.596	5.39
198	.182	.163	.148	.188	.239	.239	.388	.550	1.348	.603	5.25
199	.177	.178	.149	.182	.249	.226	.472	.532	1.259	.608	5.37
200	.191	.147	.164	.125	.249	.250	.396	.549	1.339	.645	5.33
201	.163	.130	.153	.151	.234	.216	.398	.513	1.212	.533	5.22
202	.163	.178	.154	.164	.248	.229	.427	.543	1.254	.641	4.97
203	.177	.125	.124	.193	.239	.198	.381	.516	1.213	.572	5.01
204	.153	.148	.148	.160	.246	.248	.414	.518	1.255	.572	4.93
205	.167	.207	.185	.166	.235	.237	.412	.530	1.234	.561	4.89
206	.153	.131	.159	.195	.243	.310	.387	.495	1.188	.586	4.75
207	.141	.116	.156	.174	.242	.177	.362	.403	1.159	.624	4.45
208	.146	.145	.150	.181	.221	.241	.393	.500	1.088	.586	4.68
209	.156	.154	.165	.205	.239	.249	.415	.520	1.194	.604	4.63
210	.140	.125	.144	.080	.236	.222	.384	.500	1.160	.572	4.53
211	.139	.137	.153	.156	.221	.220	.374	.467	1.152	.533	4.70
212	.105	.125	.145	.158	.253	.237	.390	.529	1.150	.580	4.57
213	.113	.138	.157	.137	.231	.244	.349	.498	1.161	.570	4.46
214	.107	.120	.143	.196	.200	.236	.407	.466	1.125	.484	4.41
215	.203	.134	.189	.194	.220	.247	.374	.485	1.146	.535	4.74
216	.125	.135	.168	.199	.213	.236	.352	.443	1.038	.442	4.37
217	.100	.089	.141	.219	.208	.218	.322	.444	1.093	.510	4.20
218	.119	.132	.140	.180	.190	.257	.353	.459	1.092	.551	4.15
219	.102	.104	.132	.168	.203	.229	.351	.442	1.085	.485	4.62
220	.126	.111	.146	.162	.234	.214	.418	.432	1.057	.529	4.12
221	.082	.143	.143	.185	.220	.192	.347	.429	1.048	.465	3.84
222	.154	.154	.120	.152	.200	.195	.366	.422	1.049	.495	3.81
223	.110	.116	.139	.162	.207	.214	.350	.393	1.022	.500	3.95
224	.081	.110	.130	.153	.207	.216	.324	.432	1.053	.491	4.03
225	.107	.095	.119	.160	.210	.226	.365	.455	1.016	.420	3.90
226	.068	.127	.129	.145	.216	.174	.323	.415	1.038	.424	3.99
227	.086	.139	.125	.144	.199	.214	.318	.416	1.026	.428	3.91
228	.085	.106	.134	.165	.183	.195	.323	.410	.976	.450	3.95
229	.088	.097	.117	.155	.202	.147	.295	.399	.981	.504	3.92
230	.090	.063	.172	.220	.232	.183	.302	.388	.960	.491	3.60
231	.079	.075	.112	.152	.180	.185	.301	.403	.963	.469	3.56
232	.110	.115	.118	.135	.187	.186	.301	.436	.998	.511	3.64
233	.098	.098	.130	.159	.194	.212	.303	.370	1.018	.487	3.70
234	.087	.115	.129	.178	.197	.174	.290	.363	.976	.435	3.47
235	.078	.091	.115	.119	.184	.225	.291	.376	1.109	.412	3.50
236	.079	.117	.121	.114	.190	.166	.263	.351	.932	.367	3.46
237	.074	.105	.123	.136	.187	.183	.259	.383	.914	.408	3.71
238	.095	.104	.118	.122	.181	.149	.305	.359	.904	.350	3.70
239	.077	.088	.127	.115	.188	.171	.283	.342	.838	.352	3.56

Table IVA. Average Spectral Radiances in Spectral Regions 1-12 (μw cm^{-2} sr^{-1} μm^{-1}). Spectral Regions are in Table III and Pressures, Temperatures and Zenith Angles are in Table II. (Continued)

Rec. No.	Spectral Region 1	2	3	4	5	6	7	8	9	10	11	12
240	.083	1.287	30.76	.226	.255	.111	.069	.055	.072	.081	.079	.073
241	.088	1.215	29.96	.253	.262	.123	.036	.049	.061	.084	.060	.075
242	.069	1.240	29.31	.252	.261	.119	.066	.064	.061	.074	.070	.082
243	.052	1.238	29.27	.134	.324	.118	.083	.046	.069	.089	.073	.067
244	.141	1.221	29.18	.338	.271	.121	.069	.053	.074	.083	.080	.080
245	.113	1.226	29.00	.293	.267	.159	.050	.070	.075	.086	.061	.069
246	.087	1.207	28.80	.204	.268	.133	.101	.036	.072	.056	.087	.072
247	.348	3.191	62.31	.808	.739	.361	.212	.162	.155	.130	.162	.177
248	.131	3.392	63.25	.813	.711	.397	.216	.145	.130	.188	.169	.194
249	.284	3.316	62.63	.714	.762	.347	.251	.191	.169	.130	.154	.202
250	.302	3.206	60.74	.724	.819	.494	.388	.313	.434	.304	.407	.456
251	.232	3.159	59.99	.827	.828	.537	.322	.286	.511	.329	.500	.556
252	.300	3.063	58.67	.708	.692	.366	.197	.115	.163	.133	.141	.123
253	.227	2.876	56.00	.695	.660	.354	.185	.115	.139	.088	.088	.146
254	.159	2.884	57.39	.690	.653	.335	.179	.093	.130	.098	.122	.113
255	.253	2.994	58.18	.787	.692	.323	.227	.113	.130	.079	.089	.118
256	.651	2.951	58.47	.704	.671	.314	.208	.125	.152	.103	.108	.111
257	.330	2.985	58.63	.720	.692	.328	.292	.154	.142	.120	.105	.126
258	.190	3.013	58.52	.684	.686	.337	.162	.108	.141	.118	.122	.125
259	.216	2.981	57.95	.708	.695	.336	.210	.135	.132	.094	.125	.123
260	.234	2.887	56.80	.719	.668	.343	.199	.119	.133	.092	.133	.120
261	.792	7.589	118.46	2.066	1.509	.803	.590	.354	.375	.314	.383	.378
262	.914	7.620	117.06	1.942	1.457	.840	.574	.356	.362	.329	.358	.349
263	.670	7.647	117.39	1.956	1.487	.738	.475	.327	.356	.293	.368	.357
264	.873	7.683	117.37	1.973	1.497	.894	.541	.315	.384	.327	.357	.390
265	.536	7.811	118.28	1.969	1.447	.766	.425	.338	.374	.324	.449	.383
266	.726	7.683	117.33	1.976	1.525	.717	.472	.320	.339	.277	.330	.341
267	.586	7.418	115.00	3.757	2.710	1.521	1.151	1.160	3.750	3.221	5.247	5.128
268	2.593	20.595	192.13	4.112	2.982	1.591	1.276	1.314	4.174	3.615	5.920	5.733
269	2.305	19.928	192.12	4.116	2.866	1.524	1.162	1.117	3.439	2.923	4.825	4.694
270	2.402	20.423	192.03	4.295	3.012	1.708	1.293	1.220	3.750	3.239	5.251	5.[illegible]92
271	2.351	20.105	193.57	4.265	3.031	1.727	1.349	1.379	3.976	3.416	5.391	5.294
272	2.080	20.388	193.63	4.250	3.080	1.817	1.480	1.356	4.046	3.496	5.503	5.428
273	2.277	20.266	193.04	4.349	2.979	1.590	1.179	1.174	3.956	3.419	5.593	5.547
278	.076	.452	15.24	.163	.096	.084	.056	.039	.045	.052	.042	.040
279	.031	.411	15.25	.158	.095	.050	.040	.041	.038	.036	.043	.036
280	.097	.408	15.23	.156	.125	.085	.031	.033	.045	.056	.068	.043
281	.037	.378	15.14	.095	.145	.018	.046	.042	.043	.049	.032	.034
282	.253	.434	15.11	.099	.144	.041	.030	.059	.042	.028	.047	.044
283	.260	.432	14.90	.109	.163	.099	.157	.059	.076	.051	.158	.131

Table IVB. Average Spectral Radiances in Spectral Regions 13-23 ($\mu w\ cm^{-2}\ sr^{-1}\ \mu m^{-1}$). Spectral Regions are in Table III and Pressures, Temperatures and Zenith Angles are in Table II. (Continued)

Rec. No.	Spectral Region										
	13	14	15	16	17	18	19	20	21	22	23
240	.077	.099	.084	.110	.163	.187	.252	.334	.896	.424	3.28
241	.061	.091	.099	.128	.186	.164	.266	.321	.826	.339	3.07
242	.039	.064	.097	.131	.170	.161	.263	.329	.876	.344	3.02
243	.078	.068	.125	.136	.176	.166	.287	.343	.866	.341	3.01
244	.072	.082	.119	.132	.188	.164	.281	.343	.878	.332	2.97
245	.058	.085	.134	.121	.145	.186	.327	.338	.834	.371	2.97
246	.061	.082	.099	.056	.186	.175	.255	.342	.840	.242	3.59
247	.168	.217	.248	.383	.526	.568	.803	1.059	2.464	1.194	8.67
248	.152	.221	.299	.387	.555	.565	.851	1.087	2.441	1.027	8.87
249	.211	.196	.252	.298	.510	.511	.935	1.052	2.414	1.197	8.38
250	.490	.547	.516	.581	.756	.716	1.066	1.233	2.488	1.227	8.51
251	.750	.571	.671	.582	.704	.712	.933	1.208	2.446	1.252	8.23
252	.184	.236	.299	.301	.445	.467	.750	.924	2.158	1.112	7.26
253	.145	.193	.253	.287	.436	.438	.739	.919	2.153	.904	7.12
254	.105	.157	.209	.275	.451	.389	.742	.933	2.226	1.017	7.35
255	.139	.153	.216	.416	.455	.472	.690	.893	2.201	1.058	7.37
256	.111	.189	.272	.462	.543	.566	.728	.999	2.222	.975	7.82
257	.119	.277	.267	.489	.554	.541	.737	.948	2.262	1.065	7.60
258	.164	.167	.234	.331	.465	.476	.672	.910	2.223	1.045	7.47
259	.128	.163	.212	.276	.467	.472	.708	.912	2.165	.997	7.49
260	.123	.170	.250	.801	1.179	1.339	2.103	2.806	5.734	3.123	19.49
261	.355	.368	.479	.770	1.179	1.425	2.137	2.776	5.585	3.221	19.86
262	.336	.339	.472	.716	1.140	1.392	2.038	2.644	5.361	3.037	18.58
263	.339	.365	.463	.782	1.186	1.381	2.044	2.672	5.480	3.082	19.05
264	.452	.365	.462	.752	1.185	1.391	2.153	2.747	5.553	3.144	19.33
265	.356	.351	.489	.816	1.197	1.382	2.086	2.765	5.616	3.286	17.60
266	.314	.327	.443	.737	1.095	1.342	1.967	2.554	5.326	3.069	17.64
267	4.274	2.467	1.771	2.321	3.412	4.120	7.209	9.196	14.551	9.897	47.29
268	4.761	2.817	1.903	2.440	3.569	4.269	7.168	9.099	14.643	9.868	49.24
269	3.905	2.450	1.687	2.263	3.365	4.162	6.950	8.852	14.549	10.001	49.57
270	4.232	2.704	1.954	2.548	3.552	4.800	7.551	9.270	14.847	9.860	52.41
271	4.412	3.000	2.015	2.502	3.672	4.401	7.214	9.184	14.812	9.901	53.26
272	4.604	3.084	2.230	2.565	3.566	4.543	7.345	9.341	14.797	9.966	54.26
273	4.519	2.876	1.810	2.223	3.300	4.159	6.936	8.865	14.433	9.762	55.39
278	.045	.090	.060	.043	.077	.059	.086	.083	.331	.117	1.48
279	.033	.018	.046	.099	.098	.071	.087	.107	.295	.105	1.47
280	.047	.034	.052	.030	.053	.080	.099	.096	.310	.057	1.46
281	.037	.059	.095	.044	.066	.063	.081	.121	.312	.093	1.44
282	.026	.076	.104	.047	.086	.198	.093	.108	.291	.037	1.31
283	.084	.040	.102	.060	.056	.055	.133	.177	.410	.273	1.40

Table V. Average Spectral Radiances in Spectral Regions 24-34 ($\mu w\ cm^{-2}\ sr^{-1}\ \mu m^{-1}$). Spectral Regions are in Table III and Pressures, Temperatures and Zenith Angles are in Table II.

Rec. No.	Spectral Region 24	25	26	27	28	29	30	31	32	33	34
56	7.300	17.737	9.332	13.084	63.840	15.957	16.586	53.579	22.154	33.188	22.973
57	7.038	16.812	9.112	13.191	63.299	16.665	16.192	52.906	19.715	25.474	21.603
58	7.233	16.149	8.407	12.199	61.032	14.575	14.560	49.771	17.714	22.725	19.640
59	6.592	14.467	7.525	11.168	57.346	12.990	12.826	46.573	15.705	17.499	17.267
60	6.337	13.226	6.393	8.273	52.726	10.215	11.592	43.177	14.788	29.438	16.466
61	4.563	10.975	5.576	8.199	50.390	9.904	9.985	41.225	12.032	14.475	14.164
62	4.341	10.080	5.241	7.597	47.370	8.983	9.005	38.841	10.985	12.833	12.925
63	4.306	9.375	4.689	7.342	44.755	8.286	8.351	36.990	10.356	9.851	11.673
64	3.560	8.381	4.143	6.261	42.141	7.279	7.326	34.674	6.357	10.489	10.927
65	3.312	7.616	3.634	5.227	38.831	6.184	6.366	32.147	7.557	11.115	9.852
66	3.301	6.936	3.401	4.667	35.361	5.476	5.682	29.553	6.535	9.695	8.765
67	3.129	6.451	3.030	4.370	32.821	4.934	5.101	27.830	5.981	7.955	7.971
68	2.733	5.575	3.093	3.905	30.370	4.931	5.010	25.941	5.330	6.812	7.191
69	2.392	5.009	2.811	3.850	29.313	4.455	4.585	24.283	5.431	5.975	6.428
70	2.234	4.535	2.537	3.347	25.742	3.929	4.061	22.185	4.717	5.635	5.728
71	1.936	4.000	2.216	2.961	23.004	3.428	3.510	20.251	4.122	4.502	5.014
72	1.914	3.543	1.970	2.523	20.603	2.976	3.077	18.439	3.642	4.771	4.493
73	1.747	3.218	1.801	2.226	18.716	2.686	2.771	16.935	3.239	4.814	4.174
74	1.642	2.952	1.667	2.044	17.087	2.450	2.513	15.654	2.932	4.194	3.714
75	1.462	2.629	1.501	1.833	15.415	2.175	2.229	14.313	2.577	3.425	3.292
76	1.319	2.387	1.347	1.643	13.728	1.936	1.980	12.671	2.323	2.756	2.929
77	1.213	2.240	1.163	1.373	11.864	1.640	1.649	11.175	1.929	2.412	2.471
78	.662	1.683	.815	.992	9.938	1.269	1.274	9.595	1.532	2.089	1.982
79	.458	1.415	.697	.830	9.417	1.093	1.078	8.223	1.313	2.021	1.720
80	.384	1.263	.632	.750	7.208	.964	.956	6.973	1.167	1.601	1.514
81	.350	1.196	.578	.673	6.190	.896	.863	6.139	1.032	1.418	1.382
82	.336	1.153	.538	.603	5.438	.625	.799	5.453	1.017	1.549	1.275
83	.311	1.090	.504	.552	4.863	.778	.746	4.831	.955	1.516	1.191
84	.294	1.047	.482	.529	4.471	.753	.721	4.504	.922	1.401	1.132
85	.285	1.025	.466	.517	4.228	.729	.694	4.265	.834	1.326	1.095
86	.280	.990	.468	.510	4.066	.714	.680	4.084	.866	1.195	1.062
87	.271	.971	.451	.482	3.780	.684	.669	3.807	.848	1.303	1.027
88	.263	.937	.439	.466	3.502	.669	.640	3.540	.821	1.257	1.003
89	.256	.926	.436	.465	3.373	.671	.624	3.376	.800	1.022	.976
90	.250	.895	.431	.472	3.229	.661	.618	3.229	.834	.956	.950
91	.239	.869	.422	.453	3.047	.637	.607	3.014	.767	.956	.924
92	.241	.863	.414	.453	2.906	.630	.600	2.894	.761	.955	.910
93	.236	.854	.407	.446	2.850	.624	.592	2.843	.760	.859	.901
94	.233	.862	.404	.444	2.753	.618	.581	2.762	.735	.792	.893
95	.226	.827	.400	.446	2.732	.609	.571	2.696	.747	.684	.875
96	.226	.818	.399	.436	2.675	.604	.584	2.633	.740	.711	.869
97	.226	.807	.383	.413	2.590	.601	.559	2.577	.709	.861	.863
98	.223	.802	.384	.406	2.542	.588	.557	[illegible]	.717	[illegible]	.857
99	.219	.809	.381	.404	2.492	.580	.554	2.455	.726	.870	.851
100	.219	.800	.381	.409	2.469	.560	.545	2.445	.705	.373	.844
101	.219	.787	.380	.412	2.423	.580	.546	2.428	.711	.777	.840
102	.219	.792	.377	.421	2.395	.570	.556	2.387	.736	.693	.837
103	.201	.781	.371	.424	2.351	.569	.557	2.354	.639	.650	.825
104	.214	.787	.373	.416	2.309	.579	.551	2.306	.696	.651	.816
105	.214	.761	.369	.407	2.271	.565	.541	2.285	.693	.735	.815

Table V. Average Spectral Radiances in Spectral Regions 24-34 (μw cm^{-2} sr^{-1} μm^{-1}). Spectral Regions are in Table III and Pressures, Temperatures and Zenith Angles are in Table II. (Continued)

Rec. No.	Spectral Region										
	24	25	26	27	28	29	30	31	32	33	34
106	.213	.761	.370	.399	2.246	.559	.541	2.235	.682	.798	.812
107	.209	.750	.363	.404	2.213	.542	.533	2.194	.669	.756	.811
108	.208	.754	.366	.399	2.166	.561	.531	2.191	.679	.616	.805
109	.203	.743	.359	.375	2.143	.542	.510	2.117	.667	.739	.799
110	.209	.742	.359	.393	2.104	.545	.533	2.143	.670	.764	.796
111	.205	.725	.359	.386	2.103	.537	.535	2.099	.674	.731	.799
112	.208	.733	.358	.383	2.054	.545	.524	2.102	.646	.699	.791
113	.206	.718	.357	.393	2.048	.530	.522	2.020	.656	.713	.78[illegible]
114	.205	.711	.357	.384	2.039	.548	.524	2.013	.661	.683	.787
115	.204	.720	.352	.381	1.970	.540	.524	2.[illegible]01	.663	.709	.775
116	.172	.674	.303	.319	1.900	.462	.434	1.915	.562	.622	.665
117	.136	.616	.245	.258	1.808	.378	.351	1.779	.432	.576	.539
118	.100	.560	.196	.210	1.715	.301	.261	1.655	.355	.435	.419
119	.067	.525	.143	.155	1.611	.231	.181	1.551	.257	.345	.314
120	.032	.483	.092	.104	1.556	.150	.104	1.403	.158	.191	.185
121	.036	.471	.095	.110	1.553	.147	.104	1.436	.170	.173	.167
122	.037	.461	.088	.093	1.493	.161	.100	1.403	.185	.292	.129
123	.037	.448	.094	.107	1.511	.321	.109	1.394	.132	.234	.185
124	.039	.453	.100	.112	1.498	.163	.113	1.348	.190	.210	.189
125	.046	.457	.107	.112	1.514	.167	.110	1.335	.180	.184	.185
126	.042	.447	.104	.120	1.481	.179	.111	1.340	.139	.165	.191
127	.043	.438	.107	.121	1.465	.167	.106	1.271	.180	.172	.181
128	.045	.416	.100	.114	1.390	.181	.107	1.274	.191	.262	.173
129	.047	.410	.100	.111	1.357	.166	.102	1.226	.181	.165	.177
130	.049	.409	.100	.115	1.340	.183	.116	1.196	.191	.207	.176
131	.051	.403	.104	.115	1.310	.175	.123	1.185	.211	.193	.182
132	.053	.403	.100	.115	1.302	.201	.117	1.177	.202	.233	.183
133	.055	.387	.104	.109	1.248	.206	.117	1.120	.205	.244	.177
134	.057	.377	.106	.115	1.236	.195	.117	1.124	.219	.199	.183
135	.059	.375	.108	.122	1.229	.206	.116	1.083	.209	.174	.182
136	.061	.365	.107	.131	1.191	.206	.115	1.077	.211	.165	.166
137	.064	.362	.109	.124	1.157	.213	.119	1.056	.229	.193	.183
138	.066	.353	.107	.120	1.118	.207	.119	1.011	.213	.203	.180
139	.068	.356	.107	.122	1.113	.214	.117	1.014	.218	.199	.181
140	.070	.337	.111	.124	1.099	.229	.117	.993	.239	.155	.181
141	.072	.331	.109	.128	1.073	.223	.123	.985	.248	.210	.179
142	.075	.335	.112	.122	1.050	.229	.126	.939	.236	.236	.150
143	.078	.332	.116	.127	1.031	.235	.126	.917	.242	.212	.184
144	.081	.325	.119	.138	1.003	.242	.131	.917	.249	.168	.186
145	.083	.321	.123	.141	1.014	.249	.133	.910	.256	.134	.183
146	.086	.313	.126	.139	.980	.256	.135	.893	.263	.159	.185
147	.089	.307	.130	.146	.958	.264	.140	.865	.270	.173	.187
148	.092	.309	.133	.144	.954	.271	.141	.866	.278	.184	.189
151	.100	.304	.142	.144	.917	.288	.150	.821	.295	.259	.193
152	.102	.286	.145	.155	.892	.294	.153	.821	.300	.194	.197
153	.105	.291	.148	.155	.889	.299	.156	.806	.336	.183	.200
154	.106	.276	.150	.160	.885	.303	.159	.792	.310	.161	.194
155	.108	.275	.152	.163	.874	.308	.160	.798	.314	.163	.195
156	.110	.272	.154	.162	.859	.312	.162	.758	.318	.165	.199
157	.112	.259	.156	.164	.844	.316	.164	.732	.322	.167	.201

Table V. Average Spectral Radiances in Spectral Regions 24-34 (μw cm^{-2} sr^{-1} μm^{-1}). Spectral Regions are in Table III and Pressures, Temperatures and Zenith Angles are in Table II. (Continued)

Rec. No.	Spectral Region 24	25	26	27	28	29	30	31	32	33	34
158	.114	.258	.159	.166	.814	.322	.167	.736	.328	.170	.205
159	.116	.258	.161	.169	.821	.326	.169	.726	.332	.186	.204
160	.118	.246	.163	.170	.805	.330	.171	.719	.337	.181	.201
161	.121	.246	.166	.172	.784	.336	.174	.702	.343	.169	.206
162	.123	.252	.169	.175	.773	.343	.177	.702	.349	.192	.211
163	.126	.256	.172	.182	.798	.349	.181	.727	.357	.184	.219
164	.128	.249	.175	.184	.791	.353	.183	.701	.360	.186	.223
168	.139	.239	.187	.192	.749	.378	.195	.665	.384	.239	.219
169	.142	.237	.190	.195	.737	.385	.198	.660	.391	.201	.236
170	.144	.247	.193	.202	.759	.389	.201	.666	.395	.211	.230
171	.148	.238	.196	.201	.741	.396	.207	.672	.402	.207	.232
172	.151	.241	.200	.214	.922	.403	.211	.816	.409	.210	.261
173	.154	.305	.203	.222	.908	.410	.211	.777	.416	.216	.252
174	.156	.292	.206	.217	.882	.415	.213	.757	.421	.245	.252
175	.159	.293	.208	.216	.867	.420	.216	.771	.426	.283	.253
176	.161	.282	.211	.214	.847	.425	.218	.717	.430	.313	.252
177	.163	.277	.213	.217	.854	.430	.221	.752	.435	.265	.255
178	.167	.283	.217	.224	.805	.437	.224	.747	.442	.267	.260
179	.169	.274	.219	.226	.844	.442	.227	.768	.447	.254	.259
180	.171	.272	.222	.232	.826	.447	.231	.741	.452	.264	.263
181	.174	.260	.224	.233	.807	.452	.232	.708	.457	.234	.263
182	.176	.264	.227	.238	.916	.457	.234	.670	.462	.237	.268
183	.178	.263	.230	.239	.809	.462	.237	.694	.467	.239	.266
184	.181	.264	.232	.238	.796	.467	.239	.692	.472	.242	.267
185	.183	.254	.235	.240	.780	.472	.242	.689	.477	.246	.268
186	.185	.252	.236	.242	.768	.475	.243	.658	.480	.246	.270
187	.187	.248	.239	.243	.765	.480	.246	.650	.485	.248	.272
188	.190	.257	.242	.245	.763	.486	.249	.654	.490	.251	.271
189	.192	.256	.244	.250	.766	.491	.251	.654	.496	.253	.429
190	.195	.251	.247	.252	.745	.496	.254	.650	.501	.256	.274
191	.197	.242	.250	.252	.747	.501	.256	.645	.506	.258	.281
192	.200	.246	.252	.255	.725	.507	.259	.634	.511	.261	.279
193	.203	.246	.255	.257	.722	.512	.262	.629	.517	.264	.276
194	.204	.247	.257	.258	.725	.515	.263	.631	.519	.275	.279
195	.207	.249	.259	.261	.727	.520	.266	.620	.525	.268	.276
196	.209	.249	.262	.264	.719	.526	.269	.611	.530	.270	.281
197	.211	.250	.264	.266	.731	.529	.270	.634	.533	.272	.283
198	.212	.241	.265	.267	.716	.532	.271	.623	.536	.273	.288
199	.215	.244	.268	.270	.714	.537	.274	.610	.541	.276	.287
200	.218	.248	.271	.274	.719	.543	.277	.610	.547	.279	.289
201	.221	.249	.274	.276	.710	.548	.280	.603	.552	.281	.291
202	.223	.251	.277	.279	.713	.554	.283	.603	.558	.284	.292
203	.226	.251	.279	.281	.702	.560	.285	.596	.563	.287	.294
204	.228	.255	.281	.283	.701	.563	.287	.592	.566	.286	.295
205	.231	.255	.284	.286	.689	.568	.290	.594	.572	.291	.298
206	.232	.258	.285	.287	.692	.571	.291	.582	.575	.293	.298
207	.235	.258	.288	.290	.669	.577	.294	.605	.580	.295	.300
208	.238	.261	.291	.293	.682	.583	.297	.577	.586	.298	.303
209	.239	.262	.293	.294	.667	.586	.298	.577	.589	.300	.304
210	.241	.262	.294	.296	.667	.589	.300	.569	.592	.301	.307

Table V. Average Spectral Radiances in Spectral Regions 24-34 ($\mu w\ cm^{-2}\ sr^{-1}\ \mu m^{-1}$). Spectral Regions are in Table III and Pressures, Temperatures and Zenith Angles are in Table II. (Continued)

Rec. No.	Spectral Region 24	25	26	27	28	29	30	31	32	33	34
211	.242	.261	.296	.298	.667	.592	.301	.572	.595	.303	.305
212	.245	.264	.299	.301	.664	.598	.304	.565	.601	.306	.309
213	.247	.265	.301	.302	.647	.601	.306	.560	.604	.307	.311
214	.248	.266	.302	.304	.658	.604	.307	.562	.607	.309	.312
215	.250	.267	.304	.305	.651	.607	.309	.566	.610	.310	.313
216	.252	.270	.305	.307	.655	.610	.310	.555	.612	.311	.313
217	.253	.272	.307	.308	.642	.613	.312	.552	.615	.313	.313
218	.253	.272	.307	.308	.643	.613	.312	.545	.615	.313	.315
219	.255	.272	.309	.310	.632	.616	.313	.541	.618	.314	.316
220	.255	.272	.309	.310	.626	.616	.313	.539	.618	.314	.315
221	.255	.272	.308	.310	.653	.616	.313	.540	.618	.314	.315
222	.253	.272	.307	.308	.628	.613	.312	.527	.616	.313	.313
223	.252	.268	.305	.307	.622	.610	.310	.533	.613	.312	.312
224	.249	.267	.302	.304	.621	.604	.308	.521	.607	.309	.311
225	.246	.266	.299	.301	.629	.598	.305	.525	.601	.306	.307
226	.243	.260	.296	.298	.601	.592	.302	.523	.595	.303	.303
227	.240	.257	.293	.295	.605	.586	.299	.512	.590	.300	.302
228	.235	.255	.289	.291	.610	.578	.294	.509	.581	.296	.298
229	.232	.252	.285	.287	.581	.572	.292	.508	.575	.293	.298
230	.228	.249	.281	.283	.597	.564	.287	.501	.567	.289	.291
231	.224	.246	.277	.279	.582	.555	.283	.493	.559	.285	.287
232	.218	.241	.271	.273	.593	.544	.278	.494	.548	.279	.284
233	.213	.231	.266	.267	.584	.533	.272	.494	.537	.274	.279
234	.209	.231	.262	.263	.557	.525	.268	.477	.529	.270	.275
235	.204	.227	.256	.258	.552	.514	.263	.463	.518	.264	.272
236	.199	.221	.251	.253	.562	.503	.257	.468	.508	.259	.266
237	.192	.220	.244	.246	.558	.490	.251	.463	.495	.253	.264
238	.185	.211	.236	.240	.551	.474	.245	.451	.479	.245	.256
239	.177	.211	.228	.237	.542	.459	.235	.442	.464	.238	.249
240	.170	.205	.221	.227	.532	.444	.228	.435	.450	.230	.243
241	.164	.204	.213	.216	.515	.430	.221	.423	.435	.226	.236
242	.161	.205	.209	.212	.510	.422	.216	.419	.426	.224	.232
243	.158	.199	.204	.207	.507	.411	.212	.417	.417	.242	.228
244	.160	.195	.199	.203	.501	.402	.207	.397	.407	.226	.224
245	.156	.196	.192	.197	.509	.388	.208	.401	.394	.228	.218
246	.152	.193	.188	.194	.502	.379	.209	.397	.383	.225	.249
247	.163	.240	.192	.215	.744	.384	.215	.576	.397	.277	.247
248	.160	.242	.192	.216	.754	.371	.209	.567	.361	.275	.240
249	.153	.233	.176	.202	.711	.347	.201	.557	.350	.286	.235
250	.158	.234	.181	.207	.715	.317	.200	.532	.309	.255	.230
251	.145	.223	.162	.188	.701	.299	.192	.533	.306	.254	.229
252	.143	.214	.162	.181	.684	.286	.180	.507	.279	.263	.213
253	.129	.203	.157	.168	.665	.267	.181	.506	.279	.271	.204
254	.141	.212	.158	.177	.663	.248	.177	.510	.260	.287	.210
255	.128	.202	.146	.164	.653	.222	.173	.500	.233	.269	.200
256	.125	.199	.152	.170	.660	.213	.172	.469	.201	.239	.196
257	.120	.191	.152	.159	.650	.213	.170	.496	.199	.250	.197
258	.119	.189	.139	.162	.656	.190	.157	.487	.233	.244	.195
259	.114	.191	.133	.155	.644	.200	.155	.468	.215	.232	.172
260	.114	.181	.172	.217	1.148	.244	.202	.850	.248	.267	.290

Table V. Average Spectral Radiances in Spectral Regions 24-34 ($\mu w\ cm^{-2}\ sr^{-1}\ \mu m^{-1}$). Spectral Regions are in Table III and Pressures, Temperatures and Zenith Angles are in Table II. (Continued)

Rec. No.	Spectral Region 24	25	26	27	28	29	30	31	32	33	34
261	.146	.292	.174	.201	1.176	.230	.299	.888	.238	.261	.283
262	.138	.289	.164	.192	1.145	.228	.191	.852	.242	.338	.283
263	.140	.292	.164	.202	1.158	.224	.196	.813	.224	.305	.286
264	.138	.284	.168	.207	1.155	.223	.189	.835	.232	.315	.284
265	.135	.288	.153	.176	1.148	.220	.186	.817	.285	.394	.287
266	.133	.281	.129	.186	1.130	.226	.199	.786	.236	.383	.295
267	.129	2.082	.729	.732	3.503	.821	.767	3.106	.908	1.126	1.319
268	.769	2.594	.768	.783	3.497	.815	.753	3.101	.851	.968	1.257
269	.616	2.125	.691	.736	3.381	.773	.729	3.036	.865	.860	1.190
270	.697	2.331	.745	.793	3.550	.809	.776	3.041	.902	.716	1.143
271	.675	2.345	.696	.757	3.482	.827	.759	3.119	.950	.832	1.197
272	.697	2.315	.770	.845	3.626	.888	.813	3.186	.953	.805	1.196
273	.680	2.429	.717	.829	3.465	.841	.815	3.106	.979	.730	1.144
278	.093	.111	.122	.128	.314	.234	.142	.259	.245	.132	.140
279	.094	.117	.122	.130	.320	.233	.148	.262	.240	.130	.144
280	.092	.112	.125	.129	.320	.226	.148	.268	.246	.138	.138
281	.092	.115	.122	.127	.316	.234	.161	.266	.251	.142	.138
282	.104	.119	.127	.131	.318	.241	.147	.267	.226	.128	.140
283	.099	.111	.128	.131	.325	.249	.151	.292	.263	.129	.144

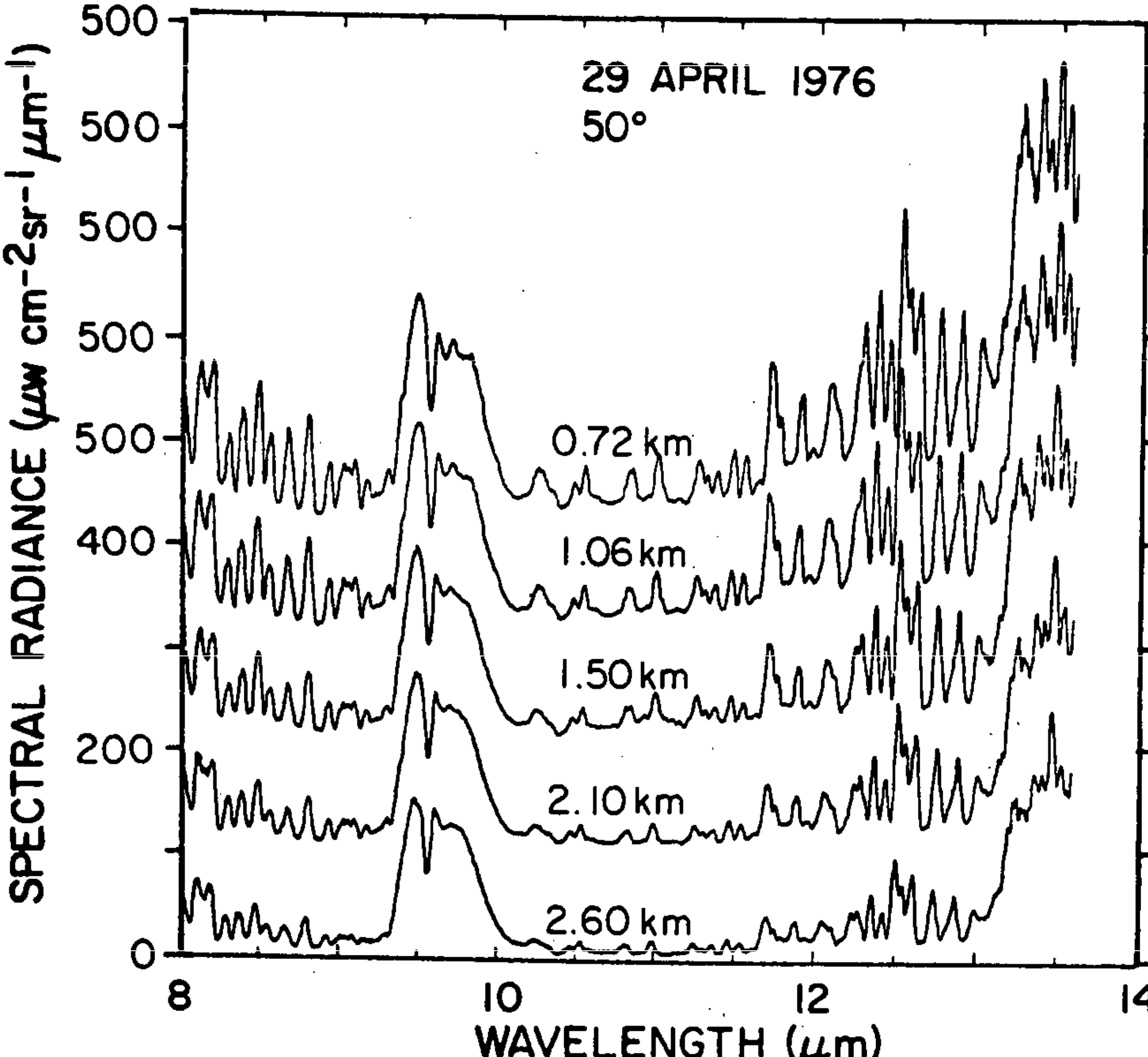

Figure 6. Linear spectral radiance in the 8-13.6μm region at 0.72, 1.06, 1.50, 2.10 and 2.60 km and a zenith angle of 50°. Spectra are offset for clarity.

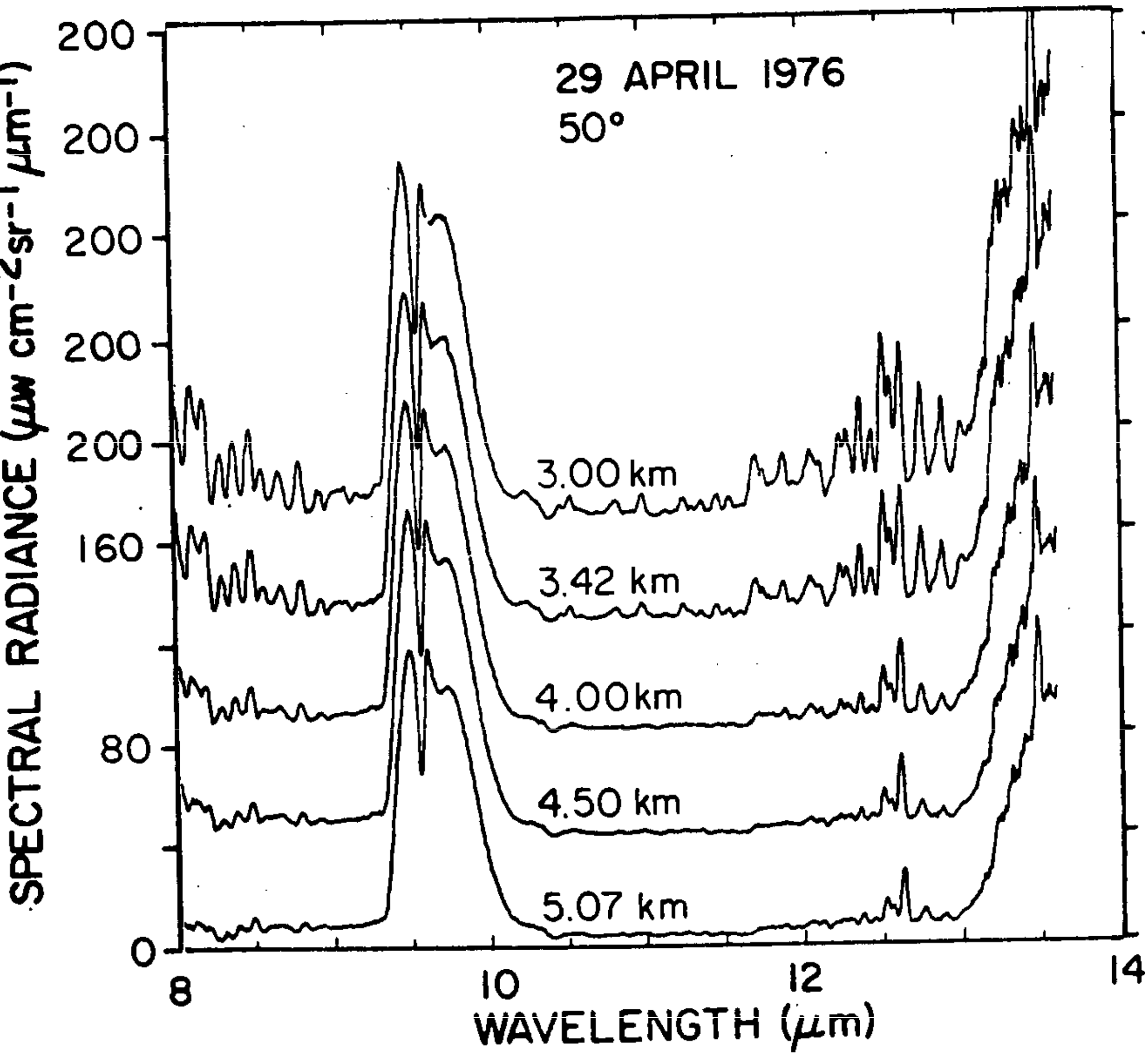

Figure 7. Linear spectral radiance in the 8-13.6μm region at 3.00, 3.42, 4.00, 4.50 and 5.07 km and a zenith angle of 50°. Spectra are offset for clarity.

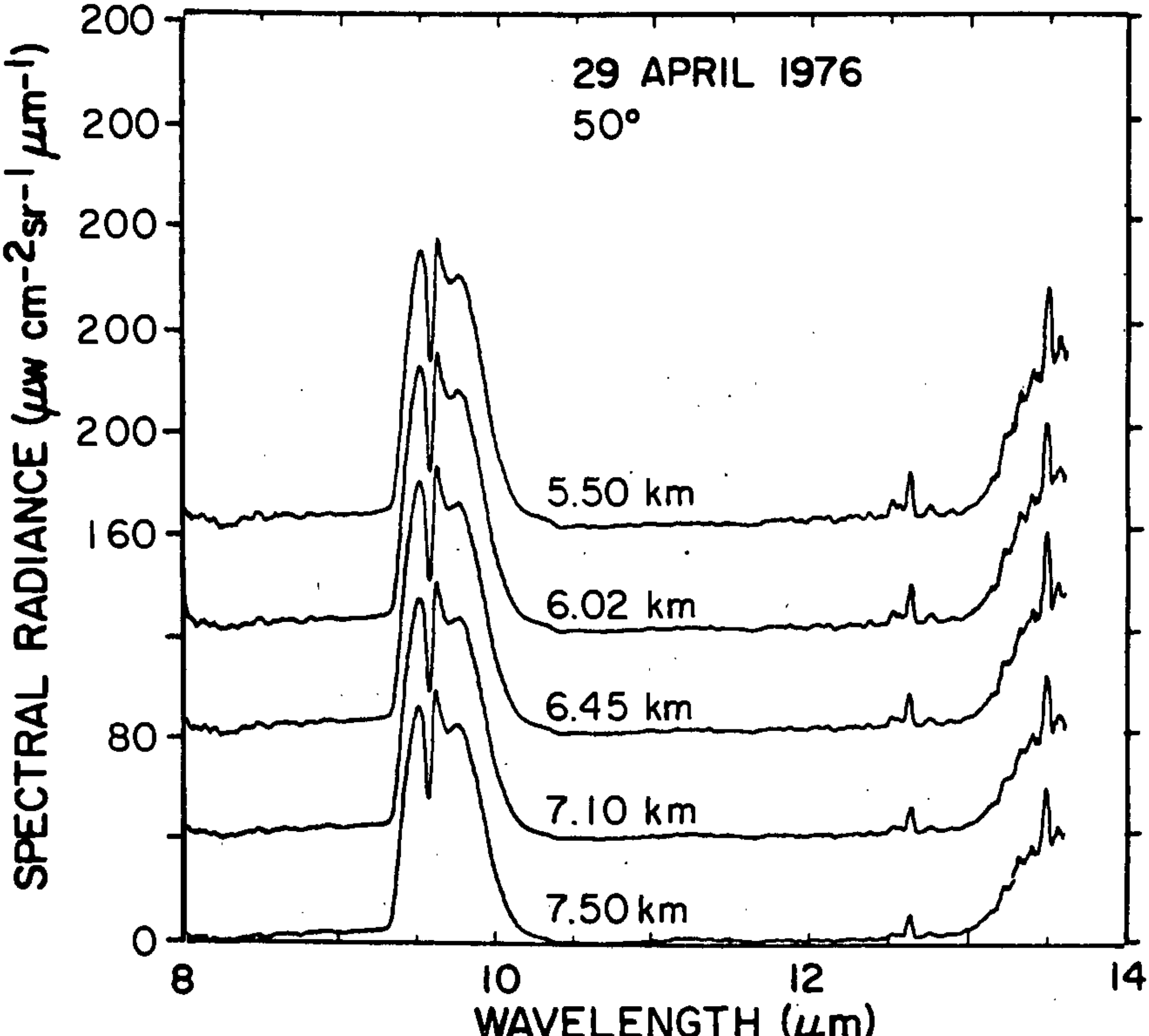

Figure 8. Linear spectral radiance in the 8-13.6μm region at 5.50, 6.02, 6.45, 7.10 and 7.50 km and a zenith angle of 50°. Spectra are offset for clarity.

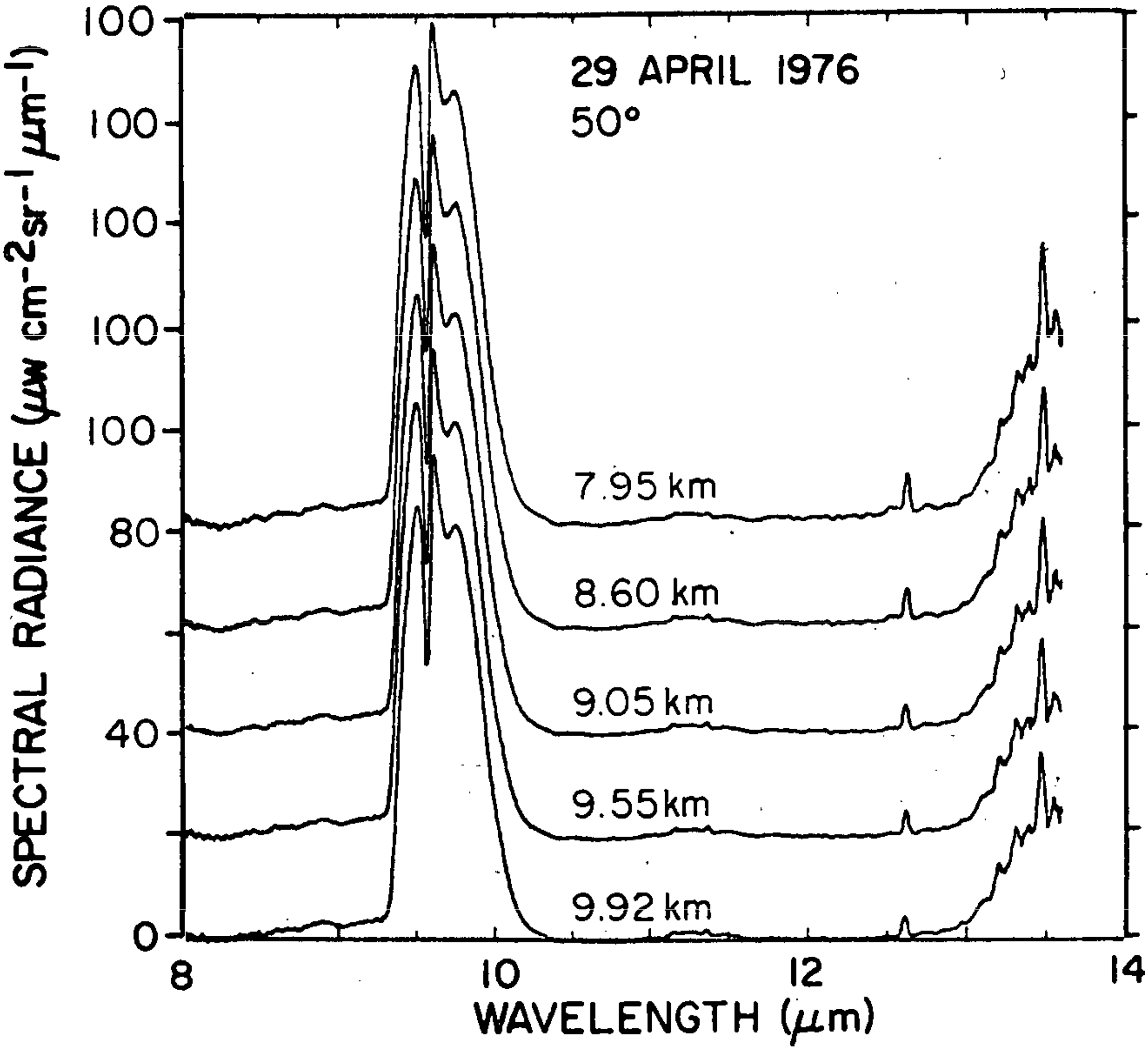

Figure 9. Linear spectral radiance in the 8-13.6μm region at 7.95, 8.60, 9.05, 9.55 and 9.92 km and a zenith angle of 50°. Spectra are offset for clarity.

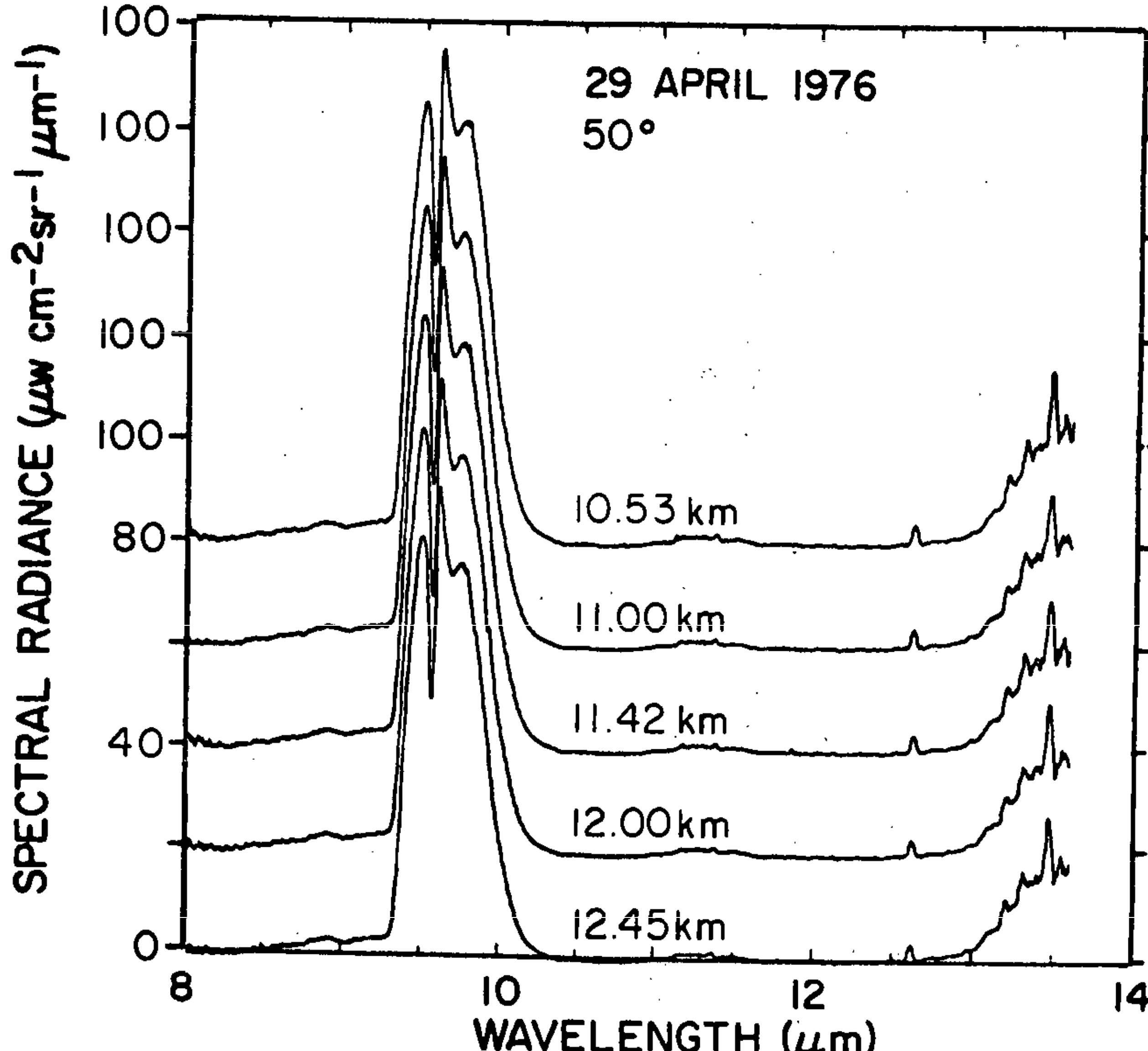

Figure 10. Linear spectral radiance in the 8-13.6μm region at 10.53, 11.00, 11.42, 12.00 and 12.45 km and a zenith angle of 50°. Spectra are offset for clarity.

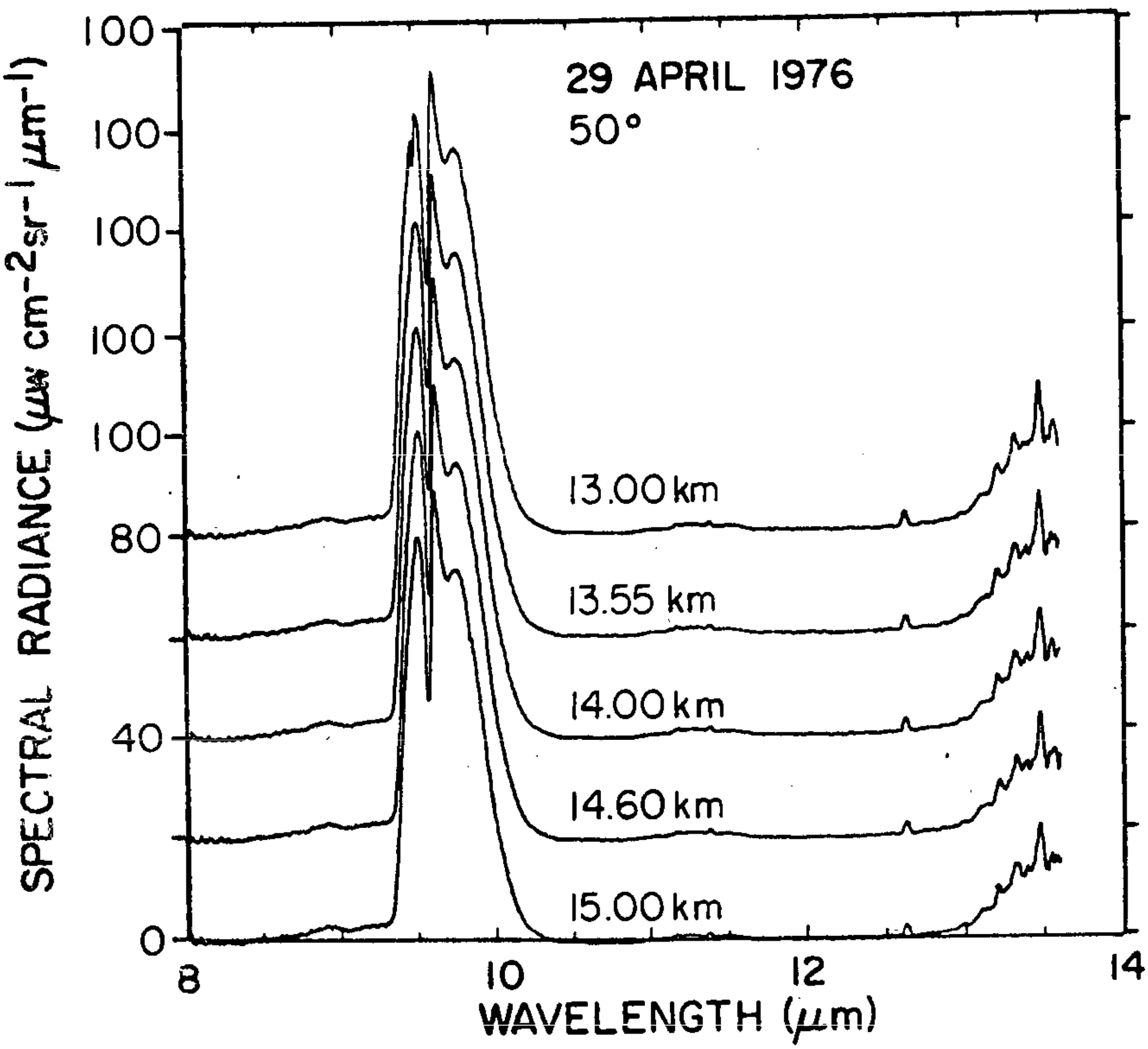

Figure 11. Linear spectral radiance in the 8-13.6μm region at 13.00, 13.55, 14.00, 14.60 and 15.00 km and a zenith angle of 50°. Spectra are offset for clarity.

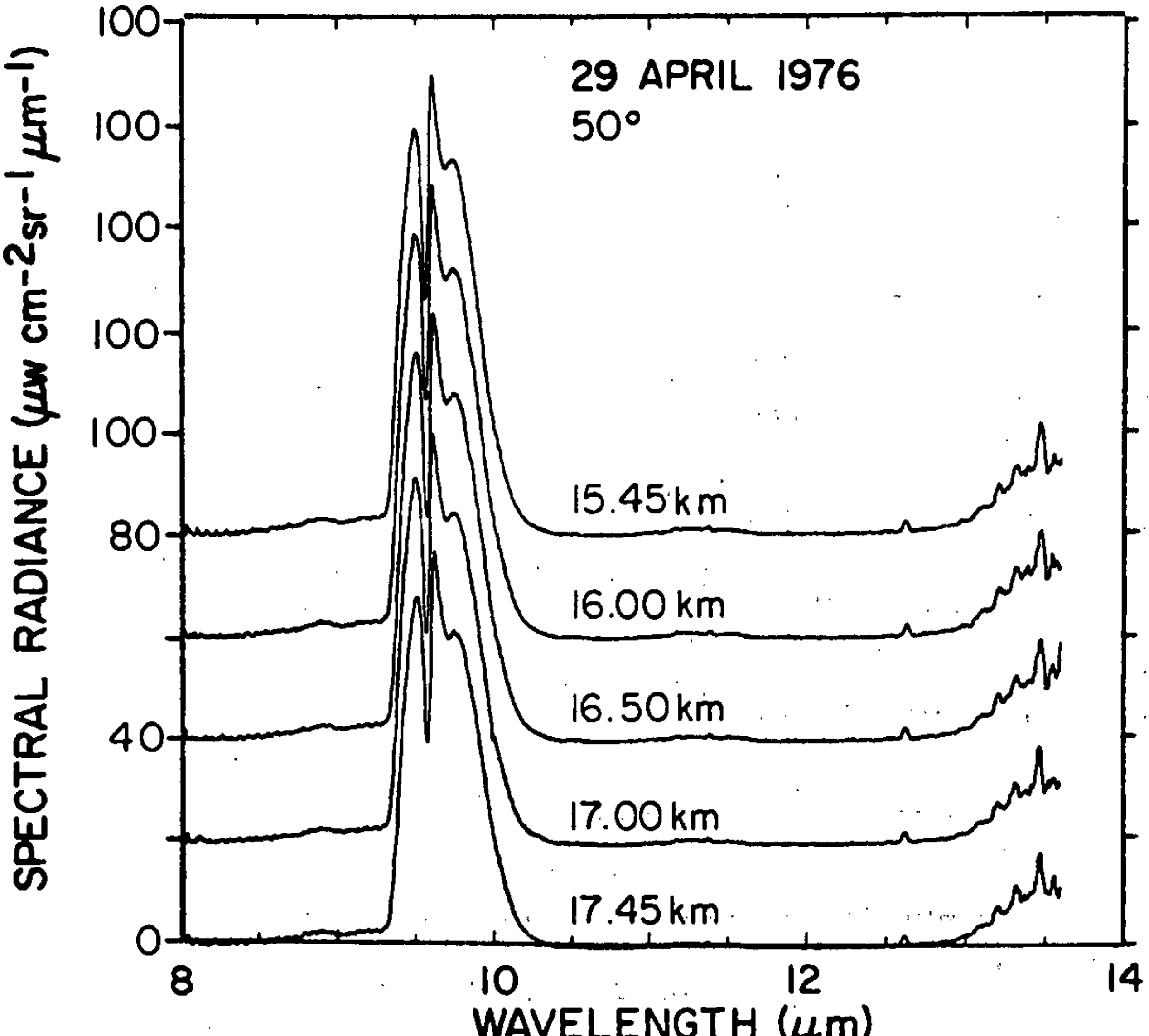

Figure 12. Linear spectral radiance in the 8-13.6μm region at 15.45, 16.00, 16.50, 17.00 and 17.45 km and a zenith angle of 50°. Spectra are offset for clarity.

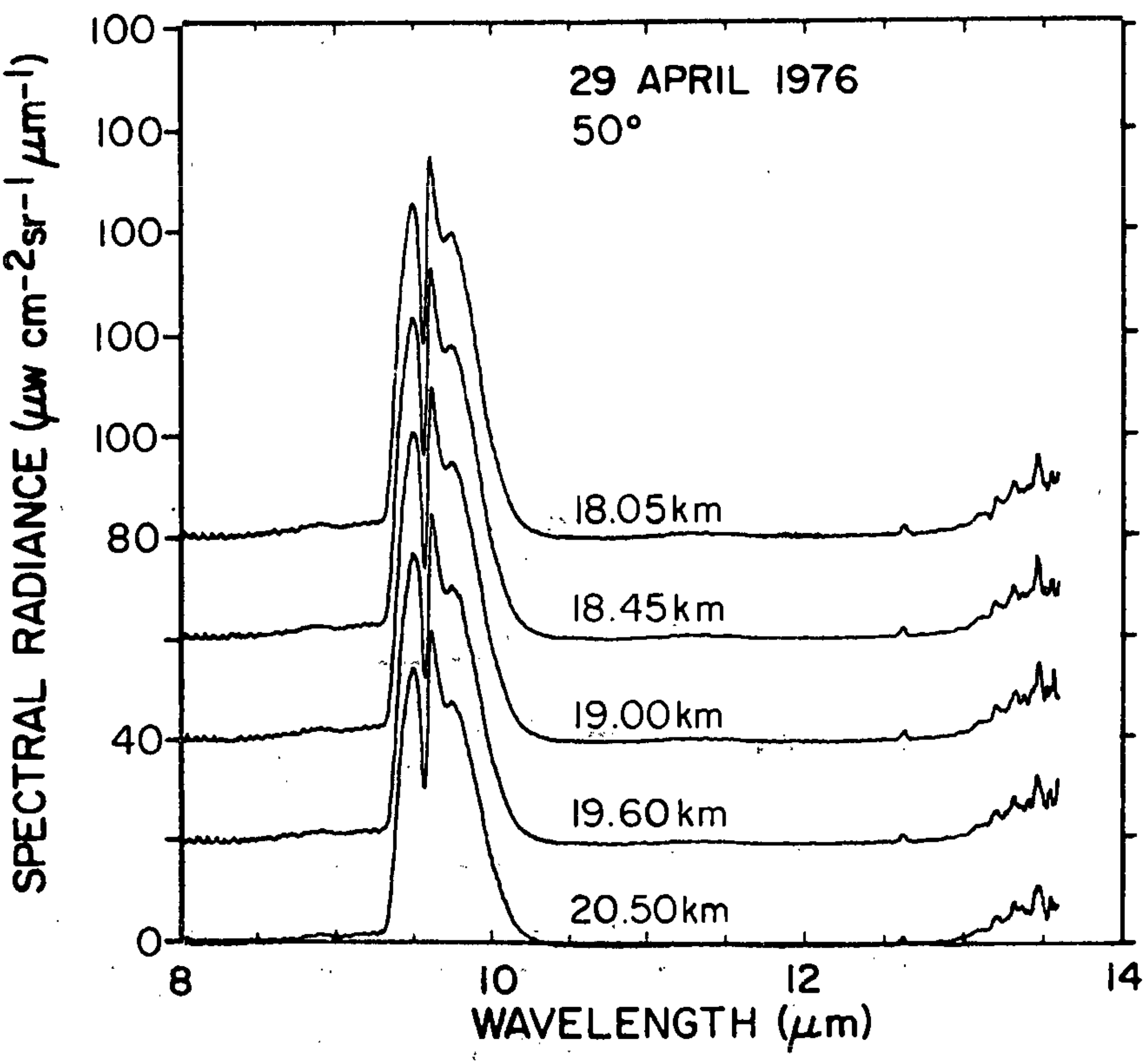

Figure 13. Linear spectral radiance in the 8-13.6μm region at 18.05, 18.45, 19.00, 19.60 and 20.50 km and a zenith angle of 50°. Spectra are offset for clarity.

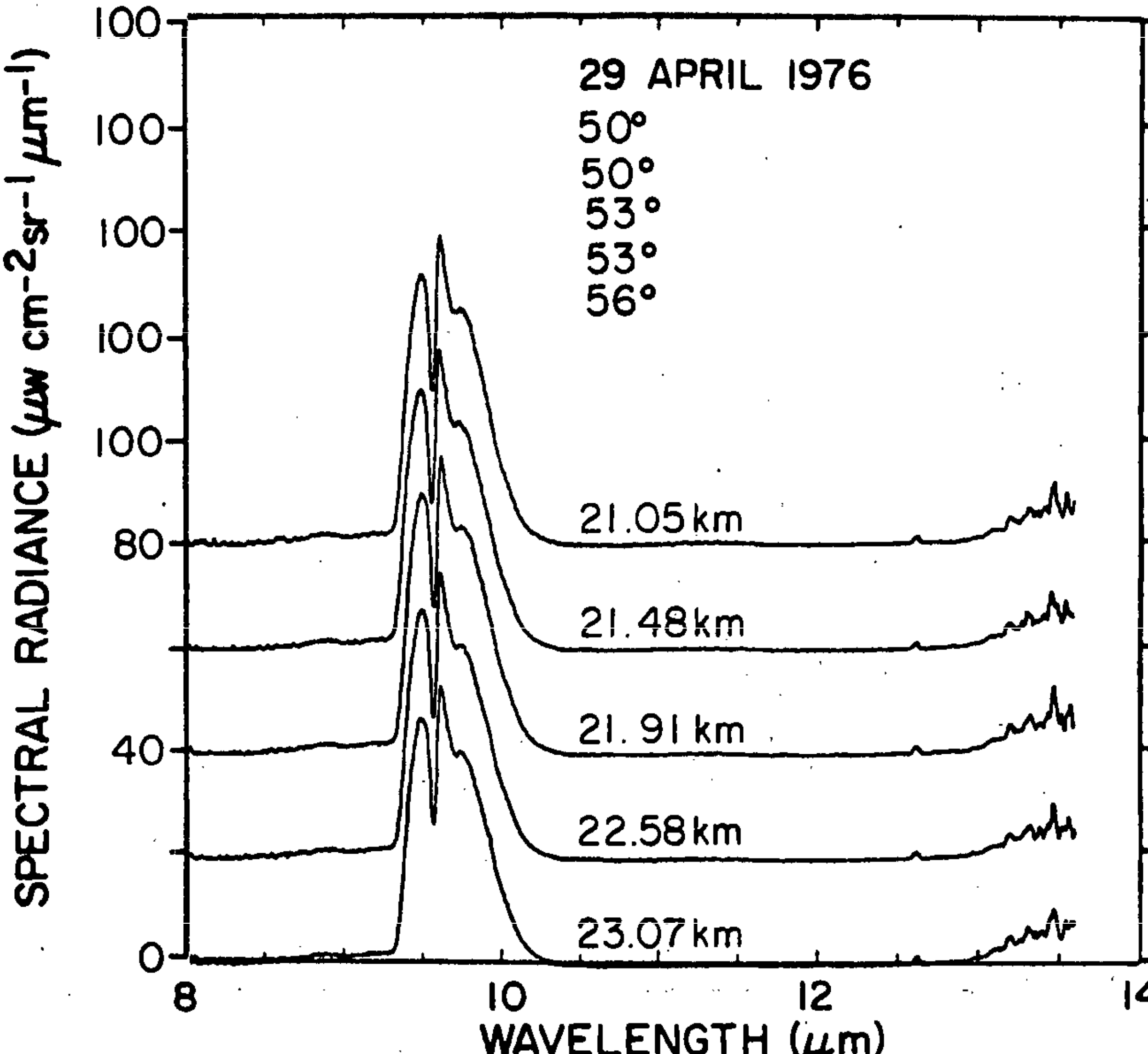

Figure 14. Linear spectral radiance in the 8-13.6μm region at 21.05, 21.48, 21.91, 22.58 and 23.07 km and zenith angles of 50°, 50°, 53°, 53° and 56°. Spectra are offset for clarity.

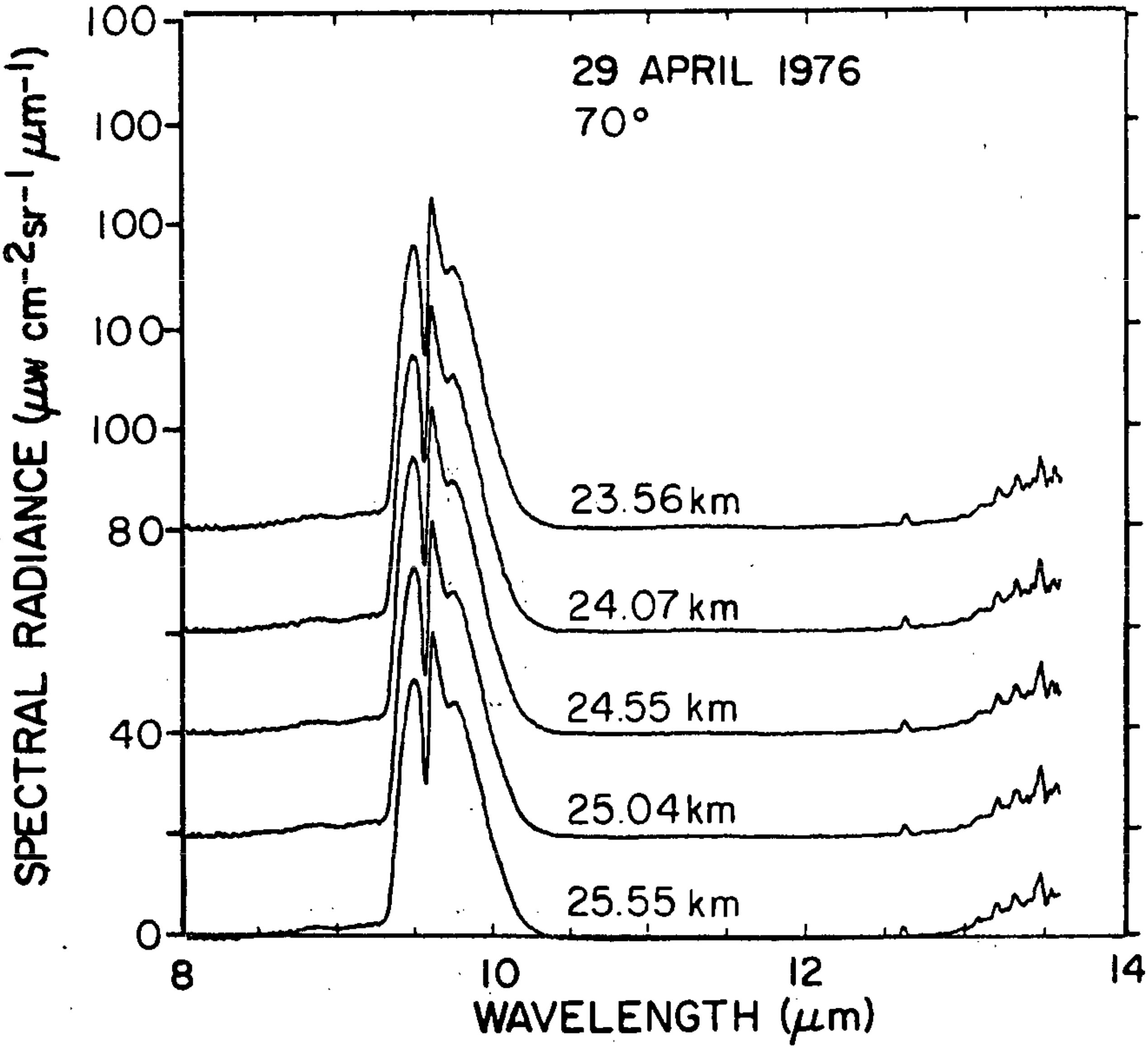

Figure 15. Linear spectral radiance in the 8-13.6μm region at 23.56, 24.07, 24.55, 25.04 and 25.55 km and a zenith angle of 70°. Spectra are offset for clarity.

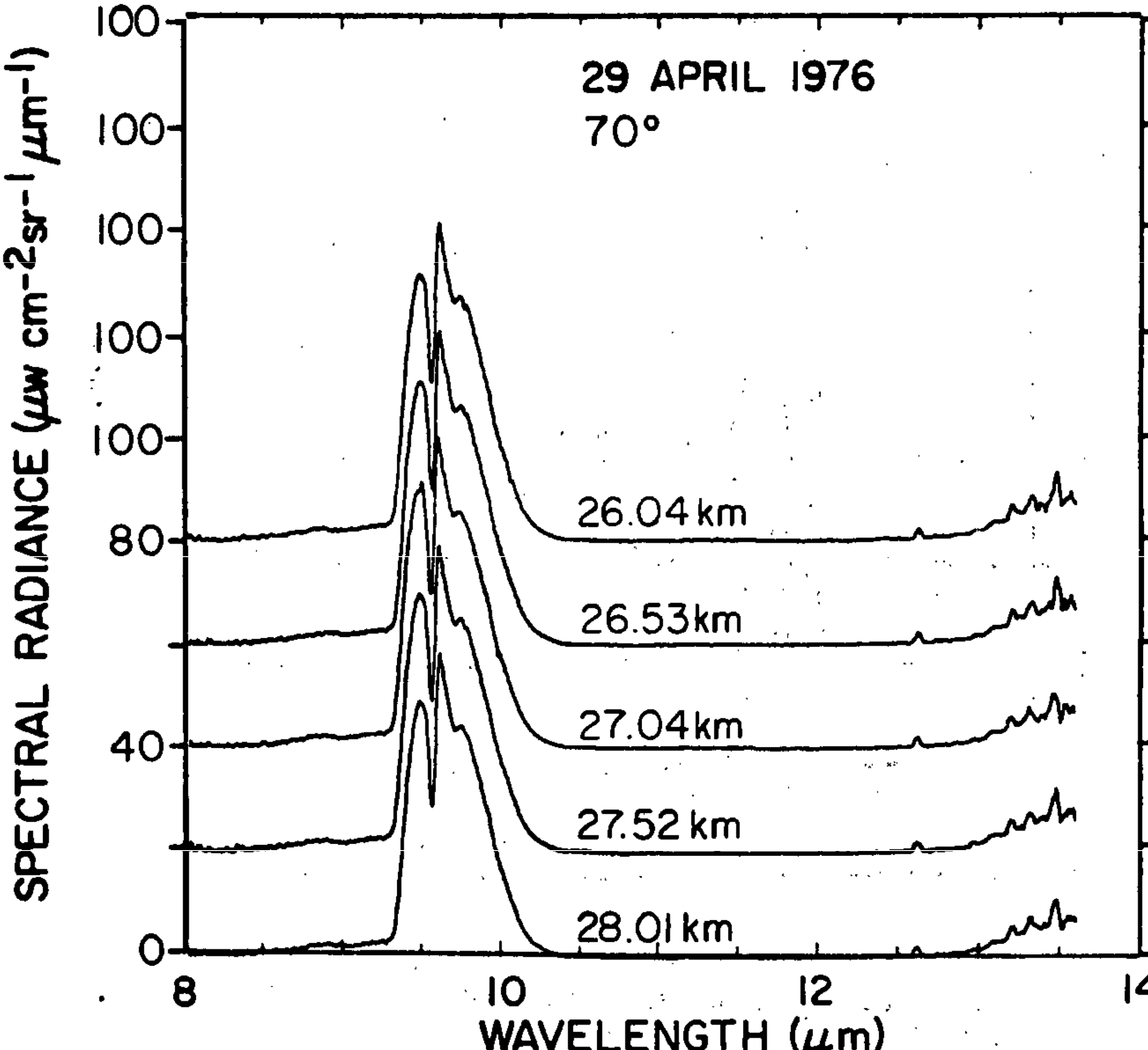

Figure 16. Linear spectral radiance in the 8-13.6μm region at 26.04, 26.53, 27.04, 27.52 and 28.01 km and a zenith angle of 70°. Spectra are offset for clarity.

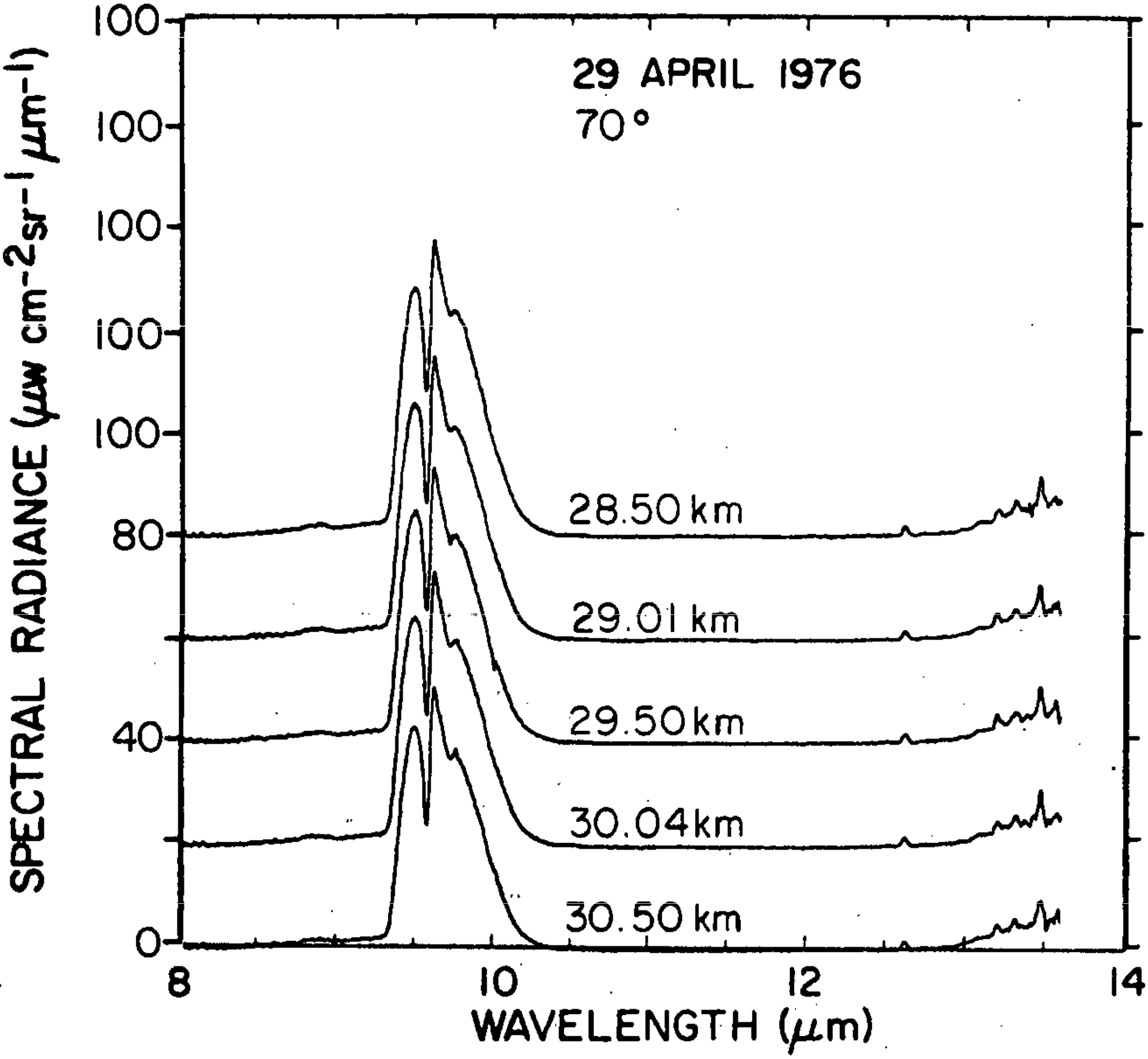

Figure 17. Linear spectral radiance in the 8-13.6μm region at 28.50, 29.01, 29.50, 30.04 and 30.50 km and a zenith angle of 70°. Spectra are offset for clarity.

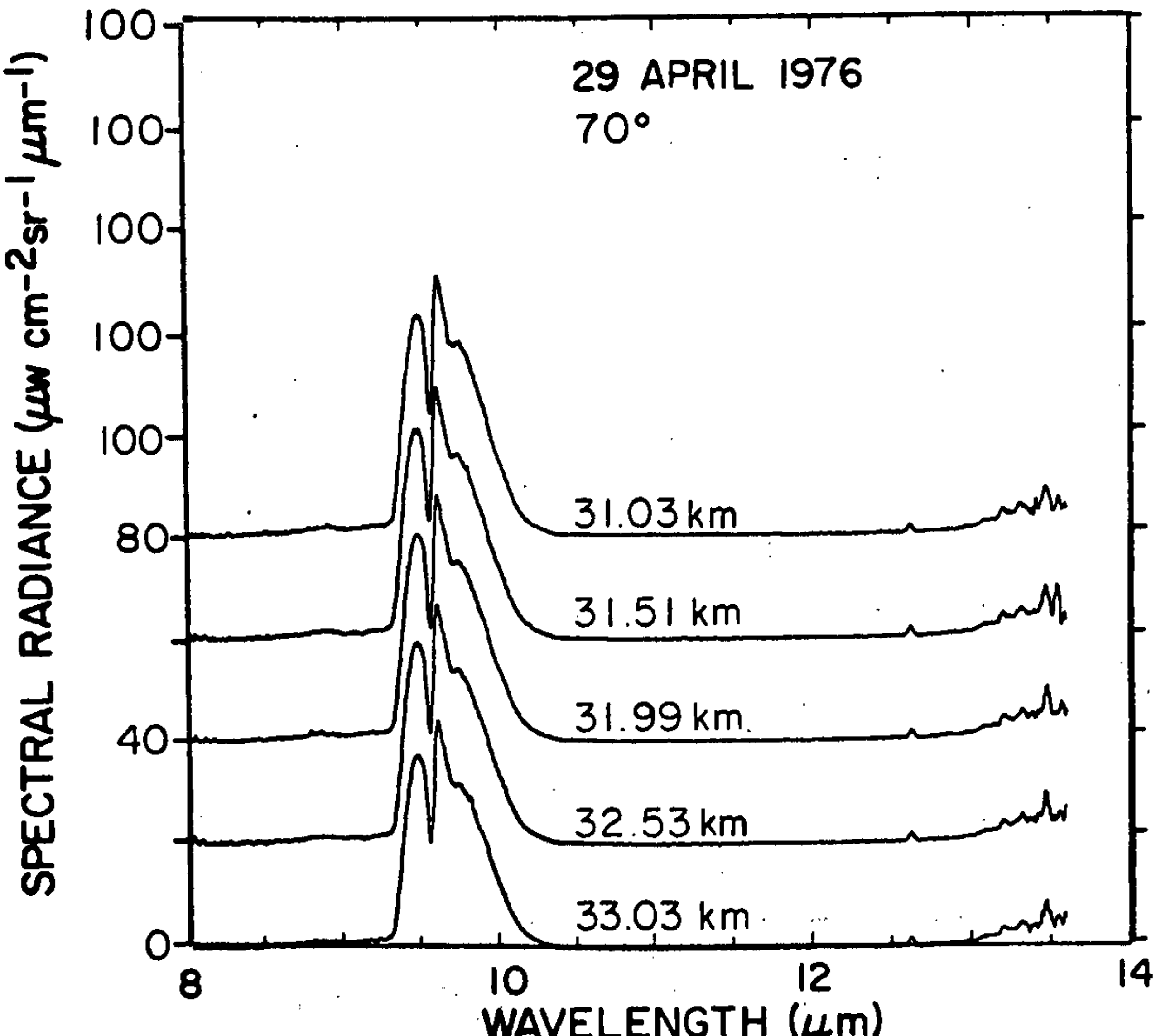

Figure 18. Linear spectral radiance in the 8-13.6μm region at 31.03, 31.51, 31.99, 32.53 and 33.03 km and a zenith angle of 70°. Spectra are offset for clarity.

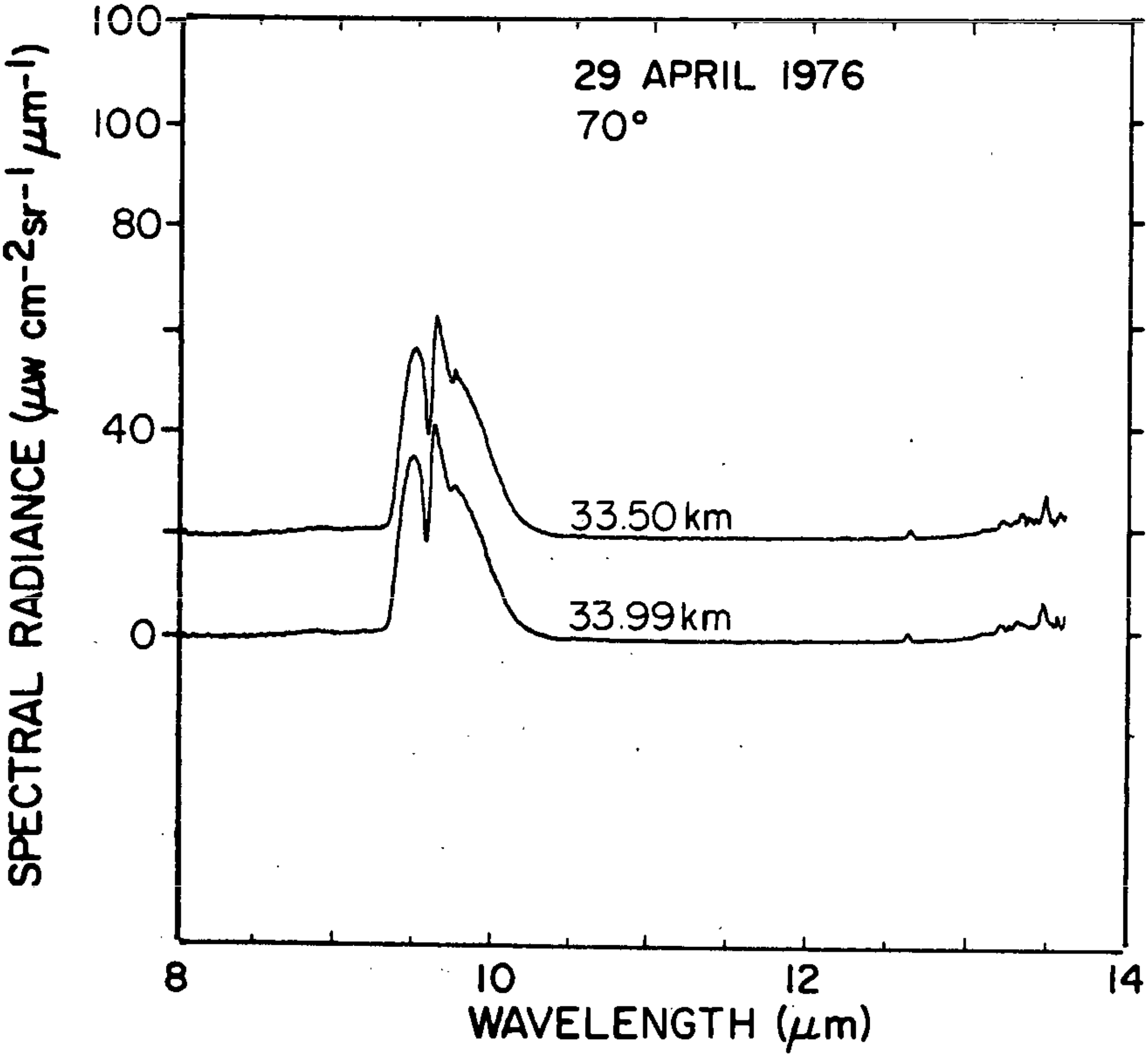

Figure 19. Linear spectral radiance in the 8-13.6μm region at 33.50 and 33.99 km and a zenith angle of 70°. Spectra are offset for clarity.

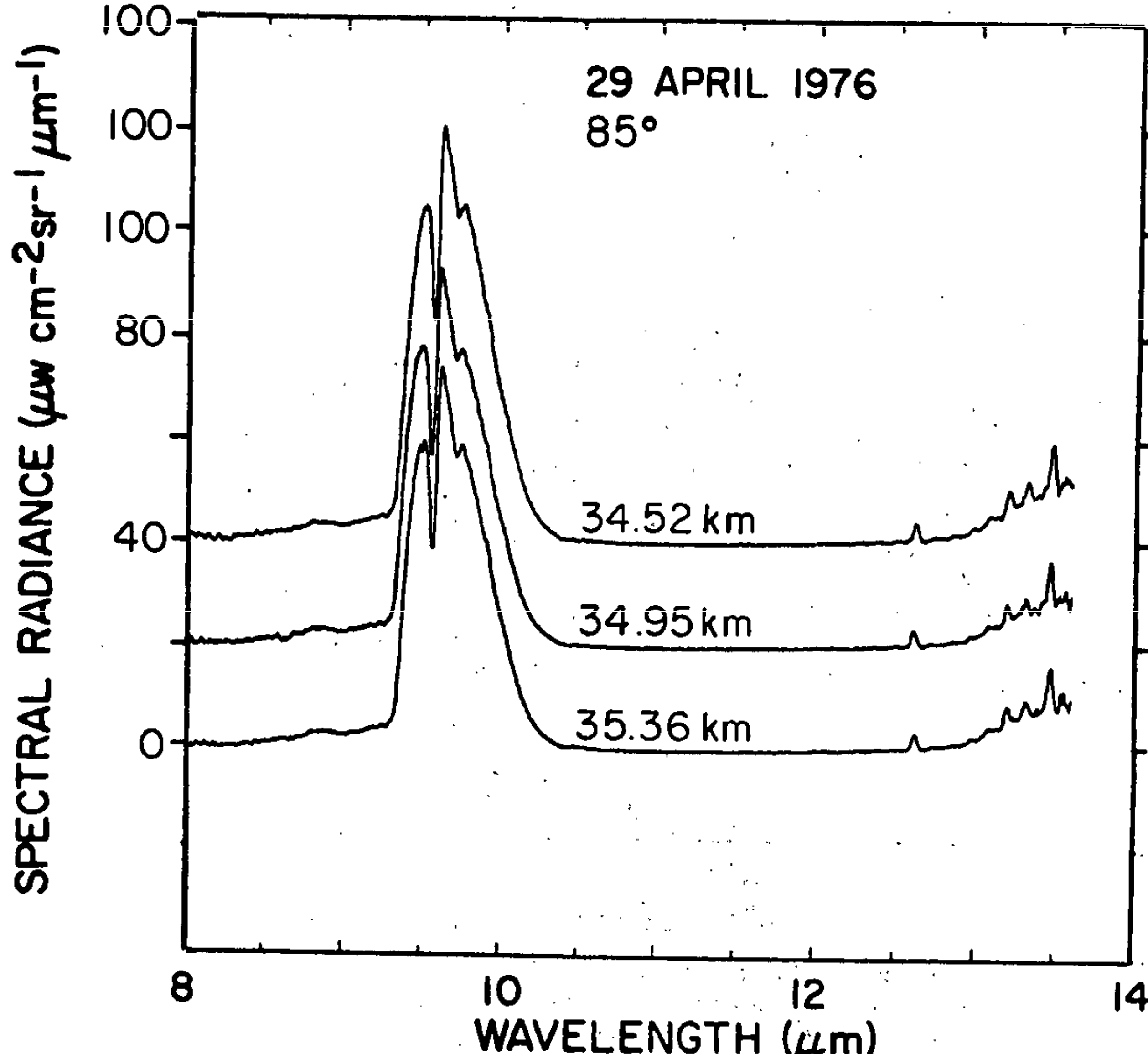

Figure 20. Linear spectral radiance in the 8-13.6μm region at 34.52, 34.95 and 35.36 km and a zenith angle of 85°. Spectra are offset for clarity.

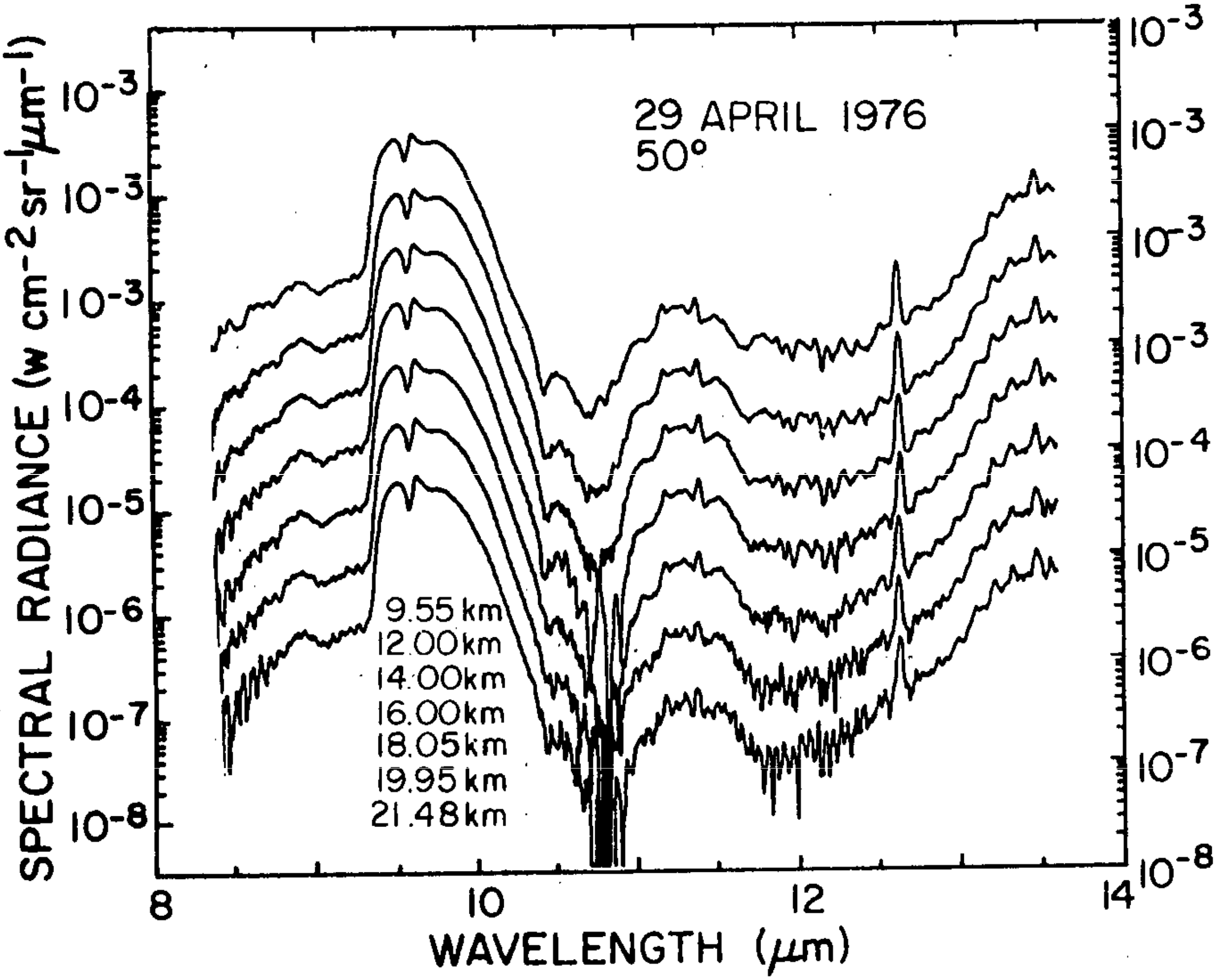

Figure 21. Log spectral radiance in the 8-13.6μm region at 9.55, 12.00, 14.00, 16.00, 18.05, 19.95 and 21.48 km and a zenith angle of 50°. Spectra are offset by 1/2 decade for clarity.

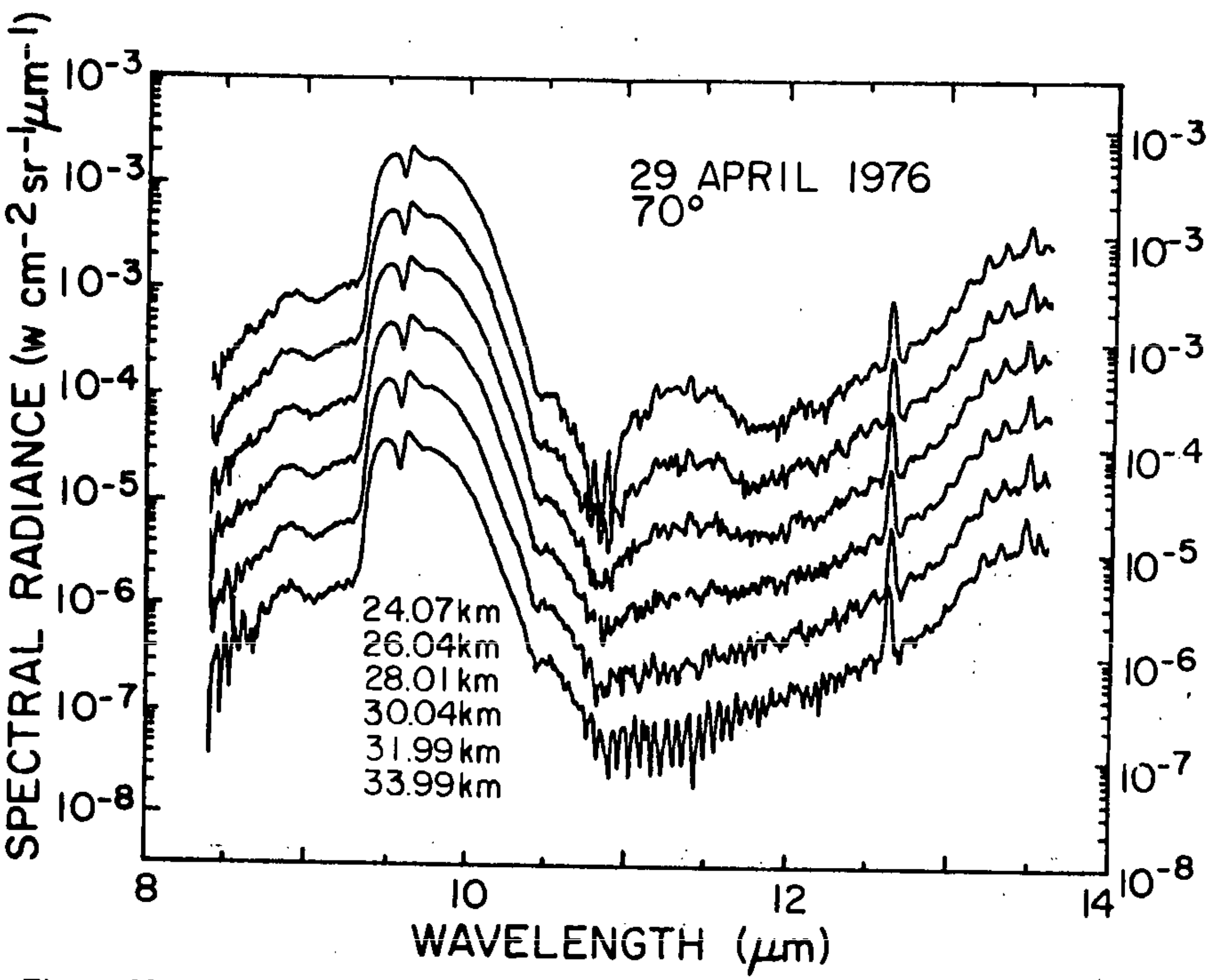

Figure 22. Log spectral radiance in the 8-13.6μm region at 24.07, 26.04, 28.01, 30.04, 31.99 and 33.99 and a zenith angle of 70°. Spectra are offset 1/2 decade for clarity.

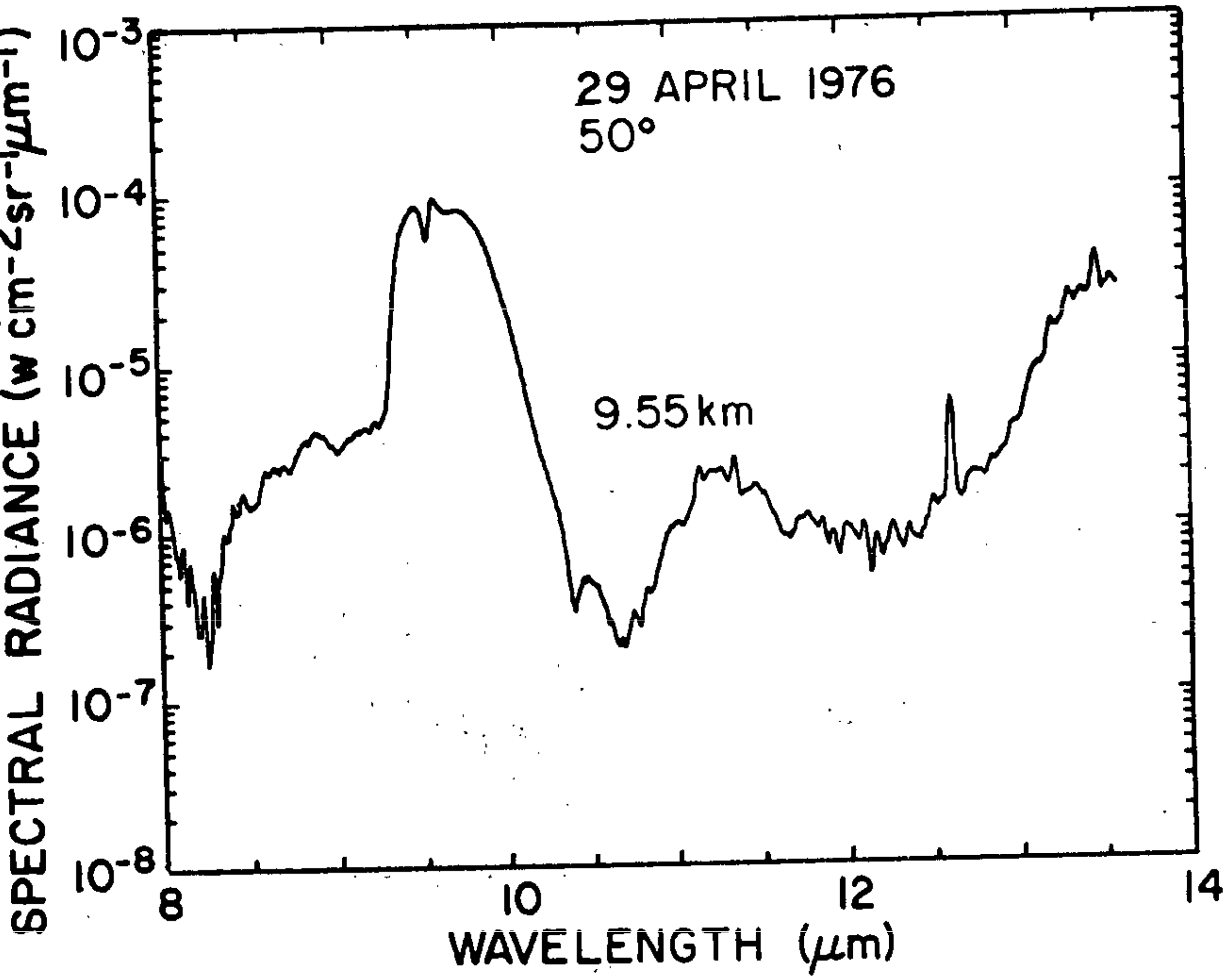

Figure 23. Log spectral radiance in the 8-13.6μm region at 9.55 km and a zenith angle of 50°. Spectrum is a composite of three scans.

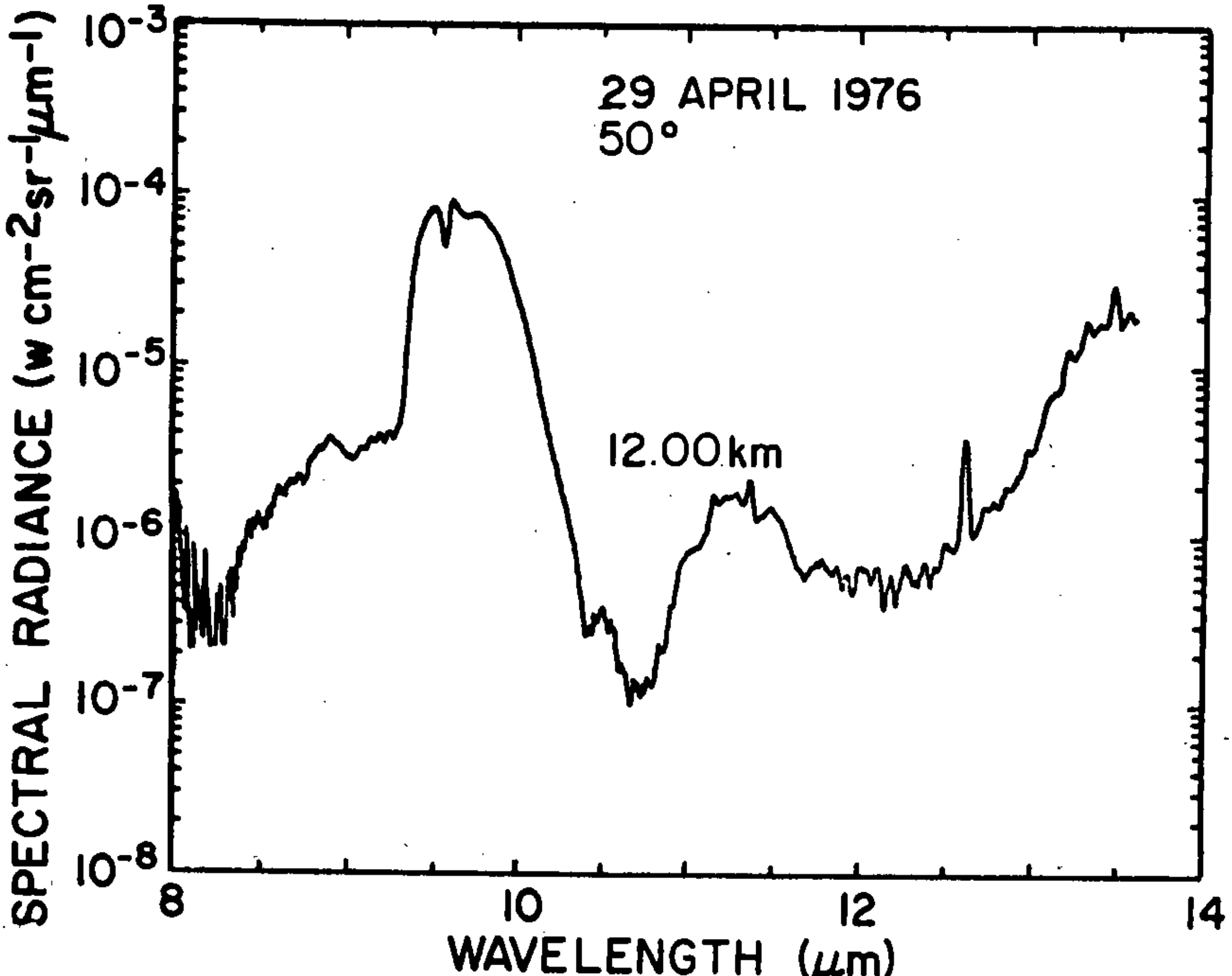

Figure 24. Log spectral radiance in the 8-13.6μm region at 12.00 km and a zenith angle of 50°. Spectrum is a composite of three scans.

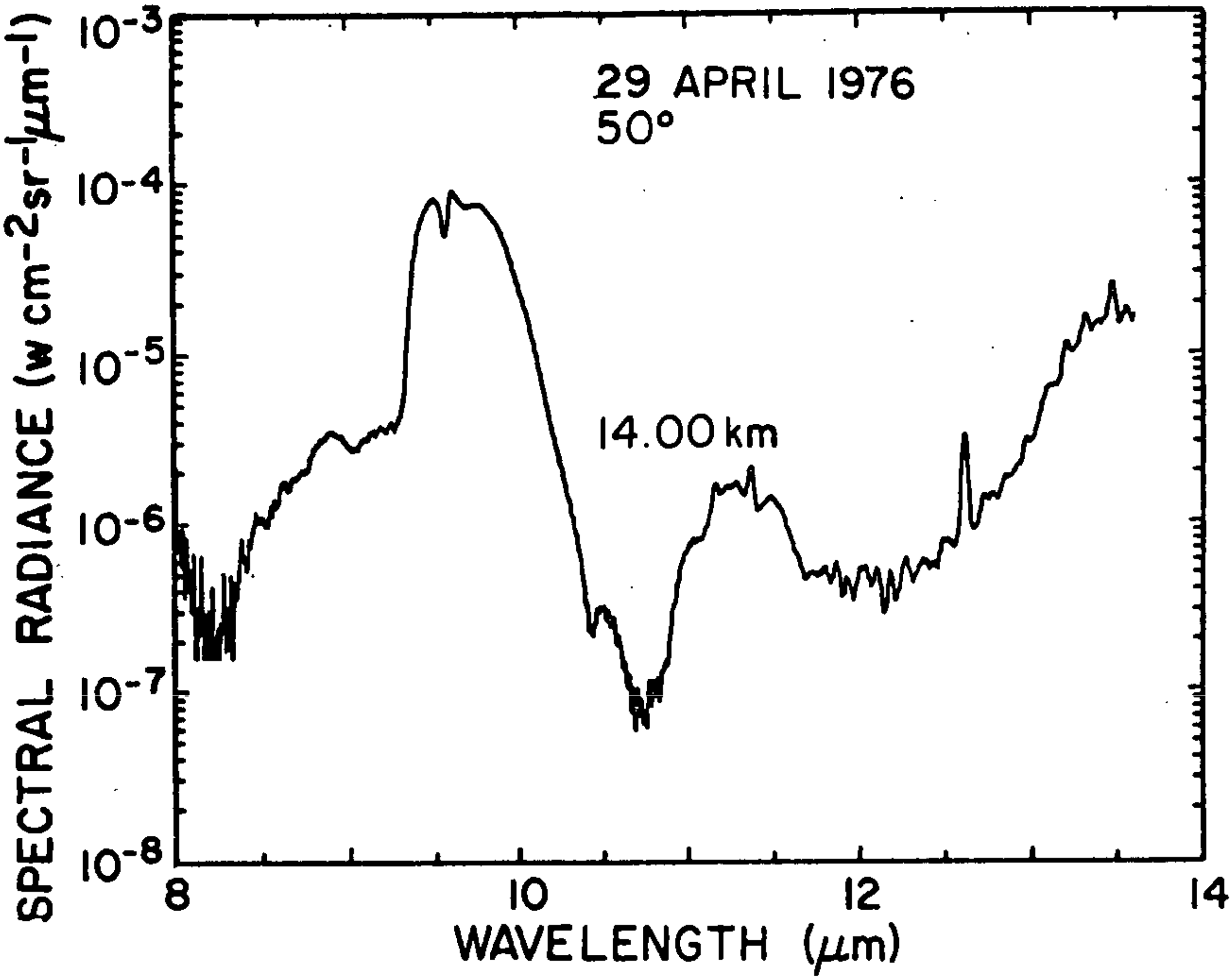

Figure 25. Log spectral radiance in the 8-13.6μm region at 14.00 km and a zenith angle of 50°. Spectrum is a composite of three scans.

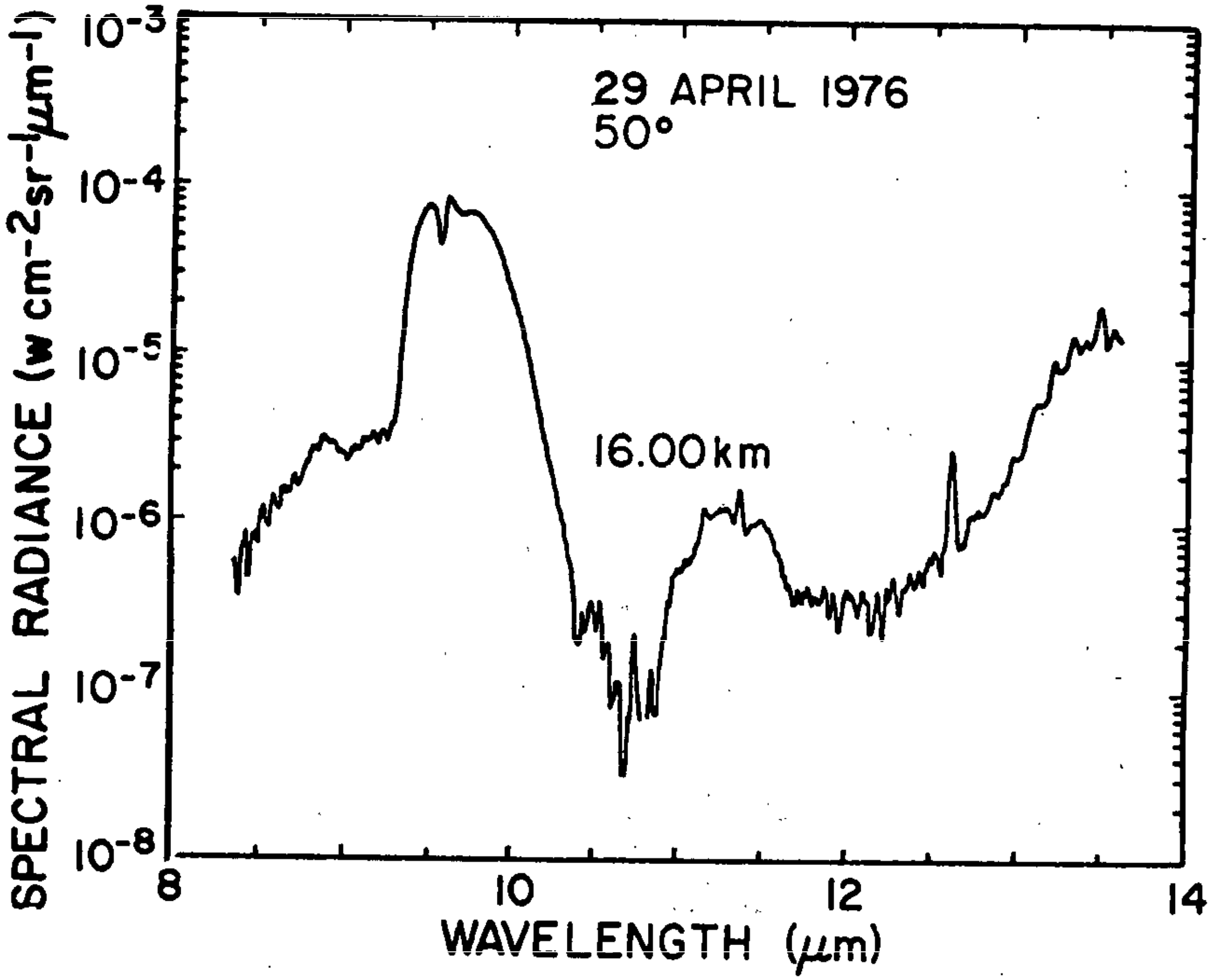

Figure 26. Log spectral radiance in the 8-13.6μm region at 16.00 km and a zenith angle of 50°. Spectrum is a composite of three scans.

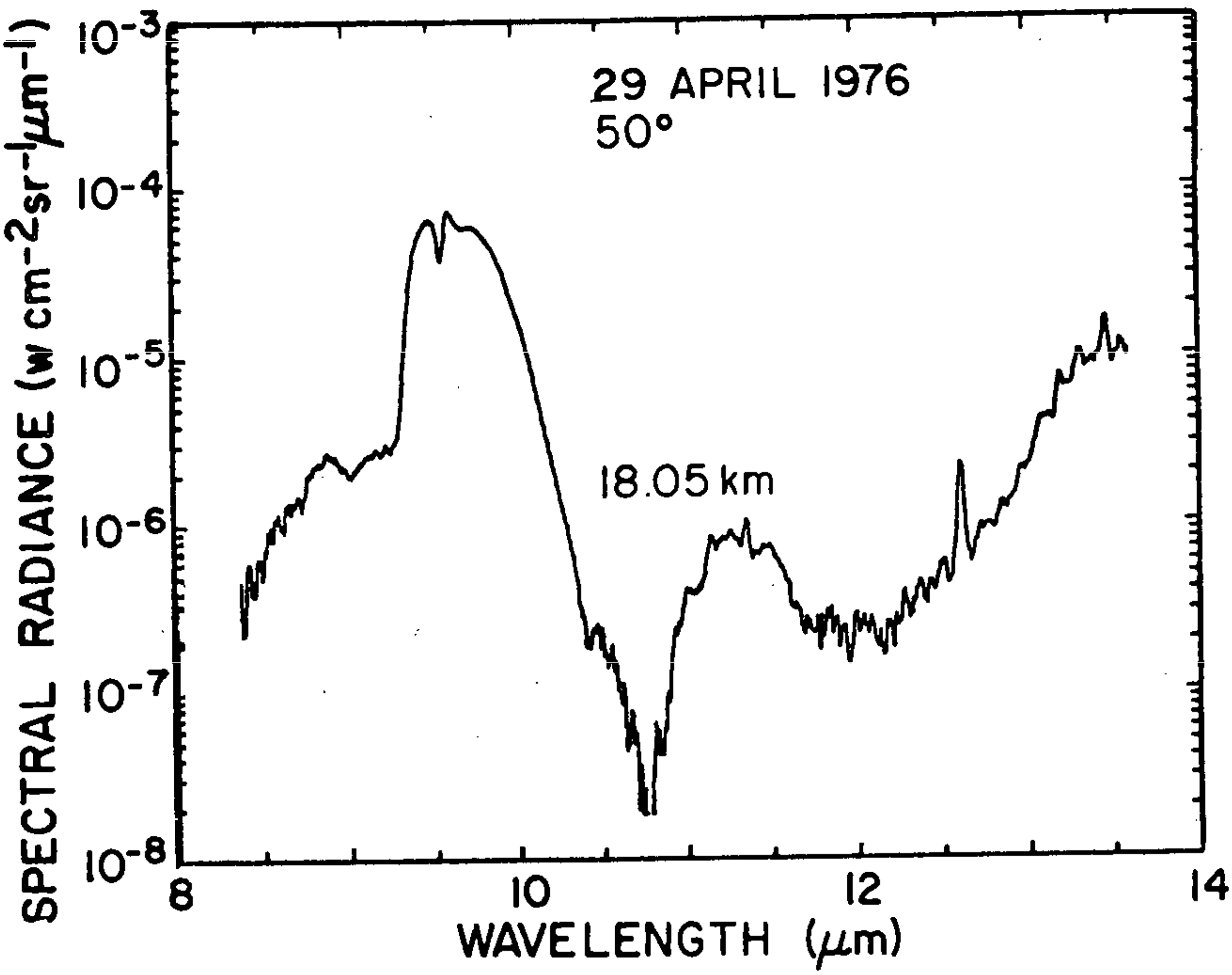

Figure 27. Log spectral radiance in the 8-13.6μm region at 18.05 km and a zenith angle of 50°. Spectrum is a composite of three scans.

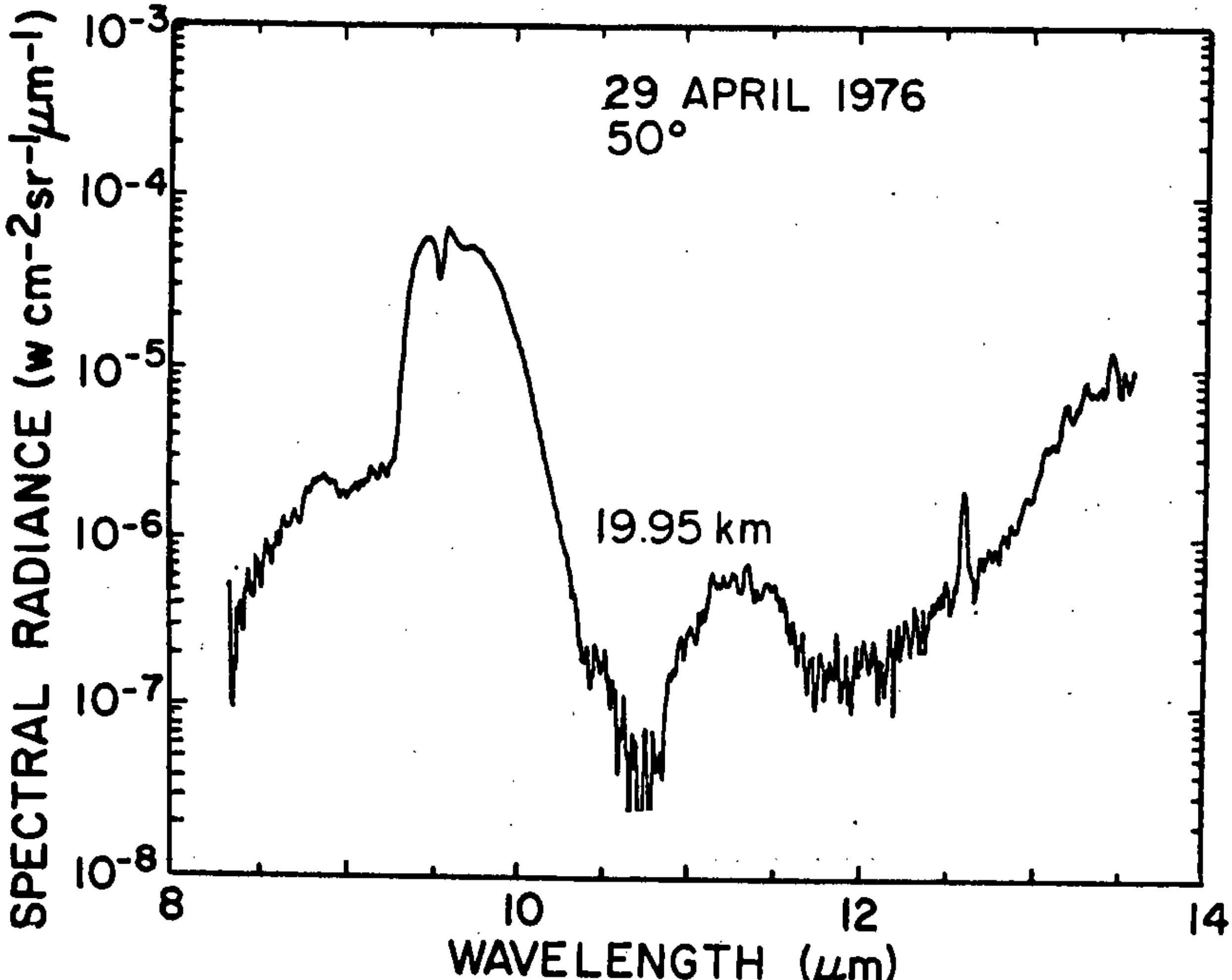

Figure 28. Log spectral radiance in the 8-13.6μm region at 19.95 km and a zenith angle of 50°. Spectrum is a composite of three scans.

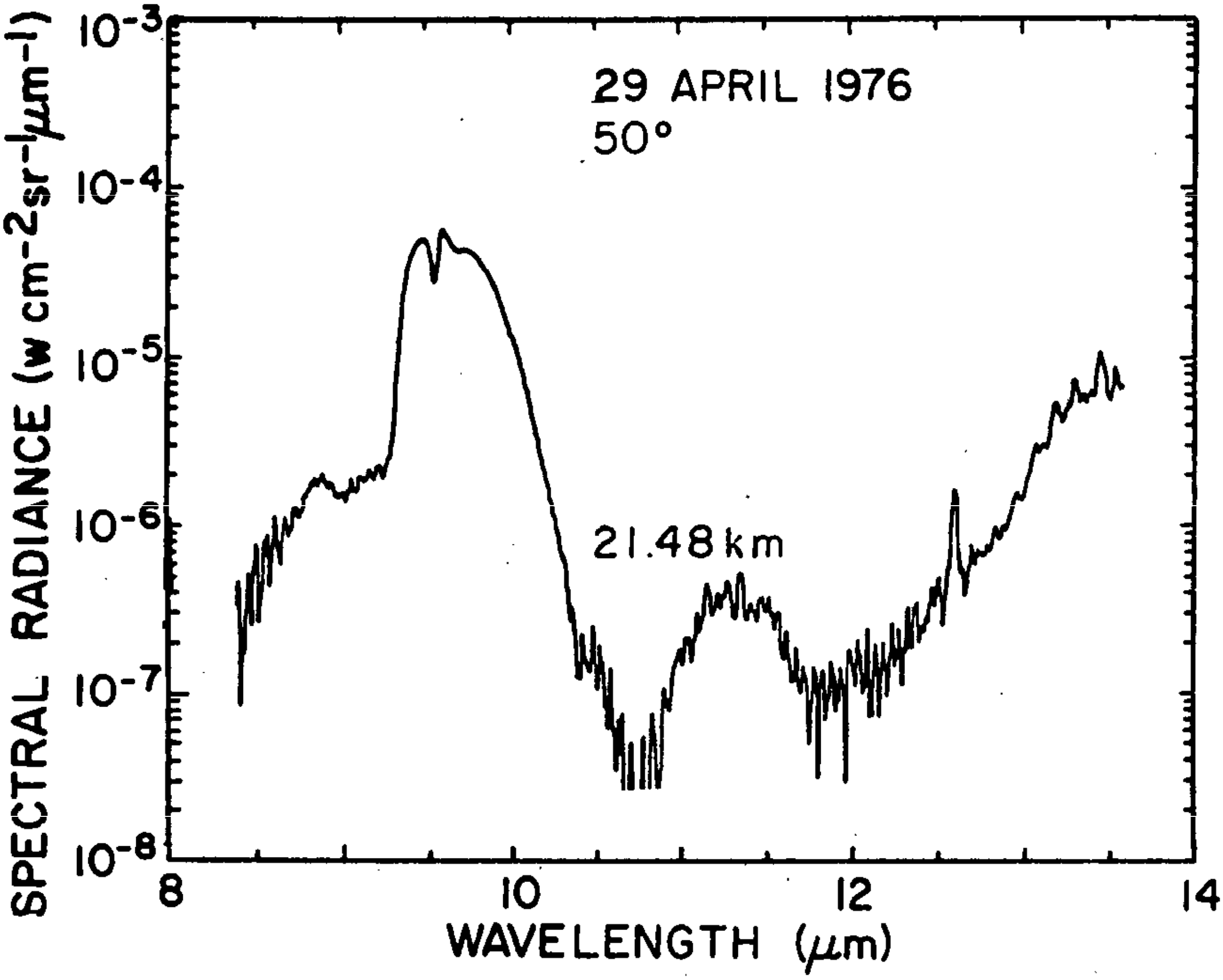

Figure 29. Log spectral radiance in the 8-13.6μm region at 21.48 km and a zenith angle of 50°. Spectrum is a composite of three scans.

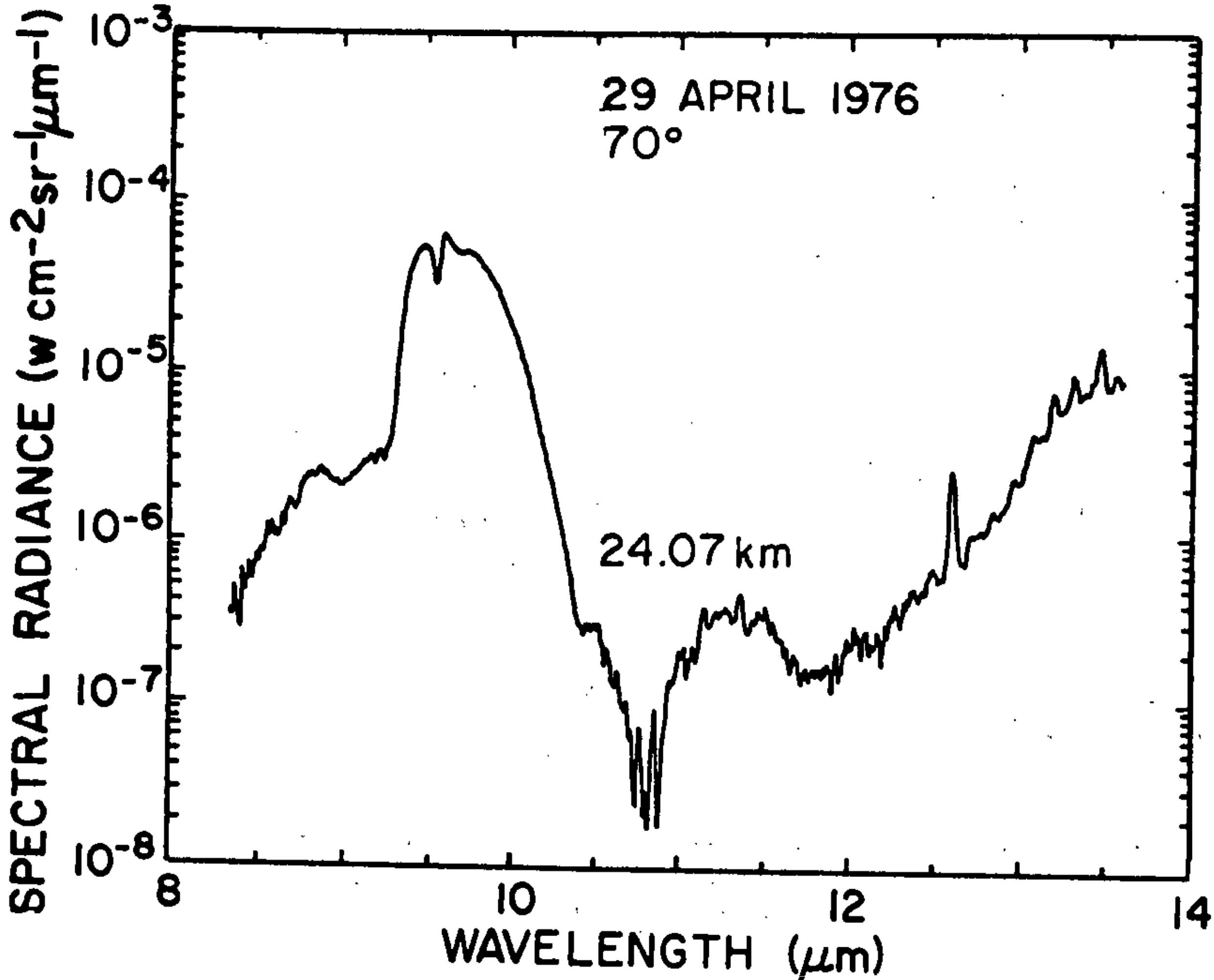

Figure 30. Log spectral radiance in the 8-13.6μm region at 24.07 km and a zenith angle of 70°. Spectrum is a composite of three scans.

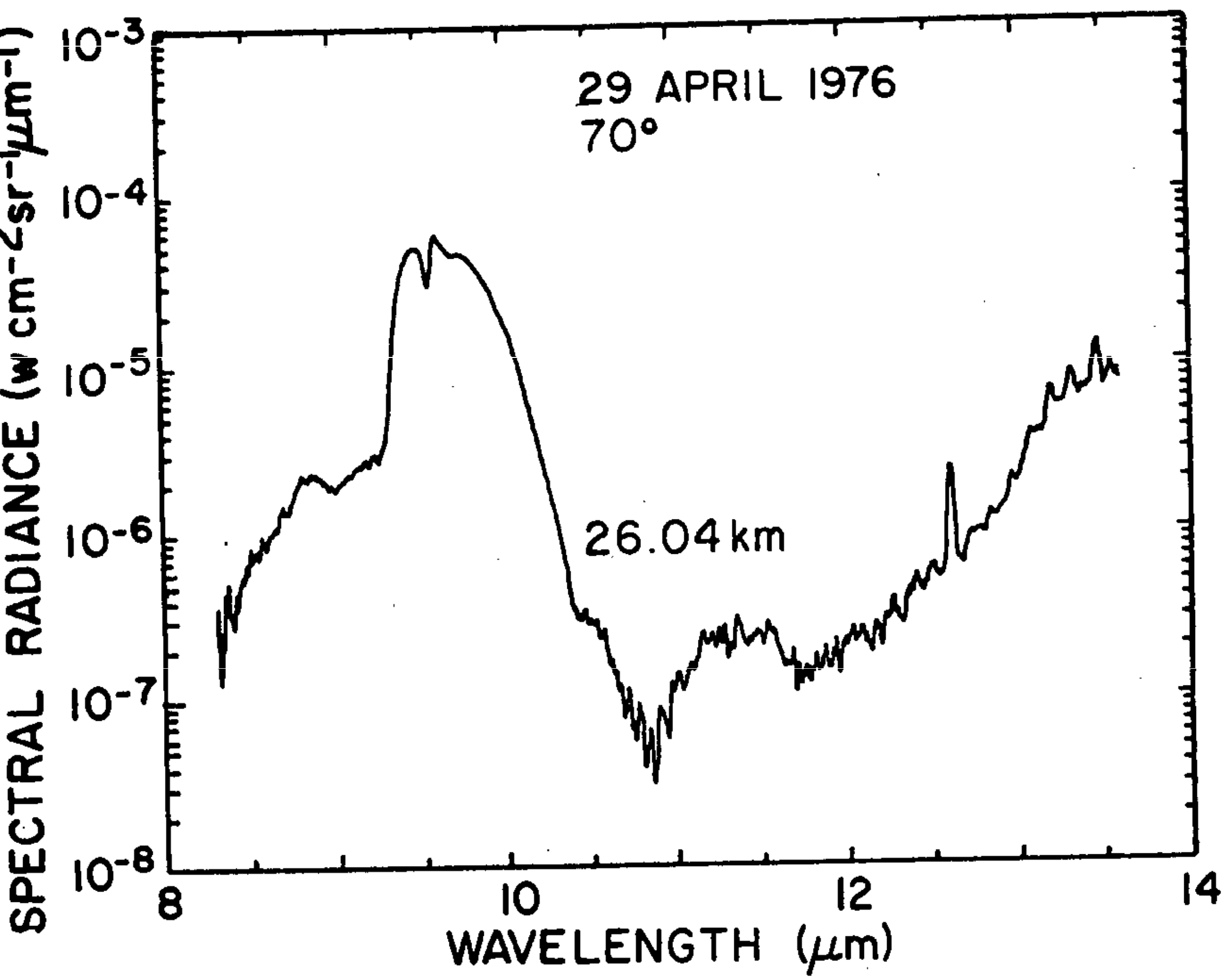

Figure 31. Log spectral radiance in the 8-13.6μm region at 26.04 km and a zenith angle of 70°. Spectrum is a composite of three scans.

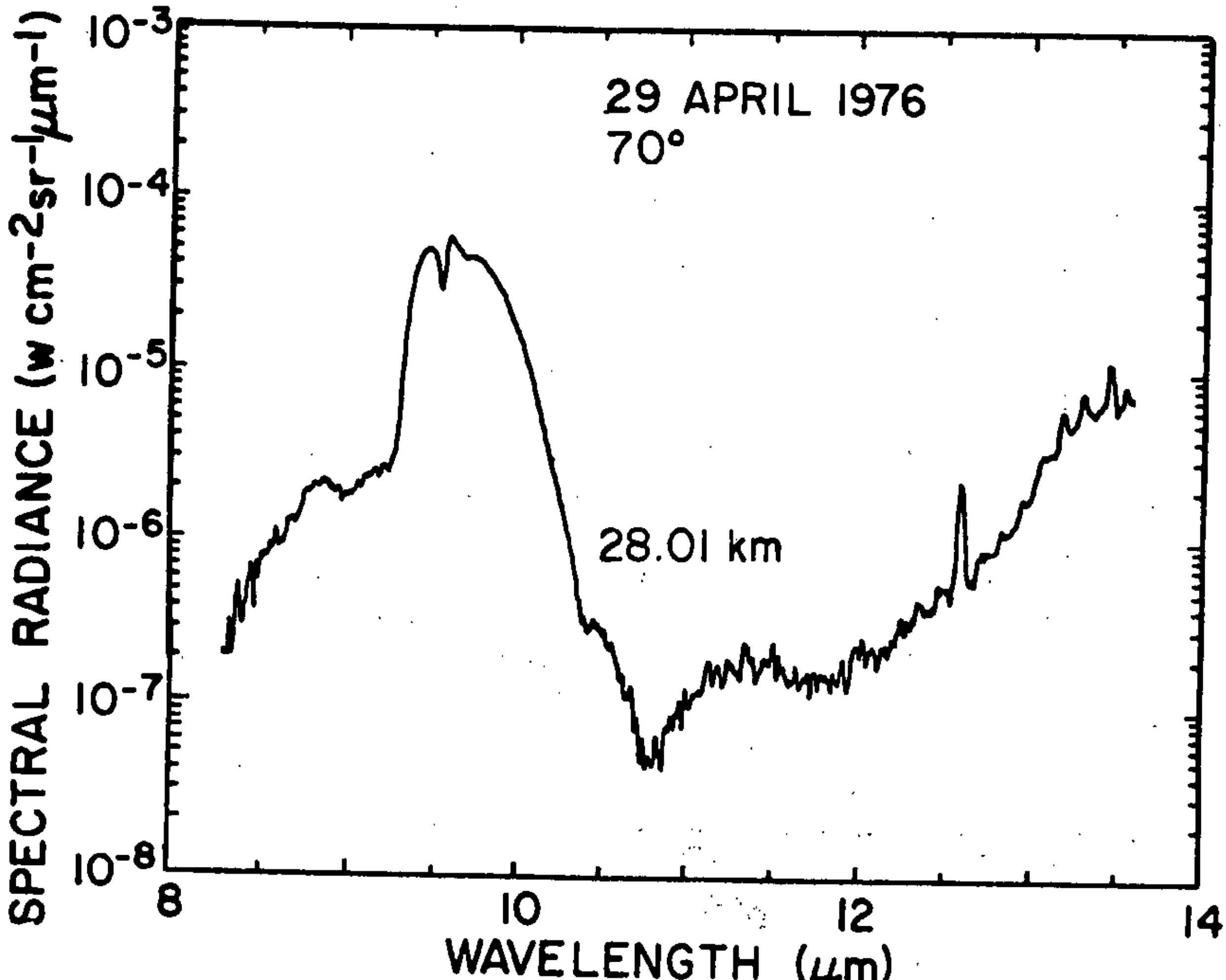

Figure 32. Log spectral radiance in the 8-13.6μm region at 28.01 km and a zenith angle of 70°. Spectrum is a composite of three scans.

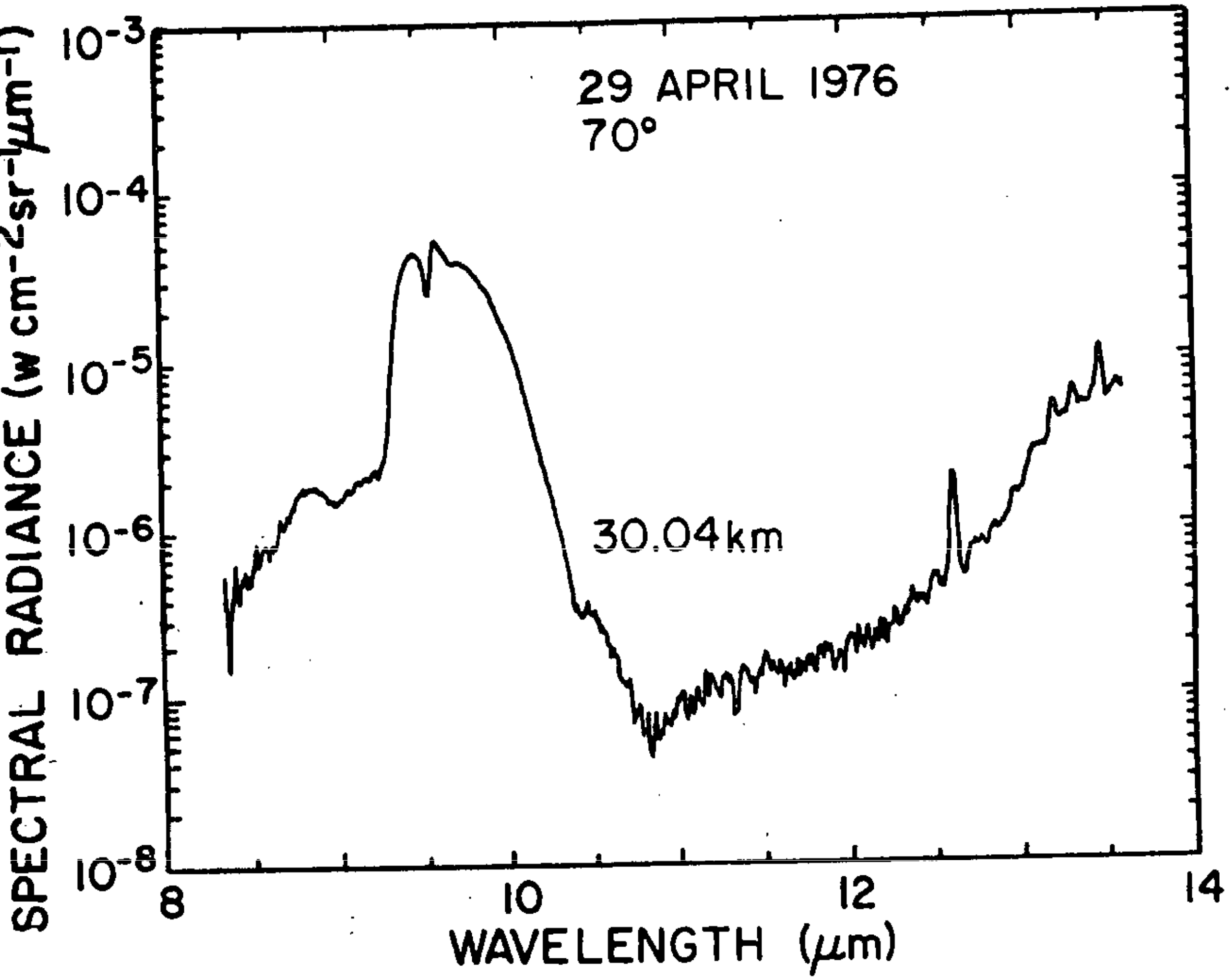

Figure 33. Log spectral radiance in the 8-13.6μm region at 30.04 km and a zenith angle of 70°. Spectrum is a composite of three scans.

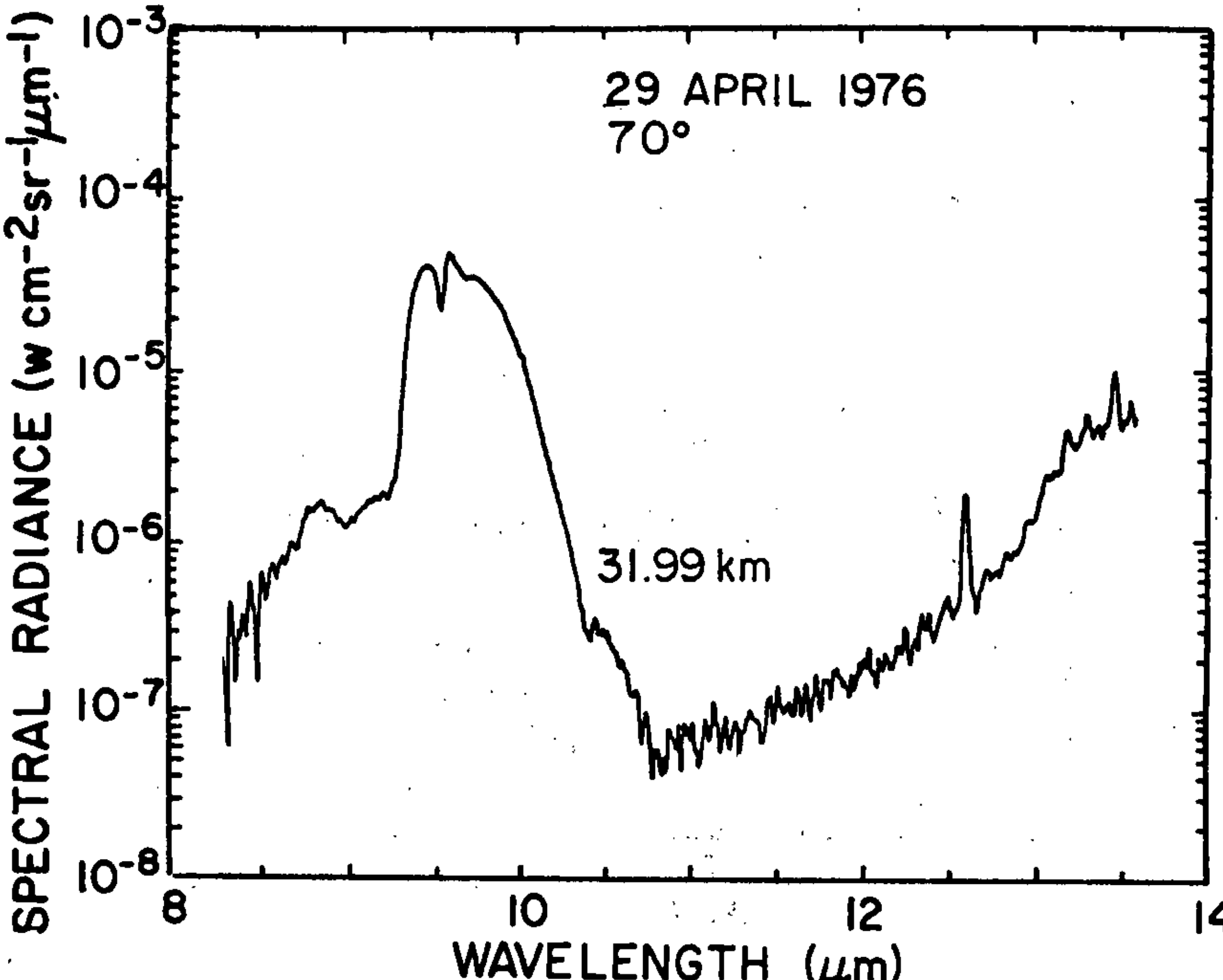

Figure 34. Log spectral radiance in the 8-13.6μm region at 31.99 km and a zenith angle of 70°. Spectrum is a composite of three scans.

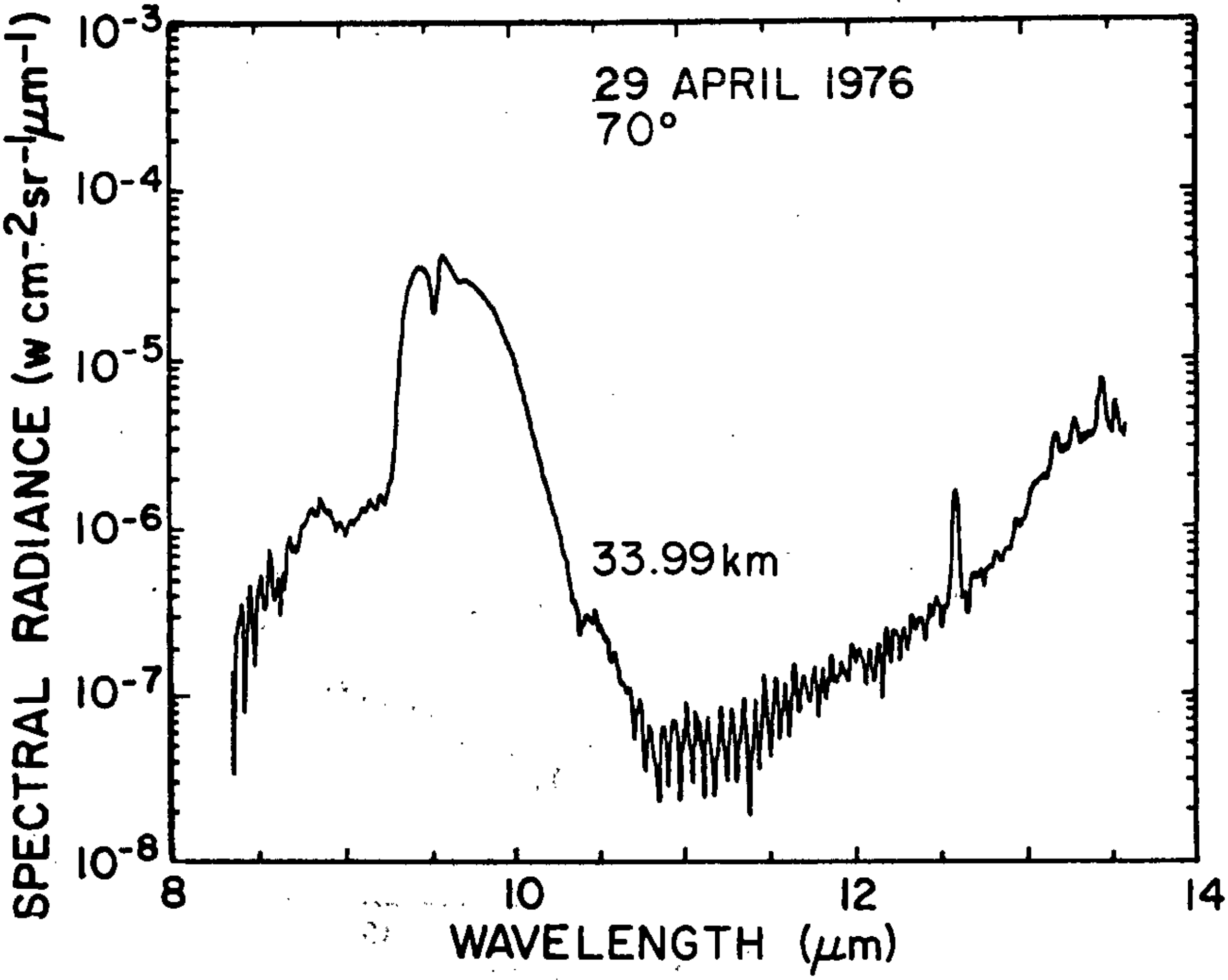

Figure 35. Log spectral radiance in the 8-13.6 μm region at 33.99 km and a zenith angle of 70°. Spectrum is a composite of three scans.

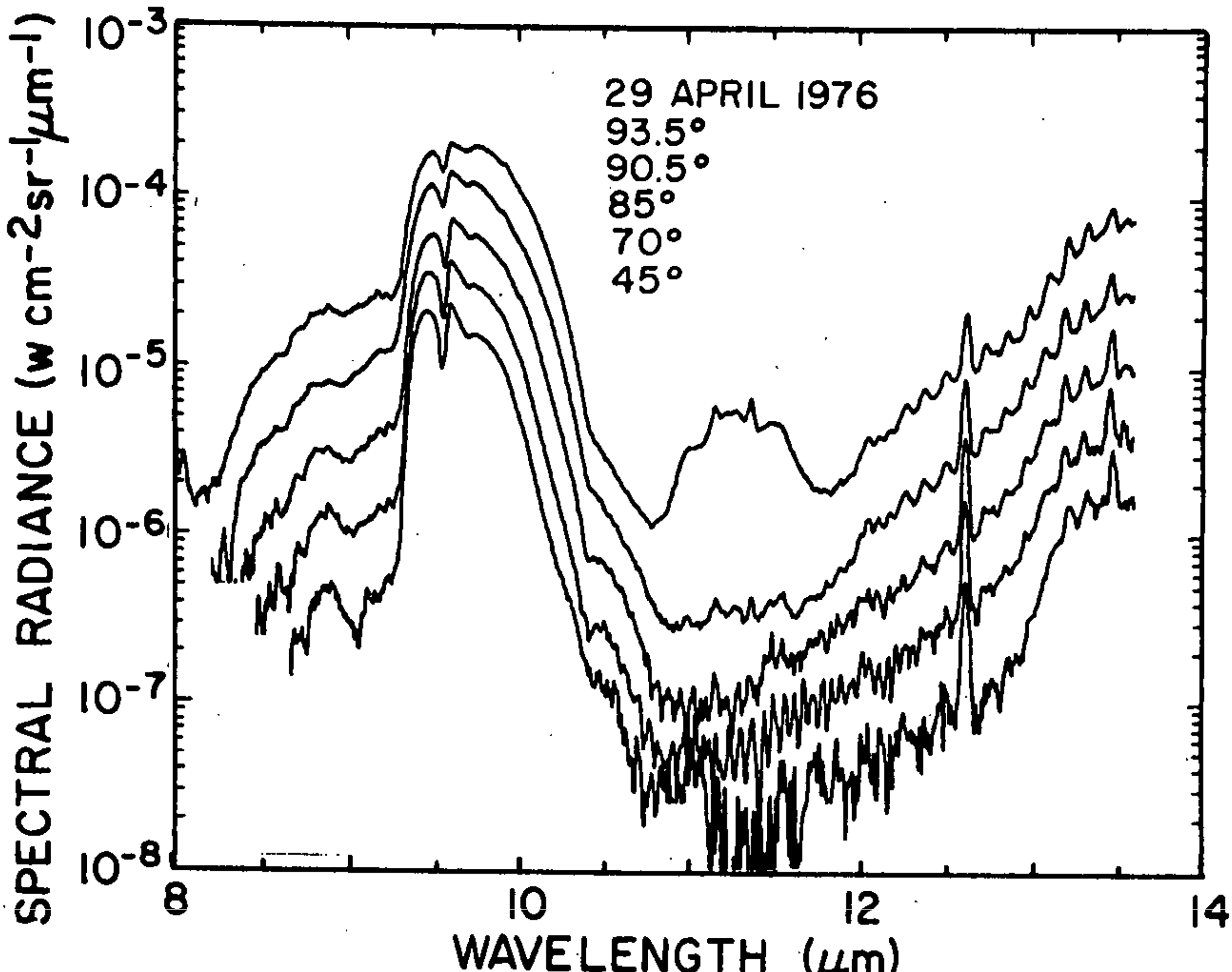

Figure 36. Log spectral radiance in the 8-13.6μm region near 36 km as a function of zenith angle. Scans are not offset. Each spectrum is a composite of four or more scans.

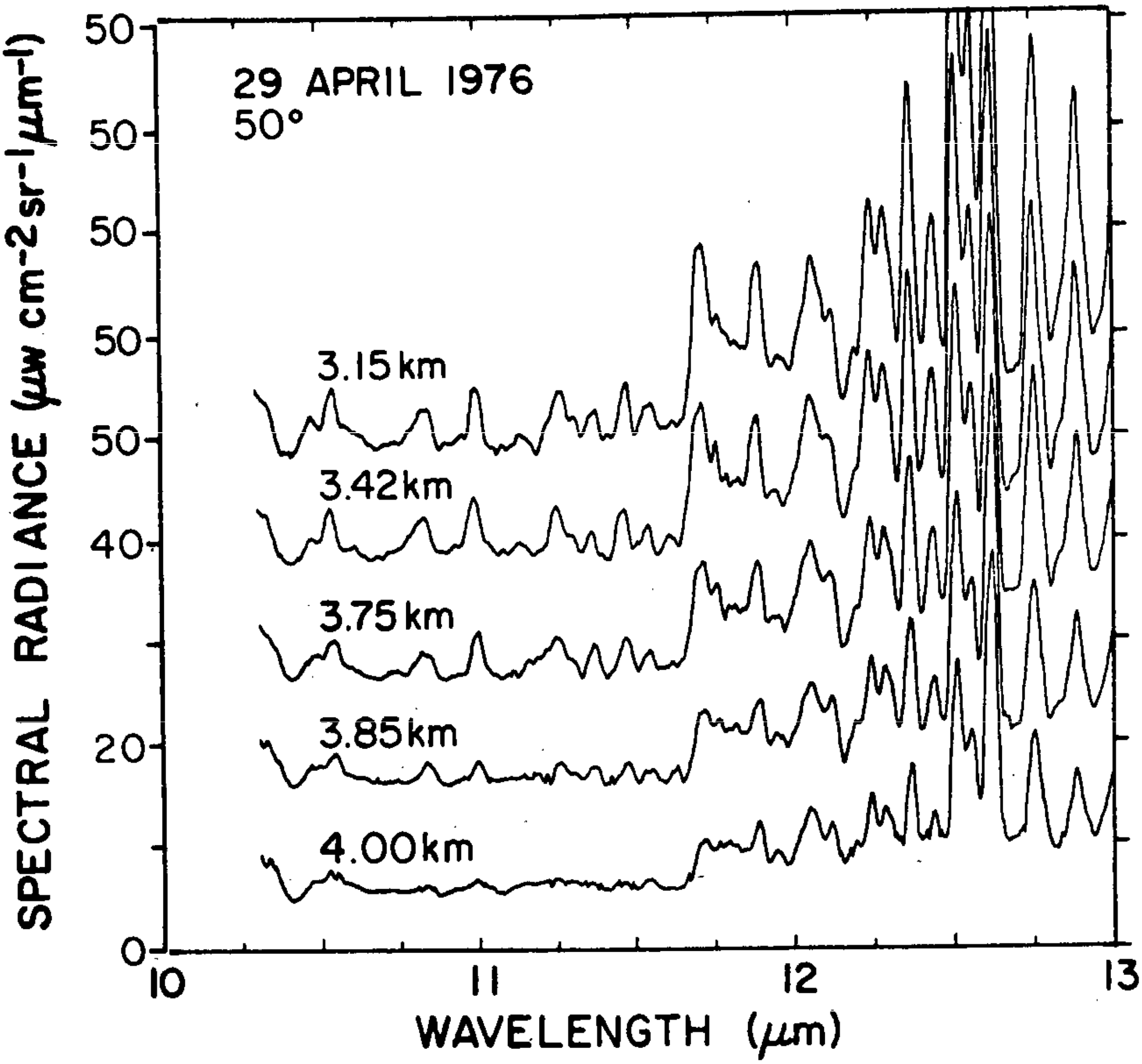

Figure 37. Linear spectral radiance in the 10.3-13μm region at 3.15, 3.42, 3.75, 3.85 and 4.00 km and a zenith angle of 50°. Spectra are offset for clarity.

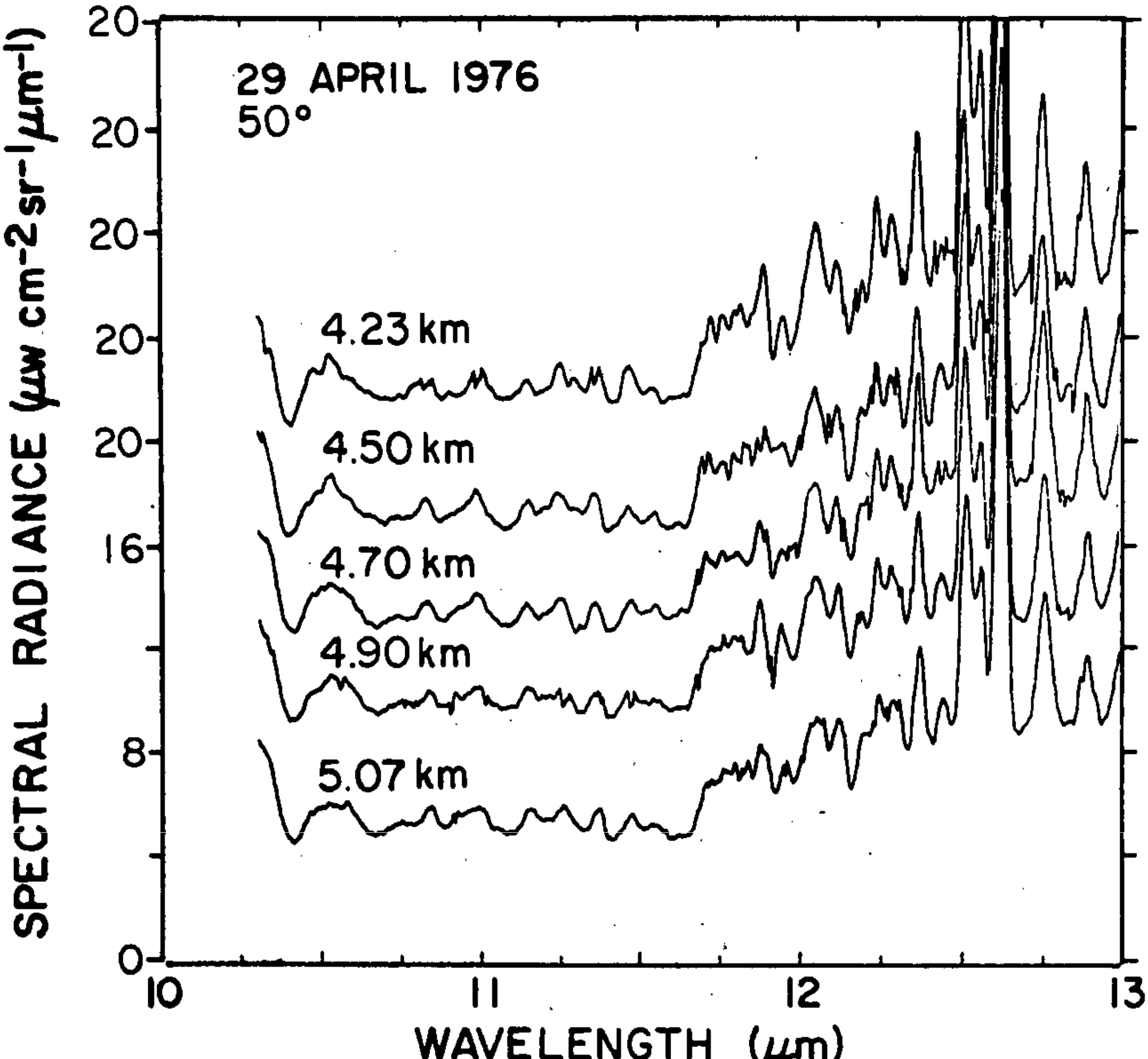

Figure 38. Linear spectral radiance in the 10.3-13μm region at 4.23, 4.50, 4.70, 4.90 and 5.07 km and a zenith angle of 50°. Spectra are offset for clarity.

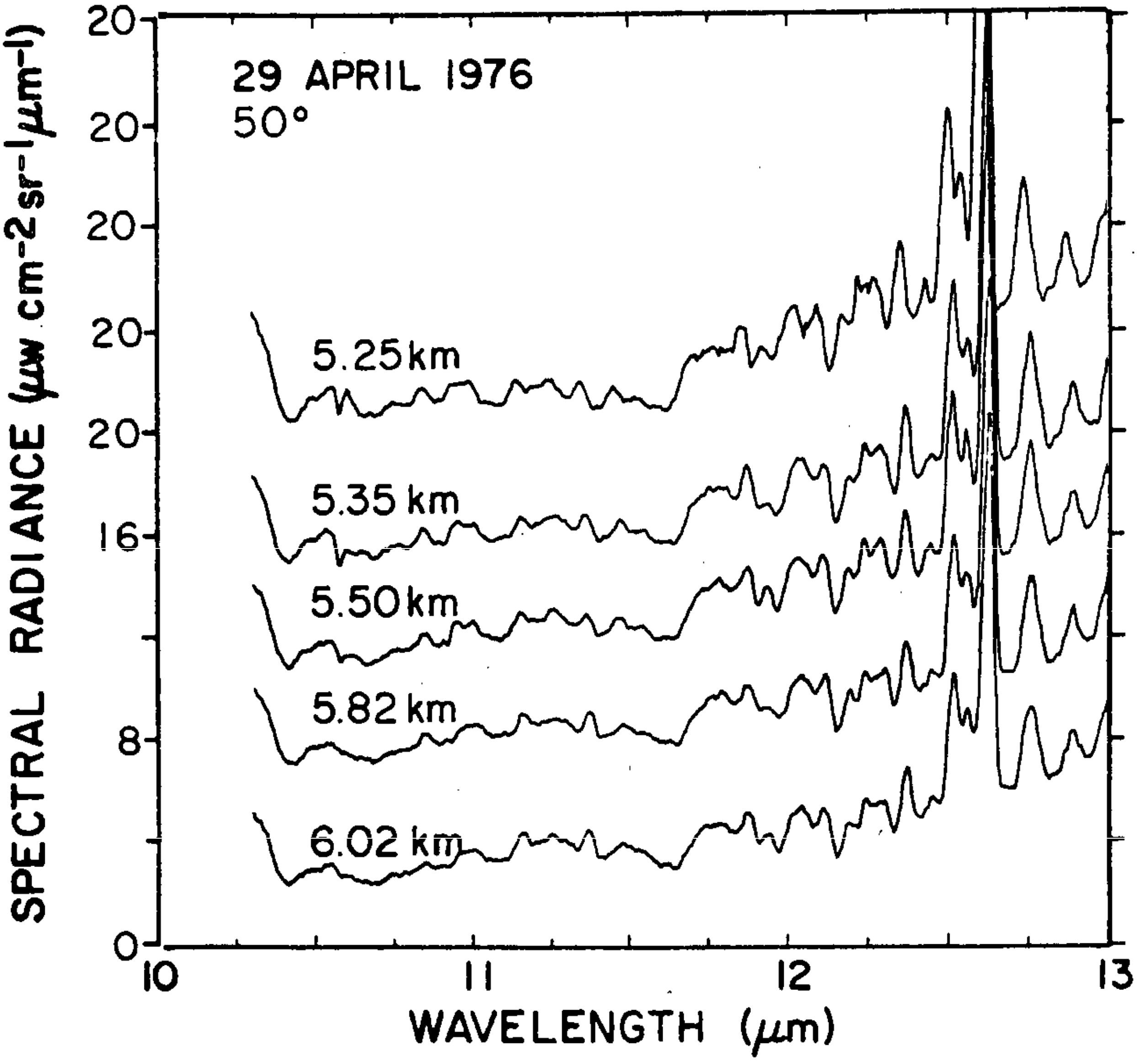

Figure 39. Linear spectral radiance in the 10.3-13μm region at 5.25, 5.35, 5.50, 5.82 and 6.02 km and a zenith angle of 50°. Spectra are offset for clarity.

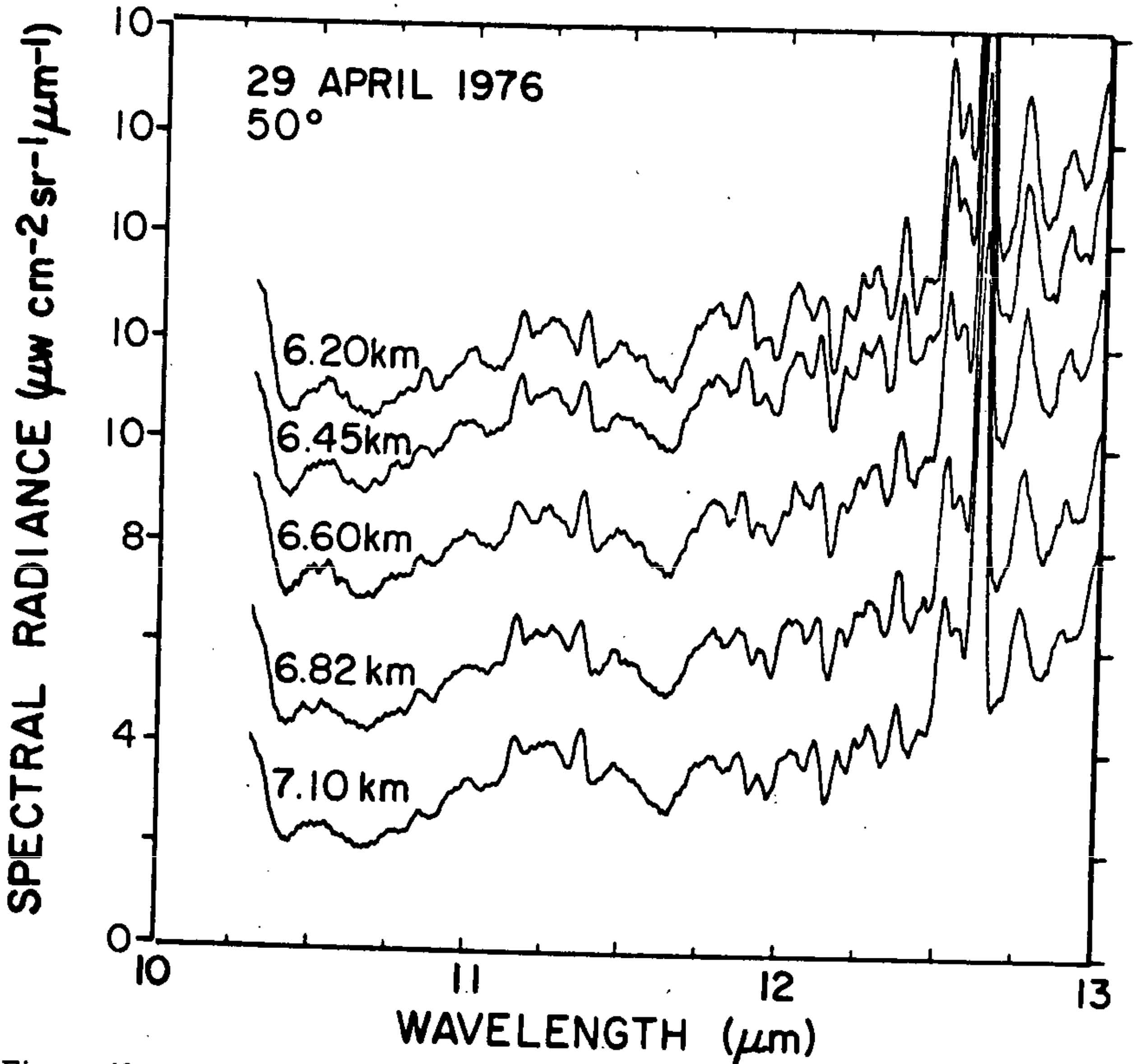

Figure 40. Linear spectral radiance in the 10.3-13μm region at 6.20, 6.45, 6.60, 6.82 and 7.10 km and a zenith angle of 50°. Spectra are offset for clarity.

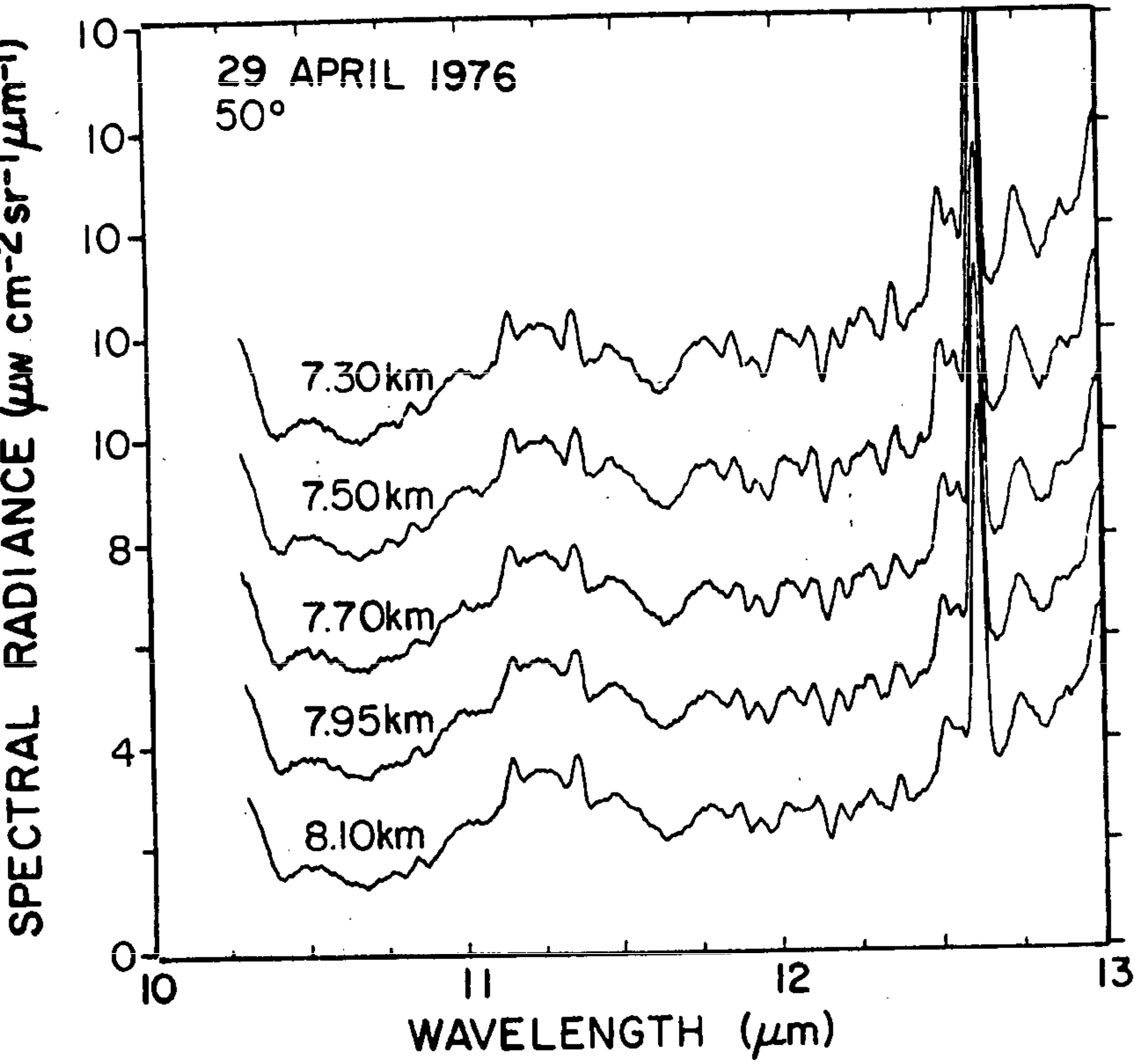

Figure 41. Linear spectral radiance in the 10.3-13μm region at 7.30, 7.50, 7.70, 7.95 and 8.10 km and a zenith angle of 50°. Spectra are offset for clarity.

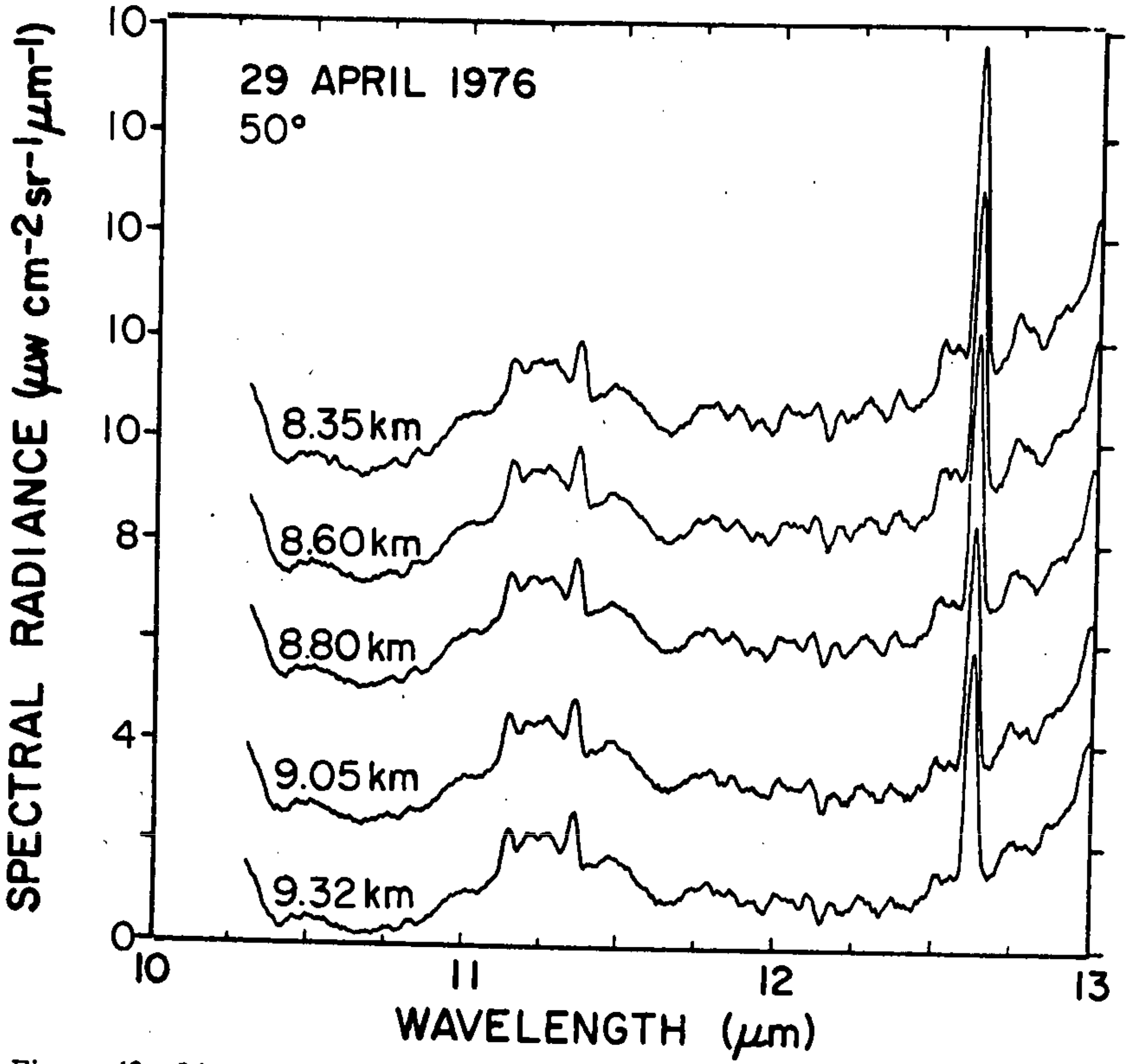

Figure 42. Linear spectral radiance in the 10.3-13μm region at 8.35, 8.60, 8.80, 9.05 and 9.32 km and a zenith angle of 50°. Spectra are offset for clarity.

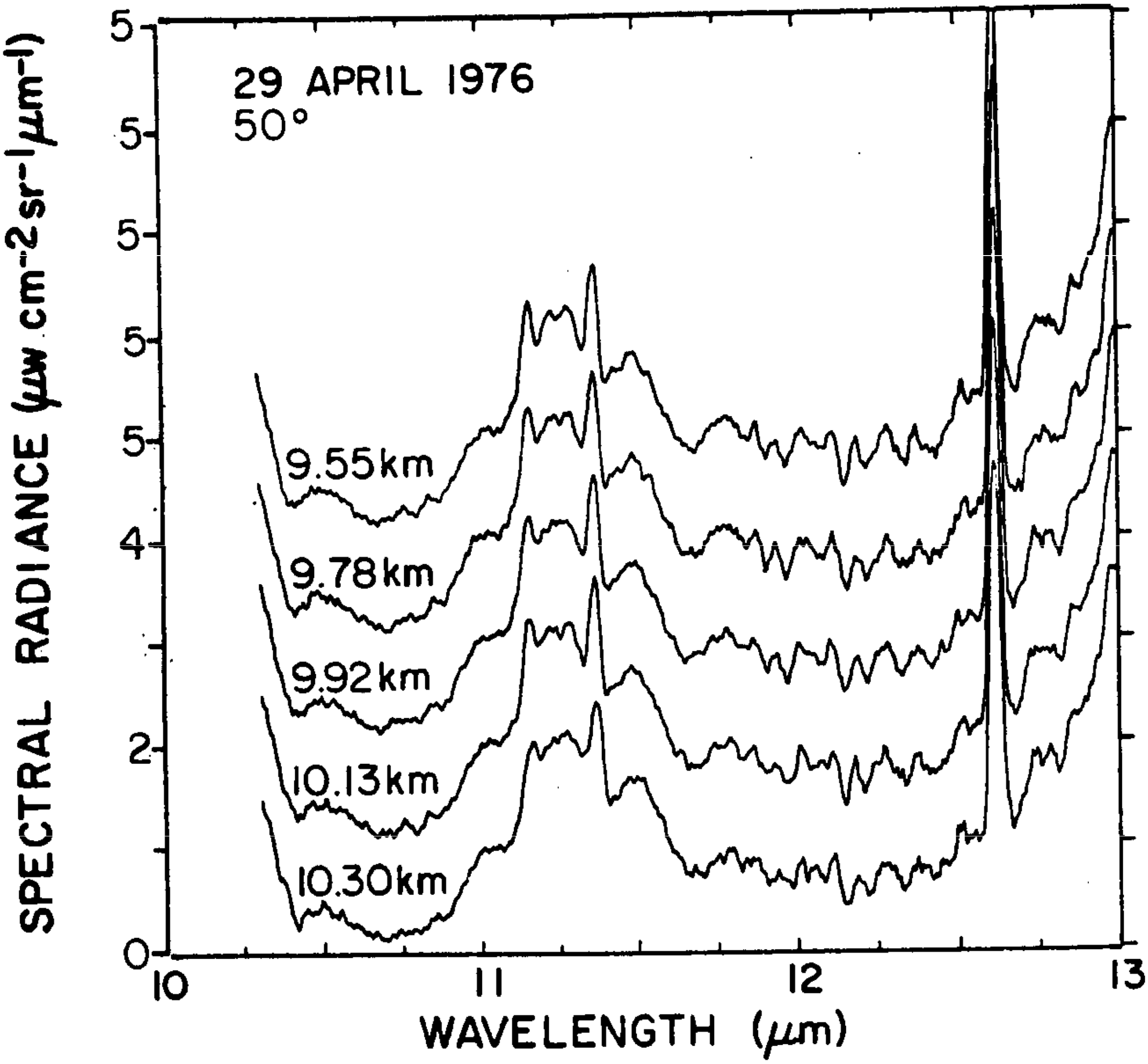

Figure 43. Linear spectral radiance in the 10.3-13μm region at 9.55, 9.78, 9.92, 10.13 and 10.30 km and a zenith angle of 50°. Spectra are offset for clarity.

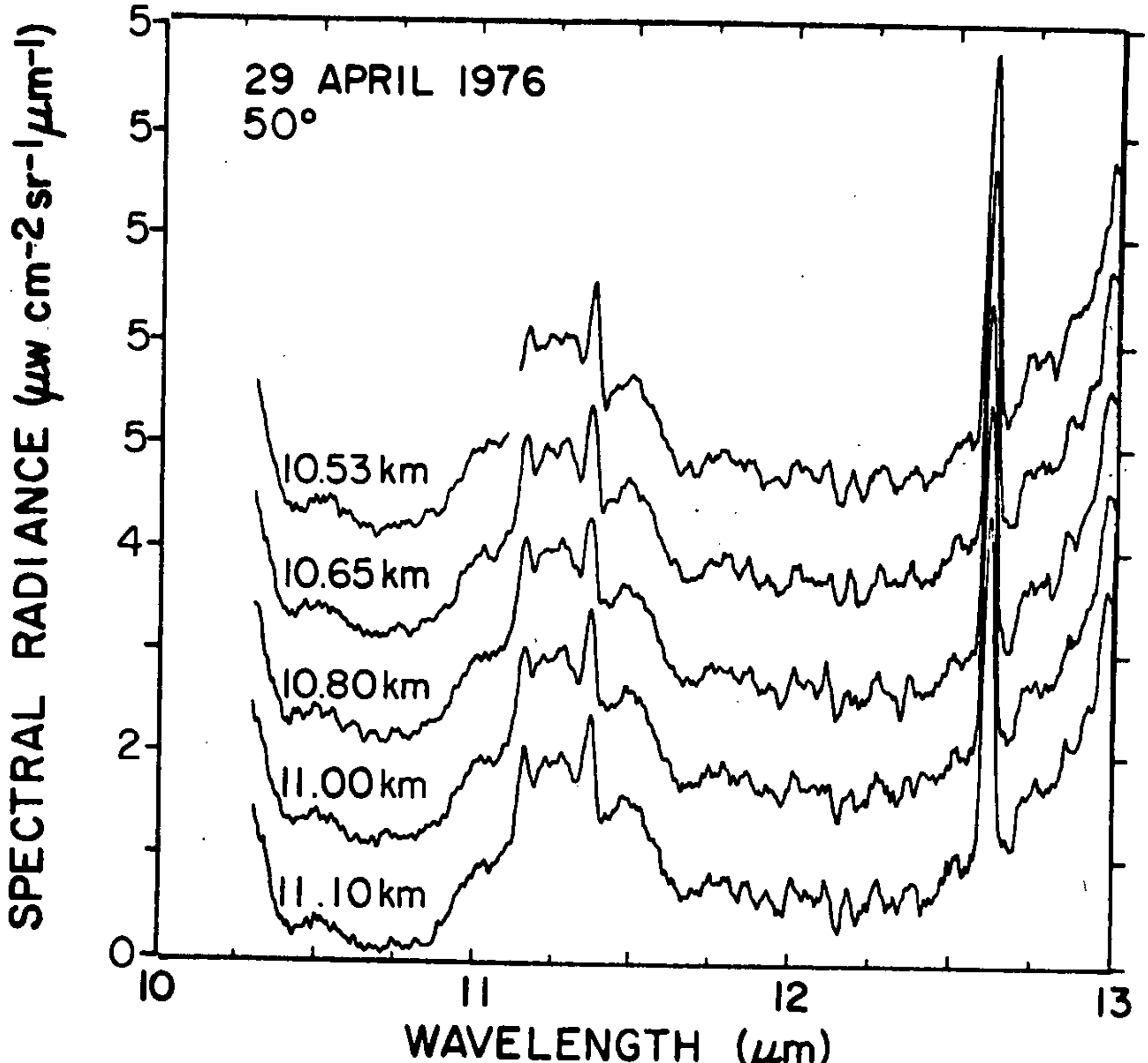

Figure 44. Linear spectral radiance in the 10.3-13μm region at 10.53, 10.65, 10.80, 11.00 and 11.10 km and a zenith angle of 50°. Spectra are offset for clarity.

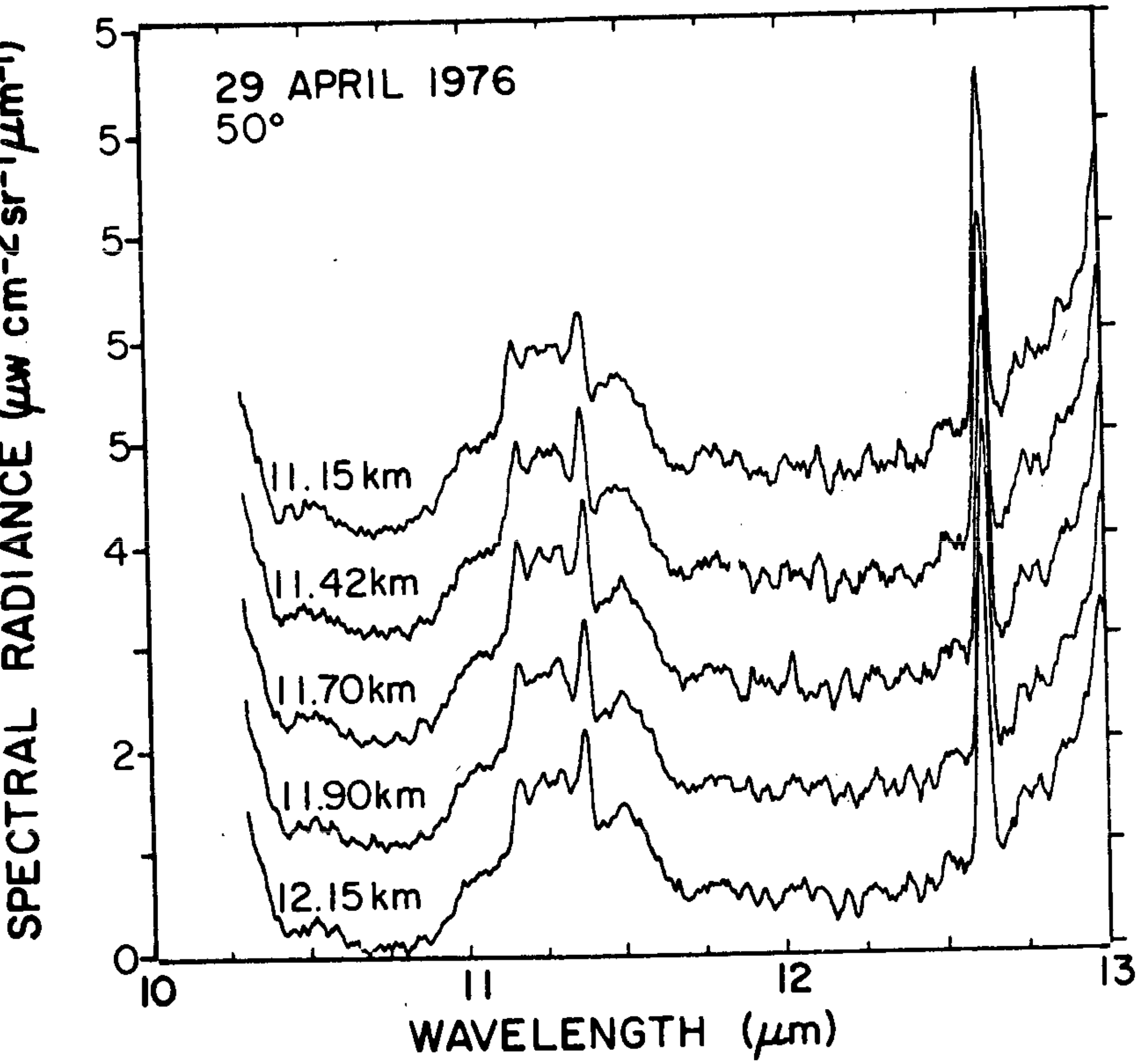

Figure 45. Linear spectral radiance in the 10.3-13μ m region at 11.15, 11.42, 11.70, 11.90 and 12.15 km and a zenith angle of 50°. Spectra are offset for clarity.

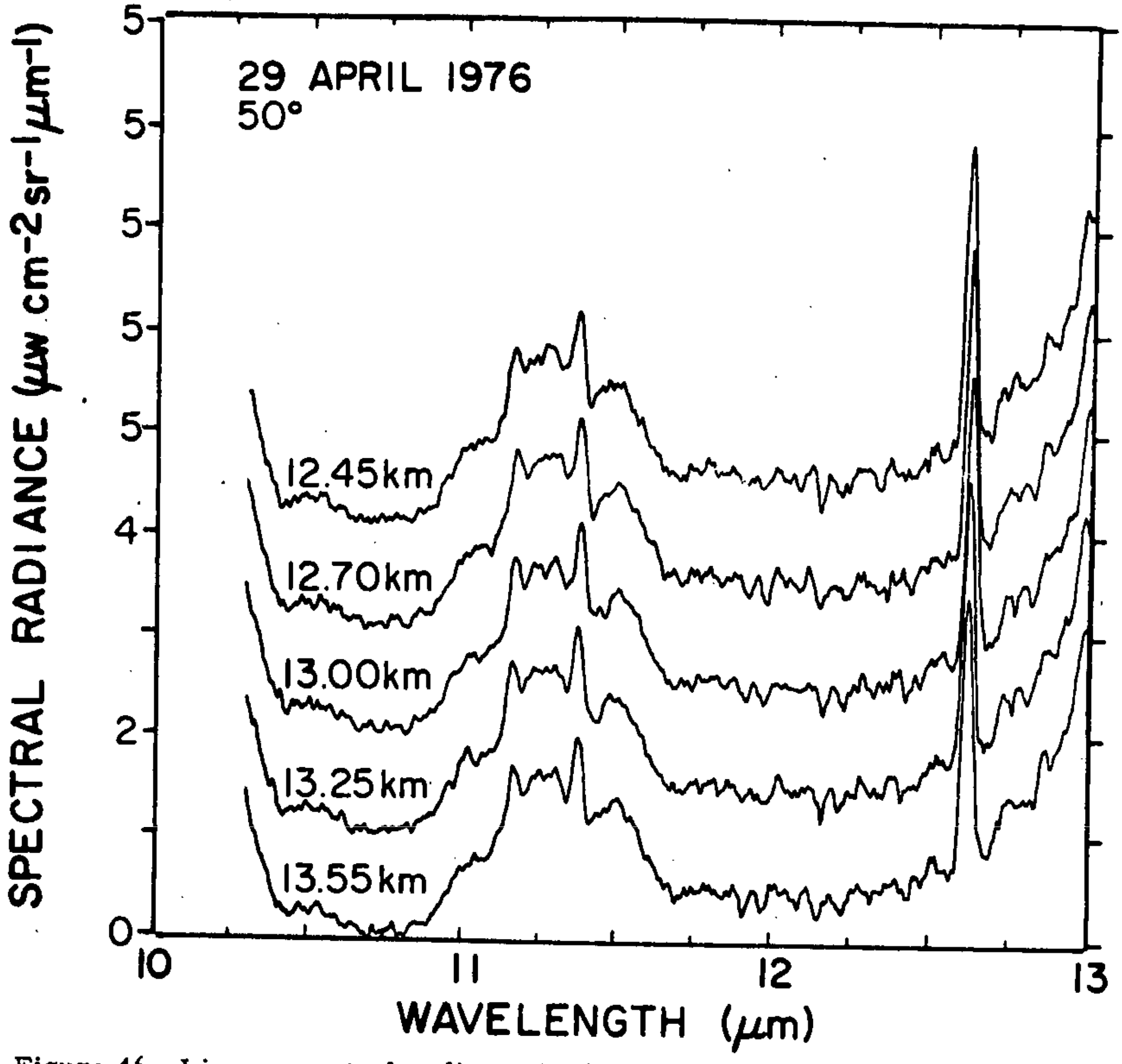

Figure 46. Linear spectral radiance in the 10.3-13μm region at 12.45, 12.70, 13.00, 13.25 and 13.55 km and a zenith angle of 50°. Spectra are offset for clarity.

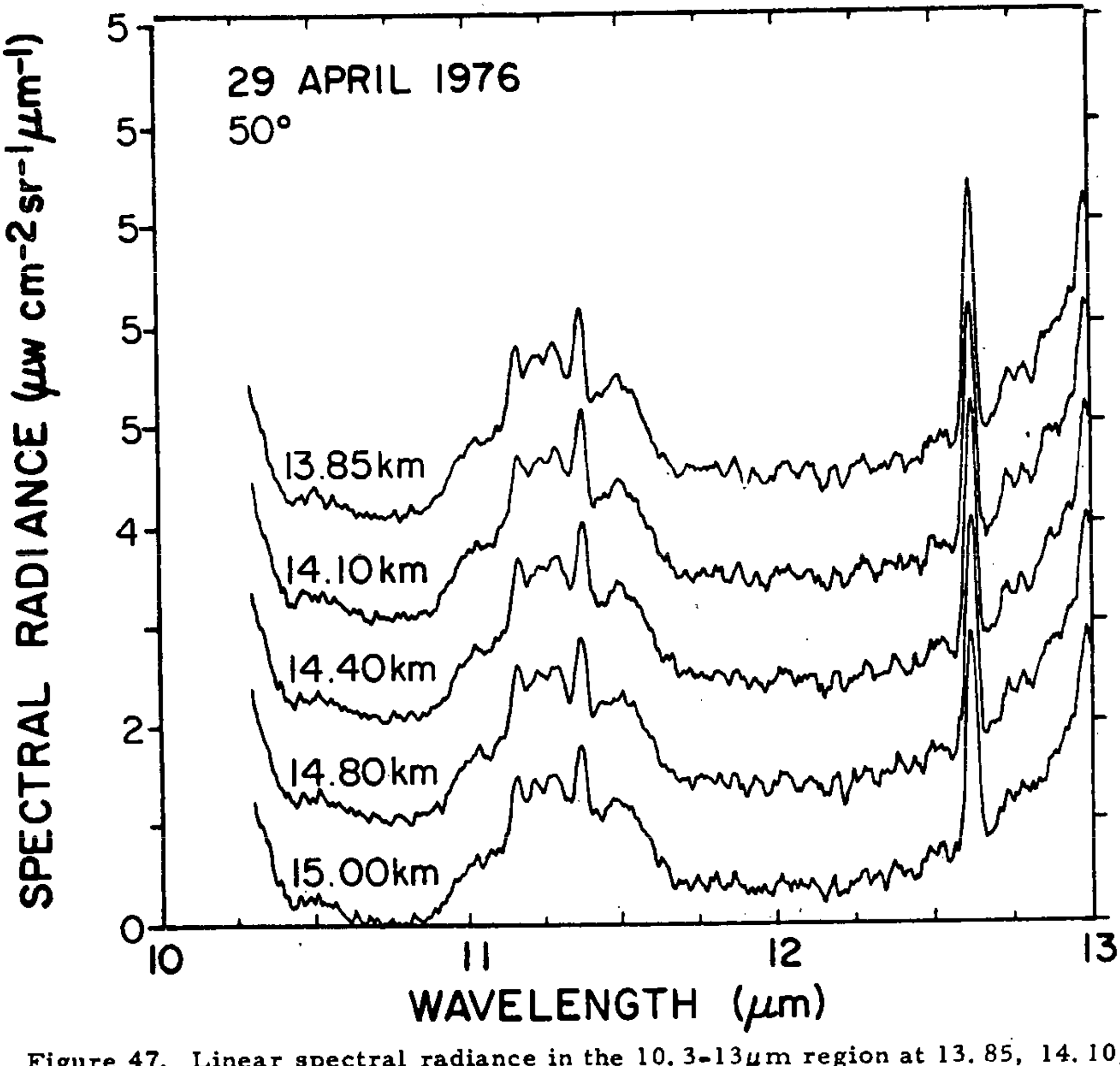

Figure 47. Linear spectral radiance in the 10.3-13μm region at 13.85, 14.10, 14.40, 14.80 and 15.00 km and a zenith angle of 50°. Spectra are offset for clarity.

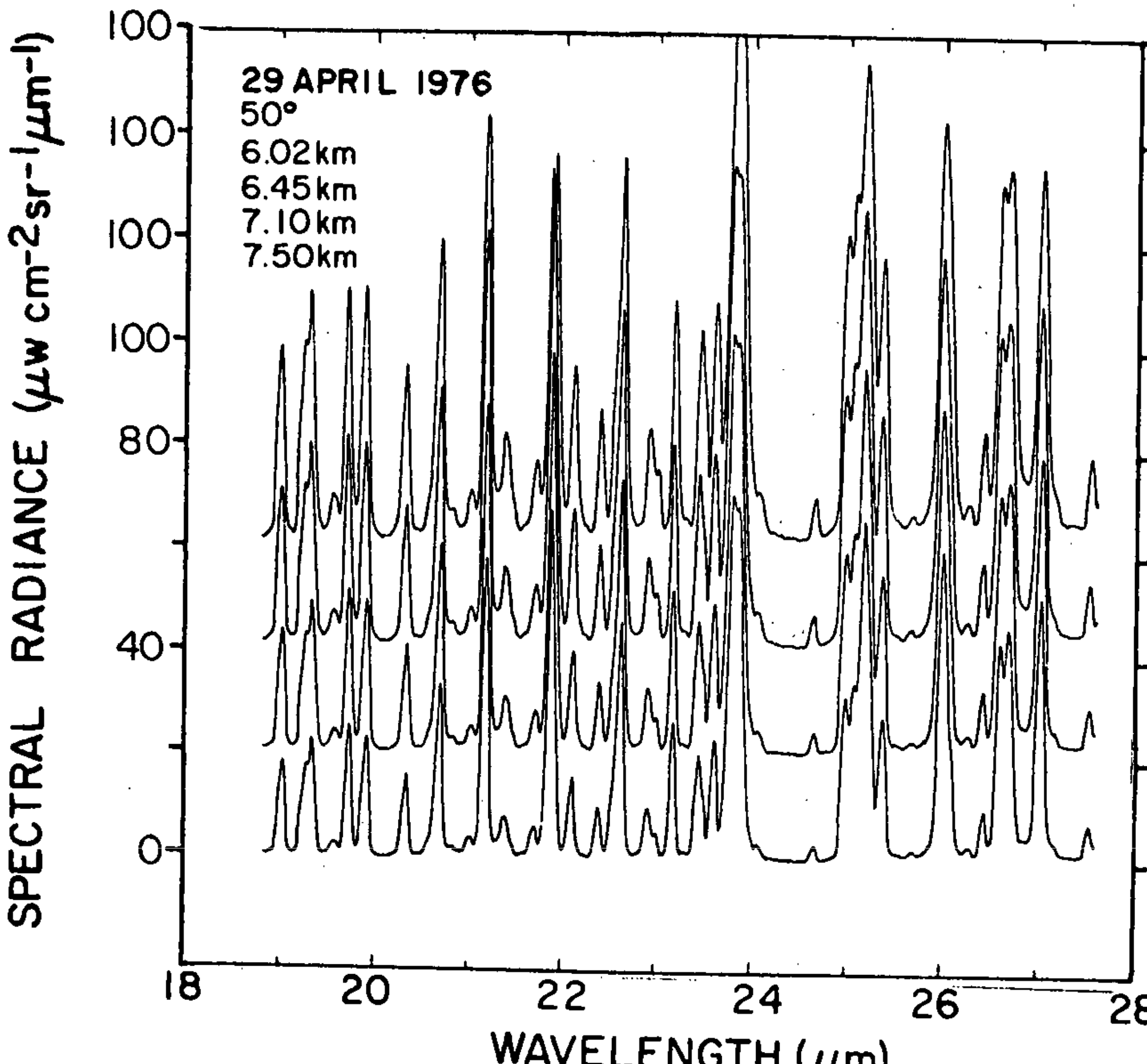

Figure 48. Linear spectral radiance in the 18.8-27μm region at 6.02, 6.45, 7.10 and 7.50 km and a zenith angle of 50°. Spectra are offset for clarity.

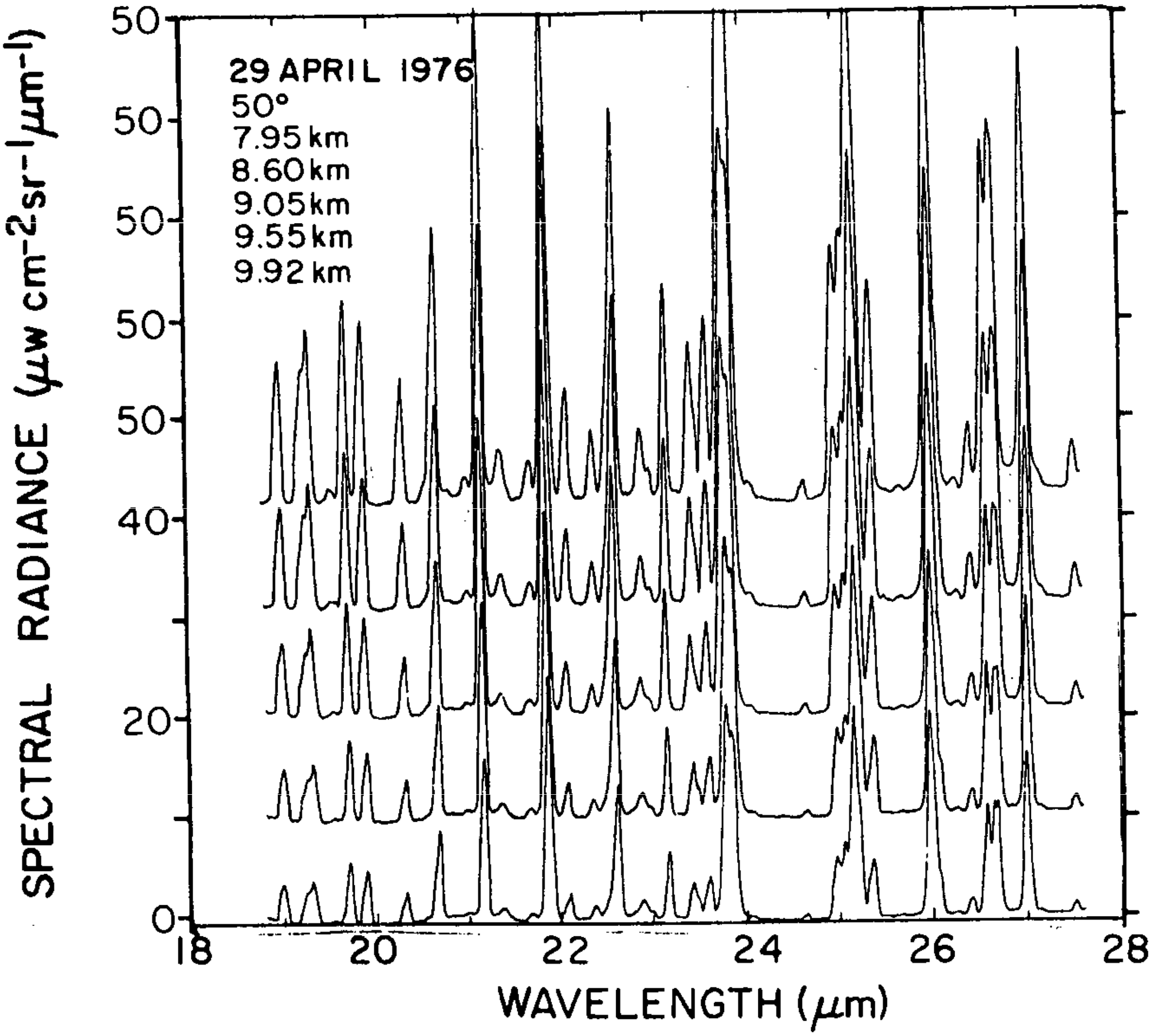

Figure 49. Linear spectral radiance in the 18.8-27μm region at 7.95, 8.60, 9.05, 9.55 and 9.92 km and a zenith angle of 50°. Spectra are offset for clarity.

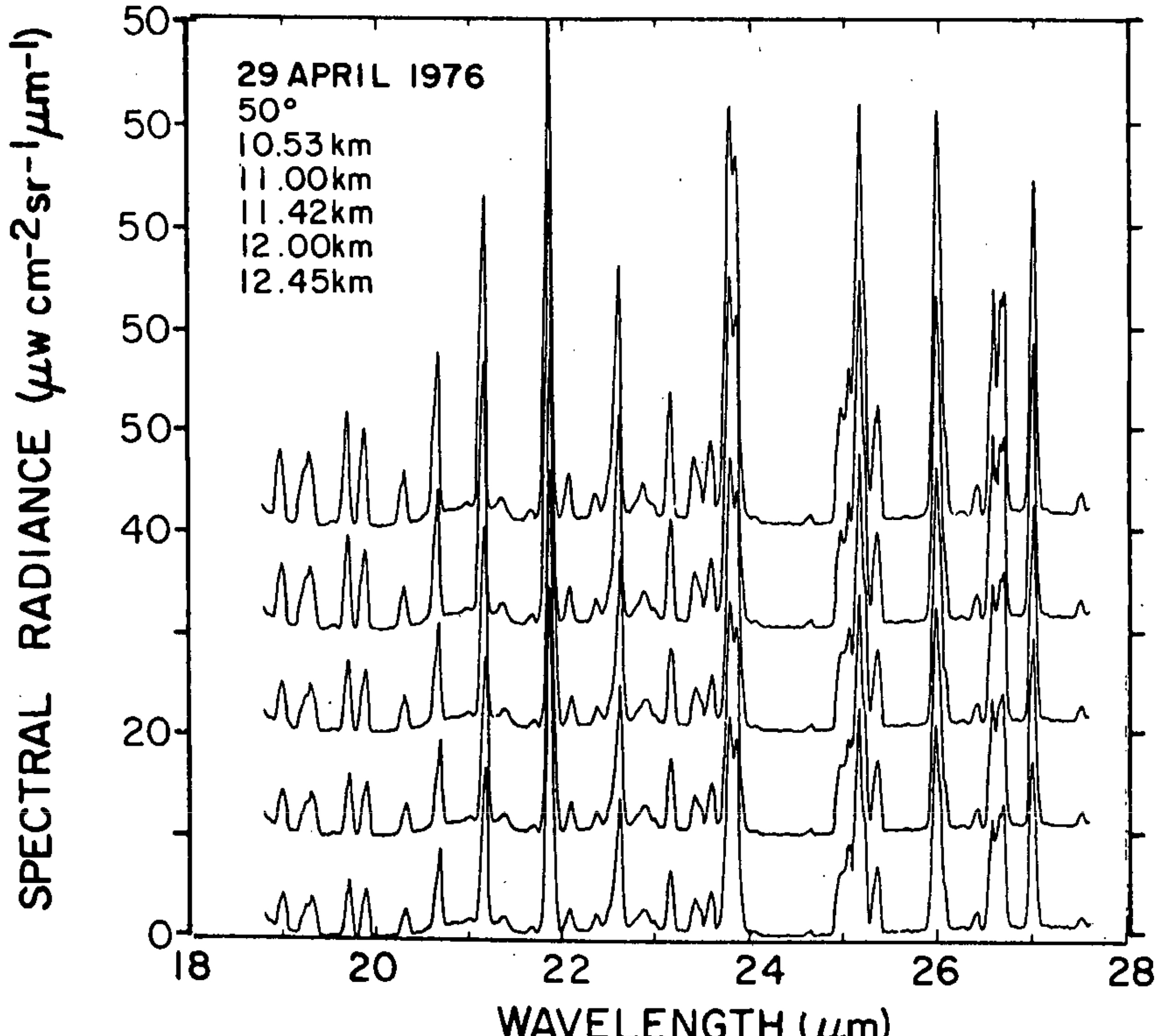

Figure 50. Linear spectral radiance in the 18.8-27μm region at 10.53, 11.00, 11.42, 12.00 and 12.45 km and a zenith angle of 50°. Spectra are offset for clarity.

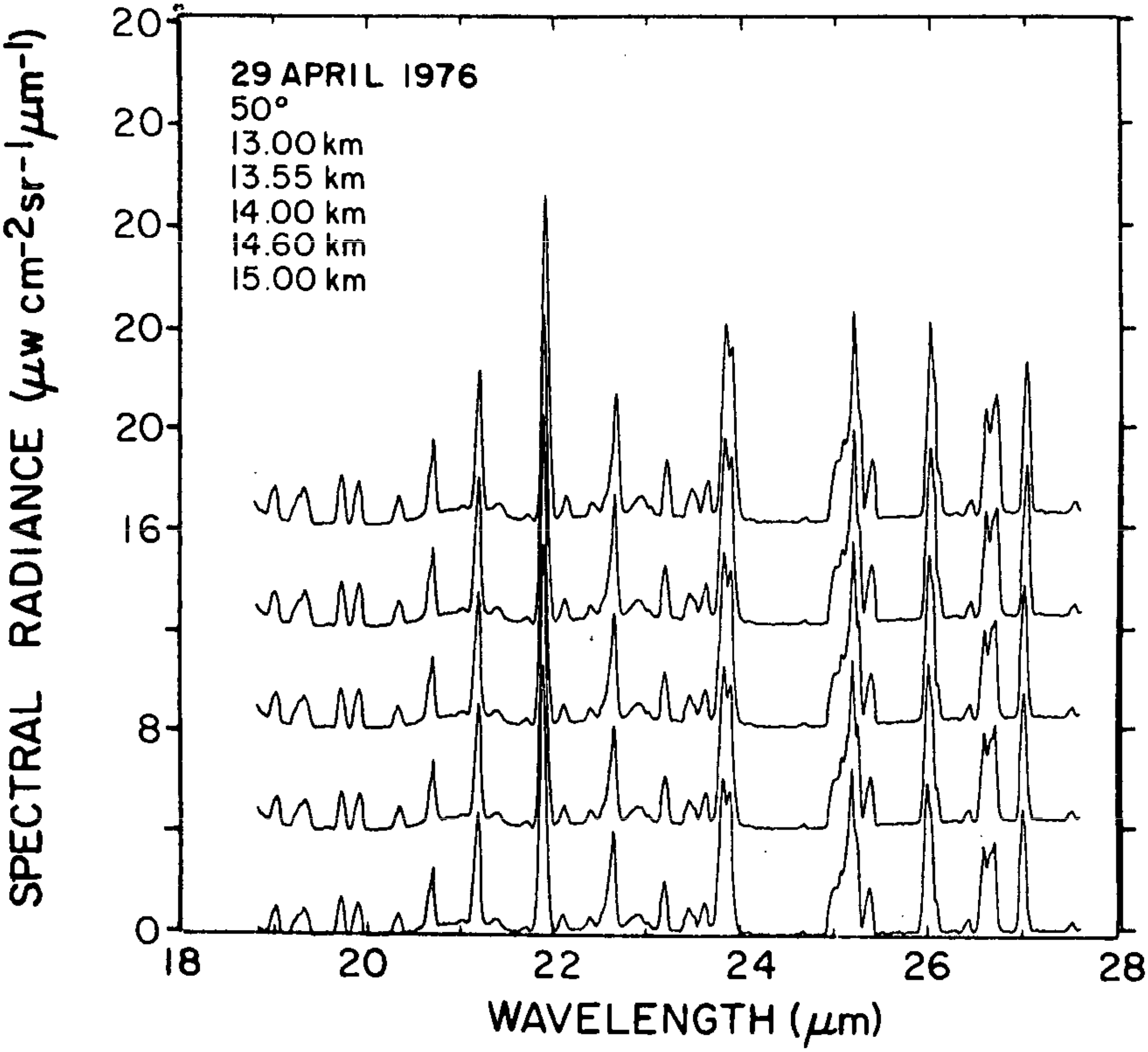

Figure 51. Linear spectral radiance in the 18.8-27μm region at 13.00, 13.55, 14.00, 14.60 and 15.00 km and a zenith angle of 50°. Spectra are offset for clarity.

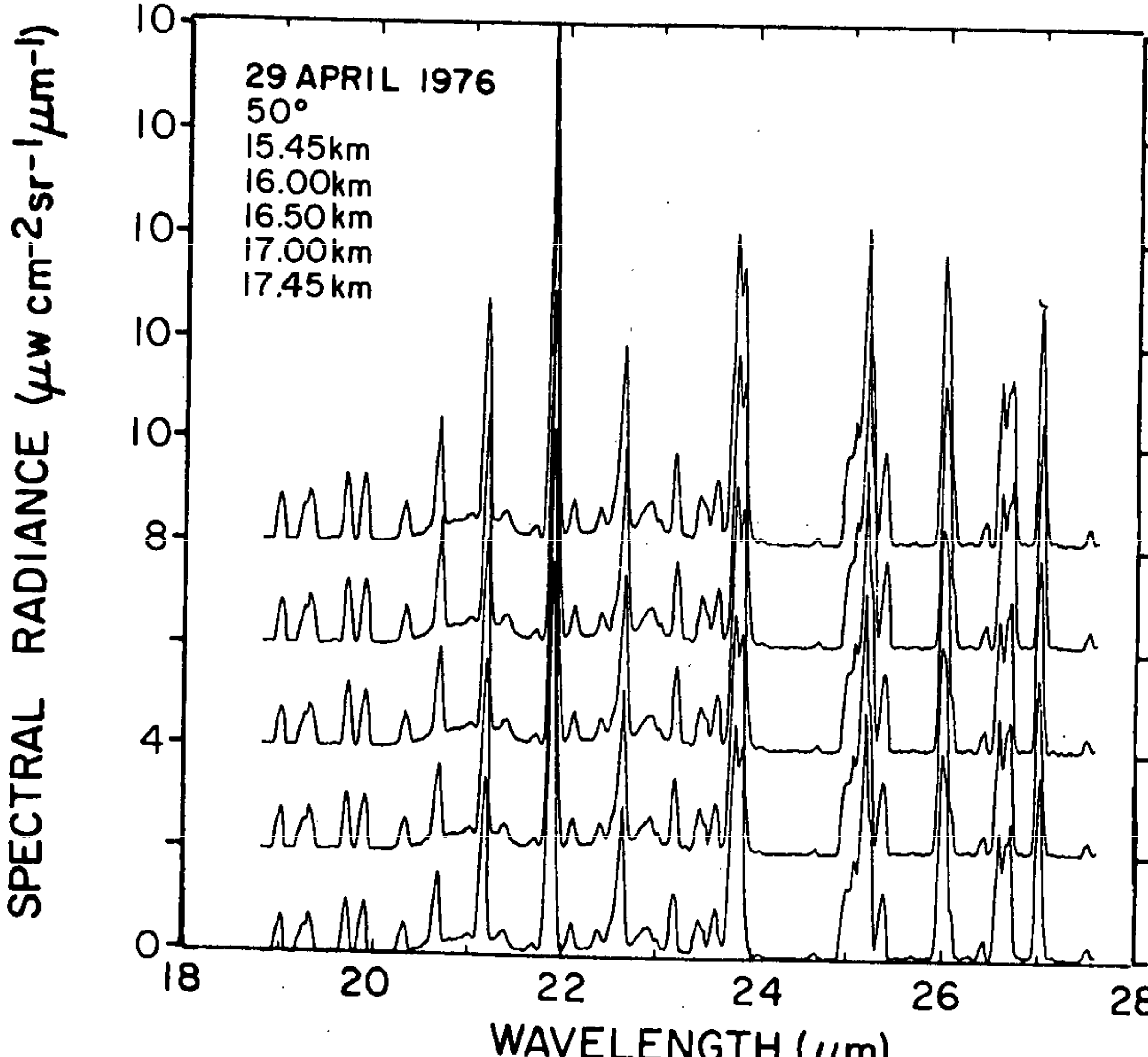

Figure 52. Linear spectral radiance in the 18.8-27μm region at 15.45, 16.00, 16.50, 17.00 and 17.45 km and a zenith angle of 50°. Spectra are offset for clarity.

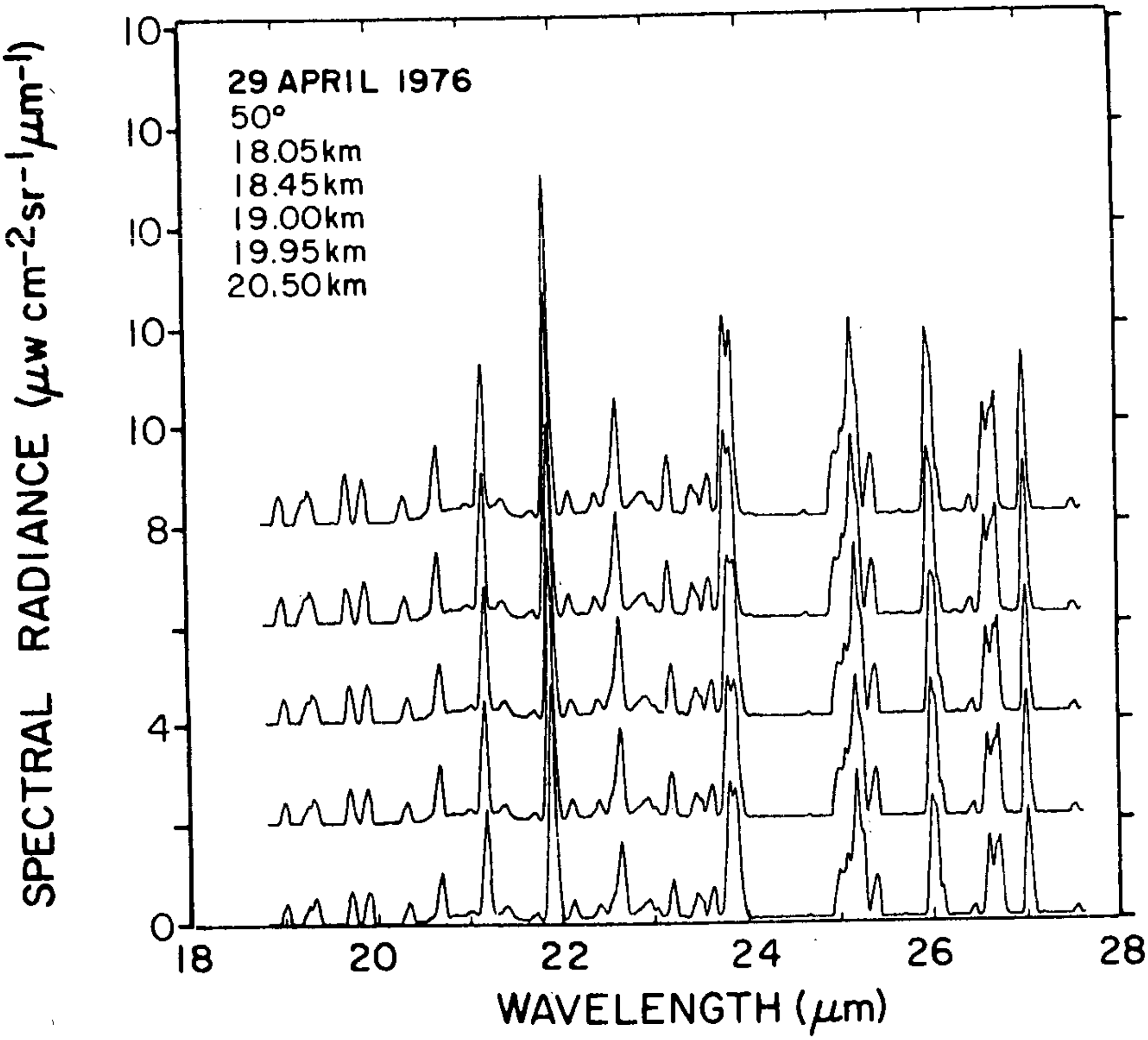

Figure 53. Linear spectral radiance in the 18.8-27μm region at 18.05, 18.45, 19.00, 19.95 and 20.50 km and a zenith angle of 50°. Spectra are offset for clarity.

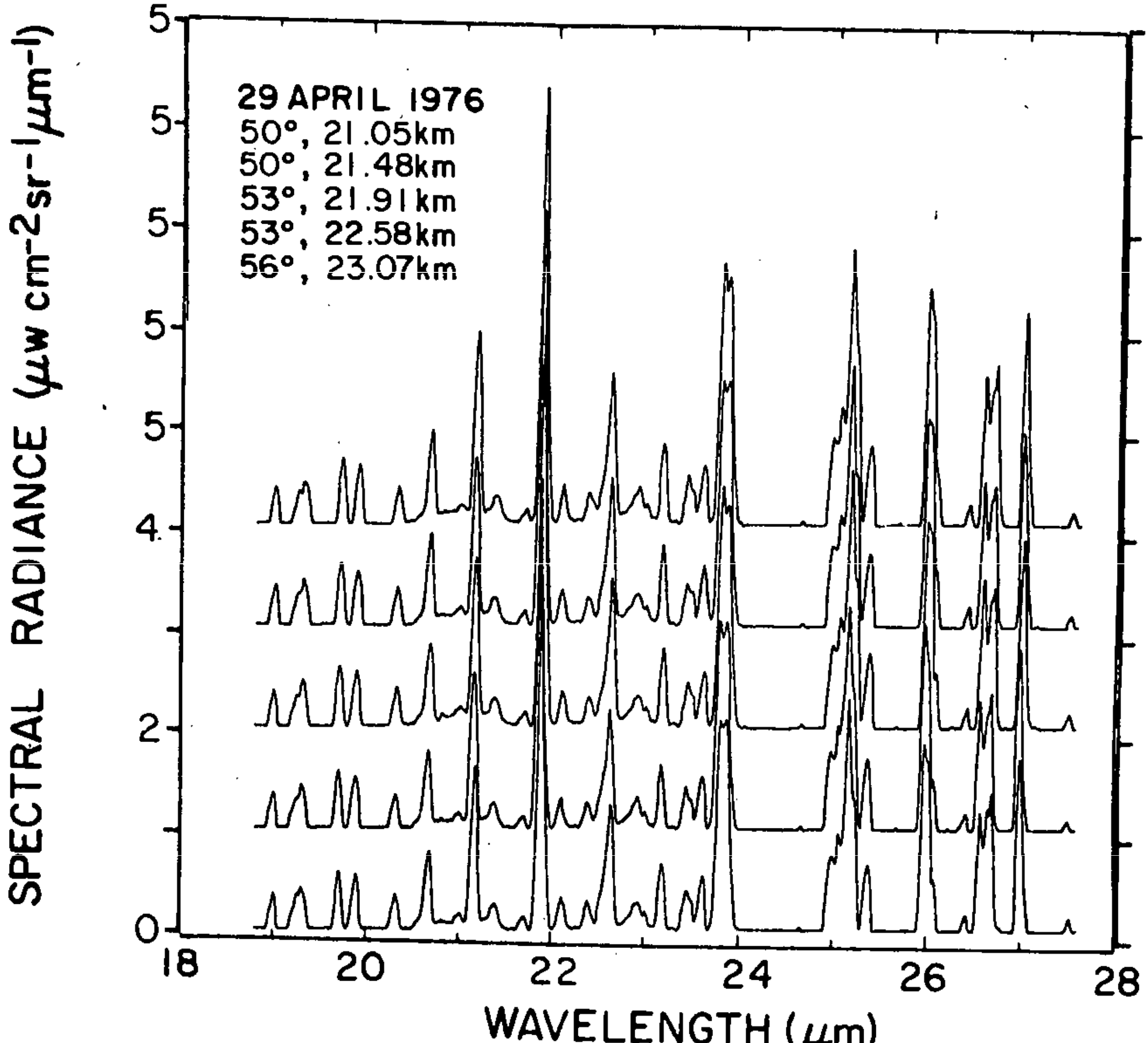

Figure 54. Linear spectral radiance in the 18.8-27μm region at 21.05, 21.48, 21.91, 22.58 and 23.07 km and zenith angles of 50°, 50°, 53°, 53° and 56°. Spectra are offset for clarity.

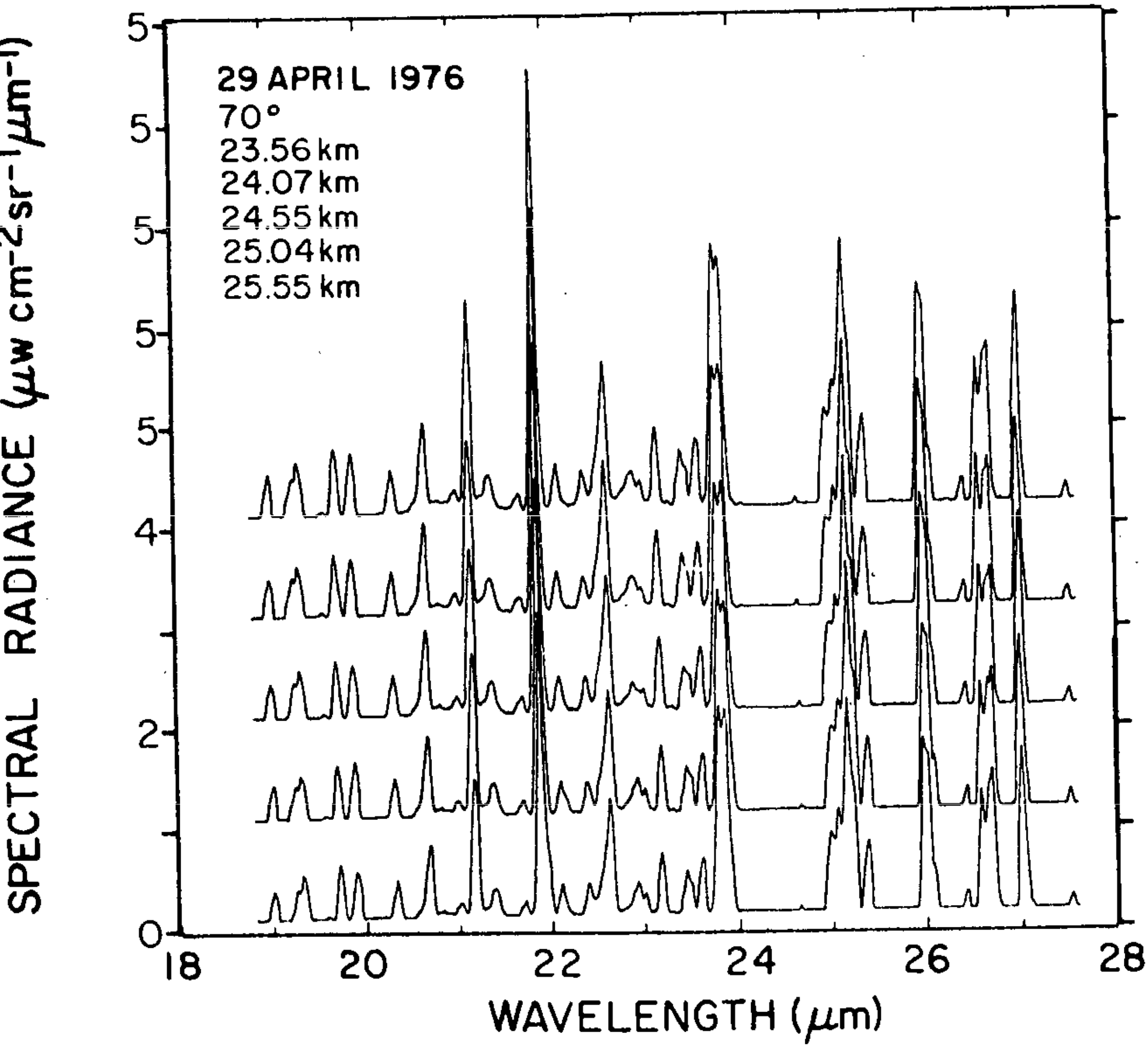

Figure 55. Linear spectral radiance in the 18.8-27μm region at 23.56, 24.07, 24.55, 25.04 and 25.55 km and a zenith angle of 70°. Spectra are offset for clarity.

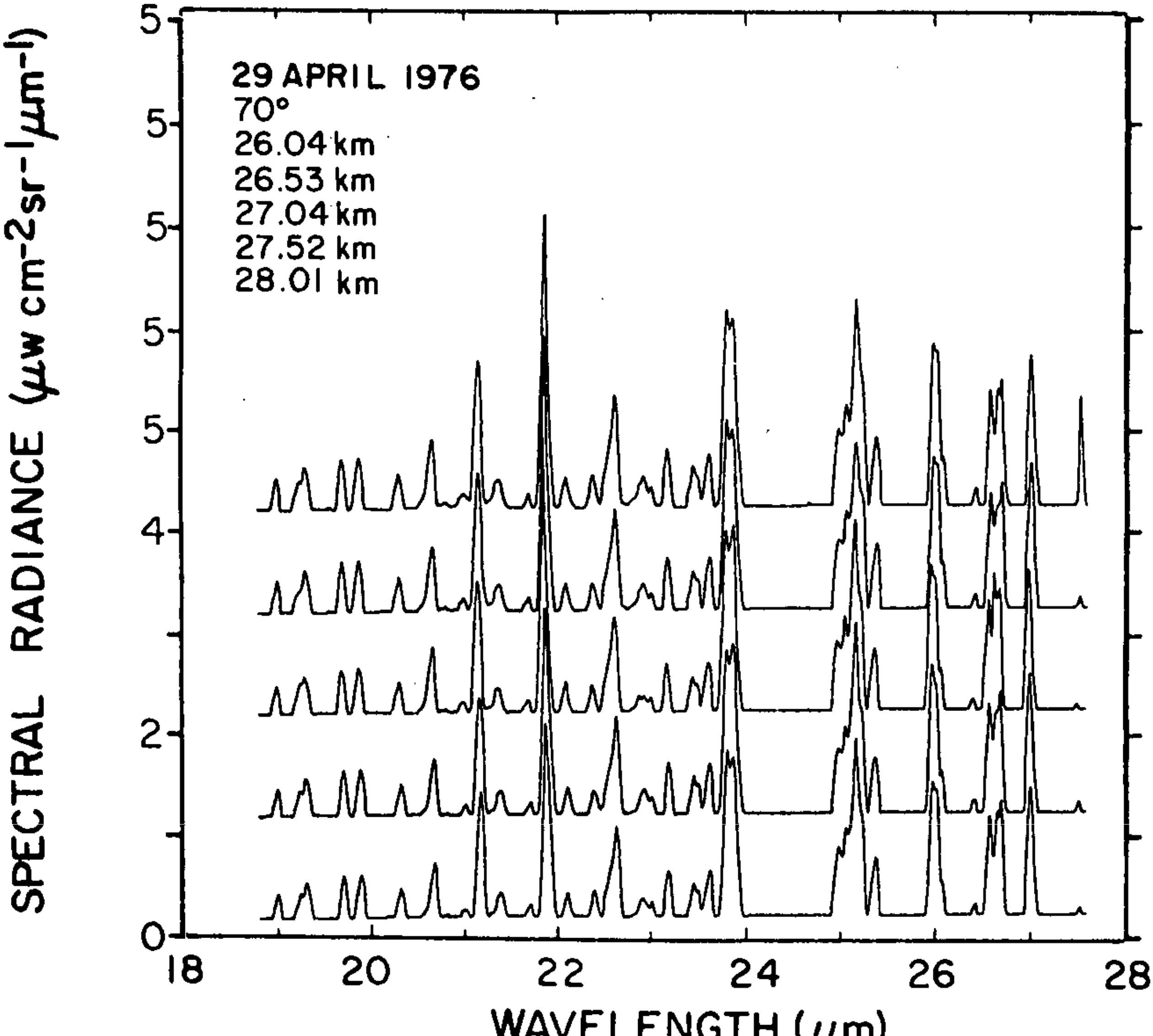

Figure 56. Linear spectral radiance in the 18.8-27μm region at 26.04, 26.53, 27.04, 27.52 and 28.01 km and a zenith angle of 70°. Spectra are offset for clarity.

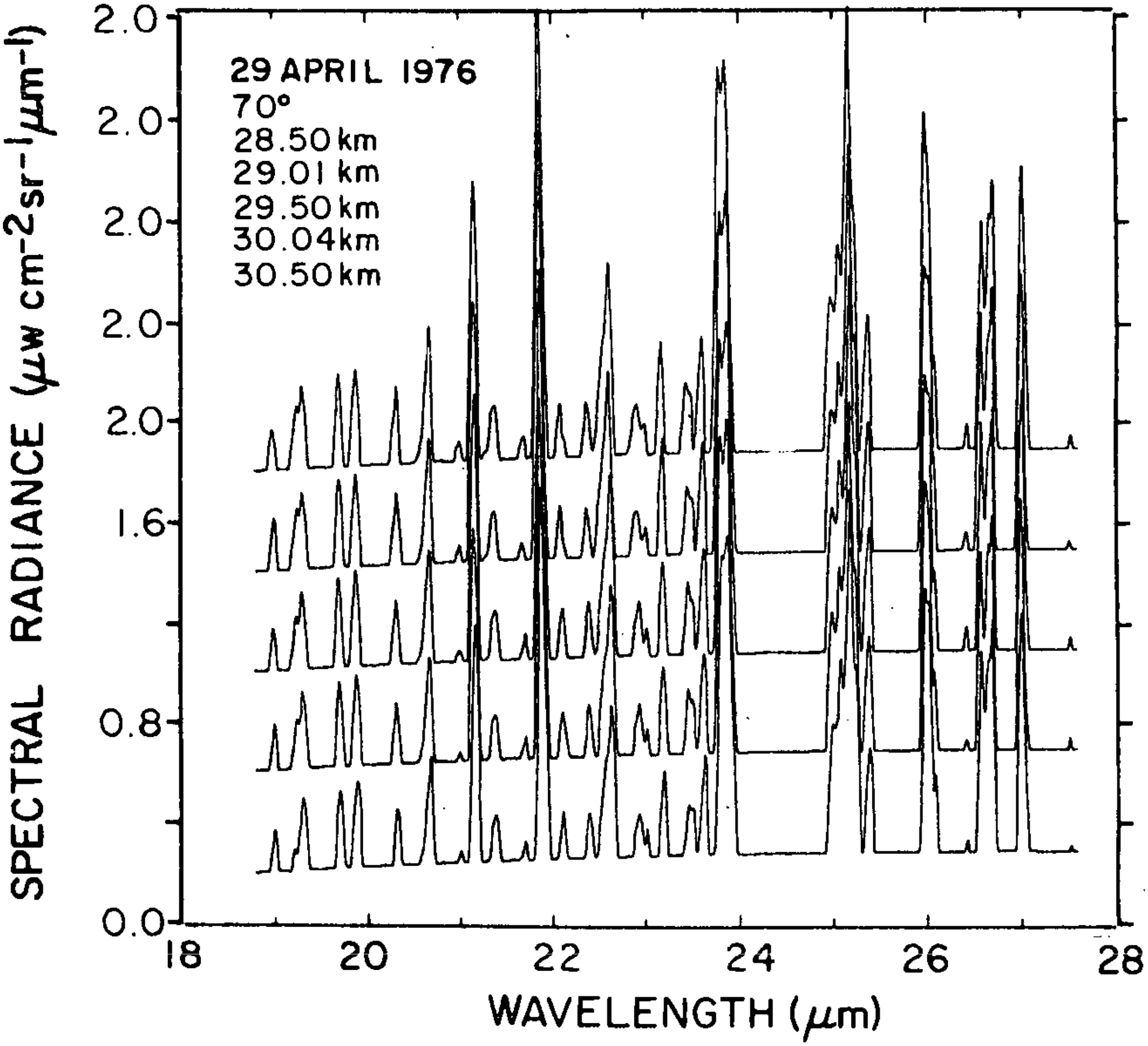

Figure 57. Linear spectral radiance in the 18.8-27μm region at 28.50, 29.01, 29.50, 30.04 and 30.50 km and a zenith angle of 70°. Spectra are offset for clarity.

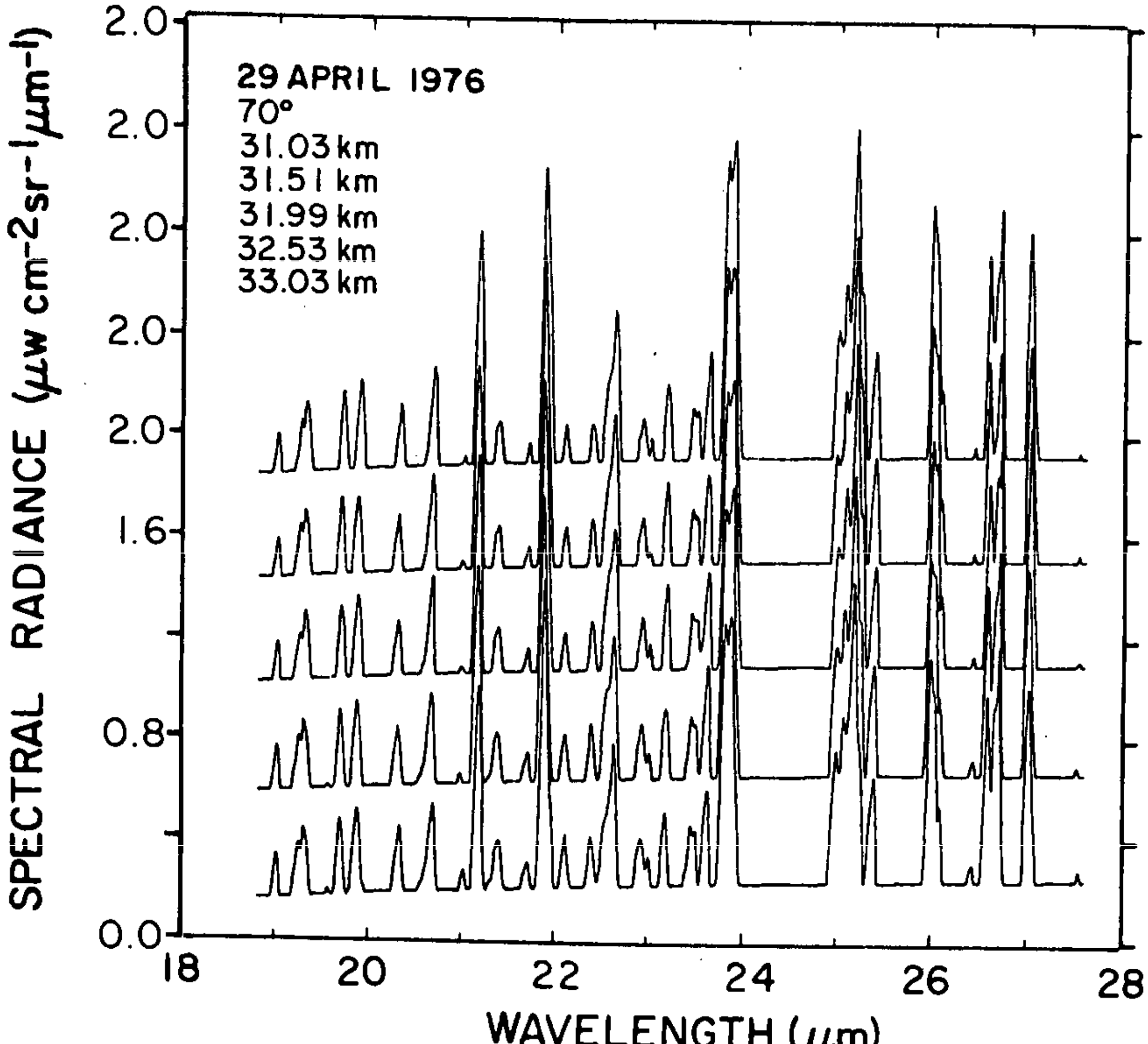

Figure 58. Linear spectral radiance in the 18.8-27μm region at 31.03, 31.51, 31.99, 32.53 and 33.03 km and a zenith angle of 70°. Spectra are offset for clarity.

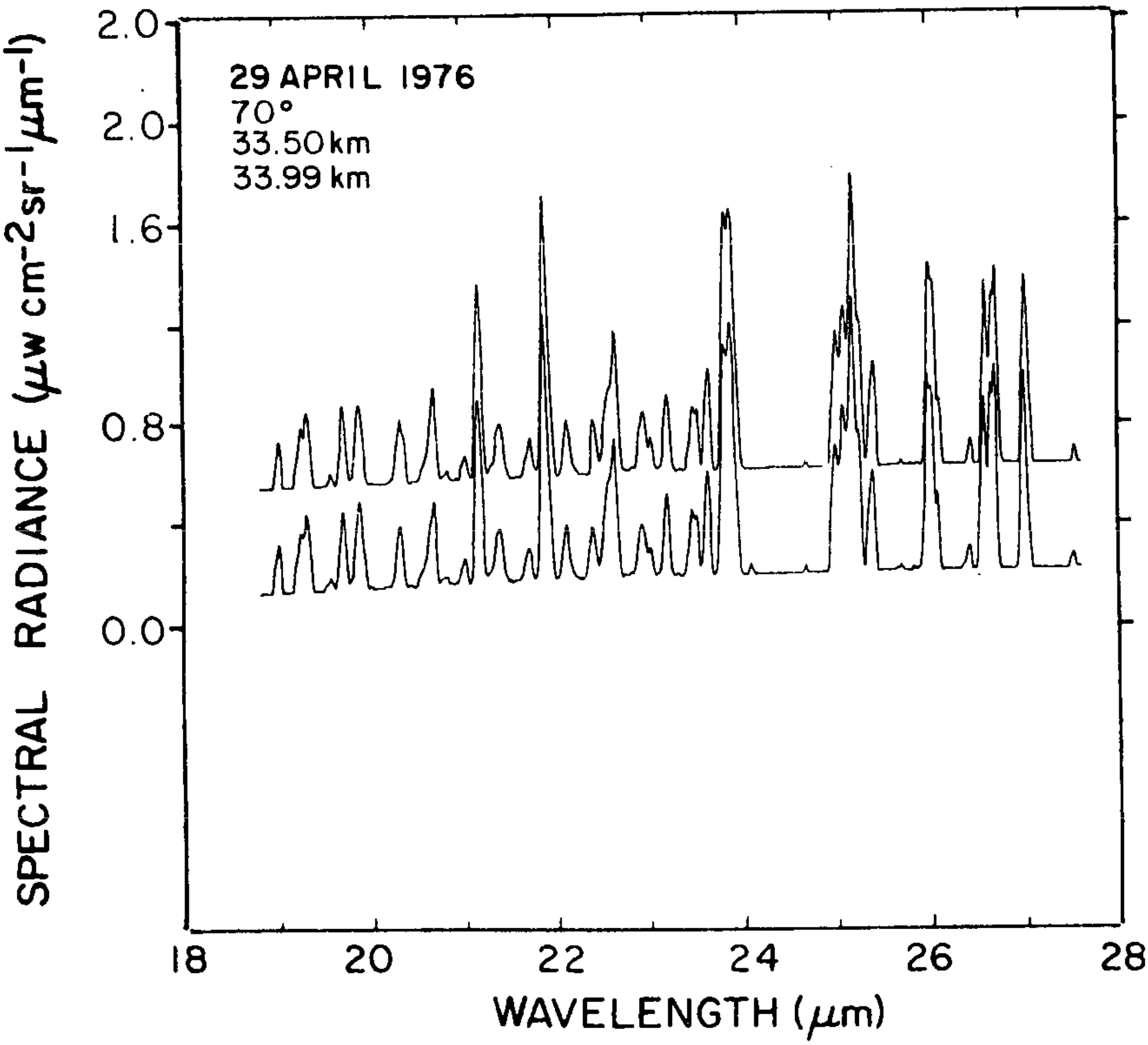

Figure 59. Linear spectral radiance in the 18.8-27μm region at 33.50 and 33.99 km and a zenith angle of 70°. Spectra are offset for clarity.

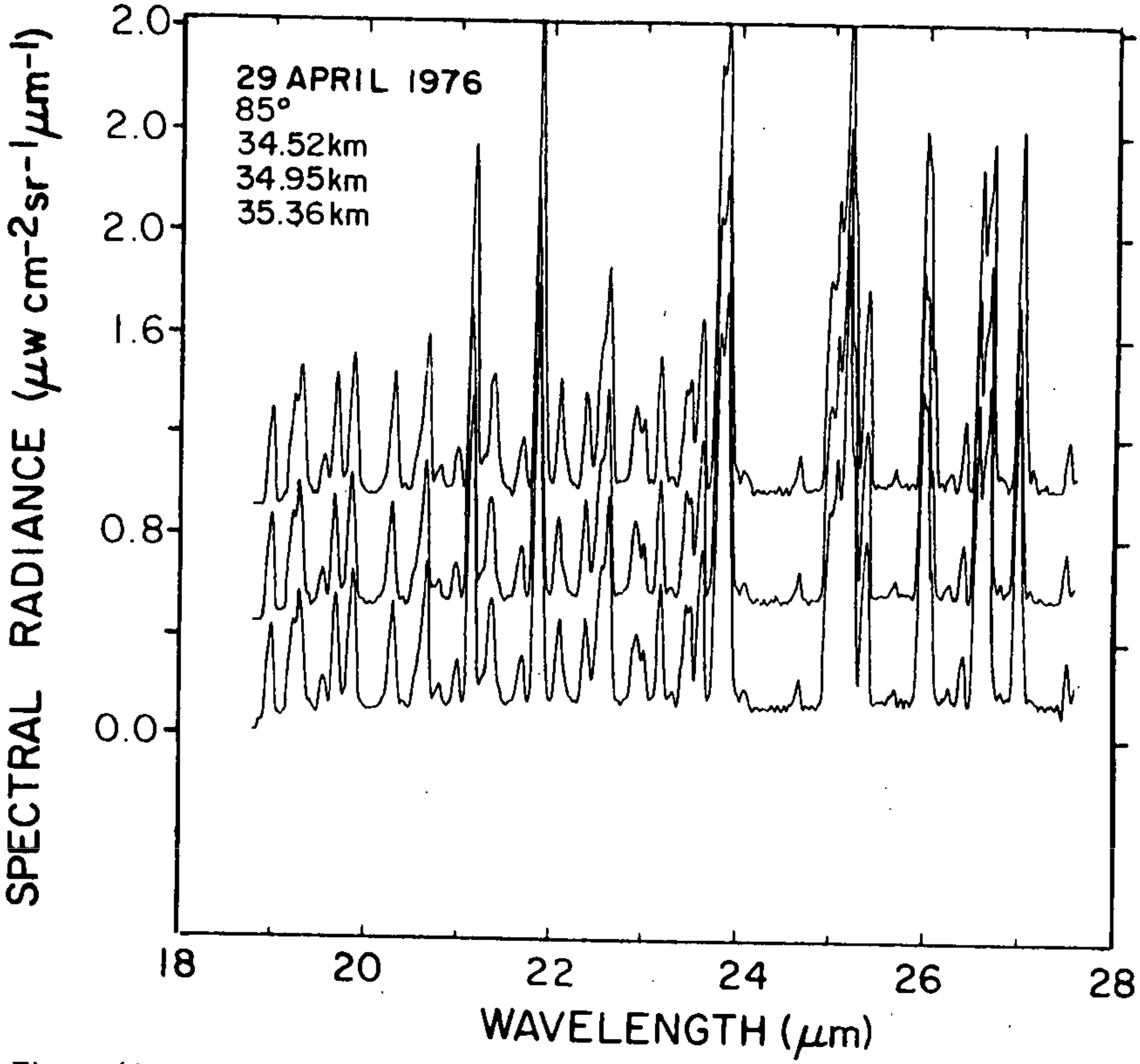

Figure 60. Linear spectral radiance in the 18.8-27μm region at 34.52, 34.95 and 35.36 km and a zenith angle of 85°. Spectra are offset for clarity.

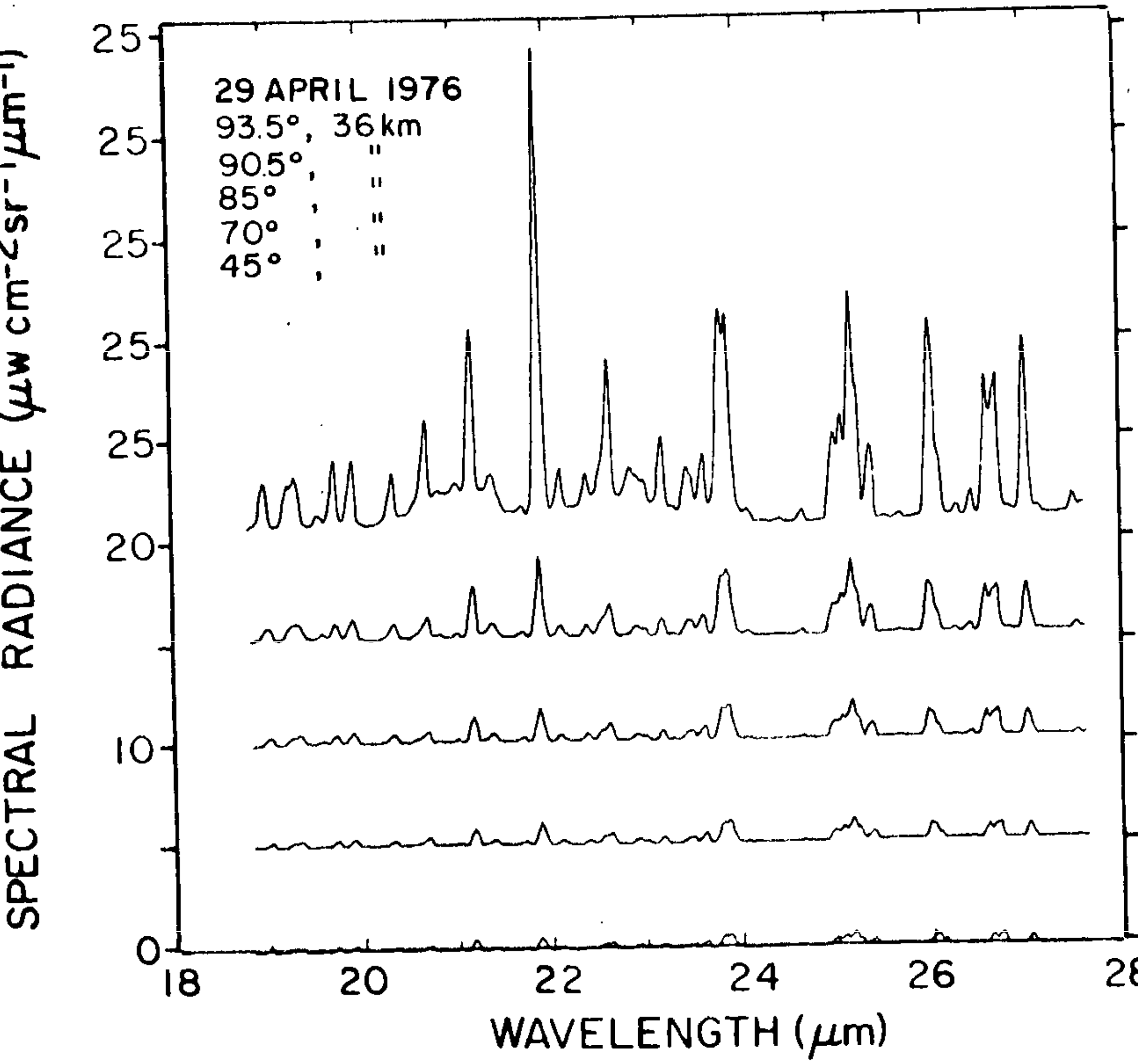

Figure 61. Linear spectral radiance in the 18.8-27μm region near 36 km as a function of zenith angle. Scans are offset for clarity. Each spectrum is a composite of 5 or more scans.

VI. ANALYSIS OF DATA

A. General Procedures

The spectral radiance is used to derive constituent height profiles by fitting either line-by-line or band molecular emission models to the radiance data at various altitudes. These models are discussed at length in the previous data report and elsewhere.[1,6,7] A short expansion of the discussion of the band model technique is included here because it is used so extensively in this report. The usual parameters of the line-by-line method, line intensity, width and energy levels, are replaced with averaged parameters over finite spectral intervals for the band model technique. Such average parameters are only meaningful if the spectral interval contains a sufficient number of lines for good statistical averaging. Instead of calculating monochromatic transmission and averaging over a resolution element (as with line-by-line), the transmission (τ) is calculated using these average parameters for a finite spectral interval.

---

[6] W. J. Williams, D. B. Barker, J. N. Brooks, A. Goldman, J. J. Kosters, F. H. Murcray, D. G. Murcray and D. E. Snider, "Spectral Radiometric Measurement of Atmospheric Constituents" Proceedings of Society of Photo-Optical Instrumentation Engineers, 91, 15-25, 1976.

[7] A. Goldman, D. G. Murcray, F. H. Murcray, W. J. Williams and J. N. Brooks, "Distribution of Water Vapor in the Stratosphere as Determined from Balloon Measurements of Atmospheric Emission Spectra in the 24-29μm Region" Appl. Opt., 12, 1045-1053, 1973.

Thus:

$$\tau = \exp - \left\{ \frac{[S^{o}(\nu) \ / \ d(\nu)] \cdot u}{\left[1 + 2 \left(\frac{x(\nu)}{L}\right) \frac{u}{p} \right]^{1/2}} \right\} \tag{2}$$

where u = optical path in atm-cm. The equivalent absorption coefficient in this expression is not only dependent on the average line intensity, but upon the pressure environment as well. The absorption coefficient is equal to the average line intensity over the average line spacing (linear fit) when the line centers are not black and pressure broadening does not dominate, and can be expressed as

$$2 \left(\frac{x}{L}\right) \frac{u}{p} << 1.$$

The gas amount, u, in a homogenous optical path can be calculated from Eq. (2) by using the measured radiance, N, to calculate a spectral emissivity, $\epsilon = \frac{N}{B}$, where B is the black body radiance. Neglecting scattering, $\tau = 1 - \epsilon$ and Eq. (2) can be solved for u. For weak emitters (or absorbers) two approximations simplify the above calculation. First, if

$$2 \left(\frac{x}{L}\right) \frac{u}{p} << 1$$

(linear region), no reiteration is required in calculating τ. Thus,

$$\tau = \exp - [S^{o} \ / \ d] u \ . \tag{3}$$

Second, an exponential expansion of Eq. (3) results in

$$\epsilon = [S^{o} / d]\, u \quad . \tag{4}$$

When Eq. (4) is valid, a simple differential technique can be used to calculate the amount of constituent material within a layer bounded by two measurements. Thus:

$$\Delta \epsilon = [S^{o}/d]\, \Delta u \ , \quad \text{or}$$

$$\frac{\Delta N}{B} = \overline{K}\, \Delta u \quad . \tag{5}$$

The amounts u or Δu in the two preceding equations can be used to calculate mixing ratios and number densities and integrated over height to yield total column densities. These relationships are summarized below:

$$\Delta u' = \Delta u \,/\, \sec\theta \qquad \text{(atm-cm at T)} \tag{6}$$

$$\Delta n = \Delta u' \frac{273}{T}\, 2.69 \times 10^{23} \qquad (\text{molecules}/\text{m}^2) \tag{7}$$

$$n_o = \Delta n \,/\, \Delta z \qquad (\text{molecules}/\text{m}^3) \tag{8}$$

$$\beta_v = \frac{\Delta u'}{\Delta p H} \ , \quad H = \frac{kT}{M_{air}\, g} \qquad \text{(vol. gas/vol. air)} \tag{9}$$

$$\text{or} \quad \beta_v = \frac{n_o}{p \,/\, kT} \tag{10}$$

$$\beta_m = \beta_v \frac{M_{gas}}{M_{air}} \tag{11}$$

$$n = \Sigma \Delta n \quad \text{or} \quad \Sigma n_o \Delta z \qquad (\text{molecules}/m^2) \tag{12}$$

$$u = \Sigma \Delta u' \frac{273}{T} \qquad (\text{atm-cm STP}) \ . \tag{13}$$

Where θ is the zenith angle of observation, T is the local atmospheric temperature (K), p is the local pressure (atm), Δ p is the pressure change through the layer being considered, Δ z (meters) is the corresponding altitude increment, β_v and β_m are the mixing ratios by volume and mass respectively, n_o and n are number density and column density, M is molecular weight, and H is a scale height. Equations (9) and (10) are equivalent.

When the above linear approximations cannot be made, the problem is significantly more difficult, because some equivalent temperature and pressure must be assumed. The appropriate assumption depends on the constituent profile and probably should be a weighted mean depending on the profile, the degree of nonlinearity and the radiance-temperature (Planckian) relationship (wavelength dependent). Usually a simplified approximation is used such as $p' = p / 2$ and $T' = T(p/2)$ or $p' = p$ (at known layer mean height) etc.

One further consideration must be noted. The linear spectral absorption coefficients, $K(\nu)$, are temperature dependent, primarily due to the relative population of the vibrational-rotational states. Line-by-line calculations take this into account with the rotational partition function (vibration partition function is approximately 1 for atmospheric temperature), but band model parameters do not

explicitly contain this temperature parameter. The following discussion is an effort to evaluate the band model temperature dependence.

B. Band Model Temperature Correction

1. Introduction

Constituent height profiles are derived from the change in radiance with altitude associated with the spectral features of a specific molecule. It should be possible to derive the same height profile from radiance data measured over different spectral intervals within a band or from radiance values integrated over the entire band. This has been done with previous spectral emission balloon data of the 11.3μm HNO_3 band by using the linear approximation of the statistical band model. The comparative results have never been as satisfactory as would be expected. There has remained a quantitative difference between the total band profile and the narrow spectral interval profiles. In addition, the laboratory spectral band model parameters of HNO_3 do not fit the long path atmospheric absorption data when the same temperature correction is used at all wavelengths. If a linear temperature correction is used for the band model absorption coefficients, concentrations derived at the center of the band are different from those at the wings of the band. In addition, a third value for the concentration was derived from the total band when a temperature power correction of 1.5 was used.

Recently, a need to quantitatively measure the 11.8μm F-11 ($CFCl_3$) band and the 10.8μm F-12 (CF_2Cl_2) band, which are superimposed on the wings of the 11.3μm HNO_3 band, has caused a re-evaluation of the discrepancies of the altitude profiles. A proper calculation of F-11 and F-12 amounts can only be done after

removing the wing effects of HNO_3 from the absorption or emission spectrum. This can best be accomplished by fitting a concentration to the center of the HNO_3 band and, using that concentration, calculating the residual absorption or emission in the F-11 and F-12 bands due to the wings of the HNO_3 band. This assumes a proper temperature correction to adjust the room temperature band model data of HNO_3 to a model at atmospheric temperature. This correction can be either theoretical or empirical, but must be accurate over the temperature range in question. Such an empirical model, partially justified by theory, is developed below.

2. Temperature Correction Model

The spectral absorption coefficient is equivalent to the average band model intensity for weak absorptions where linear approximations apply ($K_\nu = \overline{s^o / d}$). Since the average band model line intensity is temperature dependent while the average line spacing is not significantly so, the temperature dependence of the absorption coefficient is principly defined by the temperature dependence of the average band model line intensity.

The integrated intensity of a vibrational band system has been shown[8] to be independent of temperature for fundamental bands, but functionally dependent on temperature for overtone and combination bands. When only a portion of a fundamental vibration-rotation band is considered,[9] the intensity of that spectral interval may exhibit a

[8] J. C. Breeze, C. C. Ferriso, C. B. Ludwig and M. Malkmus, "Temperature Dependence of the Total Integrated Intensity of Vibrational-Rotational Band Systems" J. Chem. Phys., 42, 402-406, 1965.

[9] C. C. Ferriso and C. B. Ludwig, "An Infrared Band Ratio Technique for Temperature Determinations of Hot Gases" Appl. Opt., 4, 47-51, 1965.

temperature dependence either positive or negative. In Ferrisso's application in which the R-branch of the ν_3 H_2O fundamental band data was fit with a linear negative function, the effect was less than 2% over a range of temperatures normally associated with atmospheric measurements. Thus, any empirical model should reflect an integrated intensity nearly independent of temperature, but might also assume that, as the spectral interval becomes smaller and includes only a few vibration-rotation lines, the temperature dependence would increase.

The intensity of a single vibrational-rotational line of a band system is dependent on the rotational population levels within the band. An expression can be derived for the temperature dependence of such a line of the form

$$\frac{S(T_2)}{S(T_1)} = \left[\frac{T_1}{T_2}\right]^n \exp\left[\frac{T_2-T_1}{T_2\ T_1}\ 1.439\ E''\right] , \tag{14}$$

in which induced emission and the vibrational partition function, which have a weak temperature dependence, have been neglected (1-3% correction). E'' is the lower state energy (in cm^{-1}) and n = 1.0 for linear molecules and 1.5 for nonlinear molecules. For small changes in the temperature, a series expansion of the two parts of the right hand term gives

$$\frac{S(T_2)}{S(T_1)} \simeq \left[\frac{T_1}{T_2}\right]^{[1.5 - \frac{1.439E''}{T_1}]} \tag{15}$$

for HNO_3 or O_3. Note that this derivation defines a temperature for each E'' near which the absorption coefficient is independent of temperature ($1.5\ T_1 = 1.439\,E''$).

Previously used band model temperature corrections have been of the form $(T_1 / T_2)^{\gamma}$, and it is convenient to consider continuing this form when physically reasonable. It is, therefore, natural to consider γ of the form $\gamma \simeq 1.5 - 1.439\,E''/T_1$. However, γ as used here applies to band model absorption coefficients which have been averaged over a number of individual S values, each of which is dependent on different E'' levels. There may be significant variations in values for E'' within one spectral interval, particularly for the random band model. In addition, the levels for HNO_3 are not well-known. It is, therefore, difficult to calculate the frequency dependence of γ within an absorption band. Roughly, γ should not exceed 1.5 (2.5 if density charges are included) near the band center (small E'') and may go negative toward the band wings (large E'').

Experimentally, it is suitable to derive band model values of γ from data at two or more temperatures. This empirical approach is a substitute for more complex modeling, particularly when some of the parameters are not well-known.

3. <u>O_3 Temperature Correction</u>

Before calculating the values for γ for the HNO_3 bands at 11.3μm, it is desirable to apply this approach to a band with well-known temperature dependence. Goldman et al.[10] calculated band model parameters for ozone for three different temperatures from individual

[10] A. Goldman, "Statistical Band Model Parameters for Long Path Atmospheric Ozone in the 9-10μm Region" Appl. Opt., 9, 2600-2604, 1970.

line parameters with known temperature dependencies. Based on the empirical approach of

$$\left(\frac{T_1}{T_2}\right)^{\gamma}$$

as the form of the temperature correction, values for γ were determined from the O_3 band model data from 960 to 1176 cm^{-1}. Note that $\gamma = 1$ is a density correction to the absorption coefficient and $\gamma = 1.5$ is the suggested[11] total band correction. Since band model coefficients had been calculated for 195, 235 and 275°K, values of γ were determined for two pairs of temperatures at each frequency. The average of these two values for γ is plotted in Figure 62, with bars showing the spread in values of the separate calculations. Some things are clear from this data. 1) A linear temperature correction (for density only) is not valid over the entire frequency interval, particularly toward the wings and when there are multiple bands contributing to the absorption. 2) At any narrow frequency interval an empirical value for γ can be determined which will correct the band model parameters for temperature, probably within the general uncertainties of the band model calculation. In addition, the temperature correction for the integrated intensity is $\gamma = .991 \pm .012$ which is nearly unity and represents a density correction.

---

[11] S. S. Penner, Quantitative Molecular Spectroscopy and Gas Emissivities, Addison-Wesley Publishing Company, Inc., Reading, Mass., 1959.

The purpose of the above exercise is to validate an approach which is now applied to the 11.3μm HNO_3 bands. Band model data are available for this band at 313°K,[12] and some additional data are available at 283 and 263°K.[13] The random band model used is similar to that used for the O_3 bands, but individual line parameters are not available for HNO_3.

---

[12] A. Goldman, T. G. Kyle and F. S. Bonomo, "Statistical Band Model Parameters and Integrated Intensities for the 5.9μ, 7.5μ and 11.3μ Bands of HNO_3 Vapor" Appl. Opt., 10, 65-73, 1971.

[13] D. G. Murcray, A. Goldman and F. S. Bonomo, "Laboratory Studies of Infrared Absorption by NO_2 and HNO_3" Final Report on NASA Grant 06-004-128, Department of Physics, University of Denver, 1974.

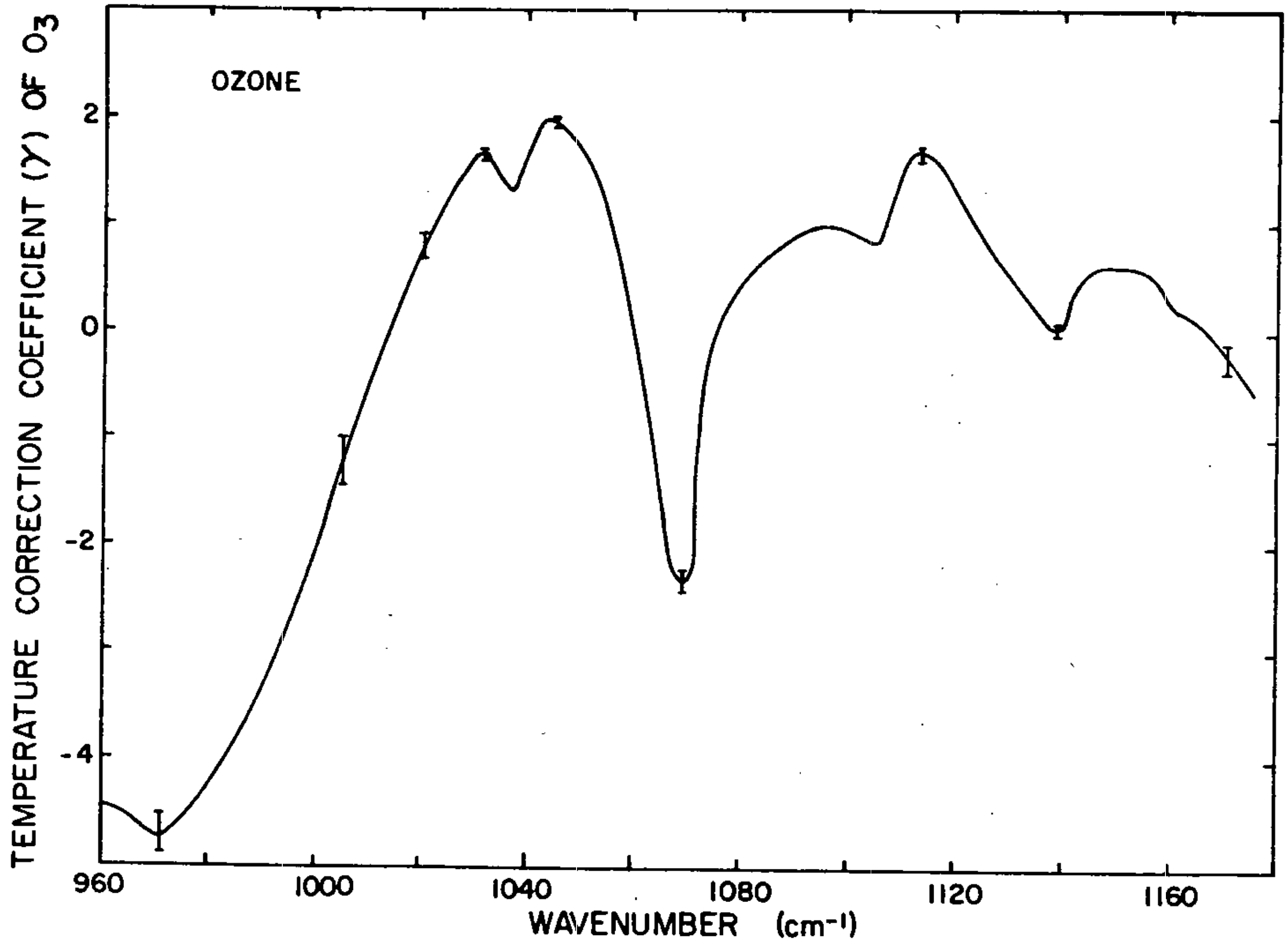

Figure 62. Temperature correction coefficients for the ozone band model absorption coefficients, $K_2 = K_1 (T_1/T_2)^{\gamma}$. $\gamma = 1$ is a density correction.

4. HNO_3 Temperature Correction

Values for γ were calculated for the HNO_3 band over the frequency range of 850 to 920 cm^{-1} for two pairs of temperatures. This data contained somewhat more scatter in the final results than the O_3 data since it was derived from experimental data and measured over a relatively small temperature interval. However, it also showed a probable deviation from $\gamma = 1$ at some frequencies, particularly toward the wings of the band. The total band intensity correction factor of γ is $0.874 \pm .021$. In an attempt to better define the functional relationship between γ and frequency, a second set of values for γ were calculated under the following assumptions. First, that the absorption coefficients calculated from the laboratory at 313°K are reasonably accurate. (This data is much more reliable than the lower temperature data.) Second, that absorption spectra measured at sunset from 30 km altitude in 1968[14] can be used as a low temperature measurement of HNO_3. Assuming a constant temperature (213°K) over most of the absorbing path and simple linear modeling ($\tau = e^{-Ku}$; where τ is transmittance, K is the absorption coefficient and u is the HNO_3 amount), values for γ can be calculated as a function of frequency. An estimate of the non-linear correction is < 1%. Since the amount of HNO_3 is not known, some point of normalization is required. An initial amount was calculated using $\gamma = 1$ at 872.5 and 875 cm^{-1} and was later adjusted slightly. (Changes in the amount of HNO_3 have the effect of shifting the curve

[14] D. G. Murcray, F. S. Bonorno, J. N. Brooks, A. Goldman, F. H. Murcray and W. J. Williams, "Detection of Fluorocarbons in the Stratosphere" Geophys. Res. Lett., 2, 109-112, 1975.

up or down on the γ scale.) Figure 63 shows two curves for the band model temperature coefficient for HNO_3. The solid curve is a hand-smoothed curve through all the data, both laboratory and atmospheric described above, and reflects a smoothing due to effects of different resolution. The dashed curve is from the laboratory absorption data only. The difference in these two curves points up the need to match the resolution of the model to that of the data, particularly in spectral regions containing sharp features such as Q-branches. Such regions are apparent at 879 and 896 cm^{-1}.

There are a number of weaknesses in this data that need to be resolved with additional measurements. However, the solid curve is presented here because it has been used at wavelengths (spectral regions 11 and 12) near the center of the band for spectral emission data from several past balloon flights and compared with results obtained by using the entire band. In all cases there was excellent agreement (within 5%) between the pairs of profiles generated, as can be seen in Figures 64, 66, 70, 71, and 72 and Table VII. This agreement was not present in some earlier attempts at comparing total band to band center profiles. The major change between the earlier calculations and those here is in using $\gamma \simeq 1$ for the total band instead of $\gamma = 1.5$.[15] The actual values used are listed in Table VI, along with the average values of γ over spectral regions 9, 10, 11, 12, and 13, for both curves in Figure 63. It is difficult at this time to state the accuracy of these values. There are large uncertainties in their derivation, but their success

---

[15] D. G. Murcray, A. Goldman, A. Csoeke-Poeckh, F. H. Murcray, W. J. Williams and R. N. Stocker, "Nitric Acid Distribution in the Stratosphere" J. Geophys. Res., 78, 7033-7038, 1973.

with field data provides some empirical justification for their use. Additional laboratory data at several temperatures is needed to better define the γ profile.

Table VI.

Absorption Coefficients and Temperature Corrections for Specified Spectral Regions

Spectral Region	$K(\text{atm-cm})^{-1}$	γ_{used}	$\gamma_{\text{Lab Data}}$
9	8.022 ($850-920\ cm^{-1}$)		$.874 \pm .021$
	8.217* ($850-940\ cm^{-1}$)		
10	7.51	.87	$.650 \pm .047$
11	11.17	1.13	$1.049 \pm .131$
12	11.13	.91	$.892 \pm .086$
13	9.42	.74	$.686 \pm .160$

*This value was derived as an average $(\Sigma \frac{kv}{n})$, the value used by Goldman et al.[16] for total band is 8.32 $(\text{atm-cm})^{-1}$.

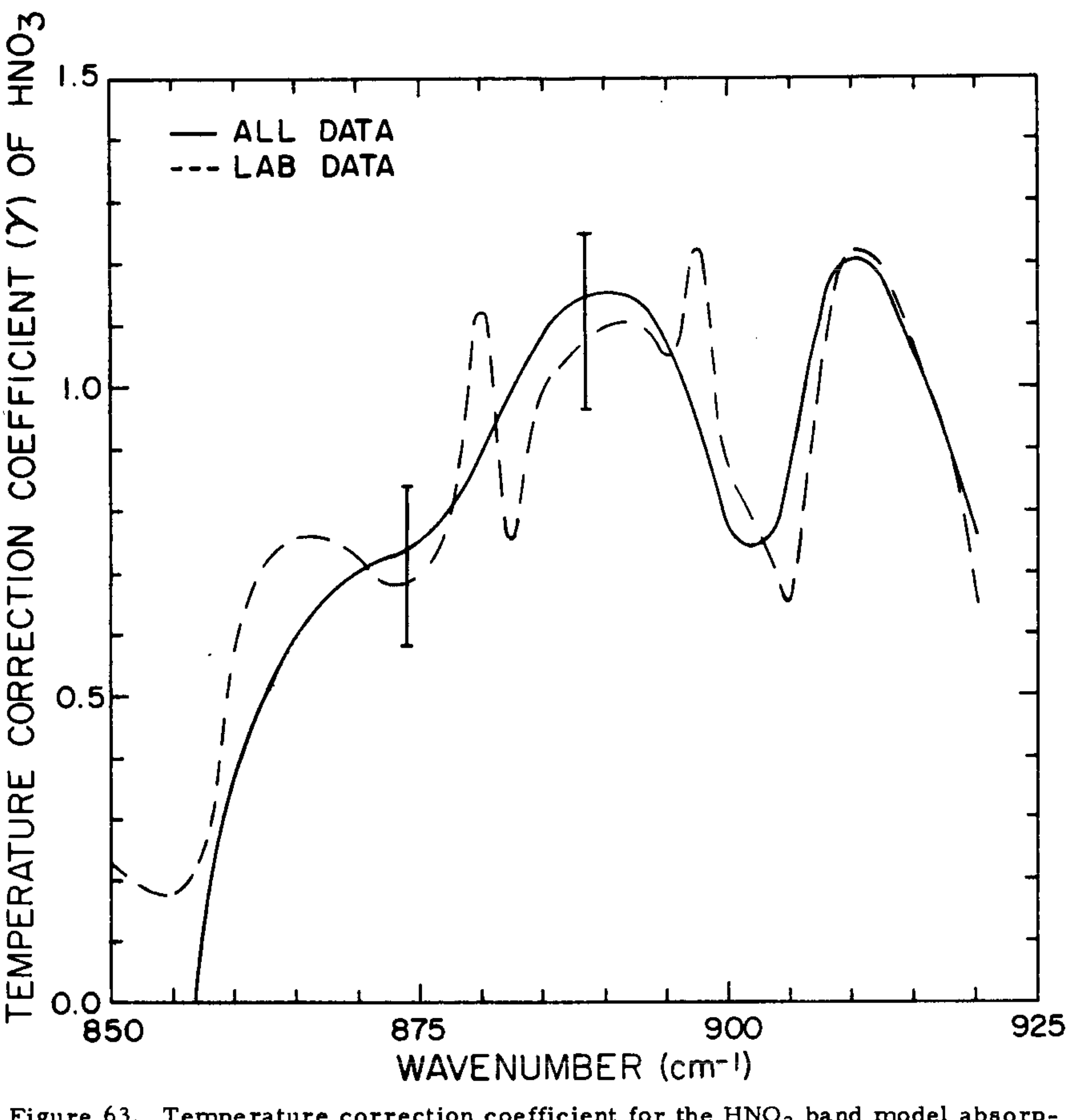

Figure 63. Temperature correction coefficient for the HNO_3 band model absorption coefficients, $K_2 = K_1(T_1/T_2)^{\gamma}$. $\gamma = 1$ is a density correction. The two curves represent differences in resolution in the data used and slight wavelength errors. While a strongly smoothed curve (solid) was used in this report, a curve similar to the dashed curve is more representative of the real band, but requires additional measurements for an accurate determination.

C. HNO_3 Profiles

The temperature dependence of the absorption coefficient was first tested by deriving the mixing ratio height profile of HNO_3 from the 29 April 1976 radiance data for several wavelengths. Figure 64 shows three superimposed curves which were derived using spectral regions 11, 12 and 9 (total band). The variation at any one height is random and due to variations in the measured radiance. Above the tropopause these integrated profiles agree to within 1%. The two profiles from regions 11 and 12 are indistinguishable from one another above 17 km. These profiles were derived from the change in radiance with height of the ascent data. Additional comparative data were obtained by observing the change in radiance as a function of zenith angle at float. Figure 65 shows this information as a series of one-layer calculations compared with the average ascent mixing ratio profile. Here, average refers to the mean of the total band profile and the band center profile at each height level.

This same data is presented in several ways in the form of number density and integrated density in Figures 66 through 68. The one-layer calculations from float are also shown in Figure 68, in which it is easier to see the apparent fit between the ascent and float data. In fact, it was from these data that the adjustment to the "effective" zenith angle of -0.2° was determined. This curve can also be used to determine quickly the fractional distribution of HNO_3 with height since scaling factors are easily read off a logarithmic scale (i.e., the center of mass of HNO_3 above the tropopause occurs at a factor of 2 down in the integrated column density scale, ~ 17 km and $< 1\%$ of the HNO_3 lies above 32 km.).

The absorption coefficient temperature corrections were then applied to the earlier spectral radiance data and, whenever possible, the band center profile was compared with the total band profile. Figures 69 through 77 show these comparisons and Table VII lists the integrated column for each case. The differences between them are only a few percent. The temperature corrections for the total band and band center are in good agreement. Corrections for the band wings probably need more laboratory data to insure their accuracy. Some of the profiles in Figures 70 through 76 are smoothed by a technique described by Goldman et al.[16] in which the measured data are fitted to functions with continuous derivatives.

The total band correction was then applied to the filter radiometer data and data that coincides with spectral measurements is included in Table VII. Here the agreement is not as good and is being studied further. Figure 78 also shows a comparison of three of these Alaskan HNO_3 profiles. Additional comparison of these data are being made and will be presented as a separate publication.

---

[16] A. Goldman, R. N. Stocker, D. Rolens, W. J. Williams and D. G. Murcray, "Stratospheric HNO_3 Distributions from Balloon-Borne Infrared Atmospheric Emission Measurements from 1970-75" Scientific Report, Department of Physics and Astronomy, University of Denver, 1976.

Table VII.

Comparison of Integrated Column of HNO_3
For Two or More Wavelength Regions

Date	Total Band (Region 9) (10^{20} mol/m^2)	Band Center (Region 11) (10^{20} mol/m^2)	Q-Branch (Region 12) (10^{20} mol/m^2)	Mean (10^{20} mol/m^2)	Filter (Total Band) (10^{20} mol/m^2)
29 Apr. 1976					
Above 12 km	1.030	1.060	1.035	1.046 ± 1.5%	
Above Trop.	1.213	1.198	1.216	1.206 ± 0.6%	
Above 8 km	1.534	1.343	1.452	1.439 ± 6.7%	
12 Sept. 1971					
Above 12.0 km		2.26		2.26	1.804
15 Sept. 1971					
Above 12.0 km	2.30	2.32		2.31 ± 0.4%	1.91
6 Sept. 1972					
Above 12.3 km	3.27	3.30		3.285 ± 0.5%	1.86
12 Sept. 1972					
Above 12.1 km	2.17	2.06		2.115 ± 2.6%	1.25
5 May 1975					
Above 12.0 km	1.71	1.97		1.84 ± 7.1%	1.31

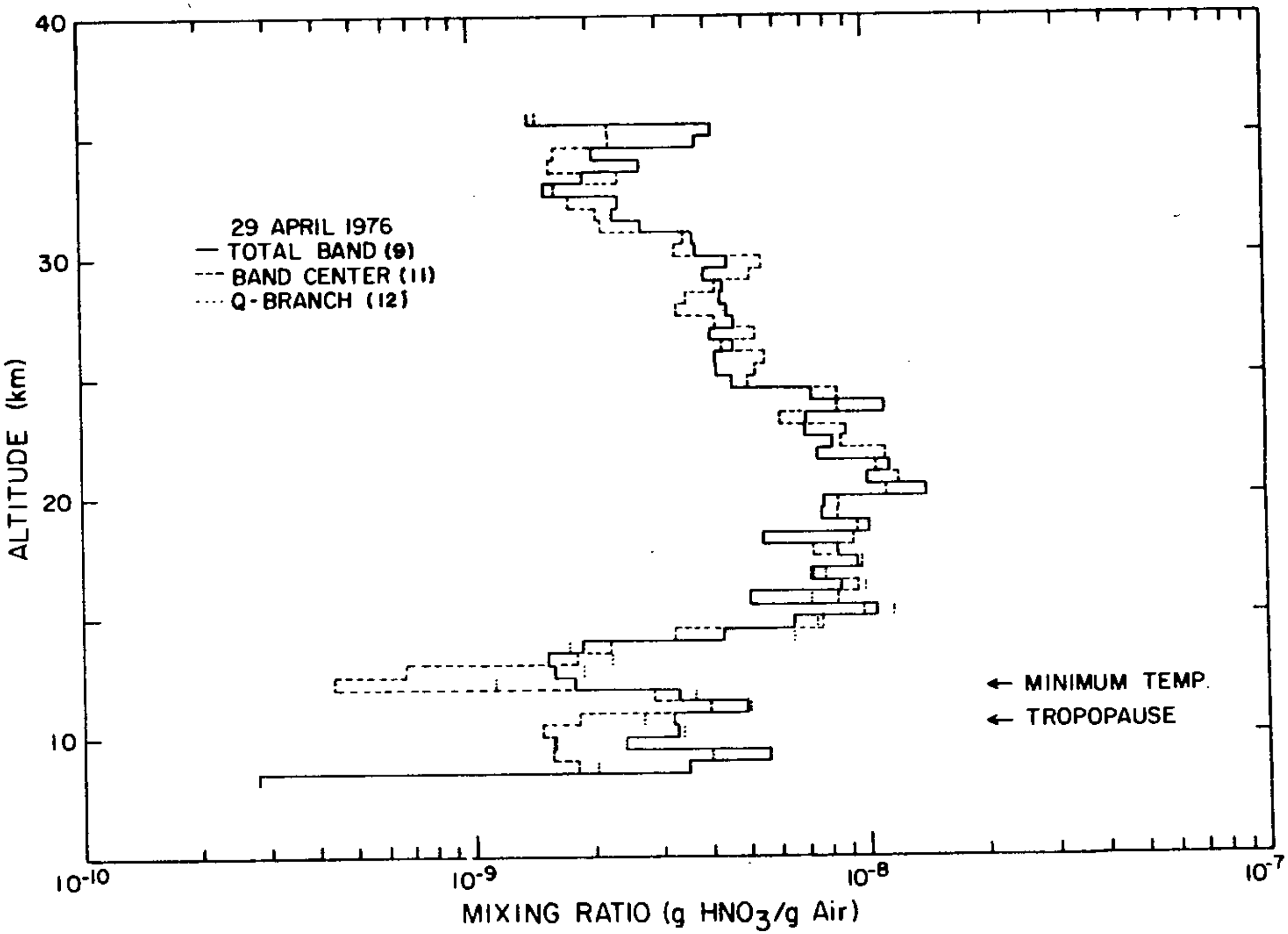

Figure 64. Mixing ratio height profile of HNO_3 using three spectral regions for comparison.

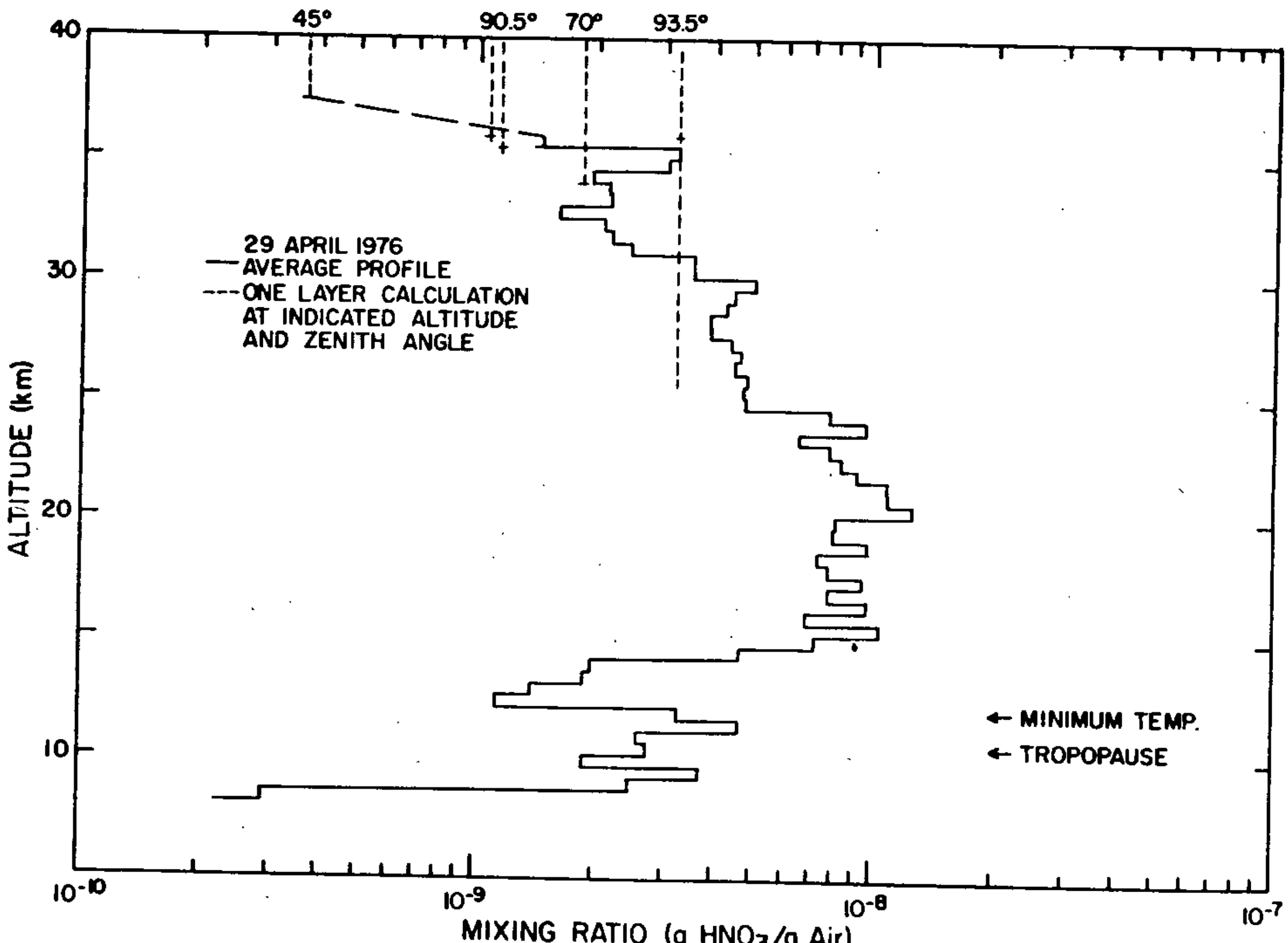

Figure 65. Average mixing ratio height profile of HNO_3 with data from one layer calculations from limb scans added. Angles associated with one layer calculations are shown at top of figure, altitude of observation is shown by (—) and minimum height of path by lower extent of dashed line.

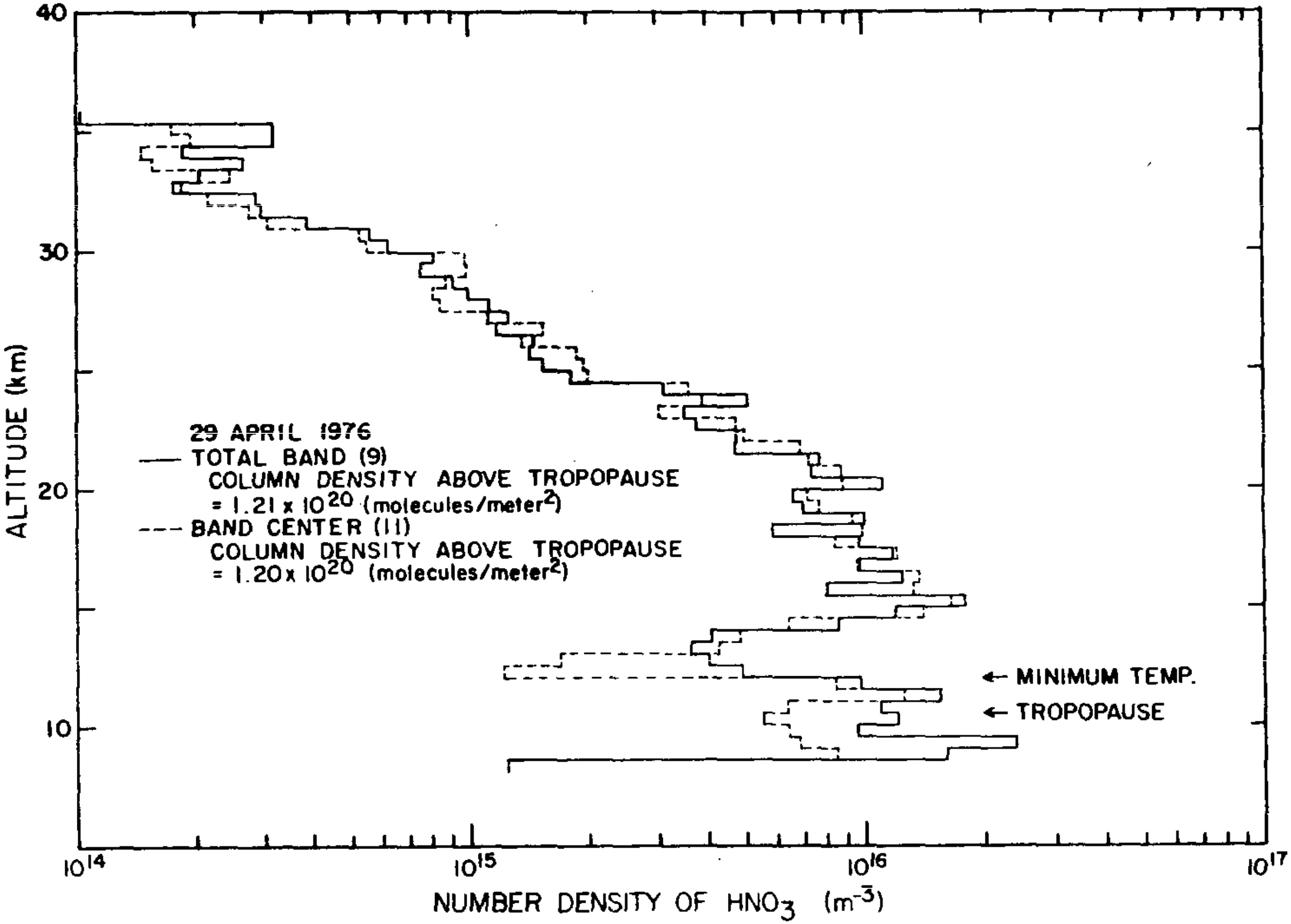

Figure 66. Number density height profile of HNO_3 for band center and total band calculations for comparison of the two models.

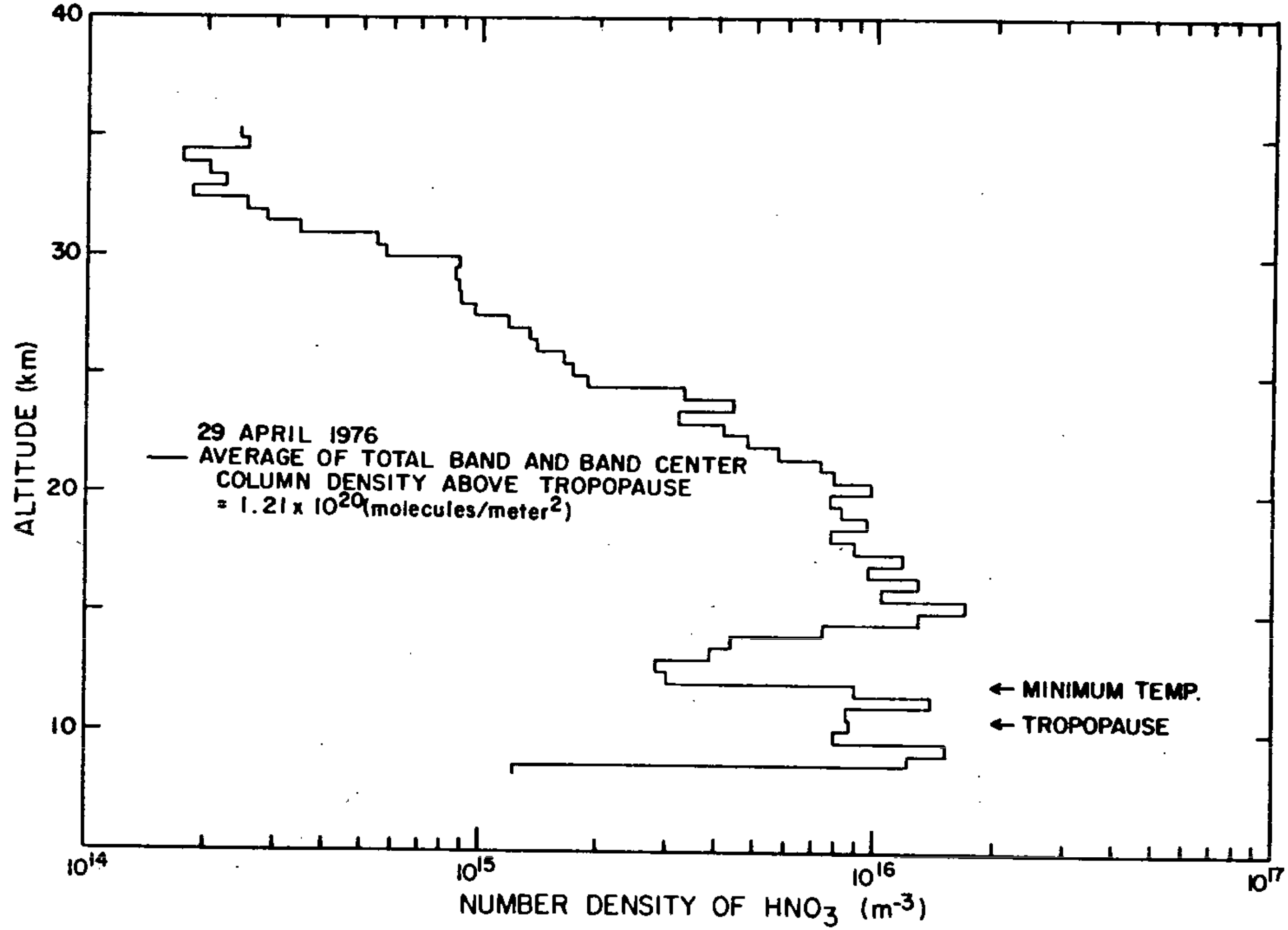

Figure 67. Average number density profile of HNO_3.

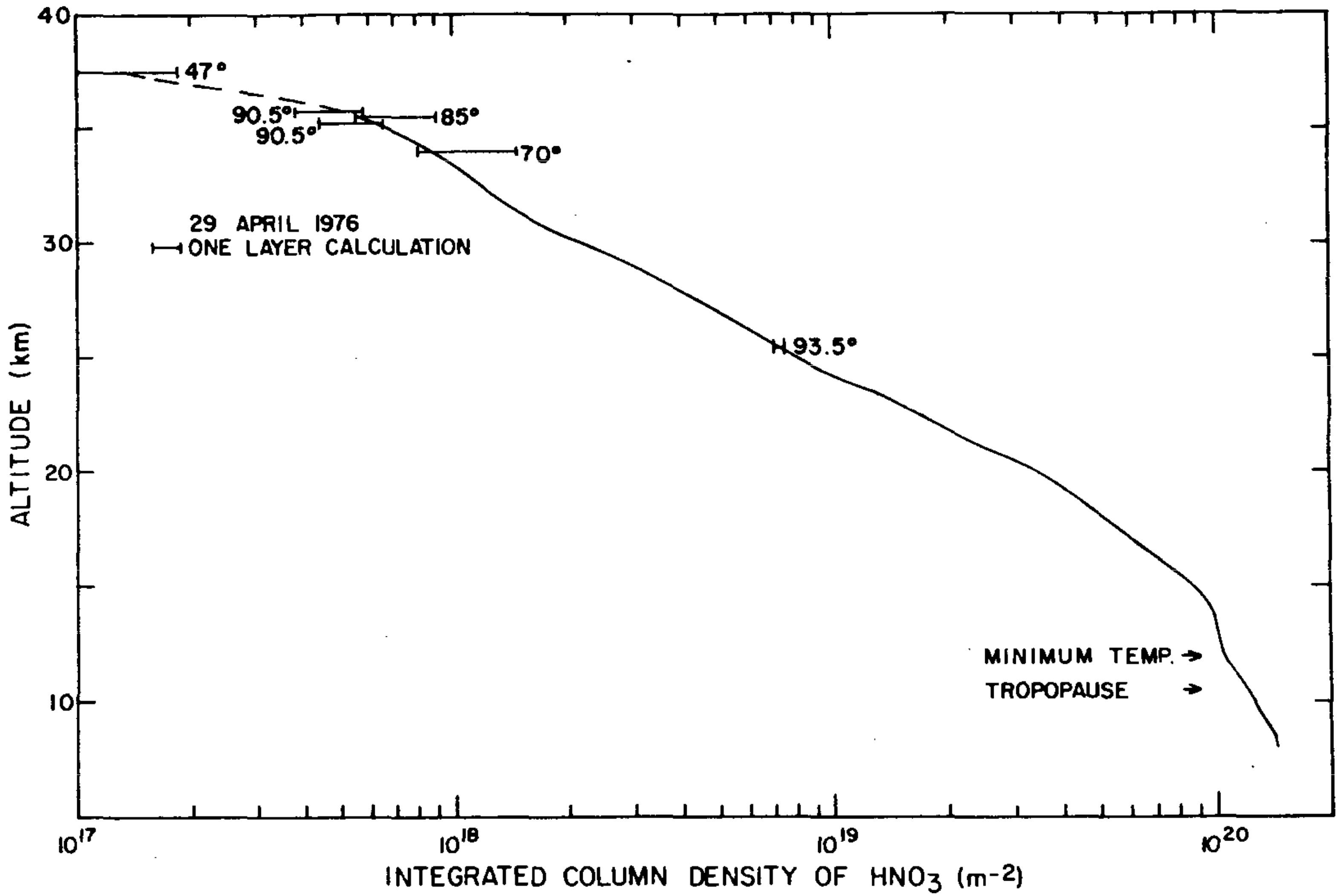

Figure 68. Integrated column density of HNO_3 as a function of height. Data from zenith angle scans near float have been added (⊢⊣) with length of bar representing range of radiance values over the five or more scans averaged for this calculation.

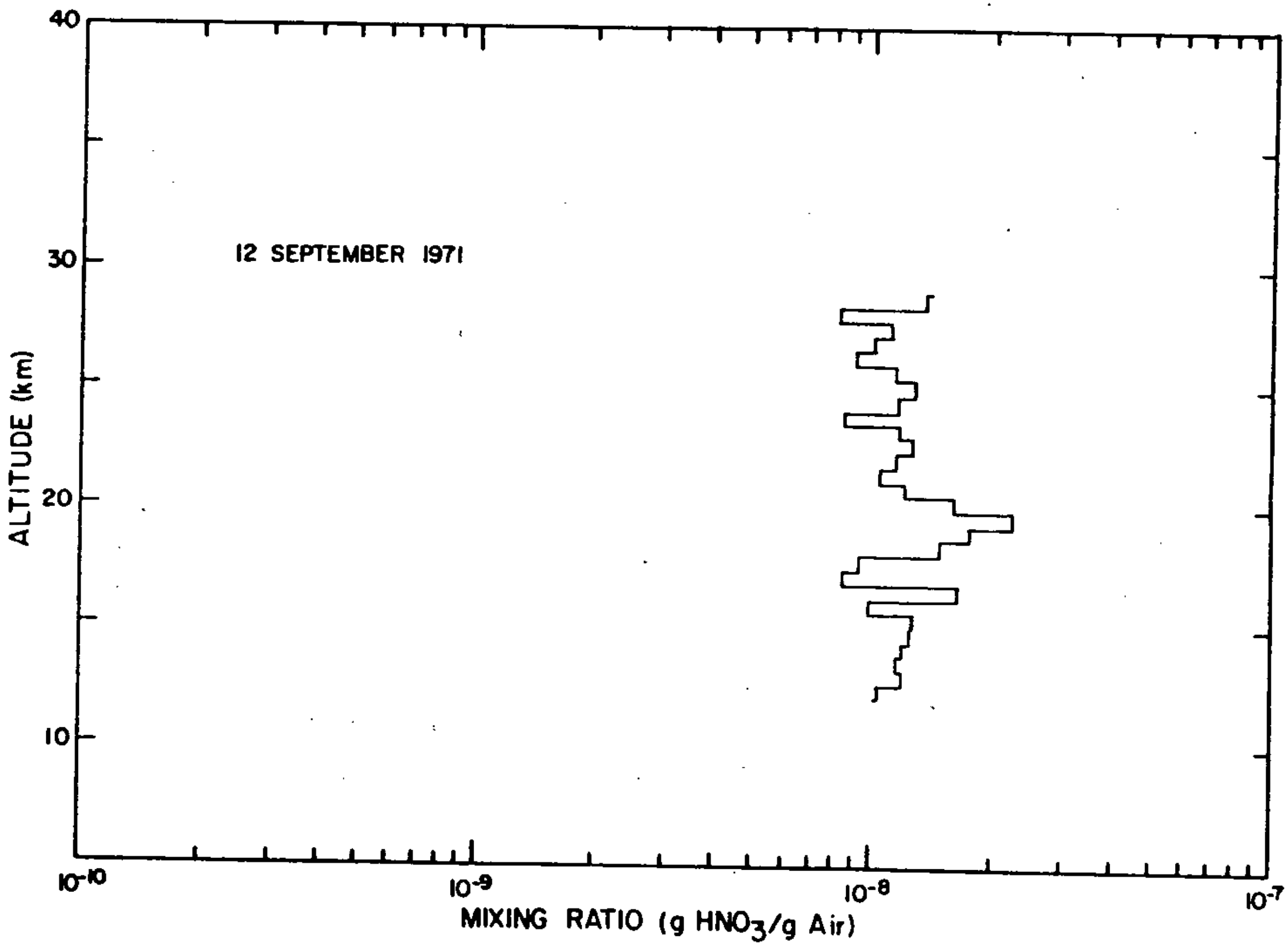

Figure 69. Mixing ratio height profile of HNO_3 for 12 September 1971 from Fairbanks, Alaska and using a LN_2 cooled spectrometer.

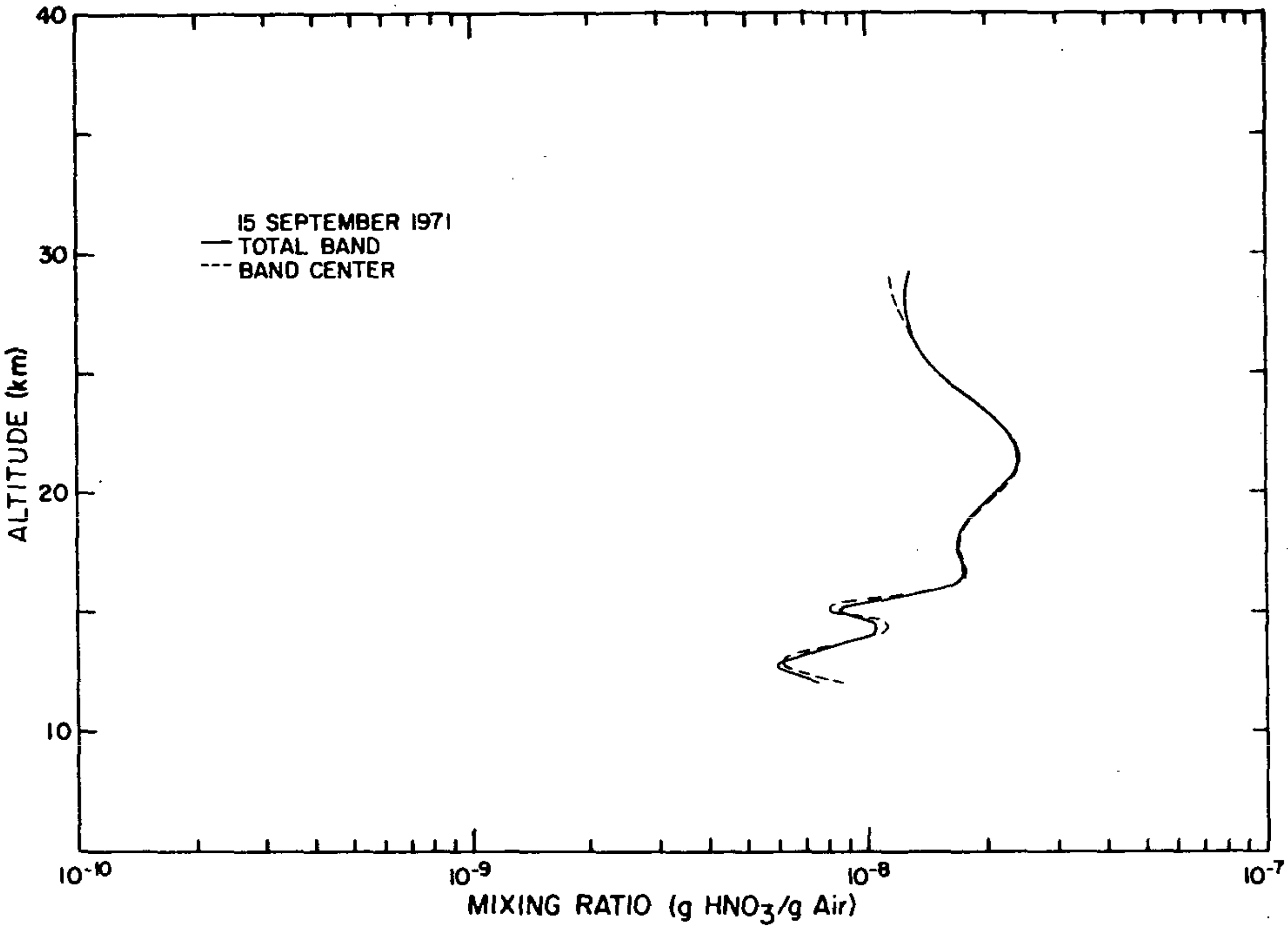

Figure 70. Mixing ratio height profile of HNO_3 for two spectral regions for 15 September 1971 from Fairbanks, Alaska and using a LN_2 cooled spectrometer.

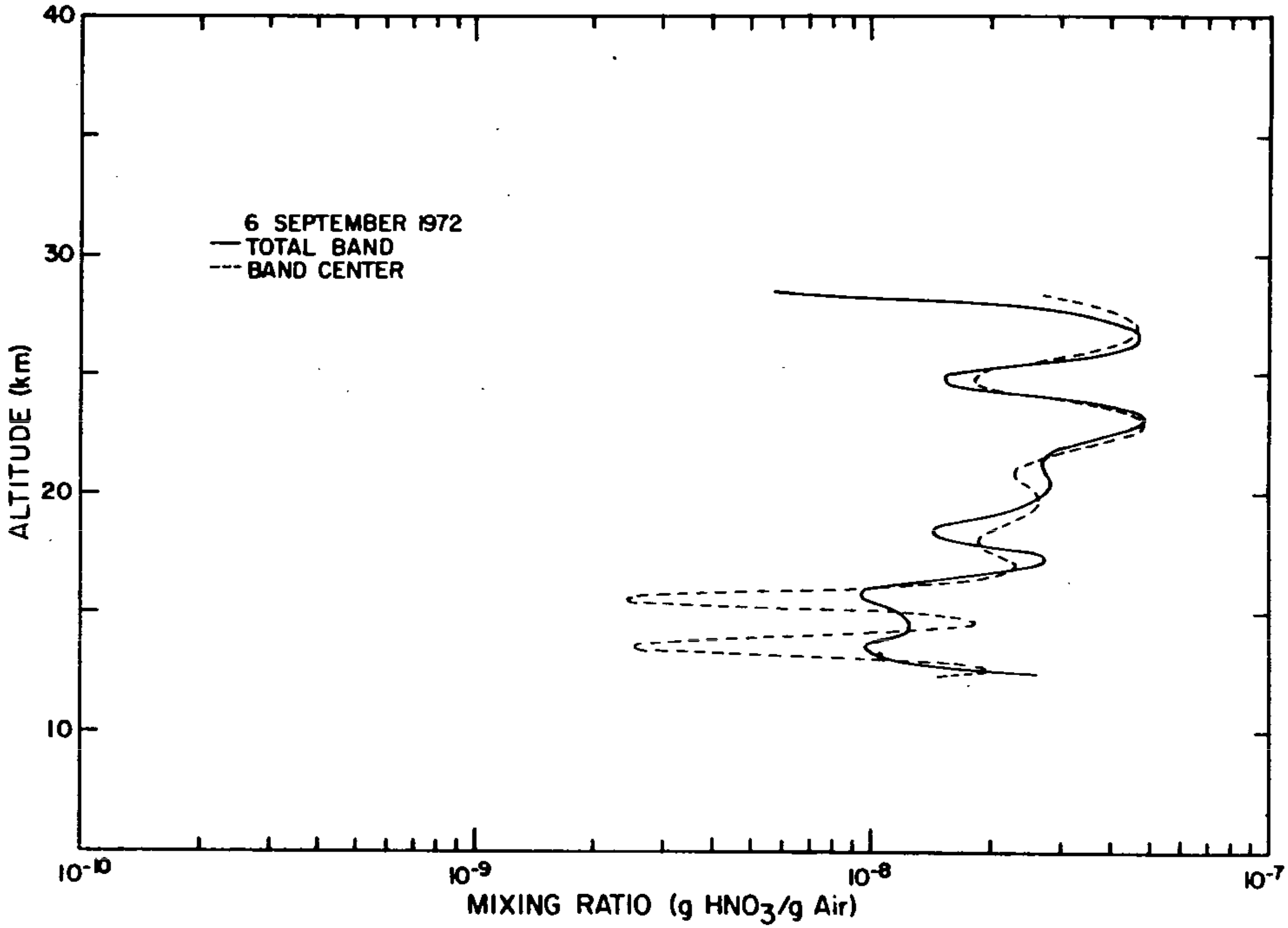

Figure 71. Mixing ratio height profile of HNO_3 for two spectral regions for 6 September 1972 from Fairbanks, Alaska and using a LN_2 cooled spectrometer.

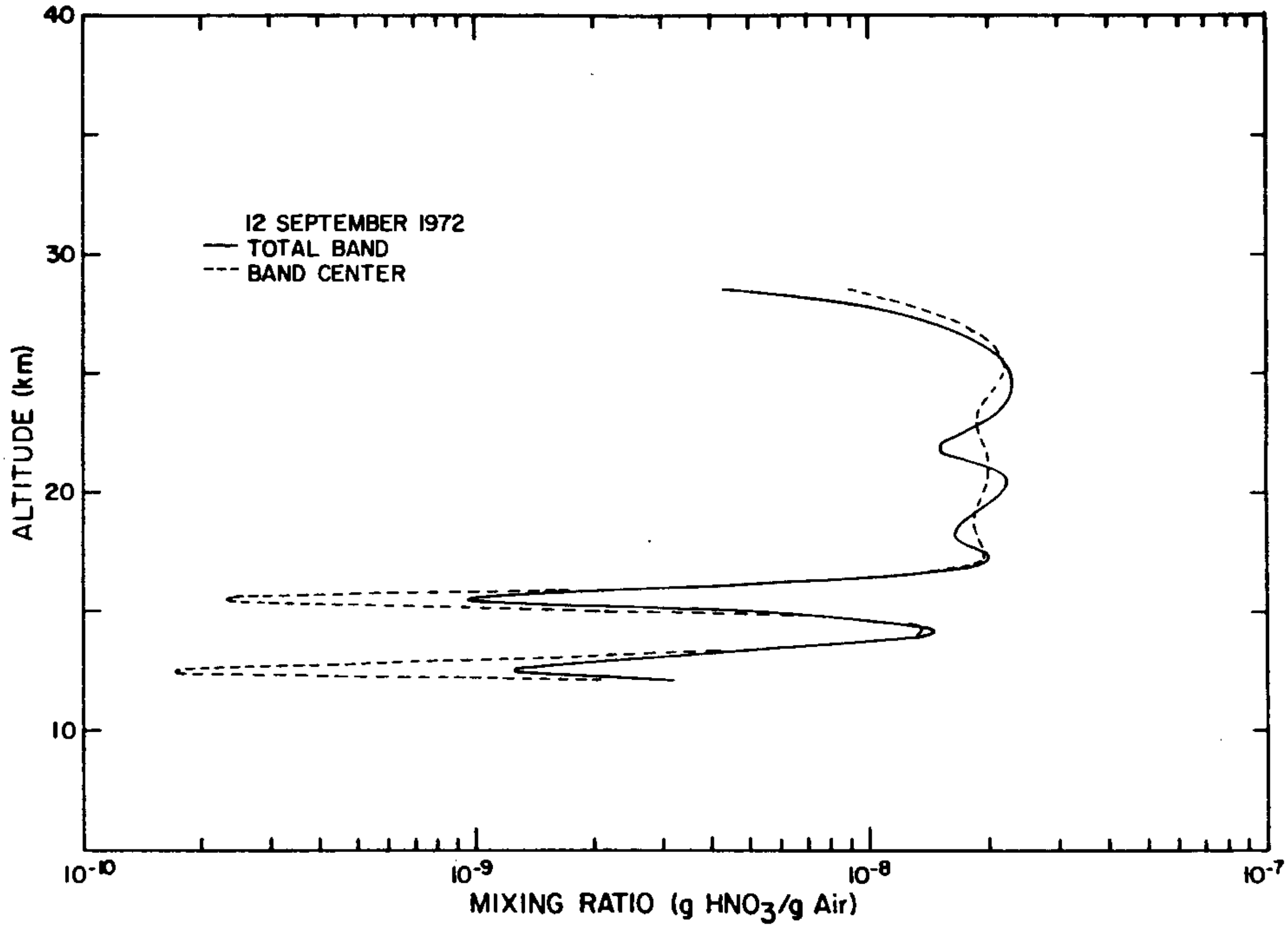

Figure 72. Mixing ratio height profile of HNO_3 for two spectral regions for 12 September 1972 from Fairbanks, Alaska and using a LN_2 cooled spectrometer.

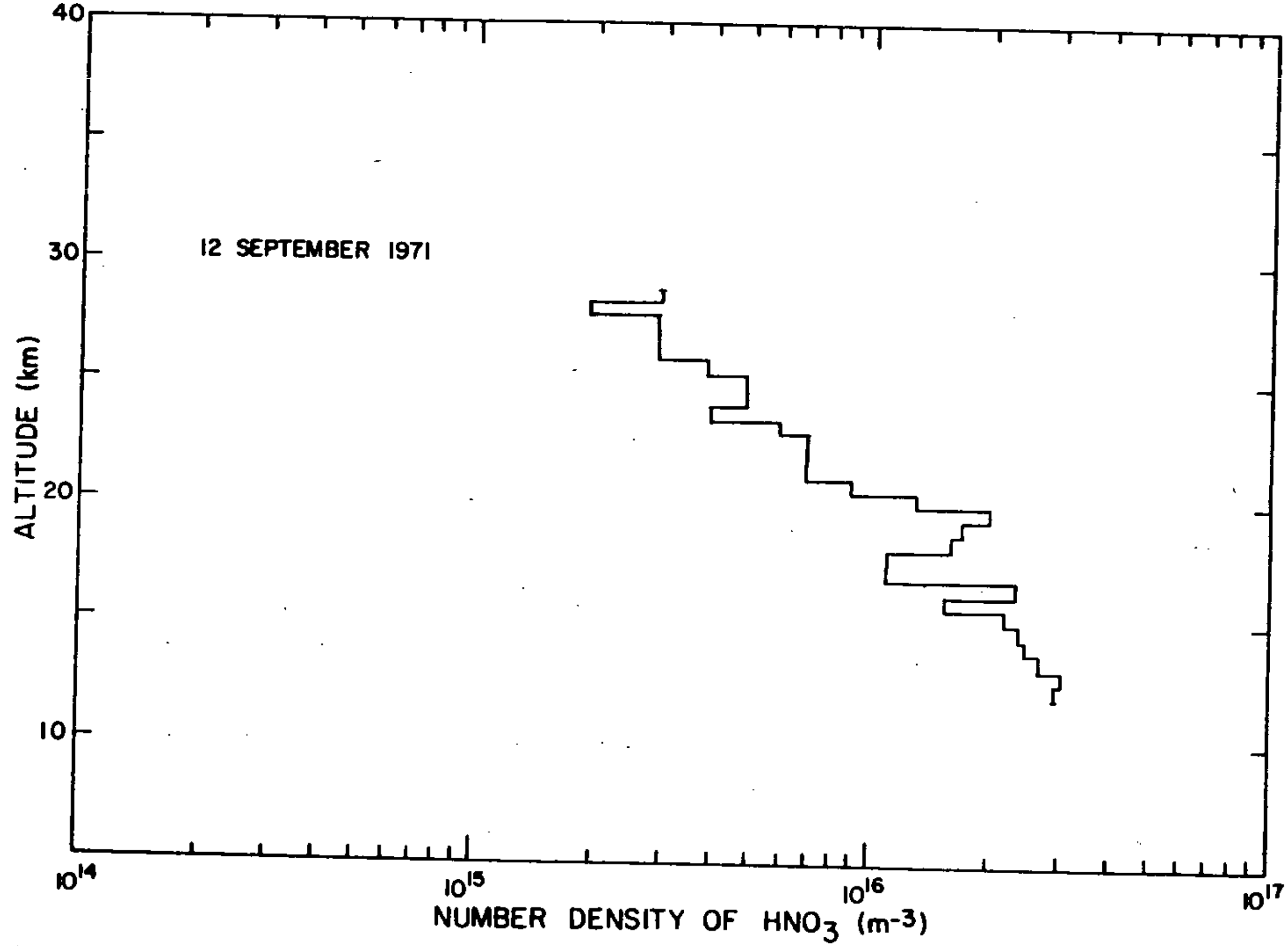

Figure 73. Number density height profile of HNO_3 for 12 September 1971.

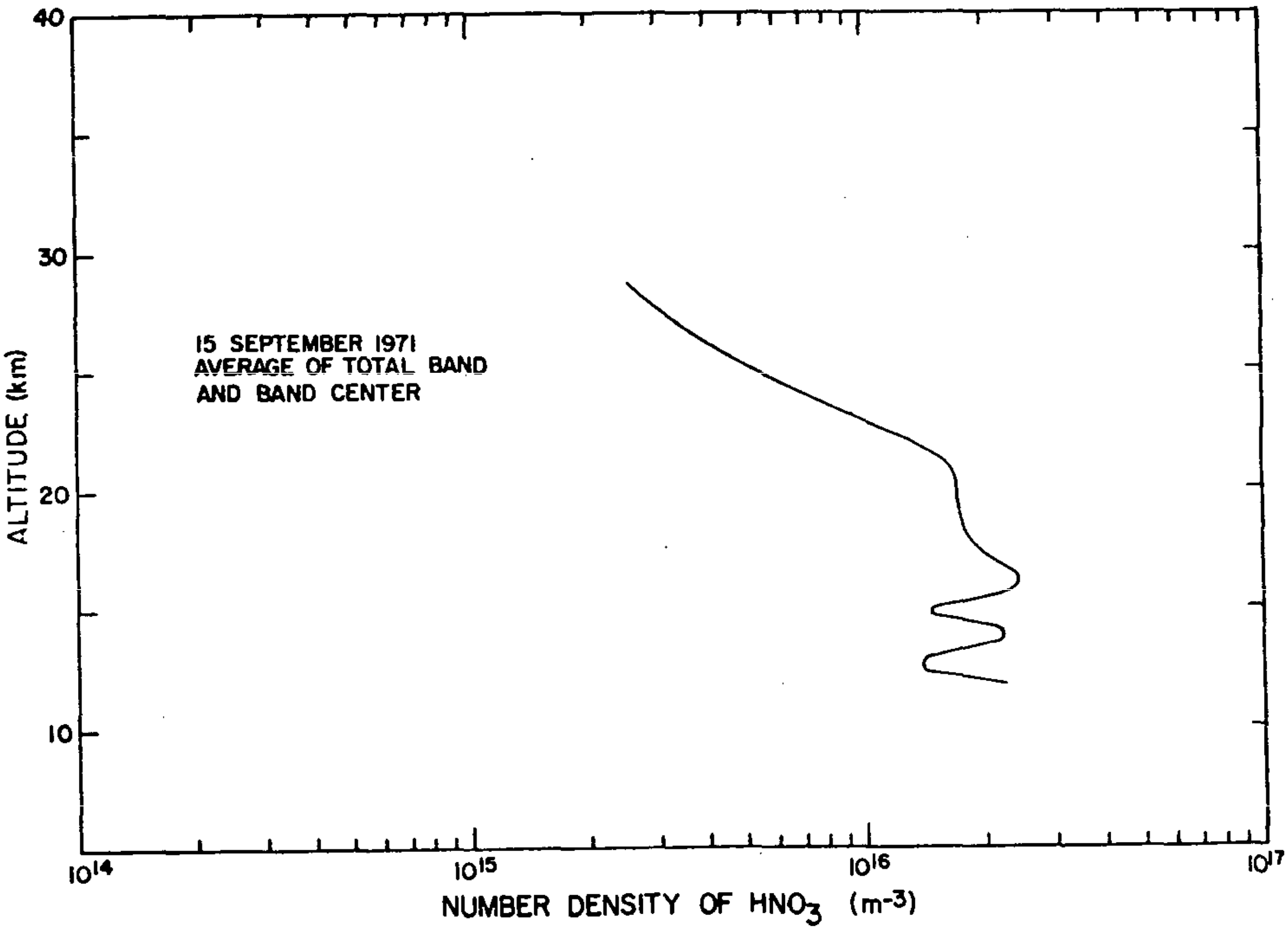

Figure 74. Average number density height profile of HNO_3 for 15 September 1971.

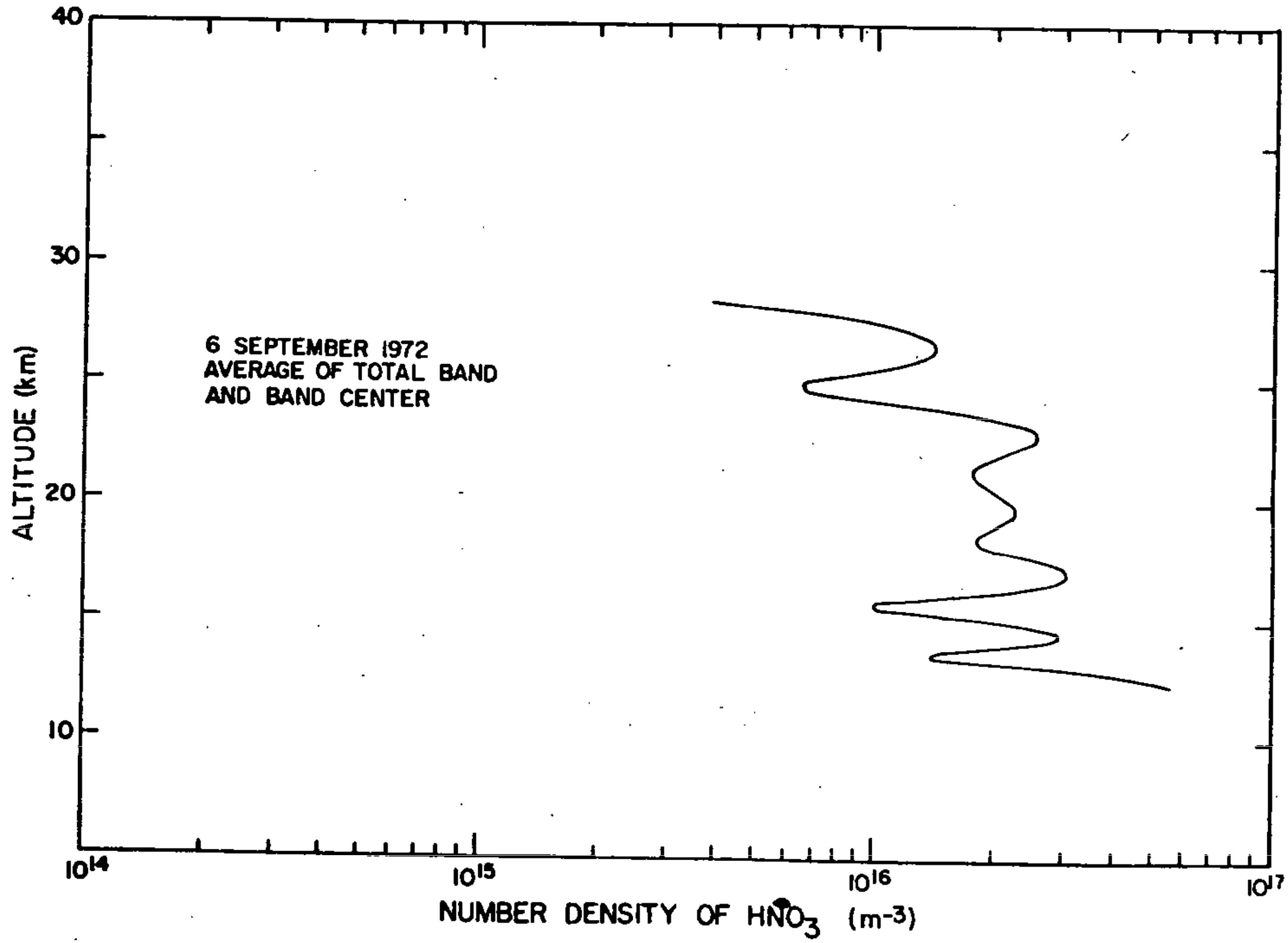

Figure 75. Average number density height profile of HNO_3 for 6 September 1972.

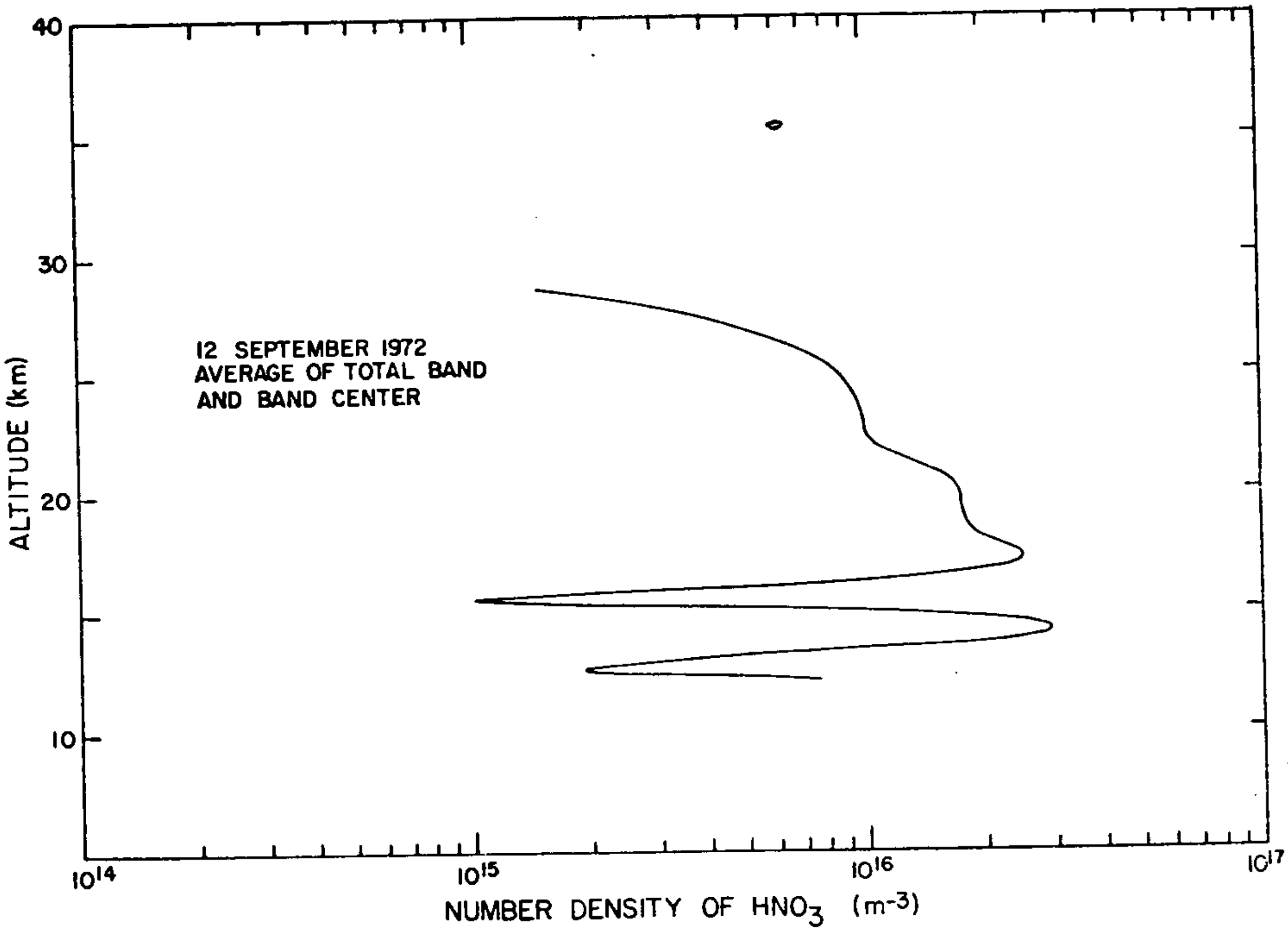

Figure 76. Average number density height profile of HNO_3 for 12 September 1972.

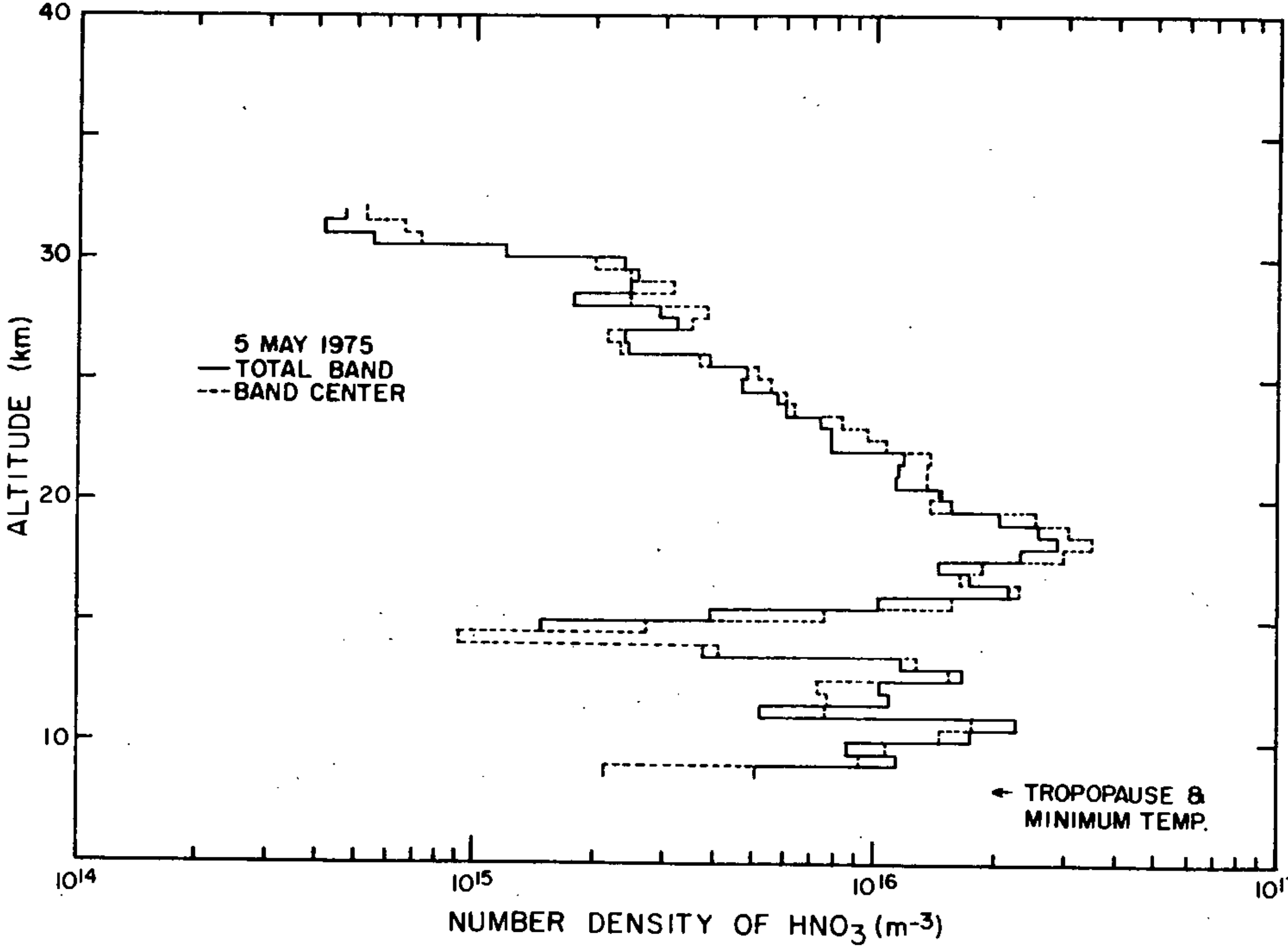

Figure 77. Number density height profile of HNO_3 for two spectral regions for 5 May 1975 from Fairbanks, Alaska and using the LHe cooled spectrometer.

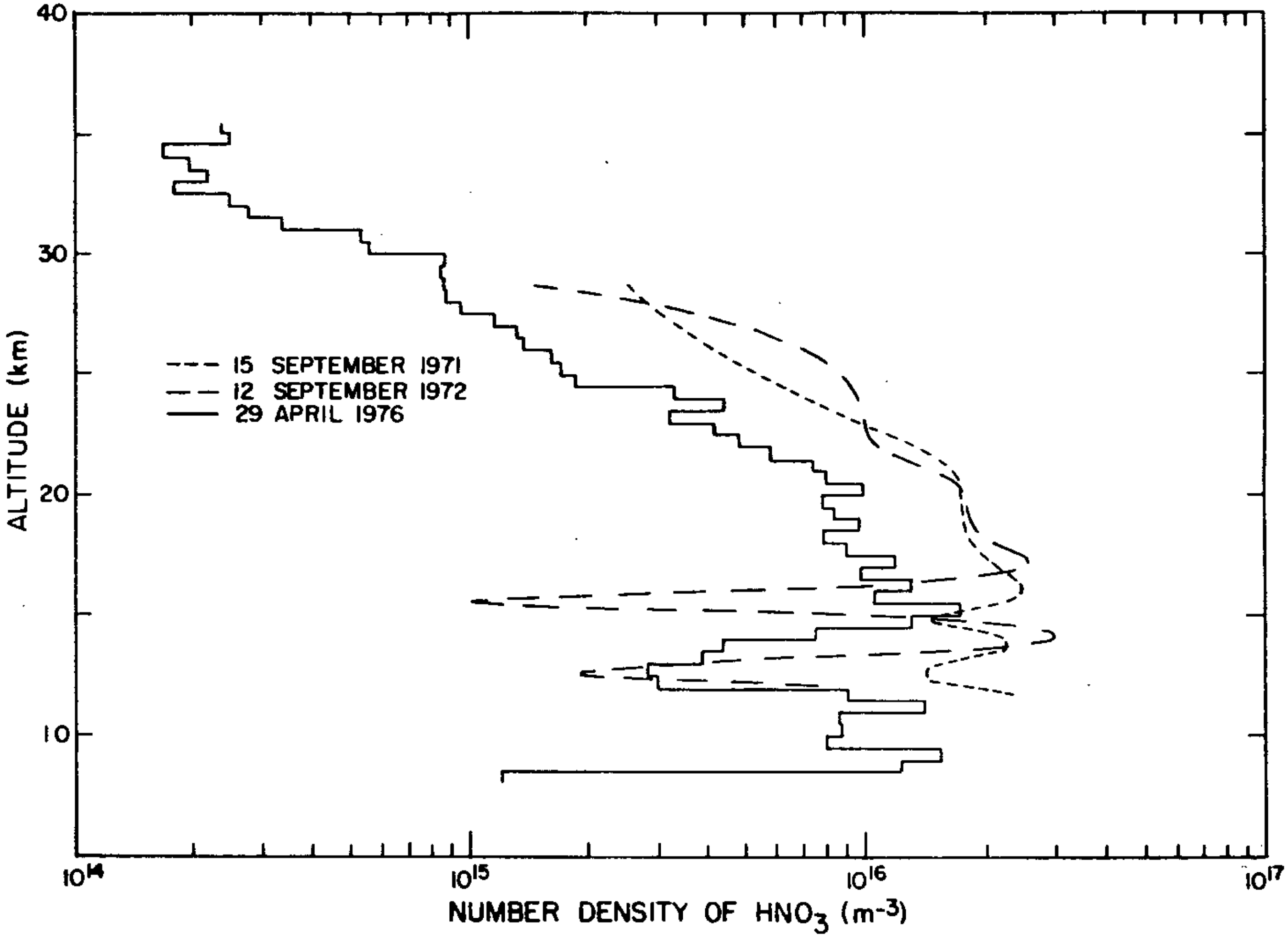

Figure 78. Comparison of selected number density height profiles of HNO_3 for Fairbanks, Alaska.

D. H_2O Profiles

The water vapor mixing ratio height profiles are derived using the line-by-line model and the long wavelength rotational water vapor emission data. This method was used because the rotational lines are very strong and are not suitable to linear modeling. Also the individual line parameters are well-known. The reiterative process of matching the measured integrated radiance over a group of lines with the calculated integrated radiance from

$$N(\nu, h_2) = \tau(\nu, 2)\ N(\nu, h_1) + \epsilon(\nu, 2)\ B(\nu, 2) \tag{16}$$

is described in the preceding report.[1] The results of this calculation for spectral region 28 are shown in Figure 79 along with results from a similar calculation for the 5 May 1975 data, also from Fairbanks. These represent significantly different profiles for the stratosphere which overlap in the upper troposphere. The differences are larger than can be explained by reasonable error analysis and represent a difference in the stratospheric model for these two dates. A profile using the water lines of region 31 will be calculated and used for additional comparison.

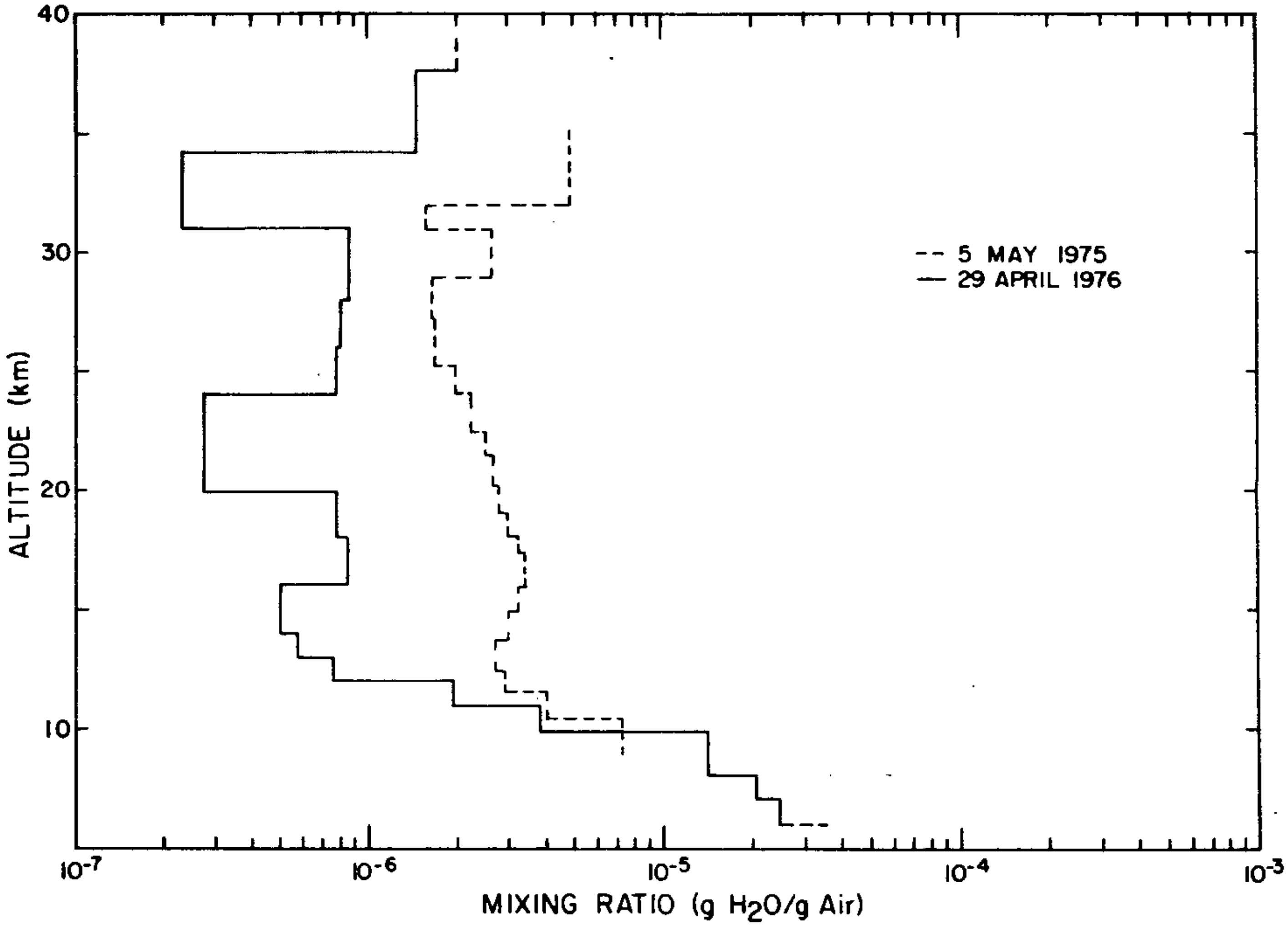

Figure 79. Comparison of the mixing ratio height profiles of H_2O for 5 May 1975 and 29 April 1976 for Fairbanks, Alaska.

E. O_3 Profiles

Ozone has a number of strong emission features in the spectral region scanned. It should be possible to calculate O_3 height profiles from this data, possibly using more than one wavelength. Goldman et al.[10] have calculated band model parameters for the O_3 bands between 960 and 1176 cm^{-1} which were used in a preceding section of this report. Within this spectral range, two regions were selected (2 and 3) which are dominated by O_3 emission. The emission at 9.7μm (region 3) is much stronger than that at 8.9μm (region 2). Yet, the calculated column density of O_3 should be the same for both regions for an observed spectrum at the tropopause (selected to be below the O_3 and above any interfering H_2O). The band model parameter $2(\frac{x}{L})\frac{u}{p}$ described above which defines the emission range for linear modeling can be evaluated for each of these spectral regions. For the 8.9μm region it has a value $\simeq 0.1$ depending on what "effective pressure" is used, while in the 9.7μm region it has a value >2. Thus, linear modeling can possibly be used in region 2, but definitely not in region 3.

One-layer calculations of atmospheric absorption or emission must, of necessity, include assumptions concerning effective temperature and pressure. This is true for both line-by-line and band model calculations. The effective temperature is not too difficult to choose for absorption, particularly in the lower stratosphere where the temperature does not change greatly. But for the emission process, the temperature also strongly influences the value of B, the Planck radiation term, and can be a major source of error. The effective pressure is important when the line centers become black. For a uniformly mixed gas the Curtis-Godson approximation

of p/2 is usually used, but many of the constituents of interest are not uniformly mixed. An alternate assumption is to use a pressure associated with the height of the center of mass of the column being measured. This method gives approximately p/2 for uniform mixing and is also appropriate for a highly-layered constituent.

A series of calculations was performed for both spectral regions 2 and 3 using the data and parameters associated with record 84 (10.3 km altitude) to show the magnitude of error associated with four different assumptions. These four assumptions are: 1) linear modeling (no pressure dependence); 2) $p_e = p/2$; 3) $p_e = p$ at the center of mass of the O_3 profile as determined from the auxiliary O_3 measurement; 4) β = const and $p = p_o e^{-z/H}$. With the fourth assumption the band model calculation takes the slightly different form of[17]

$$T = \exp -\left[\frac{\alpha_o}{d}\, p\, 2\sqrt{\pi}\, \frac{\Gamma(x_o + 1/2)}{\Gamma(x_o)}\right] \quad , \tag{17}$$

where $x_o = \frac{S^o u}{2\pi\alpha_o p}$, and α_o is the half-width and Γ is a gamma function.

Table VIII shows the values of u and the total O_3 in the slant path above the point of observation for each of the cases described. Several points can be briefly noted. For the near linear case at 8.9µm, all the techniques agree to better than 5%. For the non-linear case at 9.7µm, the use of p/2 and β = const contain similar assumptions and produce close results. However, the best agreement

[17] R. M. Goody, Atmospheric Radiation I. Theoretical Basis, Oxford University Press, London, 1964.

between the linear and non-linear calculations occurs when using the pressure at the center of mass. Since O_3 is somewhat layered, this is probably not surprising. Unfortunately, it is not always possible to know the height of the center of mass when making one-layer calculations.

It is apparent from these considerations that the 8.9µm region can be used with a linear model to derive O_3 height profiles from the differential radiance data in a manner similar to that for HNO_3. Such a profile of number density vs height is shown in Figure 80. Included in this plot is an O_3 profile measured with an ozonesonde from Poker Flats on the same day. The profiles have similar features and the infrared technique provides a detailed profile at the higher altitudes generally lacking in the sonde data. However, there is a discrepancy in the absolute magnitude of the two curves. A comparison between the two curves can be accomplished by integrating each curve over a height range where both instruments seem to be working well, say 10.5 to 24.5 km. The ratio of the two column values over this range (5.99×10^{22} / 2.58×10^{22}) (m^{-2}) is 2.3 : 1. The O_3 profiles derived from the radiance data of 27 June 1974 and 19 February 1975 also show low absolute values compared with other measurements. In contrast, data of the 5 May 1975 flight show a total column of O_3 above 10.5 km of $>10^{23}$ m^{-2}, while the total O_3 above the tropopause is 3.16×10^{22} m^{-2}. This discrepancy is under study both by this group and Dr. Snider at ASL.

The O_3 profile for 29 April has also been plotted as mass mixing ratio vs height in Figure 81. This figure also contains the mixing ratio profiles of HNO_3 and H_2O for this data. The most

notable common feature is the strong fall-off in the profiles at the minimum temperature, rather than at the tropopause (here defined as a significant change in temperature lapse rate).

Table VIII.

Comparison of Various Equivalent Pressures Used for One Layer Calculations of the O_3 Column

Parameters

	8.9μm	9.7μm
N	3.532	80.85 $\mu w\ cm^{-2} sr^{-1} \mu m^{-1}$
ϵ	.0257	.4933
S^o/d	.1366	8.354 $(atm\text{-}cm)^{-1}$
α_o/d	1.006	1.92 (atm^{-1})
x/L_e	.0214	.732
p	.245 (atm)	.245 (atm)
z	10.30 km	10.30 km
p(1/2 mass)	.058 (atm)	.058 (atm)
z(1/2 mass)	19.5 km	19.5 km

Calculated Column of O_3 (atm-cm)

	8.9μm	9.7μm
Linear	.1906	.0814
p/2	.1971	.1300
p(center of mass)	.2045	.2002
β = Const	.1948	.1126

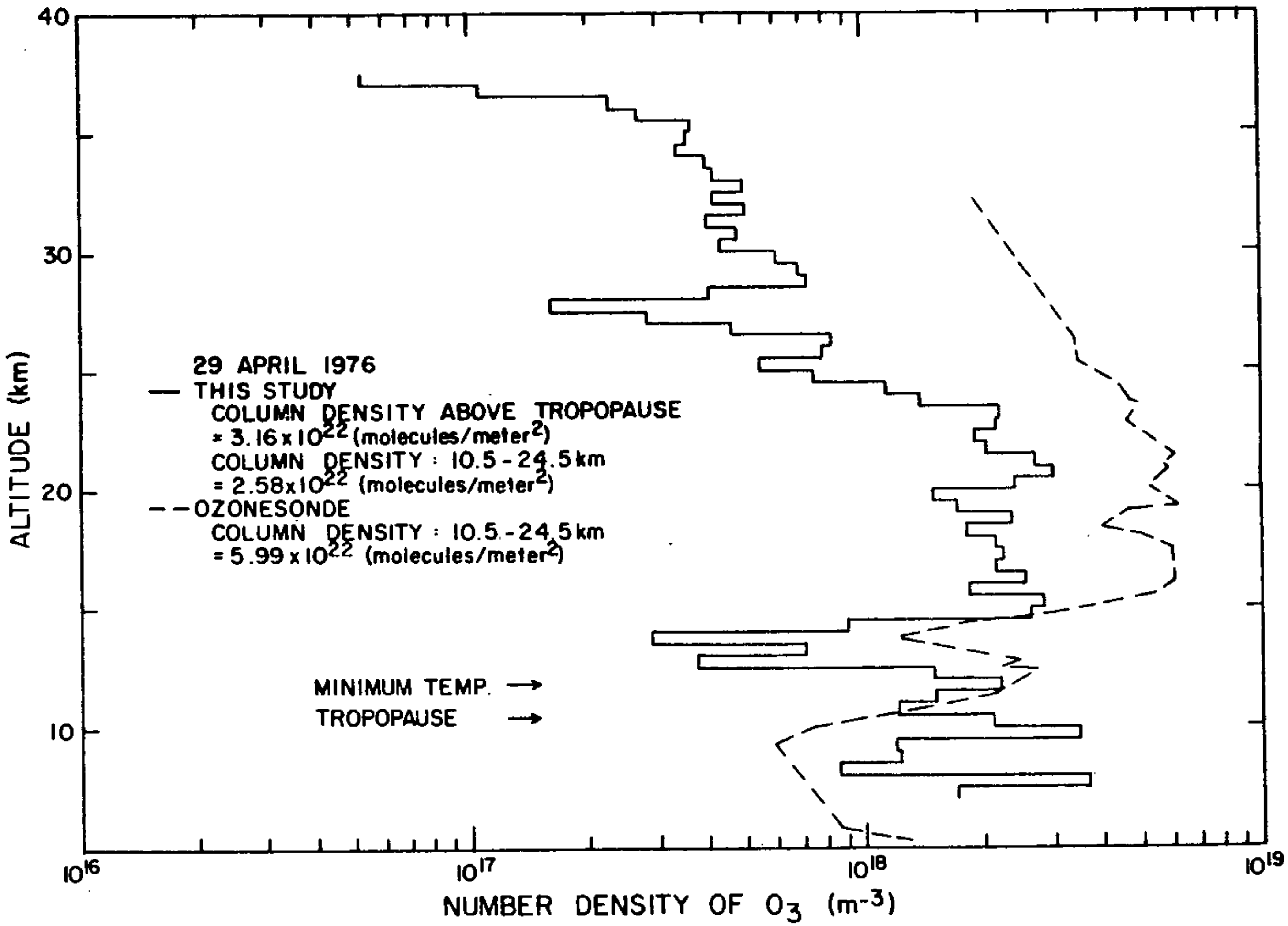

Figure 80. Number density height profile of O_3 derived from the $8.9 \mu m$ spectral radiance compared with that measured with a balloon ozonesonde.

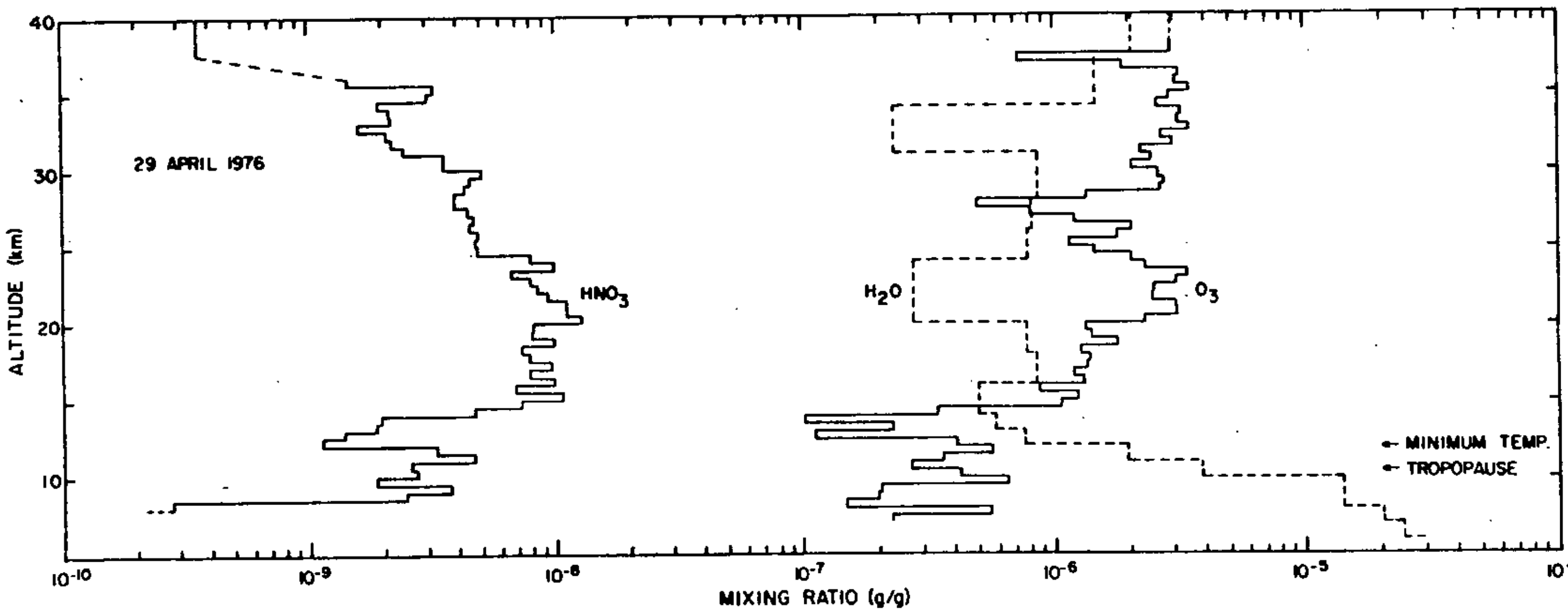

Figure 81. Comparison of mixing ratio height profiles of HNO_3, H_2O and O_3 for 29 April 1976.

F. Other Constituents

1. $CF_2Cl_2 + CFCl_3$

The spectral radiance near the tropopause in the 10-13μm region shows a great deal of structure (see Figures 39 through 46). Some of this is due to F-11 ($CFCl_3$) and F-12 (CF_2Cl_2) (regions 7, 8 and 15), and some is due to unidentified constituents (regions 17 and 18). F-11 and F-12 height profiles near the tropopause can be calculated by fitting the total spectral data as Murcray et al.[18] have done with this data (Figure 82) or by selecting specific wavelength intervals (regions 7, 8 and 15). Both approaches use the band model parameters of Goldman et al.[19,20] The difficulty in this analysis is not with the spectral parameters, but rather with the changing radiance due to gray emitters, probably cirrus clouds, as was discussed earlier. The difference between the earlier F-11 and F-12 computations and those using the selected spectral regions is the manner of dealing with this gray radiation. The earlier effort attempted to estimate the gray radiance based on the relative

---

[18] D. G. Murcray, A. Goldman, F. H. Murcray and W. J. Williams, "Measurement of CF_2Cl_2 and $CFCl_3$ Using Infrared Emission Spectra" Final Report on MCA Contract No. 75-13, Department of Physics, University of Denver, December 1976.

[19] A. Goldman, F. S. Bonomo and D. G. Murcray, "Statistical Band Model Analysis and Integrated Intensity for the 11.8μm Band of $CFCl_3$" Appl. Opt., <u>15</u>, 2305-2307, 1976.

[20] A. Goldman, F. S. Bonomo and D. G. Murcray, "Statistical Band Model Analysis and Integrated Intensity for the 10.8μm Band of CF_2Cl_2" Geophys. Res. Lett., <u>3</u>, 309-312, 1976.

intensities of different parts of the calculated spectral features. This effort was to subtract the total radiance measured in the minimas of the nearby spectral features (i.e. spectral regions 4 or 6). Figure 83 shows the profile from the earlier calculation and Figures 84 and 85 show the latter. The first probably under-compensated and the second over-compensated for gray radiation. This is a difficult problem and requires more study. Improved spectral resolution would probably be of some help, as would elimination of the optical window scattering radiation. Data of Ridley et al.[21] obtained during the same flight series is also shown in Figures 83 and 84.

[21] B. A. Ridley, "Stratospheric Measurements of $CFCl_3$ and CF_2Cl_2 at Fairbanks, Alaska" MCA Report 76-102, August 3 1976.

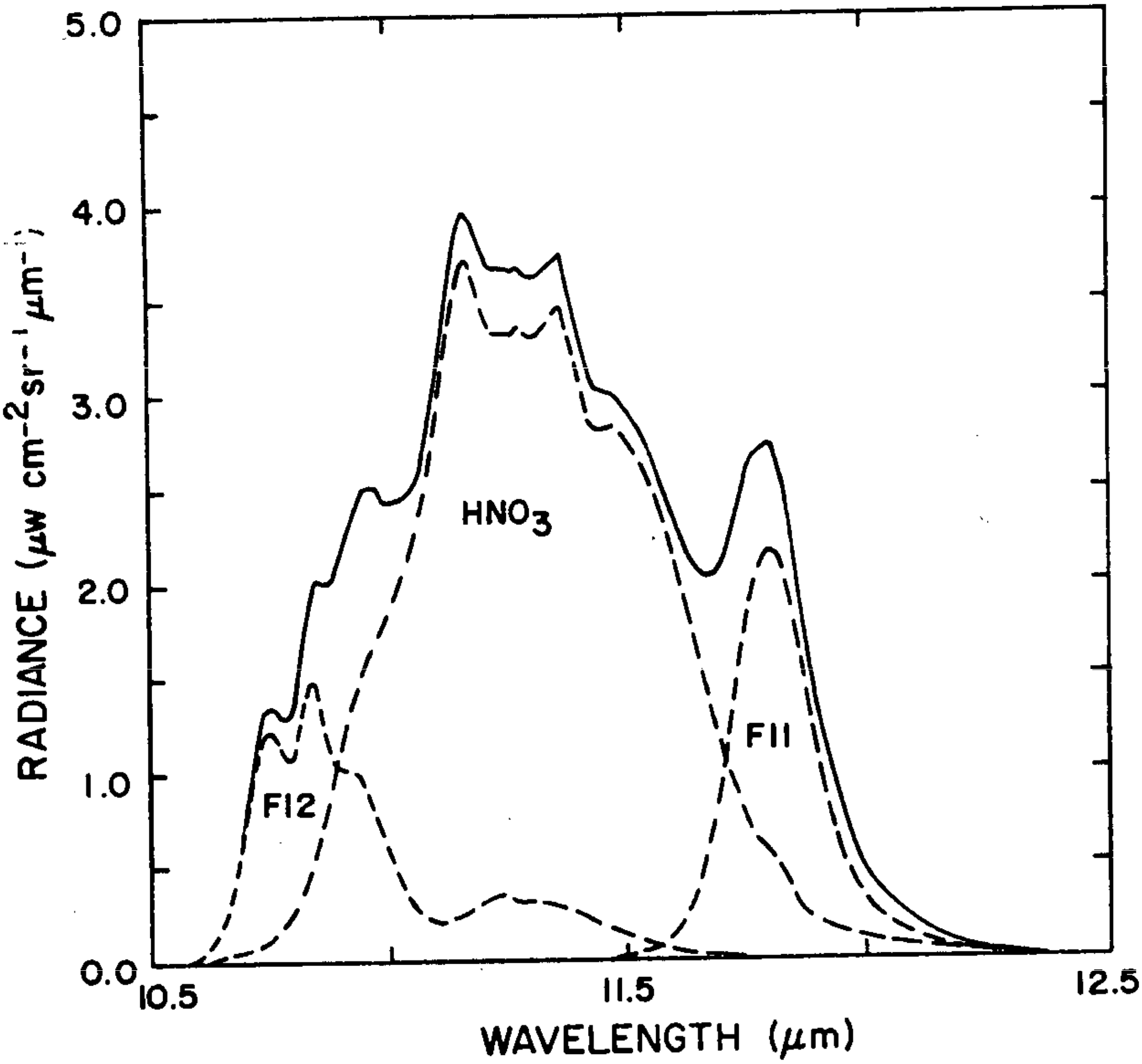

Figure 82. Calculated spectral radiance of F-11, F-12 and HNO_3 showing separate bands (dashed) and combined spectral radiance (solid curves).

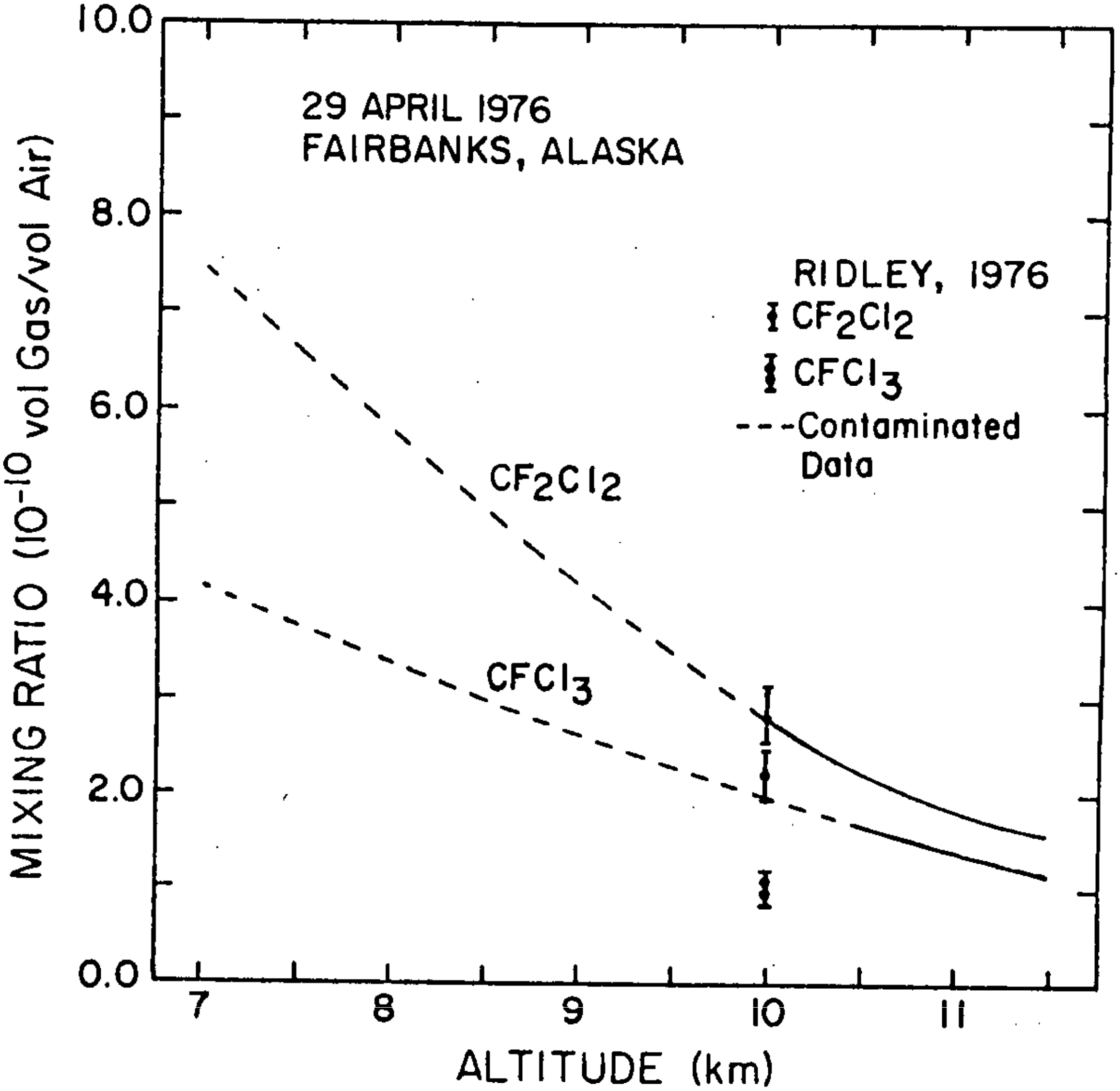

Figure 83. Mixing ratio height profiles of CF_2Cl_2 and $CFCl_3$ derived from the spectral radiance data of 29 April 1976[318] by matching spectral features in the manner shown in Figure 82.

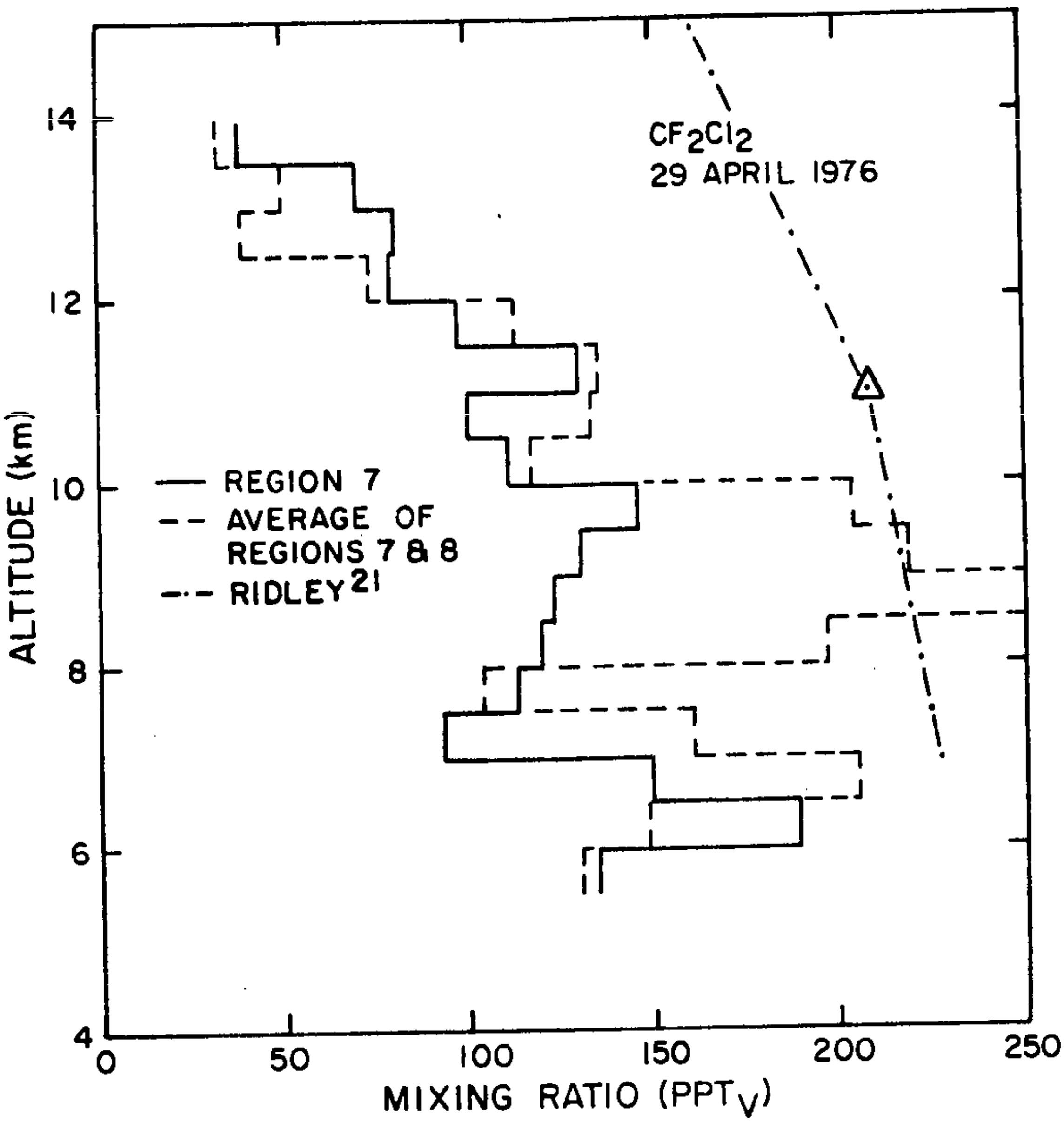

Figure 84. Mixing ratio height profiles of CF_2Cl_2 derived from the spectral radiance data of 29 April 1976 using spectral regions 7 and 8 and reference spectral regions 4 or 6.

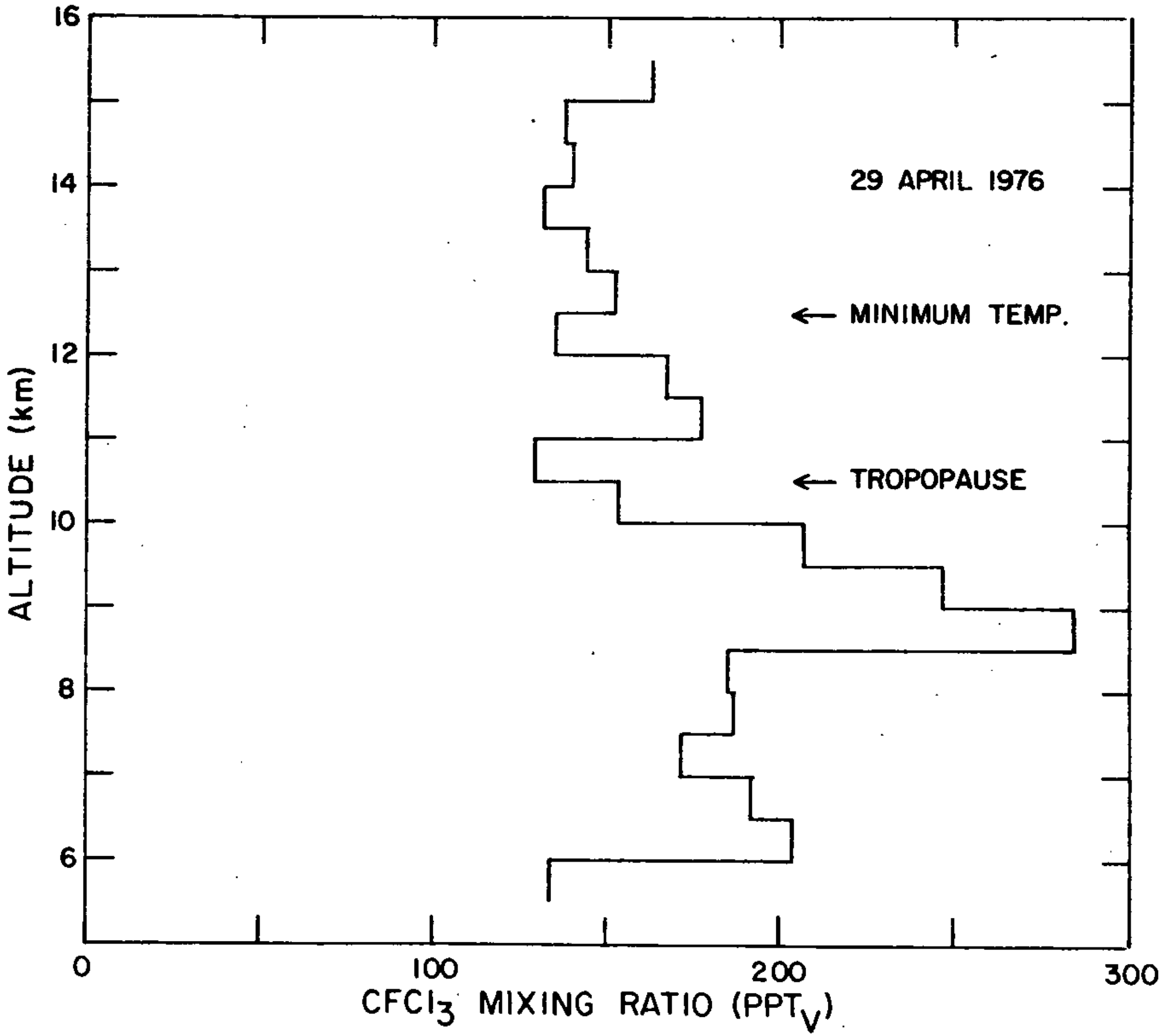

Figure 85. Mixing ratio height profile of $CFCl_3$ derived from the spectral radiance data of 29 April 1976 using spectral region 15 and referenced to spectral region 4.

2. Unknown Constituents

Emissions at $12.04\mu m$ and $12.20\mu m$ are apparent in Figures 41 through 47. The spectral source of these emissions is not certain at this time. However, it is possible to use the linear band model technique to calculate the relative shape of the height profiles of these constituents, based on the change in emissivity with pressure ($\Delta\epsilon$ / Δp). This is equivalent to a mixing ratio in relative units. It can be shown from (5) and (9) that

$$\beta_v = \frac{\Delta\epsilon}{\Delta p} \frac{1}{\overline{K} \text{ Sec}\theta \text{ H}} \quad . \tag{18}$$

As an example of this technique, a plot of the $CFCl_3$ data of Figure 85 is shown in Figure 86 using this parameter. In Figure 87, the feature at $12.04\mu m$ (region 17) shows a decrease just below the tropopause of a factor of about 2, while in Figure 88 the feature at $12.20\mu m$ (region 18) shows an even stronger decrease just below the tropopause, possibly followed by a slight increase. Clearly these two are features of two different constituents. Both of these profiles suffer from the uncertainties associated with the gray radiance correction. A similar decrease of about two is also noted when this type of analysis is applied to the CO_2 Q-branch at $12.62\mu m$, but this may be caused by a different effect. Identification of these features is part of a continuing effort under a separate contract.

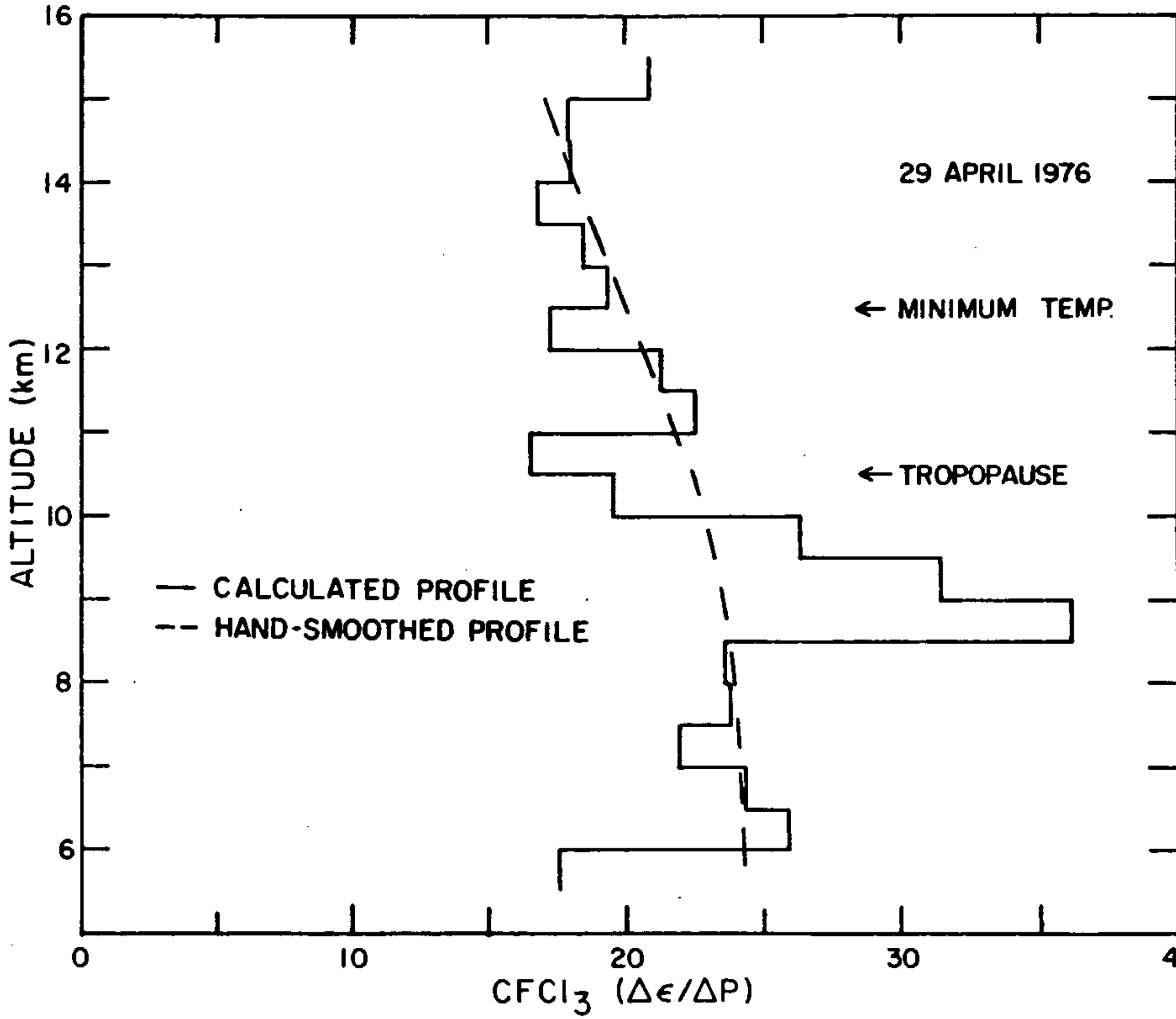

Figure 86. Relative mixing ratio height profile of $CFCl_3$ using technique of Equation 18. This is the same data shown in Figure 85.

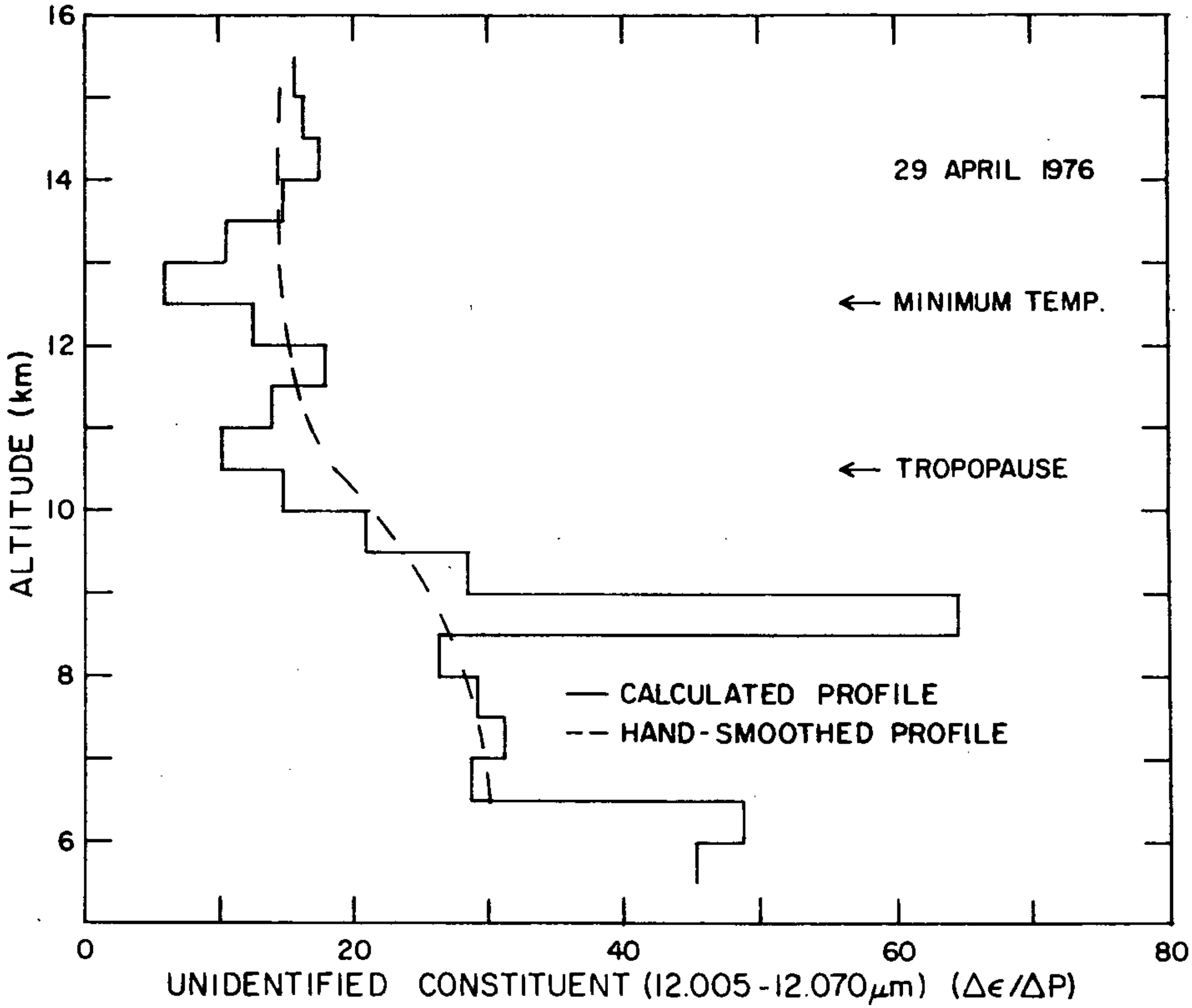

Figure 87. Relative mixing ratio height profile of an unidentified constituent emitting at 12.04μm.

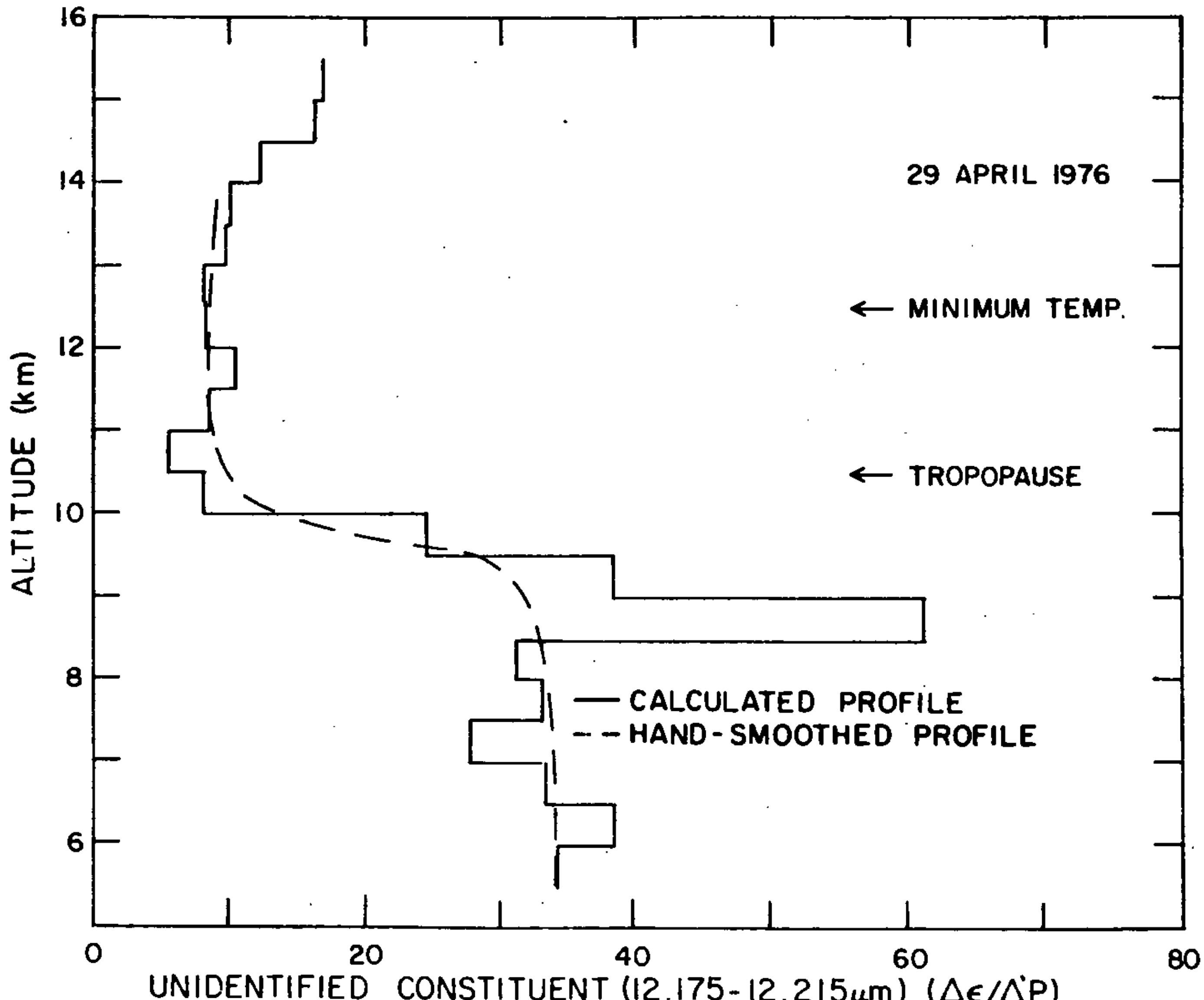

Figure 88. Relative mixing ratio height profile of an unidentified constituent emitting at 12.20μm.

G. Additional Features of the Float Data

The variation of radiance at float of several spectral regions was discussed earlier. Several other pieces of information can be derived from the float data, particularly from the data associated with observations at several secant angles within relatively short time periods. The most interesting spectral regions to consider in this way are the 25 and 26μm H_2O (regions 28 and 31). Since these regions are composed of a series of randomly spaced strong lines, one might expect the radiance change to be proportional to the square root of the optical path. Figure 89 confirms this expectation for both regions. Further, it sets an upper limit for H_2O contamination in the vicinity of the balloon at about 22% of the radiance measured at 45^o and at 37.5 km. Based on the square root approximation this represents about 5% of the total H_2O in the path. This number could be further interpreted as a H_2O density increase in the vicinity of the balloon, depending on the length of the assumed contaminated path. However, this is not attempted here because of the large number of assumptions already present in the 5% figure.

Similar analyses of other spectral regions are also of some interest. The 12.6μm CO_2 region plotted vs secant has a slope approximated by a power of 0.73, part way between a square root and a linear fit. This is in agreement with the results of the 5 May 1975 CO_2 data[3] and inferred in the previous report covering two earlier flights.[1] It makes this spectral feature somewhat difficult to work with for inferring either CO_2 amounts or atmospheric temperature profiles. The window radiances at 10.7 and 12μm fit a linear model, but due to their low values, there is some scatter in the data. This, of

course, is a check on the optical window corrections and does not yield any information about the atmosphere. (See IV B).

For observations at a zenith angle of 93.5° the measured emission is from very long geometric paths (hundreds of kilometers). Variation in the data from scan to scan would infer either inhomogeneities in the atmosphere or slight variations of the instrument angle. Analysis of data from several spectral regions (windows, H_2O, HNO_3, O_3, CO_2), provides some conclusions. Immediately following a change in angle and for 2-3 minutes, there is some variation in all the data which can be explained as a quickly damped oscillation of about 0.1°. For the remainder of a ten-minute period the changes in the radiance levels were less than 4% and generally less than 2%. The associated radiance variations were approximately 1×10^{-7} w cm^{-2} sr^{-1} μm^{-1}.

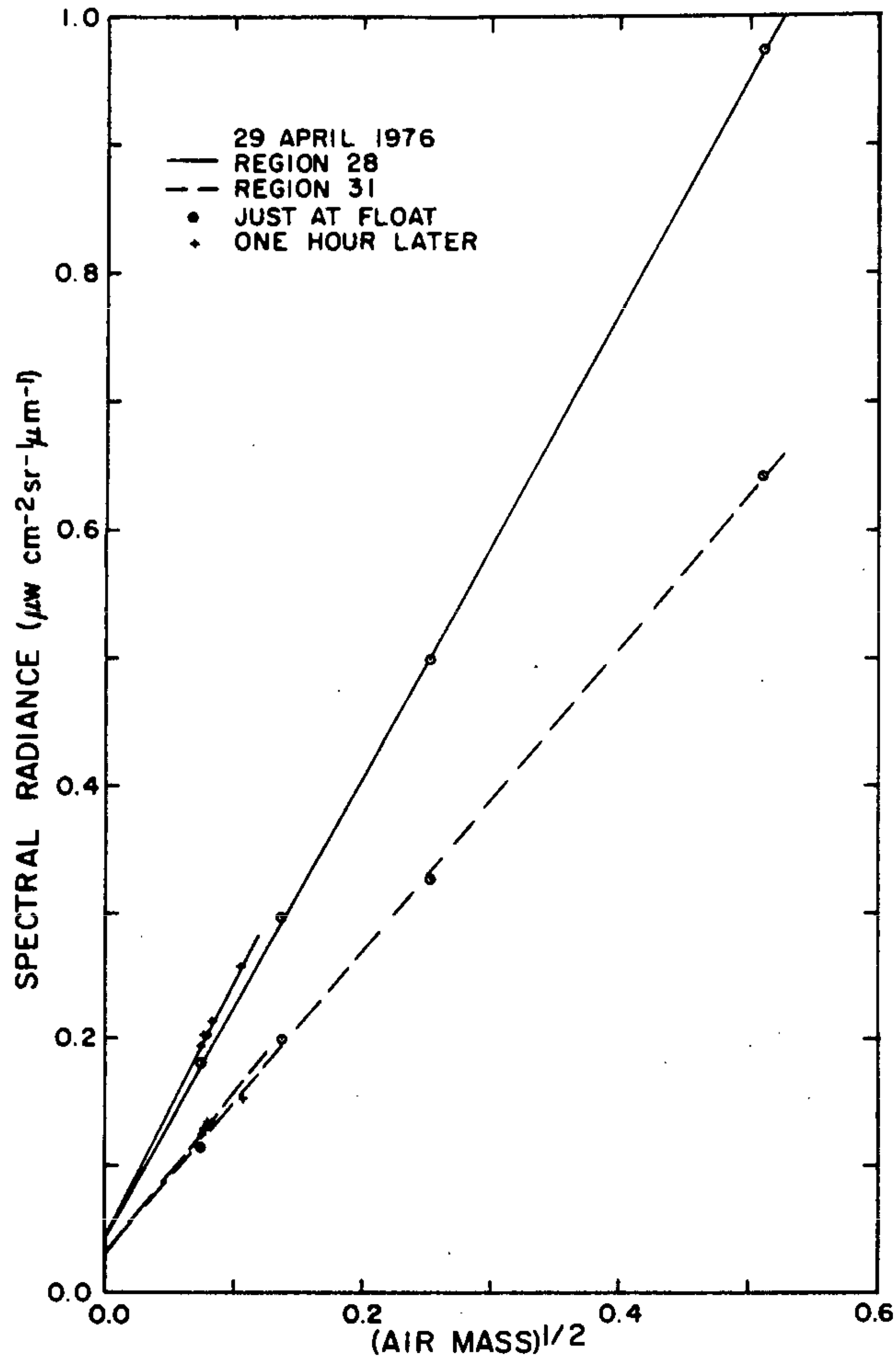

Figure 89. Dependence of the spectral radiance of water vapor emission at 25μm (region 28) and 26μm (region 31) on secant. Straight line through points represents a square root fit with zero offset.

VII. CONCLUSIONS

The liquid helium spectral radiometer has now been developed into an accurate, functional instrument capable of simultaneously measuring a large number of atmospheric constituents. A number of minor corrections suggested by the experiences of this flight and associated data reduction processes have been or are being incorporated into the spectrometer. These include reduction of the optical window scattering, changes in the antifrost gas system to allow more constant window temperatures, improvement in spectral resolution, and possibly a change in the wavelength region covered to include more species.

A number of constituent height profiles were derived from the data. The procedures which accomplish this are continuing to be refined, both to expedite the process and to provide greater accuracy. A number of questions have been raised about the best analysis techniques for dealing with gray radiation from atmospheric particulates. Also a number of spectral features continue to be unidentified.

ACKNOWLEDGMENTS

We wish to thank the National Center for Atmospheric Research, which is sponsored by the National Science Foundation, for computer time used in this research. We wish to thank C. Bauer for preparation of the figures and editing the text and K. Mutchler for preparing the text.

REFERENCES

1. D. G. Murcray, J. N. Brooks, A. Goldman, J. J. Kosters and W. J. Williams, "Water Vapor, Nitric Acid and Ozone Mixing Ratio Height Profiles Derived from Spectral Radiometric Measurements" Report No. BRL CR332 on Contract DAAD05-74-C-0795 by Department of Physics, University of Denver, Feb. 1977. (AD #A037375)

2. D. E. Snider, D. G. Murcray, W. J. Williams and F. H. Murcray, "Investigation of High Altitude Enhanced Infrared Background Emissions - Results from COSMEP III and IV" Electronics Command Report No. 5824, OSD-1366, June 1977.

3. D. G. Murcray, R. C. Amme and J. R. Olson, Final Reports on Contracts DAAD05-74-C-0795 and DAAD05-76-C-0740 by Department of Physics, University of Denver, in preparation, 1978.

4. D. G. Murcray, "Optical Properties of the Atmosphere" Six Month Technical Report on Contract F19628-68-C-0233 for AFCRL by Department of Physics, University of Denver, Sept. 1969.

5. D. E. Snider and A. Goldman, "Refractive Effects in Remote Sensing of the Atmosphere with Infrared Transmission Spectroscopy" BRL Report No. 1790, Ballistic Research Laboratories, Aberdeen Proving Ground, Maryland, June 1975. (AD #A011253)

6. W. J. Williams, D. B. Barker, J. N. Brooks, A. Goldman, J. J. Kosters, F. H. Murcray, D. G. Murcray and D. E. Snider, "Spectral Radiometric Measurement of Atmospheric Constituents" Proceedings of Society of Photo-Optical Instrumentation Engineers, 91, 15-25, 1976.

7. A. Goldman, D. G. Murcray, F. H. Murcray, W. J. Williams and J. N. Brooks, "Distribution of Water Vapor in the Stratosphere as Determined from Balloon Measurements of Atmospheric Emission Spectra in the 24-29 μm Region" Appl. Opt., 12, 1045-1053, 1973.

8. J. C. Breeze, C. C. Ferriso, C. B. Ludwig and M. Malkmus, "Temperature Dependence of the Total Integrated Intensity of Vibrational-Rotational Band Systems" J. Chem. Phys., 42, 402-406, 1965.

9. C. C. Ferriso and C. B. Ludwig, "An Infrared Band Ratio Technique for Temperature Determinations of Hot Gases" Appl. Opt., 4, 47-51, 1965.

10. A. Goldman, "Statistical Band Model Parameters for Long Path Atmospheric Ozone in the 9-10μm Region" Appl. Opt., 9, 2600-2604, 1970.

11. S. S. Penner, Quantitative Molecular Spectroscopy and Gas Emissivities, Addison-Wesley Publishing Company, Inc., Reading, Mass., 1959.

12. A. Goldman, T. G. Kyle and F. S. Bonomo, "Statistical Band Model Parameters and Integrated Intensities for the 5.9μ, 7.5μ and 11.3μ Bands of HNO_3 Vapor" Appl. Opt., 10, 65-73, 1971.

13. D. G. Murcray, A. Goldman and F. S. Bonomo, "Laboratory Studies of Infrared Absorption by NO_2 and HNO_3" Final Report on NASA Grant 06-004-128, Department of Physics, University of Denver, 1974.

14. D. G. Murcray, F. S. Bonomo, J. N. Brooks, A. Goldman, F. H. Murcray and W. J. Williams, "Detection of Fluorocarbons in the Stratosphere" Geophys. Res. Lett., 2, 109-112, 1975.

15. D. G. Murcray, A. Goldman, A. Scoeke-Poeckh, F. H. Murcray, W. J. Williams and R. N. Stocker, "Nitric Acid Distribution in the Stratosphere" J. Geophys. Res., 78, 7033-7038, 1973.

16. A. Goldman, R. N. Stocker, D. Rolens, W. J. Williams and D. G. Murcray, "Stratospheric HNO_3 Distributions from Balloon-Borne Infrared Atmospheric Emission Measurements from 1970-75" Scientific Report, Department of Physics and Astronomy, University of Denver, 1976.

17. R. M. Goody, Atmospheric Radiation I. Theoretical Basis, Oxford University Press, London, 1964.

18. D. G. Murcray, A. Goldman, F. H. Murcray and W. J. Williams, "Measurement of CF_2Cl_2 and $CFCl_3$ Using Infrared Emission Spectra" Final Report on MCA Contract No. 75-13, Department of Physics, University of Denver, Dec. 1976.

19. A. Goldman, F. S. Bonomo and D. G. Murcray, "Statistical Band Model Analysis and Integrated Intensity for the 11.8μm Band of $CFCl_3$" Appl. Opt., 15, 2305-2307, 1976.

20. A. Goldman, F. S. Bonomo and D. G. Murcray, "Statistical Band Model Analysis and Integrated Intensity for the 10.8μm Band of CF_2Cl_2" Geophys. Res. Lett., 3, 309-312, 1976.

21. B. A. Ridley, "Stratospheric Measurements of $CFCl_3$ and CF_2Cl_2 at Fairbanks, Alaska" MCA Report 76-102, Aug. 1976.

DISTRIBUTION LIST

No. of Copies	Organization
12	Commander Defense Documentation Center ATTN: DDC-TCA Cameron Station Alexandria, VA 22314
1	Director Institute for Defense Analyses ATTN: Dr. E. Bauer 400 Army-Navy Drive Arlington, VA 22202
2	Director Defense Advanced Research Projects Agency ATTN: STO, Mr. J. Justice Dr. S. Zakanyca 1400 Wilson Boulevard Arlington, VA 22209
1	Director of Defense Research and Engineering ATTN: Mr. D. Brockway Washington, DC 20305
5	Director Defense Nuclear Agency ATTN: STAP (APTL) STRA (RAAE) Dr. C. Blank Dr. G. Soper Mr. J. Mayo DDST, Dr. M. Peek Washington, DC 20305
5	DASIAC/DOD Nuclear Information and Analysis Center General Electric Company-TEMPO ATTN: Mr. A. Feryok Mr. W. Knapp Dr. T. Stevens Dr. M. Stanton Mr. T. Barrett 816 State Street P. O. Drawer QQ Santa Barbara, CA 93102

No. of Copies	Organization
1	Commander US Army Materiel Development and Readiness Command ATTN: DRCDMA-ST 5001 Eisenhower Avenue Alexandria, VA 22333
1	Commander US Army Aviation Research and Development Command ATTN: DRSAV-E 12th and Spruce Streets St. Louis, MO 63166
1	Director US Army Air Mobility Research and Development Laboratory Ames Research Center Moffett Field, CA 94035
1	Commander US Army Electronics Command ATTN: DRSEL-RD Fort Monmouth, NJ 07703
5	Commander/Director US Army Electronics Command Atmospheric Sciences Laboratory ATTN: Dr. D. E. Snider Dr. E. H. Holt Mr. F. Horning Mr. R. Olsen Dr. F. E. Niles White Sands Missile Range NM 88002
5	Commander/Director US Army Electronics Command Atmospheric Sciences Laboratory ATTN: Mr. B. Kennedy Dr. J. Randhawa Mr. H. Ballard Dr. H. Rachele Dr. M. Heaps White Sands Missile Range NM 88002

DISTRIBUTION LIST

No. of Copies	Organization
1	Commander US Army Missile Research and Development Command ATTN: DRDMI-R Redstone Arsenal, AL 35809
1	Commander US Army Tank Automotive Research & Development Cmd ATTN: DRDTA-RWL Warren, MI 48090
1	Commander US Army Mobility Equipment Research & Development Cmd ATTN: DRDME-WC, Tech Lib Fort Belvoir, VA 22060
1	Commander US Army Armament Materiel Readiness Command ATTN: DRSAR-LEP-L, Tech Lib Rock Island, IL 61299
2	Commander US Army Armament Research and Development Command ATTN: DRDAR-TSS (2 cys) Dover, NJ 07801
1	Commander US Army Harry Diamond Labs ATTN: DRXDO-TI 2800 Powder Mill Road Adelphi, MD 20783
1	Director US Army TRADOC Systems Analysis Activity ATTN: ATAA-SL, Tech Lib White Sands Missile Range NM 88002

No. of Copies	Organization
1	Commander US Army Nuclear and Chemical Agency ATTN: Dr. J. Berberet 7500 Backlick Road Springfield, VA 22150
3	Commander US Army Research Office ATTN: Dr. A. Dodd Dr. R. Mace Dr. R. Lontz P. O. Box 12211 Research Triangle Park NC 27709
2	Director US Army BMD Advanced Technology Center ATTN: Mr. W. Davies Mr. M. Capps P. O. Box 1500 Huntsville, AL 35807
1	HQDA (DAEN-RDM, Dr. F. dePercin) Washington, DC 20310
1	Commander US Army Research and Standardization Gp (Europe) ATTN: Dr. H. Lemons P. O. Box 15 FPO New York 09510
1	Chief of Naval Research ATTN: Code 418, Dr. J. Dardis Department of the Navy Washington, DC 20360
1	Commander Naval Surface Weapons Center ATTN: Dr. L. Rutland Silver Spring, MD 20910

DISTRIBUTION LIST

No. of Copies	Organization
1	Commander Naval Electronics Laboratory ATTN: M. W. Moler San Diego, CA 92152
4	Commander Naval Research Laboratory ATTN: Dr. W. Ali Dr. D. Strobel Code 7700, Mr. J. Brown Code 2020, Tech Lib Washington, DC 20375
4	HQ USAF (AFNIN; AFRD; AFRDQ; ARTAC, COL C. Anderson) Washington, DC 20330
2	AFSC (DLCAW, LTC R. Linkous; SCS) Andrews AFB Washington, DC 20334
5	AFGL (Dr. R. McClatchey; Dr. J. Garing; Dr. H. Gardiner; Mr. D. Smith; Dr. A.T. Stair) Hanscom AFB, MA 01730
5	AFGL (Dr. J. Kennealy; Dr. K. Champion; Dr. W. Swider; Dr. T. Keneshea; Dr. R. Narcisi) Hanscom AFB, MA 01730
1	Director National Oceanic and Atmospheric Administration ATTN: Dr. L. Machta US Department of Commerce 8060 13th Street Silver Spring, MD 20910
1	Director National Oceanic and Atmospheric Administration US Department of Commerce ATTN: Dr. E. Ferguson Boulder, CO 80302
1	Director Transportation System Center US Department of Transportation ATTN: Dr. T. Hard 55 Broadway Cambridge, MA 02142
1	Director Air Pollution Technical Information Center US Environmental Protection Agency ATTN: P. Halpin Research Triangle Park NC 27709
1	National Center for Atmospheric Research ATTN: Dr. J. Gille P. O. Box 3000 Boulder, CO 80303
1	Director Lawrence Livermore Laboratory ATTN: Dr. H. Ellsaesser, L-71 P. O. Box 808 Livermore, CA 94550
3	Director Los Alamos Scientific Lab ATTN: Dr. W. Maier (Gp J-10) Dr. J. Zinn (MS 664) Dr. W. Myers P. O. Box 1663 Los Alamos, NM 84544
2	Director Jet Propulsion Laboratory ATTN: Dr. C. Farmer Dr. R. Toth 4800 Oak Grove Drive Pasadena, CA 91103

DISTRIBUTION LIST

No. of Copies	Organization
4	Director National Aeronautics and Space Administration Goddard Space Flight Center ATTN: Dr. E. Hilsenrath Dr. V. Kunde Dr. A. Aikin Dr. R. Goldberg Greenbelt, MD 20771
1	Director National Aeronautics and Space Administration Langley Research Center ATTN: Dr. J. Russell Hampton, VA 23365
2	Director National Science Foundation ATTN: Dr. F. Eden Dr. G. Adams 1800 G Street, NW Washington, DC 20550
1	Boeing Aerospace Company ATTN: J. Nelson P. O. Box 3999 Seattle, WA 98124
1	Brown Engineering Company ATTN: N. Passino 300 Sparkman Drive Huntsville, AL 46807
1	Ford Aerospace and Communications Corporation ATTN: N. Cowden Ford & Jamboree Roads Newport Beach, CA 92663
1	General Electric Company Missile and Space Division ATTN: J. Burns P. O. Box 9555 Philadelphia, PA 19101

No. of Copies	Organization
2	General Electric Company Valley Forge Space Technology Center ATTN: Dr. M. Bortner Dr. T. Baurer P. O. Box 8555 Philadelphia, PA 19101
1	General Research Corporation ATTN: Dr. R. Zirkind 1501 Wilson Boulevard Arlington, VA 22209
1	General Research Corporation ATTN: J. Fowler 307 Wynn Drive Huntsville, AL 35807
1	General Research Corporation ATTN: T. Zakrzewski 7655 Old Springhouse Road McLean, VA 22101
1	Grumann Aerospace Corporation Research Division 35/588 ATTN: Dr. J. Selby Bethpage, NY 11714
1	Honeywell Radiation Center ATTN: H. Robinson No. 2 Forbes Road Lexington, MA 02173
1	Hughes Aircraft Company ATTN: J. Steffes Centinela & Teale Streets Culver City, CA 90230
1	L'Garde, Inc. ATTN: M. Thomas 1555 Placentia Avenue Newport Beach, CA 92663

DISTRIBUTION LIST

No. of Copies	Organization
1	Lockheed Aircraft Corporation Lockheed Missiles and Space Company ATTN: R. Daniels 3251 Hanover Street Palo Alto, CA 94304
3	Lockheed Palo Alto Research Laboratory ATTN: Dr. B. McCormack Dr. J. Reagan Mr. R. Sears 3251 Hanover Street Palo Alto, CA 94304
1	McDonnell Douglas Astronautics Company ATTN: H. Herdman 3322 S. Memorial Parkway Huntsville, AL 35804
1	Mission Research Corporation ATTN: Dr. R. Hendrick 735 State Street P. O. Drawer 719 Santa Barbara, CA 93101
1	MIT Lincoln Laboratory ATTN: P. Longaker/R.Espinola P. O. Box 73 Lexington, MA 02173
1	MITRE Corporation ATTN: Tech Lib P. O. Box 208 Bedford, MA 01730
1	Nichols Research Corporation ATTN: R. Nichols 7910 South Memorial Parkway Suite A Huntsville, AL 35802

No. of Copies	Organization
1	Photon Research Assoc, Inc. ATTN: D. Anding P. O. Box 1318 2223 Avenida de la Playa La Jolla, CA 92037
1	R&D Associates ATTN: Dr. F. Gilmore P. O. Box 9695 Marina del Rey, CA 90291
1	Rockwell International ATTN: Bob Fleming P. O. Box 4182 3370 Miraloma Avenue Anaheim, CA 92803
1	Sandia Laboratories ATTN: Dr. R. O. Woods Albuquerque, NM 87115
1	The Ohio State University Department of Physics ATTN: Dr. J. Shaw Columbus, OH 43210
1	Stanford Research Institute ATTN: Dr. J. Peterson 333 Ravenswood Avenue Menlo Park, CA 94025
6	University of Denver Denver Research Institute ATTN: Dr. R. Amme Dr. D. Murcray Dr. A. Goldman Dr. J. Williams Dr. F. Murcray Mr. J. Kosters P. O. Box 10127 Denver, CO 80210

DISTRIBUTION LIST

No. of Copies	Organization
1	University of Illinois Dept of Electrical Engineering ATTN: Dr. C. Sechrist, Jr. Urbana-Champaign Campus Urbana, IL 61801
2	University of Michigan High Altitude Engineering Lab ATTN: Dr. F. Bartman Dr. S. Drayson Rsch Activities Building Ann Arbor, MI 48105
1	University of Minnesota, Morris Div of Science and Mathematics ATTN: Dr. M. N. Hirsh Morris, MN 56267
1	University of Wyoming Dept of Physics and Astronomy ATTN: Dr. T. Pepin Laramie, WY 82070
4	Utah State University Center for Research in Aeronomy ATTN: Dr. L. Megill Dr. P. Williamson Dr. K. Baker Dr. D. Baker Logan, UT 84321

Aberdeen Proving Ground

Marine Corps Ln Ofc
Dir, USAMSAA